AD/A-002 144

TIME DOMAIN APERTURE ANTENNA STUDY. VOLUME II

Hugh C. Maddocks

Vermont University

Prepared for:

Rome Air Development Center

October 1974

RADC-TR-74-254, Volume II
Final Report
October 1974

TIME DOMAIN APERTURE ANTENNA STUDY

University of Vermont

Rome Air Development Center
Air Force Systems Command
Griffiss Air Force Base, New York

UNCLASSIFIED

SECURITY CLASSIFICATION OF THIS PAGE *(When Data Entered)*

AD/A002 144

REPORT DOCUMENTATION PAGE

READ INSTRUCTIONS BEFORE COMPLETING FORM

1. REPORT NUMBER: RADC-TR-74-254, Volume II (of 2)	2. GOVT ACCESSION NO.
3. RECIPIENT'S CATALOG NUMBER	
4. TITLE *(and Subtitle)*: TIME DOMAIN APERTURE ANTENNA STUDY	5. TYPE OF REPORT & PERIOD COVERED: Final Report, 21 Dec 72 - 21 May 74
	6. PERFORMING ORG. REPORT NUMBER: None
7. AUTHOR(s): Hugh C. Maddocks	8. CONTRACT OR GRANT NUMBER(s): F30602-73-C-0104
9. PERFORMING ORGANIZATION NAME AND ADDRESS: Electrical Engineering Department, University of Vermont, Burlington, Vermont 05401	10. PROGRAM ELEMENT, PROJECT, TASK AREA & WORK UNIT NUMBERS: Job Order No. 45060168
11. CONTROLLING OFFICE NAME AND ADDRESS: Rome Air Development Center (OCTS), Griffiss Air Force Base, New York 13441	12. REPORT DATE: October 1974
	13. NUMBER OF PAGES: 218
14. MONITORING AGENCY NAME & ADDRESS *(If different from Controlling Office)*: Same	15. SECURITY CLASS. *(of this report)*: UNCLASSIFIED
	15a. DECLASSIFICATION/DOWNGRADING SCHEDULE: N/A

16. DISTRIBUTION STATEMENT *(of this Report)*

Approved for public release; distribution unlimited.

17. DISTRIBUTION STATEMENT *(of the abstract entered in Block 20, if different from Report)*

Same

18. SUPPLEMENTARY NOTES

RADC Project Engineer:
John A. Potenza (OCTS)
AC 315 330-4437

19. KEY WORDS *(Continue on reverse side if necessary and identify by block number)*

Antennas
Transient Aperture Radiation
Pulsed Paraboloid/Horn Radiation
Time Domain Antenna Response

20. ABSTRACT *(Continue on reverse side if necessary and identify by block number)*

This final report contains the results of a study to develop a time-domain analysis for impulse-excited aperture antennas such as the paraboloid/TEM horn system. The principal approach used is the Chernousov aperture-fields formulation, based upon the Huygens-Kirchoff principle, to obtain time domain equations for antenna radiation.

The aperture fields over the front and two side apertures of a constant-impedance TEM horn are obtained by modeling it as a transmission-line,

DD FORM 1 JAN 73 1473 EDITION OF 1 NOV 65 IS OBSOLETE

UNCLASSIFIED

SECURITY CLASSIFICATION OF THIS PAGE *(When Data Entered)*

20. Abstract (Cont'd)

TEM-mode, traveling-wave system with TDR-measured reflection coefficients. The equations derived from this approach were programmed for digital-computer numerical calculation. A second approach developed for the horn is the vector potential formulation using a current distribution on the conductors consistent with the fields in the TEM traveling-wave model. A third approach used for small-aperture horns is to model them as V-dipoles. Equations are given for calculating transient radiation from linear dipoles in any direction, including near endfire, from the currents on the dipole. Approximate closed-form expressions are derived for small-aperture horns for the radiation waveform in the boresight or backfire directions, using all three above approaches, which agree with each other. Comparison on a relative basis between computed and available experimental radiation vs. time curves for four TEM horns in various directions shows reasonably good agreement.

The paraboloid aperture fields are obtained by a point-to-point transformation from the fields at the paraboloid surface. The latter fields are calculated from a non-isotropic point source with arbitrary time excitation at the focus. Any given horn is replaced by an equivalent point source through an approximate closed-form equation characterizing the horn's fields in its principal planes. For gaussian pulse excitation, computed radiation vs. time curves are presented for an isotropic feed and for a particular 8" TEM horn both feeding a 48" paraboloid, in the boresight direction and other directions to display the sidelobe structure. Comparison, on a relative basis, with experimental curves for the boresight direction, shows reasonably good agreement.

The report consists of two volumes, each of which is self-contained. In addition, Volume I references, discusses, and incorporates the results of Volume II in such a manner that the reader, if desired, can obtain an overview of the entire project from Volume I.

TIME DOMAIN APERTURE ANTENNA STUDY

Hugh C. Maddocks

University of Vermont

FOREWORD

This two-volume, final technical report was prepared by the Electrical Engineering Department, University of Vermont, Burlington, Vermont. Partial support for this research was received from the Air Force Systems Command, Rome Air Development Center, Griffiss Air Force Base, New York under Contract F30602-73-C-0104, Job Order Number 45060468. The work was performed during the period from 21 December 1972 through 21 May 1974.

John A. Potenza (OCTS) was RADC Project Engineer.

The author expresses his gratitude to Dr. Morris Handelsman of the University of Vermont for professional guidance and advice during the course of this research.

This report has been reviewed by the Office of Information (OI), RADC, and approved for release to the National Technical Information Service (NTIS).

This report has been reviewed and is approved.

APPROVED: John Potenza

JOHN POTENZA
Project Engineer

APPROVED: William T. Pope

WILLIAM T. POPE
Assistant Chief
Surveillance and Control Division

FOR THE COMMANDER: James G. McGinnis

JAMES G. McGINNIS, Lt Col, USAF
Deputy Chief, Plans Office

ABSTRACT

Volume 2 is identical to a Ph.D. thesis with the title The Transient Electromagnetic Far Fields of a Paraboloid Reflector/TEM Horn Antenna Using Time Domain Techniques, submitted to the University of Vermont.

This research employs a direct time domain model applicable to aperture antennas of any shape excited by fields of any form in space and time to study theoretically the electromagnetic far fields of a paraboloid reflector when fed by a transverse electromagnetic (TEM) horn antenna. First, the TEM horn antenna is considered as an aperture antenna with an arbitrary excitation V(t) applied to its apex. The time domain model is then applied to determine the electric far fields of the TEM horn, and the theoretical results are compared with published experimental data on a relative basis. Reasonable agreement is obtained. Approximate closed form solutions for the electric far fields of the TEM horn in the azimuth plane are also found. Secondly, the TEM horn is studied in terms of current sheets using the vector potential formulation in order to confirm the approximate closed form solutions found in the azimuth plane using the aperture model.

From the theoretical results of the aperture model of the TEM horn, this feed is then reduced to an anisotropic point source located at the focus of the paraboloid reflector. The fields arising from this point source are then transformed to the resulting fields over the exit aperture of the paraboloid by utilizing the geometrical optics approximation. The time domain model is then applied to the exit aperture of the paraboloid to determine the electric far fields of the antenna system. Theoretical results are obtained for both the boresight direction and directions away from boresight, in order to characterize the sidelobe structure of the system. The theoretical boresight response is compared, also on a relative basis, with published experimental data, with reasonable agreement.

TABLE OF CONTENTS

LIST OF FIGURES

Chapter 1

STATEMENT AND BACKGROUND OF PROBLEM

1.1 INTRODUCTION

The primary objective of this research was to study theoretically, directly in the time domain, the electromagnetic far fields of a paraboloid reflector fed by a TEM horn. The TEM horn, located near the focus of the paraboloid, is excited at its apex by a voltage V(t). The TEM horn consists of two metallic circular sectors separated by a small gap at the apex and flared apart away from the apex. The paraboloid reflector/TEM horn antenna system is shown in Figure 1.1. At the present time, no direct time domain models to describe the radiation of the TEM horn or the paraboloid reflector/TEM horn antenna system at an arbitrary observation point in the far field exist.

Specifically, the study of the above antenna system was accomplished as follows. The general theoretical model applicable to aperture antennas of any type excited by electromagnetic fields of any form in space and time is a set of time domain integrals which were derived by Chernousov (1965). The electromagnetic fields at the aperture surface must be known (or guessed at).

First, the TEM horn was considered as an aperture antenna supporting a TEM spherical wave within the antenna region due to the excitation V(t) at the apex. The Chernousov (1965) expressions for

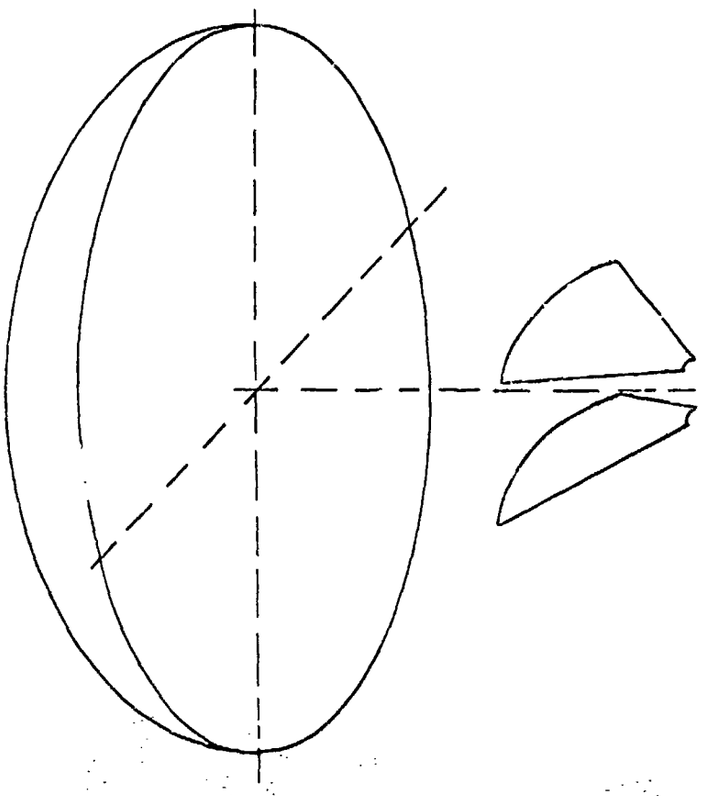

Figure 1.1

The Paraboloid Reflector/TEM Horn Antenna System

the TEM horn apertures were then applied, and the general expressions for the resulting electric far fields were found. Approximate closed form solutions for the TEM horn far fields in the azimuth plane were also determined. These approximate fields were interpreted in terms of travelling and standing waves to facilitate engineering interpretation of the behavior of the TEM horn. The general expressions for the electric far fields were then programmed and executed on a digital computer. The theoretically computed results were then compared to experimental results obtained by Susman and Lamensdorf (1970:42-44) and Martins et al. (1973:254).

Secondly, the electric far fields of the TEM horn were also formulated in terms of the current sheets flowing on the two metallic wedges which comprise the TEM horn. This formulation was also performed directly in the time domain. Approximate closed form solutions for the electric far fields in the azimuth plane were determined and compared to the approximate closed form results obtained by using the Chernousov (1965) formulation.

Thirdly, the Chernousov (1965) formulation was applied to find the electric far fields of a paraboloid reflector in terms of the fields over the exit aperture for excitation by a general spherical-wave point source located at the focus of the paraboloid. The paraboloid was assumed to be perfectly conducting, to be in the far field of the point source, and to be sufficiently smooth to allow application of the plane wave boundary conditions at the paraboloid surface. The geometrical optics approximation was invoked to allow a one-to-one, point-

to-point transformation of the fields at the paraboloid surface to the fields over the exit aperture. A solution in the boresight direction for an isotropic feed was also determined.

Finally, the general expressions for the electric far fields of a TEM horn utilizing the Chernousov (1965) formulation were executed on a digital computer to characterize the fields of the eight-inch TEM horn, studied by Martins et al. (1973), over the angular aperture of the paraboloid. The eight-inch TEM horn was then theoretically reduced to a point source radiator located at the focus of the paraboloid. This reduction was accomplished by interpreting the results of the computer runs and then approximating the fields of the eight-inch TEM horn with a closed form expression. The general expressions for the electric far fields of the paraboloid reflector/point source feed antenna system were then programmed for a digital computer using the approximate closed form solution for the eight-inch TEM horn fields. Computer runs were performed in both characteristic planes of the paraboloid reflector to demonstrate not only the theoretical boresight response of the antenna system, but also the theoretical sidelobe structure of the antenna system. The theoretically computed boresight response of the system was compared to the experimental boresight response obtained by Martins et al. (1973:235).

1.2 HISTORICAL BACKGROUND OF TRANSIENT ANTENNA STUDIES

The two major thrusts of transient antenna studies have been

(a) to investigate theoretically and experimentally antennas whose electric far fields are replicas or high fidelity derivatives of the pulse or step applied to the antenna, and (b) to investigate antennas which not only have the above property, but also have directive characteristics. Among transient antennas which have been studied both theoretically and experimentally are the monopole over a ground plane (dipole) and the conical antenna over a ground plane (biconical). Among transient antennas which have been studied experimentally are the monopole exciting a disk, corner reflector, or paraboloid; the TEM horn; and the paraboloid reflector/TEM horn antenna system.

Recently, Martins et al. (1973) have studied a wide variety of antennas both theoretically and experimentally. These include the TEM horn and the paraboloid reflector/TEM horn antenna system. The theoretical formulation of the various antennas studied by Martins et al. (1973) is performed in the frequency domain. These frequency domain models are then interpreted in the time domain only for specific observation points in the far field. (Note--The Fourier approach is a steady-state frequency domain solution, from which the time domain solution can be obtained only by an inverse transformation. The Chernousov (1965) formulation is a direct time domain approach.) Cronson and Proud (1970a) also studied the paraboloid reflector/TEM horn antenna experimentally. However, the TEM horn used by Cronson and Proud (1970a) had a considerably different geometry from the eight-inch TEM horn studied by Martins et al. (1973) or the TEM horns studied by Susman and Lamensdorf (1970,1971).

Schmitt (1960) first studied the step function response of the finite monopole over a ground plane using Fourier techniques. He interprets the electric far field at the ground plane to consist of a series of damped oscillations rather than delayed replicas of the exciting step. Wu (1961) solved the current distribution in an infinitely long dipole excited by a step function using Fourier techniques and contour integration. Morgan (1962) obtained the same current distribution as Wu (1961) using the same techniques and a more direct approach.

Four years later, Schmitt, Harrison, and Williams (1966) studied the finite monopole over a ground plane using Fourier transforms and computed values of input impedance and effective height (Harrison; 1962,1963b). The electric far field at the ground plane is shown to be a superposition of delayed replicas of the exciting pulse, emanating from the base and tip of the monopole. These theoretical predictions are confirmed experimentally. Harrison and King (1967) used the same theoretical techniques as Schmitt, Harrison, and Williams (1966) to determine the electric far field of an infinitely long monopole over a ground plane. The far field at the ground plane is shown to be a replica of the exciting Gaussian pulse. Palciauskas and Beam (1970) generalized the results of Schmitt, Harrison, and Williams (1966) to observation points not on the ground plane utilizing the same theoretical techniques. The resultant far field is a superposition of pulses which are no longer delayed replicas of the exciting pulse, but are compressed or stretched in time. The results

of Palciauskas and Beam (1970) have also been obtained approximately by using time domain techniques from an accelerated charge viewpoint (Handelsman, 1972:59-69).

From the studies of the monopole over a ground plane (dipole), it is clear that this antenna has an electric far field which is a replica of the exciting pulse only along the ground plane and only for an infinitely long monopole. Also, the monopole suffers from the characteristic that it has no directivity in the azimuth plane (the plane perpendicular to the monopole).

Another transient antenna which has been studied is the conical antenna over a ground plane (biconical). Harrison and Williams (1963, 1965) theoretically studied this antenna using Fourier transforms and computed values of input impedance and effective height (Harrison, 1963a). This study shows that the electric far field along the ground plane is a replica of the exciting pulse only if the cone is electrically extremely long (essentially infinite) and has a certain cone angle (about 46°). Susman and Lamensdorf (1971) experimentally studied the response of electrically short cones to incident transient excitation and interpret the electric far field at the ground plane to be an approximate time derivative of the exciting transient signal. No known studies of the transient response of the biconical antenna at far field points not in the azimuth plane have been performed. However, the biconical antenna, as the dipole, has no directivity in the azimuth plane.

Knop (1970) studied the response of a log-periodic dipole

array using a simplified theoretical model and rectangular pulse excitation. Although a log-periodic has fine directivity, the results unfortunately indicate that the electric far field is a highly distorted version of the exciting pulse.

Transient aperture antenna studies were begun by Polk (1960). He employed Fourier integrals and the Kirchhoff solution of the scalar diffraction problem. The vector wave solution was not attemted. Corrections to Polk (1960) are given by Mayo (1961). Cheng and Tseng (1964) and Tseng and Cheng (1964) state that due to the evaluation of infinite integrals by the theory of residues, the method of Polk (1960) is involved even for simple time signals and aperture distributions. Therefore, they offer a simple expression for a one-dimensional aperture with a known current distribution $i(x,t)$ and state that extension to a two-dimensional aperture is trivial when the spatial distribution is separable in the two dimensions. However, this trivial extension is not carried out. Finally, Chernousov (1965) employed the Huygens-Kirchhoff principle to derive time domain equations for the electromagnetic fields arising from aperture antennas of any shape excited by electromagnetic fields of any form in space and time. Nonetheless, the general equations are not restricted to the radiation fields, but also include the static and induction fields.

Investigation of the scattered fields from a rectangular plate was conducted by DeLorenzo (1967) using a long monopole transmitter and a modified short monopole receiver. The boresight response is shown to be the negative time derivate of the field incident upon

the plate. The properties of the receiving antenna used by DeLorenzo (1967) are described by Ross (1967). Cronson (1969) employed a pulse radiated from the base of a long monopole to study the radiation field of disks in the azimuth plane of the exciting monopole. He interprets the radiated fields of the disks to be delayed replicas of the exciting pulse. Cronson and Proud (1970b) used the same excitation technique as Cronson (1969) to study the radiated fields of disks, corner reflector, and a paraboloid. They make the same interpretation as Cronson (1969).

Lamensdorf (1970) studied the coaxial cone antenna (a flared coaxial line with the aperture located in the ground plane) experimentally in the receive mode. The received terminal voltage is shown to be the time derivative of the incident field. Abo-Zena and Beam (1972) studied the radiation fields of a circular loop antenna using moment methods and Fourier techniques for excitation by a band-limited rectangular pulse. The results indicate that the radiation fields in general are a series of oscillatory and damped replicas of the exciting pulse.

By inspection of the Chernousov (1965) equations (1-3) and (1-5) in the following section of this chapter, the far fields of aperture antennas are interpreted more precisely as surface integrals of the negative time derivative of the electromagnetic fields at the aperture surface. The Chernousov (1965) results can also be interpreted in terms of the radiation from equivalent accelerating charges (Handelsman, 1972:95).

1.3 OUTLINE OF THE CHERNOUSOV FORMULATION

Chernousov (1965) derived equations for the electromagnetic fields everywhere due to a closed aperture surface S_a in a homogeneous source-free medium excited by electromagnetic fields of any form in space and time. The aperture fields must be known (or guessed at).

The geometry for the problem is shown in Figure 1.2. This figure is identical to Figure A.1, and it is repeated here for the convenience of the reader. The various quantities shown in Figure 1.2, and the symbols used in the derivation, are discussed on the first and third pages of Appendix A. The complete mathematical details of the derivation are also furnished in Appendix A.

A brief outline of the derivation follows. The development of the basic equations parallels the development given in Jordan and Balmain (1968:313-315,466-469).

First, Maxwell's equations are written for electric charges and currents only and then for fictitious magnetic charges and fictitious magnetic currents only. Using standard techniques and appropriate electric and magnetic Lorentz gauge conditions, equations for the electric and magnetic fields are found in terms of the electric and magnetic vector potentials.

At this point, the fictitious magnetic current $\bar{M}$ is expressed in terms of the electric field $\bar{E}$ at the aperture surface. The electric current $\bar{J}$ is expressed in terms of the magnetic field $\bar{H}$ at the aperture surface (Jordan and Balmain, 1968:468-469). Assuming that S_a is a

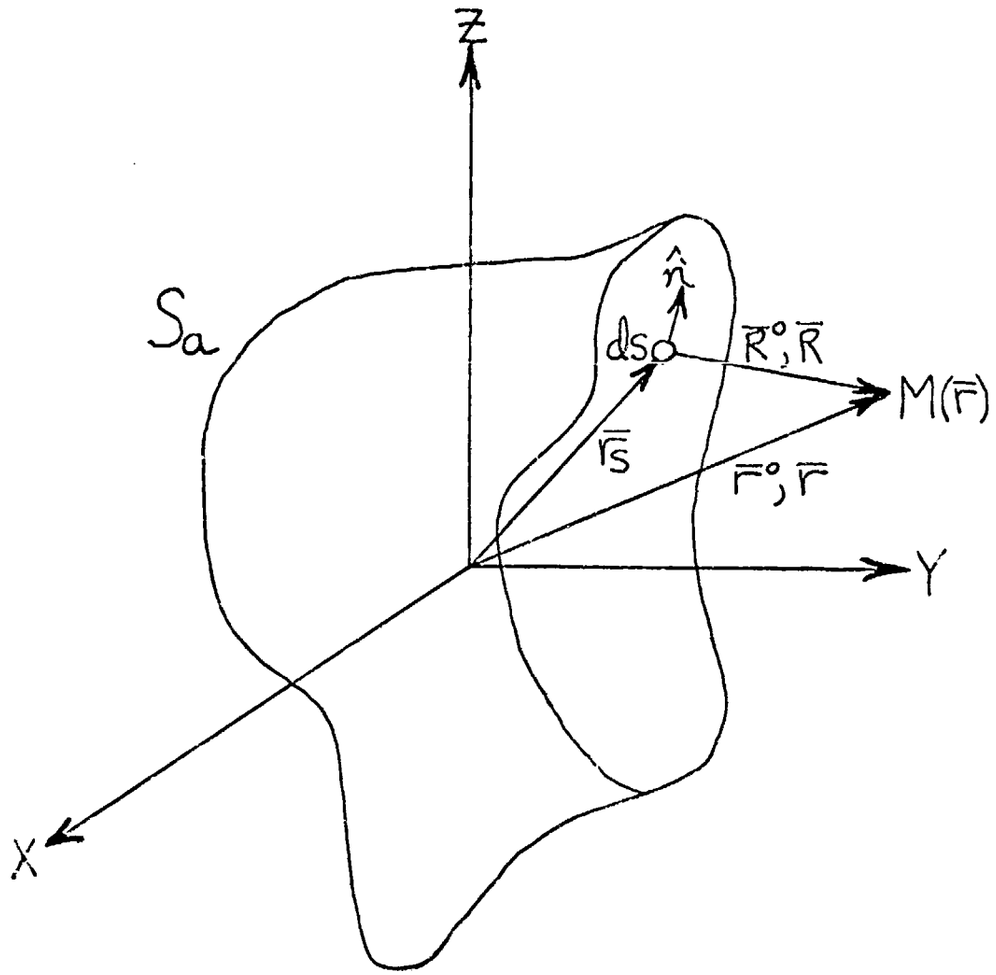

Figure 1.2

Geometry for the Chernousov Derivation

source-free aperture surface,

$$\bar{M}\left(\bar{r}_s, t - R/v\right) = -\hat{n} \times \left(\bar{E}\left[\bar{r}_s, t - R/v\right]\right) \quad (1\text{-}1)$$

$$\bar{J}\left(\bar{r}_s, t - R/v\right) = \hat{n} \times \bar{H}\left(\bar{r}_s, t - R/v\right) \quad (1\text{-}2)$$

Using (1-1) and (1-2), the electric and magnetic fields everywhere due to the electric and magnetic source fields at the aperture surface may be written as (A-45) and (A-46) as given on the tenth and eleventh pages of Appendix A.

After utilizing numerous mathematical manipulations, $\bar{E}(\bar{r},t)$ and $\bar{H}(\bar{r},t)$ <u>everywhere</u> may be written as (A-92) and (A-93) on the twentieth and twenty-first pages of Appendix A. (Note--Equations (A-92) and (A-93) are not restricted to the far fields of an aperture antenna. They also account for the induction and static fields.)

To find the electric far fields of the aperture antenna, $1/R^2$ and $1/R^3$ terms are neglected with respect to 1/R terms. The appropriate conditions for this assumption are discussed in Appendix A. Also, employing standard approximations for R in the far field as applied to the numerator and denominator of (A-92), and using trivial identities, $\bar{E}(\bar{r},t)$ in the far field may be written as

$$\bar{E}\left(\bar{r},t\right) = -\frac{1}{4\pi v r}\left[\bar{r}^{\circ} \times \oint_{S_a}\left\{\left[\hat{n} \times \frac{\partial \bar{E}\left(\bar{r}_s, T + \frac{\bar{r}^{\circ}\cdot\bar{r}_s}{v}\right)}{\partial t}\right]\right.$$
$$\left. - \eta\left[\bar{r}^{\circ} \times \left[\hat{n} \times \frac{\partial \bar{H}\left(\bar{r}_s, T + \frac{\bar{r}^{\circ}\cdot\bar{r}_s}{v}\right)}{\partial t}\right]\right]\right\} dS\Big] \quad (1\text{-}3)$$

where

$$T = t - \left(r/v\right) \quad (1\text{-}4)$$

Equation (1-3) is the same as equation (A-102) on the final page of Appendix A. (1-3) is the central general theoretical equation used in the research. Also, in the far field, $\bar{H}(\bar{r},t)$ is given in terms of $\bar{E}(\bar{r},t)$ by the simple relationship

$$\bar{H}(\bar{r},t) = \frac{1}{\eta}\left[\bar{r}^{\circ} \times \bar{E}(\bar{r},t)\right] \qquad (1\text{-}5)$$

Chapter 2

THE TRANSIENT ELECTRIC FAR FIELDS OF TEM HORN ANTENNAS UTILIZING THE CHERNOUSOV METHOD

2.1 DISCUSSION OF THE FIELDS EXCITING THE HORN AND THE APERTURES CONSIDERED

The TEM horn antenna, shown in Figure 2.1, consists of two perfectly conducting circular sectors of angle ϕ_0 and radius r_a separated by a small gap at the apex and by a distance 2h at $r' = r_a$. Figure 2.1 is the same as Figure B.1 in Appendix B, and it is repeated here for the convenience of the reader. The TEM horn, first studied experimentally by Susman and Lamensdorf (1970,1971), is similar to the dihedral horn first described by Schelkunoff and Friis (1952:528-531).

Assume that due to the excitation V(t) at the apex of the TEM horn, there exists a spherical TEM wave between the wedges described by

$$\bar{E}(\bar{r}',t) = \frac{\hat{\alpha}\, f(\alpha,\beta)}{r'} \left[V\left(t - \frac{r'}{v}\right) + k_v V\left(t + \frac{r'}{v} - \frac{2r_a}{v}\right) \right] \quad (2\text{-}1)$$

and

$$\bar{H}(\bar{r}',t) = \frac{\hat{\beta}\, f(\alpha,\beta)}{\eta r'} \left[V\left(t - \frac{r'}{v}\right) - k_v V\left(t + \frac{r'}{v} - \frac{2r_a}{v}\right) \right] \quad (2\text{-}2)$$

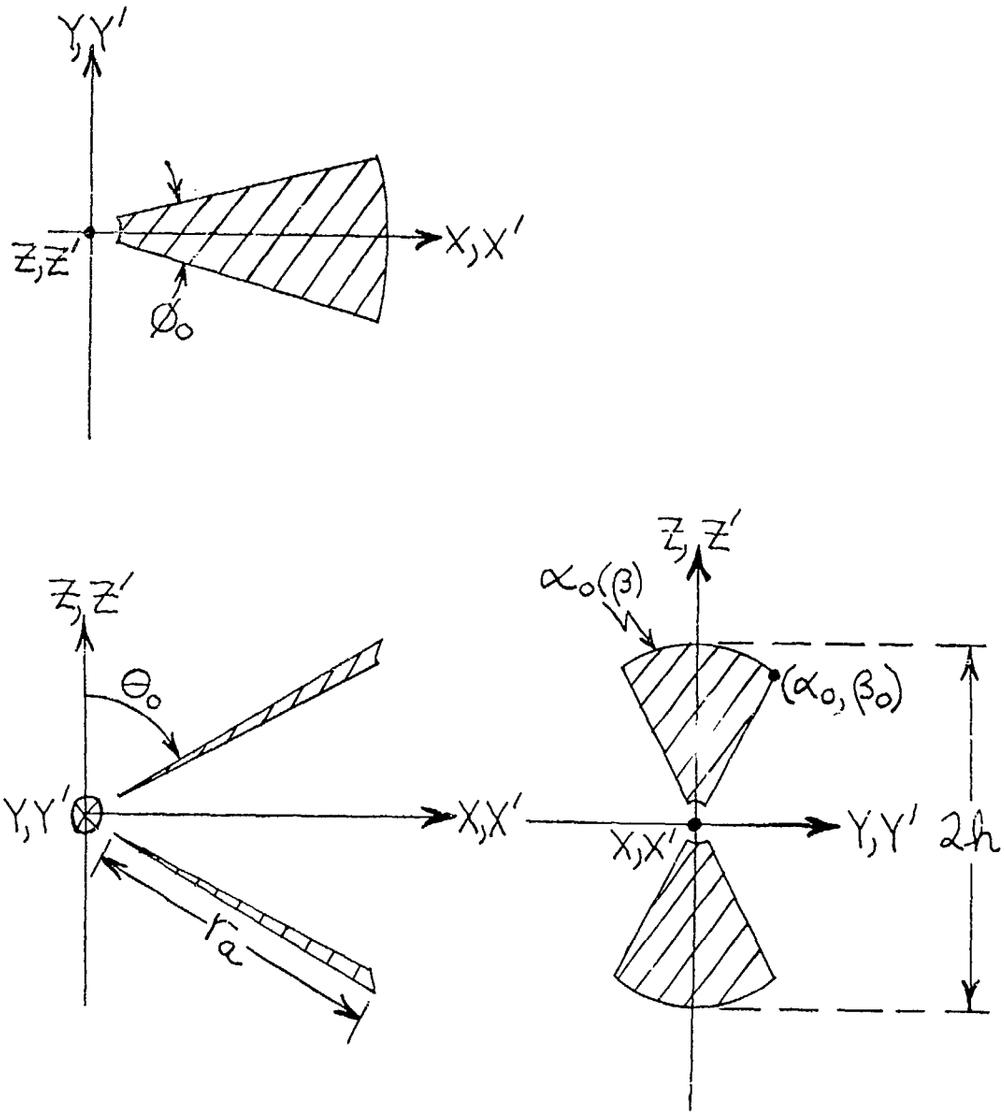

Cartesian source coordinates (x',y',z')
Spherical source coordinates (r',α, β)
Cartesian observation coordinates (x,y,z)
Spherical observation coordinates (r,θ,ϕ)

Figure 2.1

The TEM Horn Antenna

where η is the impedance of the medium and k_v is the effective voltage reflection coefficient determined from

$$k_V = \frac{Z_{eff} - Z_o}{Z_{eff} + Z_o} \tag{2-3}$$

Z_{eff} is the effective terminating impedance of the front aperture located at $r' = r_a$, and Z_o is the characteristic impedance of the TEM horn.

That is, if the apex is excited by V(t), the $\bar{E}$ field within the horn arises from a forward propagating voltage $V(t - r'/v)$ and a reflected voltage $k_v V(t + r'/v - 2r_a/v)$ propagating backward toward the apex from the front aperture. $f(\alpha, \beta)$ is a function which describes the taper of the fields in the two angular coordinates α and β. However, $f(\alpha, \beta)$ is not the standard illumination function used in antenna engineering practice. Let the standard illumination function be designated by $F_o(\alpha, \beta)$. Then, for TEM horns with small flare in the E-plane--that is, when $2h \ll r_a$, $f(\alpha, \beta)$ is related to $F_o(\alpha, \beta)$ by

$$f(\alpha, \beta) \simeq \frac{F_o(\alpha, \beta)}{\pi - 2\theta_o} \tag{2-4}$$

Thus, for TEM horns with small flare in the E-plane, when $F_o(\alpha, \beta) = 1$ (the case for uniform illumination of the front aperture, $f(\alpha, \beta) \simeq 1/(\pi - 2\theta_o)$. Equation (2-4) results from the simple principle that the line integral of the $\bar{E}$ field from one wedge to the other must be the voltage existing between the two wedges.

The closed surface S_a required by the Chernousov formulation,

encompassing the TEM horn, is shown in Figure 2.2. (Note--The gap at the apex was enlarged for the sake of clarity in Figure 2.2.) The closed surface S_a consists of six parts as follows:

1. a front aperture which is a spherical sector at $r' = r_a$ extending from $\alpha = \alpha_o(\beta)$ to $\alpha = \pi - \alpha_o(\beta)$ and from $\beta = -\beta_o$ to $\beta = \beta_o$,
2. a wedge-shaped side aperture located at $\beta = \beta_o$ extending from $r' = 0$ to $r' = r_a$ and from $\alpha = \alpha_o$ to $\alpha = \pi - \alpha_o$,
3. another wedge-shaped side aperture located at $\beta = -\beta_o$ extending from $r' = 0$ to $r' = r_a$ and from $\alpha = \alpha_o$ to $\alpha = \pi - \alpha_o$,
4. a surface on top of the upper wedge of the TEM horn,
5. a surface on the bottom of the lower wedge of the TEM horn, and
6. a small spherical sector located at the apex.

Consider first part 1. The outward normal $\hat{n}$ to this part is in the $\hat{r}'$ direction. Therefore, both $\hat{n}\times\bar{H}$ and $-\hat{n}\times\bar{E}$ current sheets exist at the front aperture.

Consider next part 2. The outward normal to this part is in the $\hat{\beta}_o$ direction. Therefore, there is no $\hat{n}\times\bar{H}$ current sheet, but there is a $-\hat{n}\times\bar{E}$ current sheet at the first wedge-shaped side aperture.

Consider next part 3. The outward normal to this part is in the $-\hat{\beta}_o$ direction. Therefore, as for part 2, there is no $\hat{n}\times\bar{H}$ current sheet, but there is a $-\hat{n}\times\bar{E}$ sheet at the second wedge-shaped side aperture.

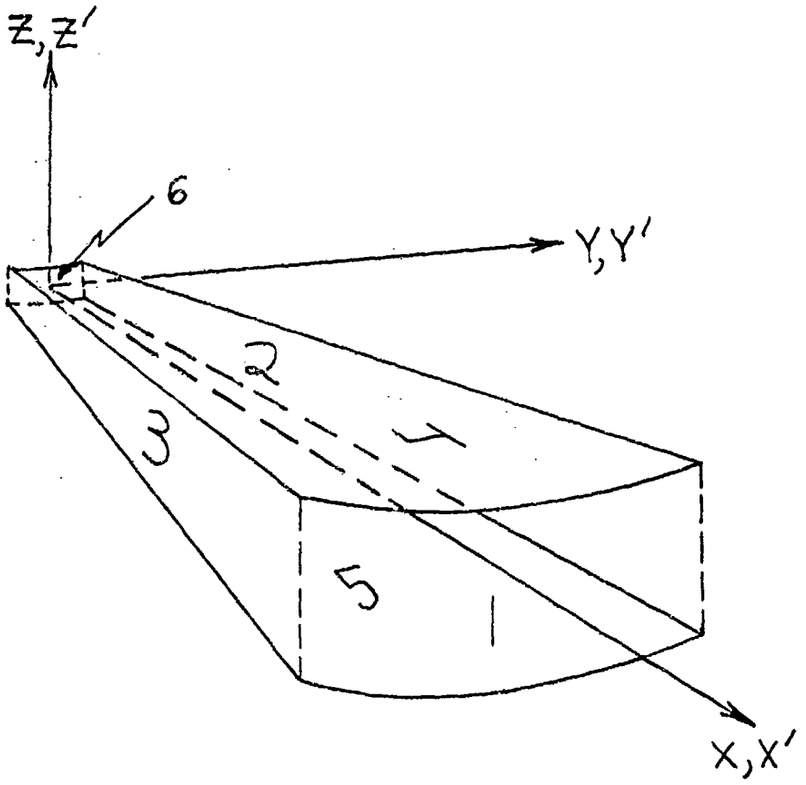

Figure 2.2

The Closed Surface Encompassing the TEM Horn

Consider now parts 4 and 5. The outward normal to part 4 is approximately in the $-\hat{\alpha}$ direction for horns with small flare in the E-plane. The outward normal to part 5 is approximately in the $\hat{\alpha}$ direction for horns with small flare in the E-plane. The tangential $\bar{E} = 0$ over conduction surfaces 4 and 5. Therfore, there are negligible $-\hat{n}x\bar{E}$ current sheets over parts 4 and 5. Theoretically, however, there exist $\hat{n}x\bar{H}$ current sheets over parts 4 and 5. The exclusion of these current sheets from the Chernousov formulation was motivated by the following statement made by Jordan and Balmain (1968:495):

> If it can be assumed that the currents on the outside walls of an open-ended wave guide have negligible effect on the radiation from the guide, the problem of diffraction through an aperture has direct application ... . Since experimentally measured radiation patterns are found to agree roughly with patterns computed by neglecting these outside currents, such calculations may be used if only approximate answers are sufficient.

Thus, the $-\hat{n}x\bar{E}$ current sheets over parts 4 and 5 are undoubtedly small and negligible, while the $\hat{n}x\bar{H}$ current sheets were assumed to be negligible in the subsequent Chernousov analysis.

Finally, the small spherical sector, part 6, was neglected in the subsequent analysis.

From a physical vector potential viewpoint, the $\hat{n}x\bar{H}$ current sheets on the bottom surface of the upper wedge of the TEM horn and the top surface of the lower wedge of the TEM horn account totally for the radiation from the structure if currents on the outer surfaces of the wedges are neglected. This vector potential formulation is discussed in Chapter 3 by approximating the TEM horn shown in Figure 2.1 by a section of a biconical antenna. The same spherical TEM wave as discussed on the first page of this chapter is assumed to exist between

the two wedges, so that the assumed current distribution is self-consistent with the fields distribution. As a check, approximate closed form solutions for the electric far fields in the azimuth plane in the boresight and backfire directions are shown to be the same as for the aperture model.

Therefore, the closed surface S_a consisting of six parts has been approximated by three surfaces with radiating fields; namely parts 1, 2, and 3; and three surfaces with zero fields. The three radiating surfaces are the front aperture and two wedge-shaped side apertures of the TEM horn respectively.

It should be emphasized that a useful consequence of the equivalence theorem applied to the closed surface S_a, as pointed out by Schelkunoff and Friis (1952:516-520), is that the $\hat{n}x\bar{H}$ and $-\hat{n}x\bar{E}$ current sheets at the three apertures of the TEM horn radiate as though they were in free space. That is, they radiate as if the metal wedges were removed.

2.2 THE TRANSIENT ELECTRIC FAR FIELDS OF A SPERRY RAND TEM HORN

The Sperry Rand TEM horn shown in Figure 2.1 is assumed to be excited at its apex by a voltage V(t). The fields exciting the TEM horn are then the spherical wave described by equations (2-1) and (2-2). The Chernousov formulation, namely equation (B-1) on the first page of Appendix B, was then applied to the TEM horn considering both the front aperture and two wedge-shaped side apertures. The resulting theta and phi components of the electric far field are then given by

equations (B-89) and (B-90) in Section B.5 of Appendix B. Equations (B-89) and (B-90) describe the electric far fields of the TEM horn at an arbitrary observation point $P(\theta,\phi)$ in the far field.

Equations (B-89) and (B-90) were programmed in Fortran for execution on a digital computer. Two programs were written--one for gaussian excitation $V(t)$ at the apex, and another for error function excitation $V(t)$ at the apex. A complete description and listing of the computer program for gaussian excitation is given in Section D.1 of Appendix D. A complete description and listing of the computer program for error function excitation is given in Section D.2 of Appendix D.

Before applying the Chernousov formulation to the TEM horn, two other solutions were attempted. First, because of the similarity of the TEM horn to a section of a biconical antenna, the boundary value problem solution for sinusoidal excitation at the apex was attempted using methods paralleling those used by Schelkunoff (1952:35-49). Secondly, the time domain fields were formulated in terms of the current sheets flowing on the two metallic sectors for step function excitation at the apex using the geometry shown in Figure 2.1. Both of these attempts led to results which were intractable and gave no engineering insight into the behavior of the TEM horn.

Recently, however, the TEM horn was approximated by a section of a biconical antenna. Then, the current sheets flowing on the biconical section due to the spherical TEM wave described by equations (2-1) and (2-2) were determined. Subsequently, the vector potential

formulation in the time domain was used to determine the resultant electric far fields of the biconical section. This biconical formulation is discussed in Chapter 3. Approximate closed form results for the theta component of the electric far field in the azimuth plane are also determined in Chapter 3. The boresight and backfire closed form solutions are shown to be self-consistent with the closed form solutions found in the following section.

2.3 APPROXIMATE CLOSED FORM SOLUTIONS FOR THE ELECTRIC FAR FIELDS OF THE SPERRY RAND TEM HORN: THE ROLES OF THE FRONT APERTURE AND WEDGE-SHAPED SIDE APERTURES

Consider first the theta component of the electric far field due to the front aperture of a Sperry Rand TEM horn in the azimuth ($\theta = 90^{\circ}$) plane. The general expression for an arbitrary observation point $P(\theta,\phi)$ in the far field is given by equation (B-25) on the seventh page of Appendix B. In the azimuth plane, $\cos\theta = 0$. Therefore, the third and fourth terms of (B-25) are zero. Thus,

$$
\begin{aligned}
&rE_{\theta_{FRONT}}(\bar{r},t)\Big|_{\theta = 90^{\circ}} \\
&= \frac{r a}{4\pi v}\Bigg\{(1+k_v)\sin\phi \int_{-\beta_0}^{\beta_0}\int_{\alpha_0(\beta)}^{\pi-\alpha_0(\beta)} \sin\beta \sin\alpha f(\alpha,\beta) V_1' \, d\alpha \, d\beta \\
&+ (1+k_v)\cos\phi \int_{-\beta_0}^{\beta_0}\int_{\alpha_0(\beta)}^{\pi-\alpha_0(\beta)} \cos\beta \sin\alpha f(\alpha,\beta) V_1' \, d\alpha \, d\beta \\
&+ (1-k_v)\int_{-\beta_0}^{\beta_0}\int_{\alpha_0(\beta)}^{\pi-\alpha_0(\beta)} \sin^2\alpha f(\alpha,\beta) V_1' \, d\alpha \, d\beta \Bigg\}
\end{aligned}
\tag{2-5}
$$

In the azimuth plane, from equations (B-22) and (B-23) on the sixth and seventh pages of Appendix B,

$$V_1' = \frac{dV\left[T - \frac{r_a}{v} + \frac{r_a}{v}\sin\alpha\cos(\beta-\phi)\right]}{d\left[T - \frac{r_a}{v} + \frac{r_a}{v}\sin\alpha\cos(\beta-\phi)\right]} \qquad (2\text{-}6)$$

T is the retarded time given by $T = t - (r/v)$.

Consider the case when the front aperture is electrically small--that is, when $2r_a\beta_o/v$ and $r_a(\pi - 2\theta_o)/v$ are less than or comparable with the excitation waveform's characteristic time dimensions. The following approximations are then in order. 1) $\sin\alpha \approx 1$ and $\cos\beta \approx 1$. 2) For β_o small, V_1' is not strongly dependent on β and may be considered approximately as an even function of β. 3) $\cos\beta$ is an even function of β and $\sin\beta$ is an odd function of β. Therefore, the first term of (2-5) is small with respect to the second and third terms.

Then, the theta component of the radiation due to the front aperture may be approximated as

$$rE_{\theta_{FRONT}}(\vec{r},t)\Big|_{\theta = 90^\circ}$$

$$\approx \frac{r_a}{4\pi v}\left\{(1+k_v)\cos\phi\int_{0}^{\beta_o}\int_{\alpha_o(\beta)}^{\pi-\alpha_o(\beta)} f(\alpha,\beta)V_1'\,d\alpha\,d\beta \right.$$

$$\left. + (1-k_v)\int_{-\beta_o}^{0}\int_{\alpha_o(\beta)}^{\pi-\alpha_o(\beta)} f(\alpha,\beta)V_1'\,d\alpha\,d\beta\right\} \qquad (2\text{-}7)$$

The double integral is approximated as follows. For horns with small flare in the $\bar{E}$-plane, $f(\alpha,\beta) \simeq 1/(\pi - 2\theta_o)$. Using the mean value

theorem of the calculus,

$$\int_{-\beta_o}^{\beta_o}\int_{\alpha_o(\beta)}^{\pi-\alpha_o(\beta)} f(\alpha,\beta)V_1'\,d\alpha\,d\beta \approx \left[\frac{1}{\pi-2\theta_o}\right]2\beta_o(\pi-2\theta_o)V_1'(\hat{\beta}) \qquad (2\text{-}8)$$

where $\hat{\beta}$ is some angle between $-\beta_o$ and β_o.

The approximate closed form result for radiation from the front aperture in the azimuth plane is then

$$4\pi r E_{\theta_{FRONT}}(\bar{r},t)\Big|_{\theta = 90^o}$$

$$\approx \frac{2\Gamma_a\beta_o}{v}\left[(1+\cos\phi)-k_v(1-\cos\phi)\right]$$

$$\times\left\{V'\left[T-\frac{\Gamma_a}{v}\left(1-\cos(\hat{\beta}-\phi)\right)\right]\right\} \qquad (2\text{-}9)$$

An electrically small front aperture thus radiates an electric far field which is the time derivative of the excitation V(t) applied to the apex of the TEM horn.

Define

$$4\pi r E_{\theta_{FRONT}}(\bar{r},t)\Big|_{\theta = 90^o} \triangleq \tilde{V}_{FRONT} \qquad * \quad (2\text{-}10)$$

and suppose that β_o is small enough so that $\cos(\hat{\beta}-\phi)\approx\cos\phi$. For the boresight ($\phi = 0^o$) direction,

$$\tilde{V}_{FRONT}\Big|\phi = 0^o \approx \frac{4\Gamma_a\beta_o}{v}V'[T] \qquad (2\text{-}11)$$

For the $\phi = 90^o$ direction, edge on to the front aperture,

---

* $\tilde{V}_{(\ )}$ is defined as $4\pi r E_{(\ )}$.

$$\tilde{v}_{FRONT}\Big|_{\phi = 90^\circ} \approx \frac{2r_a\beta_o(1-k_v)}{v} V'\left[T - \frac{r_a}{v}\right] \qquad (2\text{-}12)$$

For the backfire ($\phi = 180^\circ$) direction,

$$\tilde{v}_{FRONT}\Big|_{\phi = 180^\circ} \approx \frac{-4r_a\beta_o k_v}{v} V'\left[T - \frac{2r_a}{v}\right] \qquad (2\text{-}13)$$

Therefore, the time delay of the derivative radiation progresses from T to T - ($2r_a/v$) when changing from the boresight to backfire direction. Also, the ratio of the maximum amplitude of the backfire radiation to the maximum amplitude of the boresight radiation is $-k_v$.

Consider now the theta component of the electric far field due to the wedge-shaped side apertures of a Sperry Rand TEM horn in the azimuth ($\theta = 90^\circ$) plane. The general expression for an arbitrary point P(θ,ϕ) in the far field is the sum of equations (B-42) and (B-56) on the eleventh and fourteenth pages of Appendix B respectively. Assuming that the front aperture is electrically small, $\sin\alpha \approx 1$ and $f(\alpha, \beta_o) \simeq 1/(\pi - 2\theta_o)$. Thus,

$$rE_{\theta_{WEDGES}}(\bar{r},t)\Big|_{\theta = 90^\circ}$$

$$\approx \frac{\sin(\phi-\beta_o)}{4\pi v}\int_{0}^{\pi-\alpha_o}\int_{0}^{r_a}\frac{V_2'}{\pi-2\theta_o}\,dr'd\alpha$$

$$- \frac{\sin(\phi+\beta_o)}{4\pi v}\int_{\alpha_o}^{\pi-\alpha_o}\int_{0}^{r_a}\frac{V_3'}{\pi-2\theta_o}\,dr'd\alpha \qquad (2\text{-}14)$$

In the azimuth plane, from equations (B-39) and (B-40) on the eleventh page of Appendix B,

$$V_2' \approx \frac{dV\left[T - \frac{r'}{v} + \frac{r'}{v}\cos(\phi - \beta_o)\right]}{d\left[T - \frac{r'}{v} + \frac{r'}{v}\cos(\phi - \beta_o)\right]} + k_V \frac{dV\left[T + \frac{r'}{v} - \frac{2r_a}{v} + \frac{r'}{v}\cos(\phi - \beta_o)\right]}{d\left[T + \frac{r'}{v} - \frac{2r_a}{v} + \frac{r'}{v}\cos(\phi - \beta_o)\right]} \quad (2\text{-}15)$$

Also, in the azimuth plane, from equations (B-52) and (B-53) on the fourteenth page of Appendix B,

$$V_3' \approx \frac{dV\left[T - \frac{r'}{v} + \frac{r'}{v}\cos(\phi + \beta_o)\right]}{d\left[T - \frac{r'}{v} + \frac{r'}{v}\cos(\phi + \beta_o)\right]} + k_V \frac{dV\left[T + \frac{r'}{v} - \frac{2r_a}{v} + \frac{r'}{v}\cos(\phi + \beta_o)\right]}{d\left[T + \frac{r'}{v} - \frac{2r_a}{v} + \frac{r'}{v}\cos(\phi + \beta_o)\right]} \quad (2\text{-}16)$$

T is the retarded time given by $T = t - (r/v)$. Since the front aperture was assumed to be small, $\pi - 2\alpha_o \approx \pi - 2\theta_o$. Therefore,

$$\int_{\alpha_o}^{\pi-\alpha_o}\int_0^{r_a} \frac{V_2' dr' d\alpha}{\pi - 2\theta_o} \approx \int_0^{r_a} V_2' dr' \quad (2\text{-}17)$$

Utilizing the substitutions

$$\xi_1 = T - \frac{r'}{v} + \frac{r'}{v}\cos(\phi - \beta_o) \quad (2\text{-}18)$$

and

$$\xi_2 = T + \frac{r'}{v} - \frac{2r_a}{v} + \frac{r'}{v}\cos(\phi - \beta_o), \quad (2\text{-}19)$$

$$\int_0^{r_a} V_2' dr' = \frac{v}{1 - \cos(\phi - \beta_o)}\left\{V[T] - V\left[T - \frac{r_a}{v}\left(1 - \cos(\phi - \beta_o)\right)\right]\right\}$$

$$+\frac{k_V\, v}{1+\cos(\phi-\beta_o)}\left\{V\left[T-\frac{r_a}{v}\left(1-\cos(\phi-\beta_o)\right)\right]-V\left[T-\frac{2r_a}{v}\right]\right\} \quad (2\text{-}20)$$

The second term of equation (2-14) is the same as the first term with $-\sin(\phi + \beta_o)$ replacing $\sin(\phi - \beta_o)$ and $\cos(\phi + \beta_o)$ replacing $\cos(\phi - \beta_o)$. The approximate closed form result for radiation from the wedge-shaped side apertures in the azimuth plane is then

$$4\pi r E_{\theta_{WEDGES}}(\bar{r},t)\Big|_{\theta = 90^o}$$

$$\approx\left[\frac{\sin(\phi-\beta_o)}{1-\cos(\phi-\beta_o)}-\frac{\sin(\phi+\beta_o)}{1-\cos(\phi+\beta_o)}\right]V[T]$$

$$-\left\{\frac{\sin(\phi-\beta_o)}{1-\cos(\phi-\beta_o)}V\left[T-\frac{r_a}{v}\left(1-\cos(\phi-\beta_o)\right)\right]\right.$$

$$\left.-\frac{\sin(\phi+\beta_o)}{1-\cos(\phi+\beta_o)}V\left[T-\frac{r_a}{v}\left(1-\cos(\phi+\beta_o)\right)\right]\right\}$$

$$+k_V\left\{\frac{\sin(\phi-\beta_o)}{1+\cos(\phi-\beta_o)}V\left[T-\frac{r_a}{v}\left(1-\cos(\phi-\beta_o)\right)\right]\right.$$

$$\left.-\frac{\sin(\phi+\beta_o)}{1+\cos(\phi+\beta_o)}V\left[T-\frac{r_a}{v}\left(1-\cos(\phi+\beta_o)\right)\right]\right\}$$

$$-k_V\left[\frac{\sin(\phi-\beta_o)}{1+\cos(\phi-\beta_o)}-\frac{\sin(\phi+\beta_o)}{1+\cos(\phi+\beta_o)}\right]V\left[T-\frac{2r_a}{v}\right] \quad (2\text{-}21)$$

Equation (2-21) might appear at first to be rather involved. However, great simplification of (2-21) is possible in the boresight and backfire directions, and in directions well removed from boresight and backfire.

Consider first the boresight ($\phi = 0^\circ$) direction. Define

$$4\pi r E_{\theta_{WEDGES}}(\bar{r},t)\Big|_{\theta = 90^\circ} \triangleq \tilde{V}_{WEDGES} \tag{2-22}$$

Then

$$\tilde{V}_{WEDGES}\Big|_{\phi = 0^\circ}$$

$$\approx -\frac{2\sin\beta_o}{1-\cos\beta_o}\left\{V\left[T\right]-V\left[T-\frac{r_a}{v}\left(1-\cos\beta_o\right)\right]\right\}$$

$$-\frac{2k_v\sin\beta_o}{1+\cos\beta_o}\left\{V\left[T-\frac{r_a}{v}\left(1-\cos\beta_o\right)\right]-V\left[T-\frac{2r_a}{v}\right]\right\} \tag{2-23}$$

For β_o small, the first and second terms in (2-23) may be combined to form an approximate derivative as follows.

$$\frac{V\left[T\right]-V\left[T-\frac{r_a}{v}(1-\cos\beta_o)\right]}{\frac{r_a}{v}(1-\cos\beta_o)} \triangleq \frac{V\left[T\right]-V\left[T-\epsilon\right]}{\epsilon} \approx V'\left[T\right] \tag{2-24}$$

Therefore, (2-23) may be written as

$$\tilde{V}_{WEDGES}\Big|_{\phi = 0^\circ} \approx -\frac{2r_a\beta_o}{v}V'\left[T\right]$$

$$-k_v\beta_o\left\{V\left[T-\frac{r_a}{v}\left(1-\cos\beta_o\right)\right]-V\left[T-\frac{2r_a}{v}\right]\right\} \tag{2-25}$$

Therefore, in the boresight direction, the wedge-shaped side apertures contribute two forms of radiation. The first term of (2-25) is a negative derivative of the excitation, whose magnitude is half

the magnitude of the positive derivative radiation of the front aperture. Thus, the wedges reduce the amplitude of the radiation from the front aperture by a factor of two. The second and third terms of (2-25) account for the backward radiation due to the reflected waves travelling along the wedges from the front aperture back toward the apex. This backward radiation consists of delayed replicas of the excitation.

For the sake of completeness, the approximate theta component of the radiation from the TEM horn in the boresight direction is

$$E_{\theta_{BORESIGHT}}(\bar{r},t) \approx \frac{r_a \beta_o V'[T]}{2\pi v r} - \frac{k_v \beta_o}{4\pi r}\left\{V\left[T - \frac{r_a}{v}(1-\cos\beta_o)\right] - V\left[T - \frac{2r_a}{v}\right]\right\} \quad (2\text{-}26)$$

Consider next the contribution from the wedges in the backfire ($\phi = 180^\circ$) direction. From (2-21) and (2-22),

$$\tilde{V}_{WEDGES}\Big|\phi = 180^\circ \approx \frac{2\sin\beta_o}{1+\cos\beta_o}\left\{V[T] - V\left[T - \frac{r_a}{v}(1+\cos\beta_o)\right]\right\} + \frac{2k_v \sin\beta_o}{1-\cos\beta_o}\left\{V\left[T - \frac{r_a}{v}(1+\cos\beta_o)\right] - V\left[T - \frac{2r_a}{v}\right]\right\} \quad (2\text{-}27)$$

For β_o small, the third and fourth terms of (2-27) may be combined to form an approximate derivative as follows.

$$\frac{V\left[T - \frac{r_a}{v}(1+\cos\beta_o)\right] - V\left[T - \frac{2r_a}{v}\right]}{\frac{r_a}{v}(1-\cos\beta_o)}$$

$$\underline{\Delta}\ \frac{V\left[T-\frac{2r_a}{v}+\epsilon\right]-V\left[T-\frac{2r_a}{v}\right]}{\epsilon}\approx V'\left[T-\frac{2r_a}{v}\right] \quad (2\text{-}28)$$

Therefore, (2-27) may be written as

$$\tilde{V}_{WEDGES}\Big|_{\phi = 180^\circ}$$

$$\approx \beta_o\left\{V[T]-V\left[T-\frac{r_a}{v}(1+\cos\beta_o)\right]\right\}$$

$$+\frac{2k_v r_a \beta_o}{v}V'\left[T-\frac{2r_a}{v}\right] \quad (2\text{-}29)$$

Thus, in the backfire direction, the wedges again contribute two forms of radiation. The first and second terms of (2-29) account for the forward radiation due to waves traveling along the wedges from the apex toward the front aperture. This forward radiation consists of delayed replicas of the excitation. The third term of (2-29) is a positive derivative radiation, whose magnitude is half the magnitude of the negative derivative radiation from the front aperture. The total radiation of the TEM horn in the backfire direction is the sum of (2-13) and (2-29).

In directions well removed from boresight and backfire (ϕ neither near 0° nor near 180°), equation (2-21) may be greatly simplified by considering β_o small and approximating $1 \pm \cos(\phi - \beta_o) \approx 1 \pm \cos\phi$ and $1 \pm \cos(\phi + \beta_o) \approx 1 \pm \cos\phi$. Then, using standard triginometric identities,

$$\tilde{V}_{WEDGES}\Big|_{\substack{\phi \not\approx 0^\circ \\ \phi \not\approx 180^\circ}} \approx \frac{2\beta_o}{1-\cos\phi}\left\{V[T]-V\left[T-\frac{r_a}{v}(1-\cos\phi)\right]\right\}$$

$$-\frac{2k_v\beta_o}{1+\cos\phi}\left\{V\left[T-\frac{r_a}{v}(1-\cos\phi)\right]-V\left[T-\frac{2r_a}{v}\right]\right\} \qquad (2\text{-}30)$$

In directions well removed from the boresight and backfire directions, the wedges radiate a series of delayed replicas of the excitation. The amplitudes and time occurrences of the replicas depend upon the observation point in question. The total radiation of the TEM horn in directions away from boresight and backfire is the sum of (2-9) and (2-30).

2.4 THEORETICAL AND EXPERIMENTAL RESULTS FOR SPERRY RAND TEM HORNS

Susman and Lamensdorf (1970:42-44) studied three different TEM horns in the receive mode using an incident electric field which was a gaussian pulse. All three horns had h = 2" and r_a = 24". The wedge angles of the three horns were ϕ_o = 2.5°, 30°, and 90° respectively. Due to the time domain consequences of the Carson-Rayleigh Reciprocity Theorem (Schmitt, 1960:293), the voltage V(t) received at the apex of the TEM horn will be of the same form as the radiated fields if the TEM horn is excited at its apex by the time integral of V(t). Therefore, to compare the experimental receive mode results with the theoretical formulation using the Chernousov approach, the TEM horns were excited at the apex by the unit error function*

$$V(t)=\frac{1}{\tau\sqrt{\pi}}\int_{-\infty}^{t} e^{-\left(\frac{\xi}{\tau}\right)^2}d\xi \qquad (2\text{-}31)$$

Equations (B-89) and (B-90) in Section B.5 of Appendix B were

* The integral of gaussian function = error function.

then programmed in Fortran for execution on a digital computer using the unit error function excitation. Since Susman and Lamensdorf (1970) did not perform time domain reflectometry measurements to determine the voltage reflection coefficient, k_v, the effective terminating impedance of the front aperture was determined numerically as follows. First, the characteristic impedance of the particular horn in question was read from Susman and Lamensdorf (1970:29), which are experimentally measured characteristic impedance curves. Then, the effective terminating impedance of the front aperture, Z_{eff}, was varied until the ratio of the maximum amplitude of the boresight response to the maximum amplitude of the backfire response was the same theoretically and experimentally. Also, because only relative amplitudes were measured experimentally, the maximum amplitude of the theoretical boresight response was made the same as the maximum amplitude of the experimental boresight response.

The theoretical and experimental results are shown in Figures 2.3, 2.4, and 2.5. In general, these figures show reasonable agreement between theory and experiment. (Note-- the time retardation between the maximum boresight response and the maximum negative backfire response is due to the fact that the horns were rotated about the center of the two wedges rather than about the apex for the receive mode measurements.)

In Figure 2.3, the theoretical results show spikes on the fields at $\phi = 60^{\circ}$, 90°, and 120°. This effect is due to the theoretical superposition of the time derivative radiation from the front

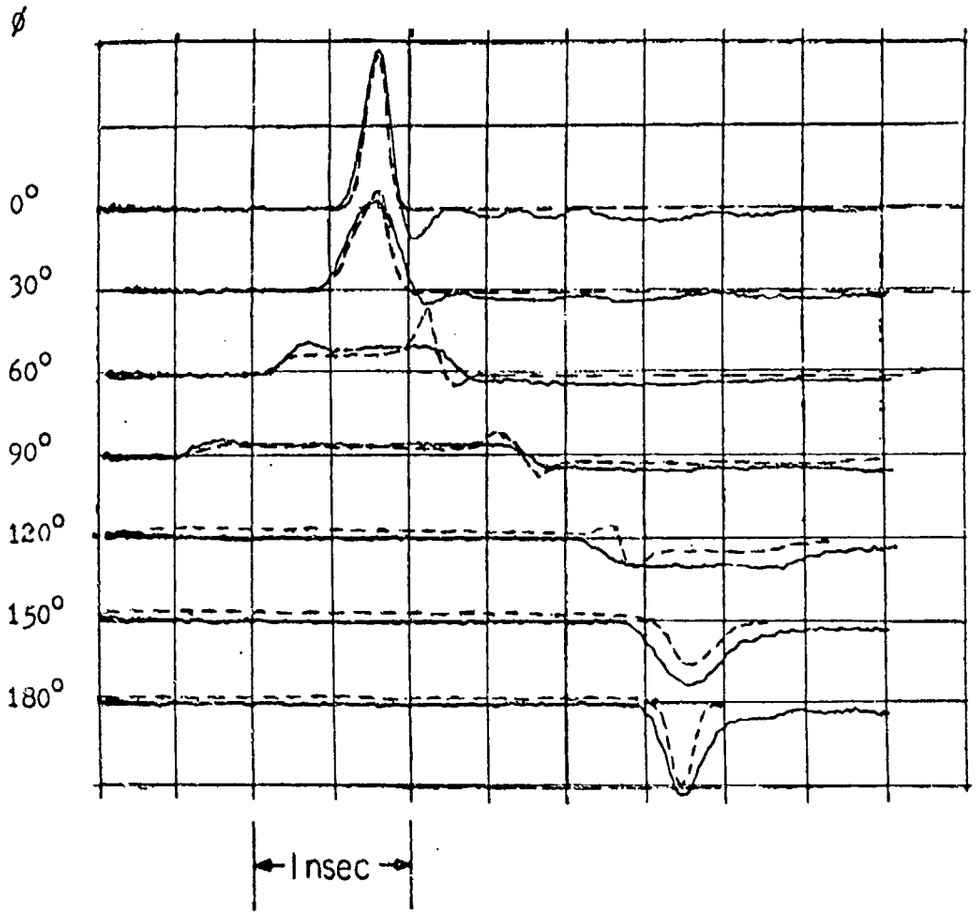

—— Experimental Results (Susman and Lamensdorf, 1970:42)
----- Theoretical Results from Chernousov Formulation and Computer Runs

$\phi_o = 2.5^o$, $h = 2"$, $r_a = 24"$

Figure 2.3

Azimuth Plane $rE_\theta(\bar{r},t)$ for the
First Sperry Rand TEM Horn

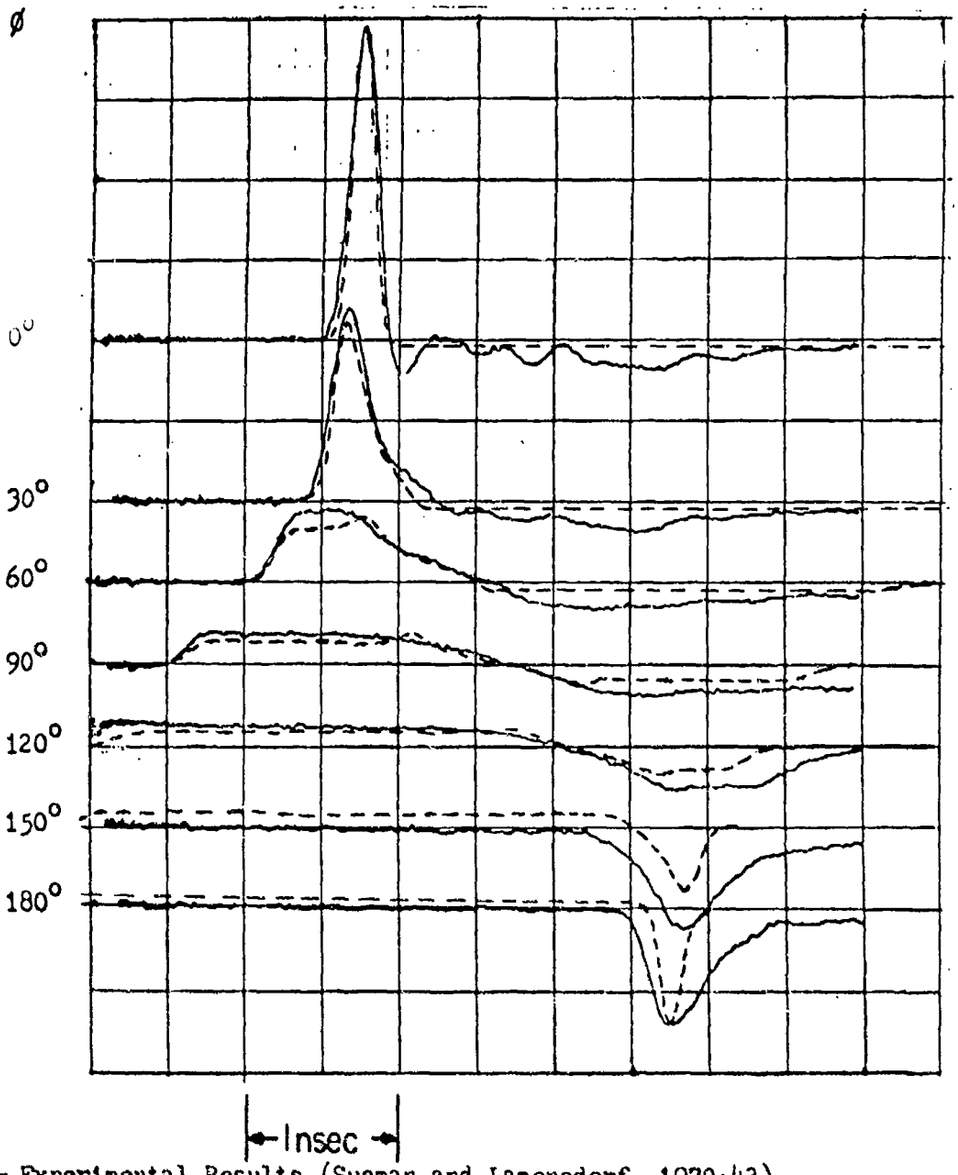

——— Experimental Results (Susman and Lamensdorf, 1970:43)
----- Theoretical Results from Chernousov Formulation and Computer Runs

$\phi_o = 30^o$, $h = 2"$, $r_a = 24"$

Figure 2.4

Azimuth Plane $rE_\theta(\bar{r},t)$ for the
Second Sperry Band TEM Horn

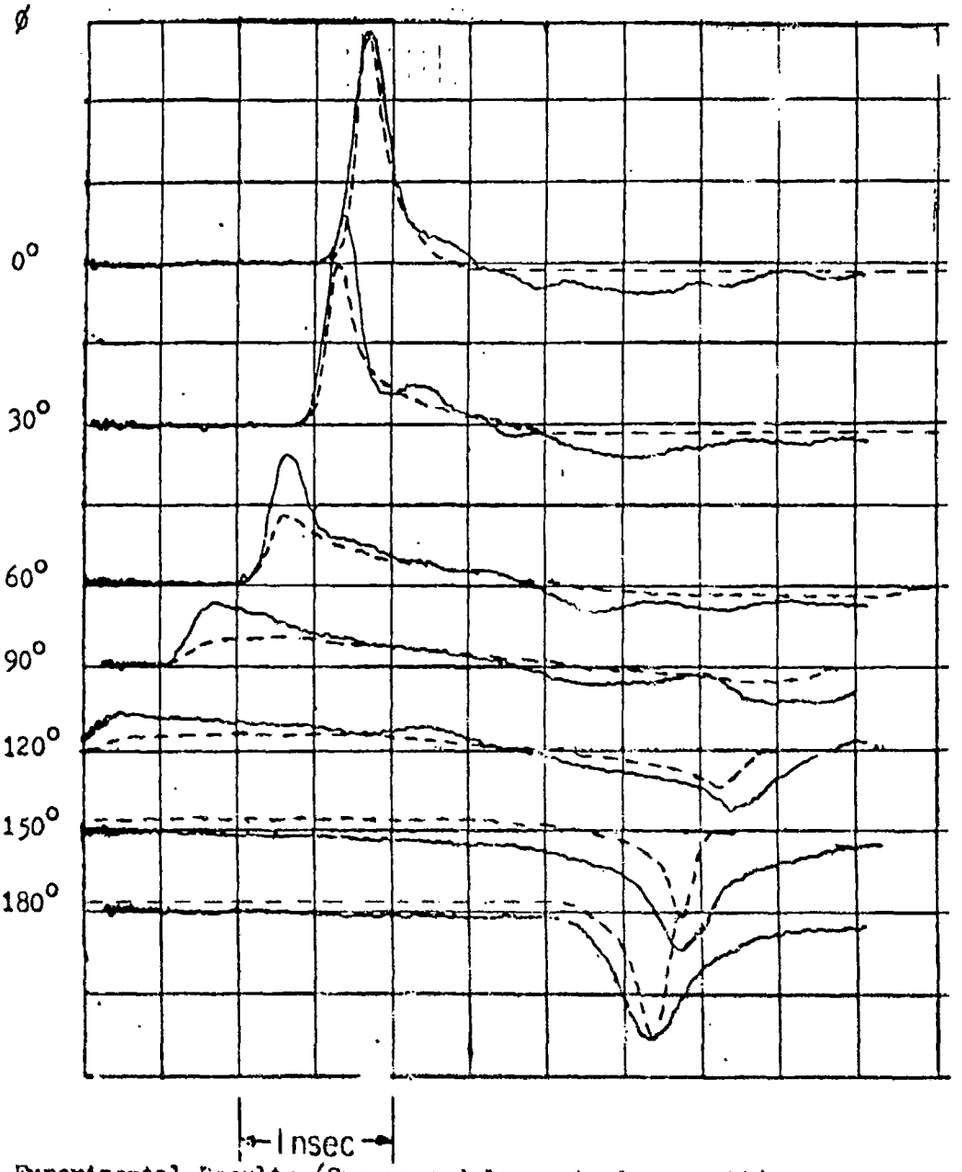

—— Experimental Results (Susman and Lamensdorf, 1970,44)
----- Theoretical Results from Chernousov Formulation and Computer Runs

$\phi_o = 90^\circ$, $h = 2''$, $r_a = 24''$

Figure 2.5

Azimuth Plane $rE_\theta(\bar{r},t)$ for the
Third Sperry Rand TEM Horn

aperture as given approximately by equation (2-9) upon the delayed replica radiation from the side wedges as given approximately by equation (2-30). This phenomenon, which does not occur when using a theoretical current sheet approach, as discussed in Chapter 3, is felt to be due to the approximation of the horn as a set of three distinct apertures. This highlights the separate derivative contribution of the front aperture, whereas the current model constitutes a single radiating system. The spike phenomenon does not occur in directions at or near boresight, which is the important direction for the paraboloid/horn system. In addition, the spike phenomenon does not occur for the larger ($\phi_o = 30^\circ$ and $\phi_o = 90^\circ$) horns.

Also, there are differences in the dc levels of the theoretical and experimental results for ϕ between 120° and 180°. This effect is believed to be due to the fact that Susman and Lamensdorf (1970) established the experimental zero level in these directions to be the amplitude of the positive delayed replica response when this amplitude was small and not noticeable experimentally.

Finally, for ϕ between 90° and 180°, the experimental responses are smeared in time with respect to the theoretically computed responses. This effect has not been explained theoretically.

2.5 APPROXIMATION OF THE EIGHT-INCH TEM HORN BY A SPERRY RAND TEM HORN

The eight-inch TEM horn studied by Martins et al. (1973) is shown in Figure 2.6. This horn is very similar to the Sperry Rand TEM horns except that the front aperture is rectangular rather than being

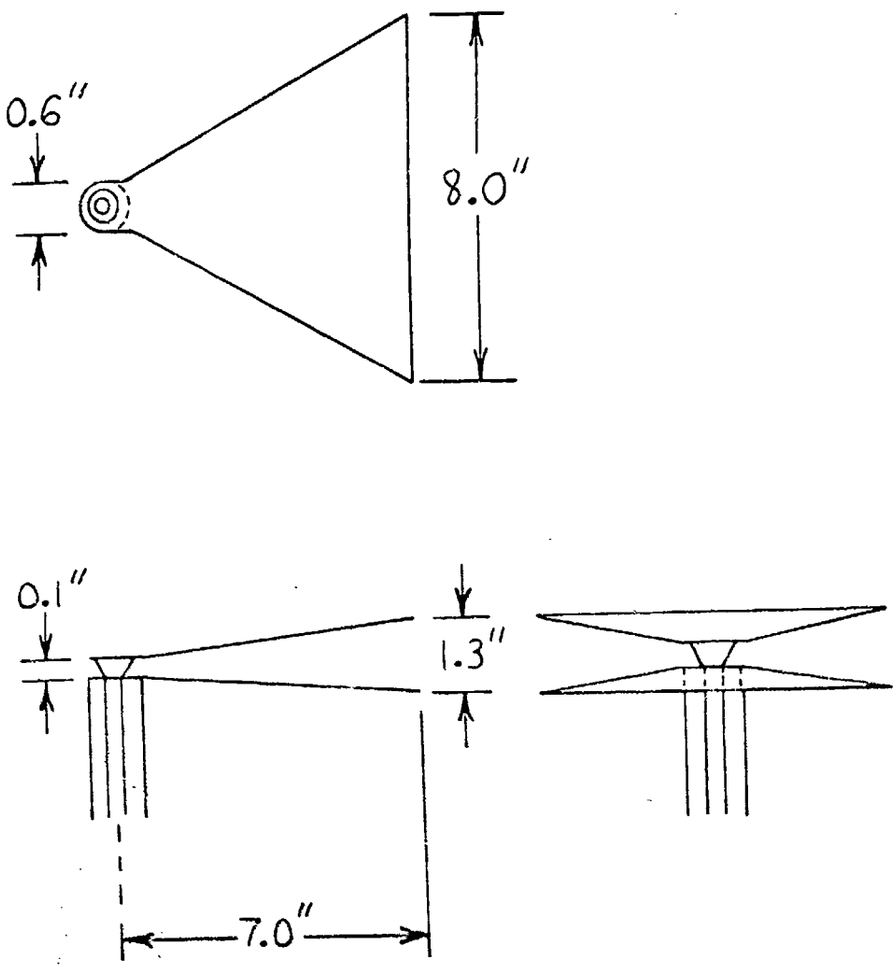

Figure 2.6

The Eight-Inch TEM Horn Antenna

a spherical sector located at $r' = r_a$. However, this difference does not greatly affect the basic characteristics of the electric far fields.

Therefore, the eight-inch TEM horn was approximated by a Sperry Rand TEM horn with the following parameters: $\phi_o = 59^o$, $h = 0.65"$, and $r_a = 7.3"$.

2.6 THEORETICAL AND EXPERIMENTAL RESULTS FOR THE EIGHT-INCH TEM HORN

Equations (B-89) and (B-90) in Section B.5 of Appendix B were programmed in Fortran for execution on a digital computer using unit amplitude gaussian excitation at the apex. The gaussian excitation is described by

$$V(t) = e^{-\left(\frac{t}{\tau}\right)^2} \qquad (2\text{-}32)$$

The parameters stated in Section 2.5 above were used. Martins et al. (1973:147) used time domain reflectometry to measure the characteristic impedance Z_o and voltage reflection coefficient k_v of the eight-inch TEM horn. The effective terminating impedance Z_{eff} was computed from Z_o and k_v. They obtained $Z_o = 50$ ohms, $k_v = 0.7$, and $Z_{eff} = 283$ ohms. These parameters were used in the input for the theoretical numerical computations.

Martins et al. (1973) studied the eight-inch TEM horn experimentally in the transmit mode using a short asymmetric stub sensor. The stub sensor's terminal voltage is an approximate replica of the incident electric field (Stekert and Fitzgerald, 1973).

The theoretical and experimental results are shown in Figures 2.7, 2.8, and 2.9. The experimental results were scaled so that the

BDM 8-INCH TEM HORN--BORESIGHT

-----Experimental Results (Martins et al., 1973:234)
———Theoretical Results from Chernousov Formulation and Computer Runs

$T' = t - (r/v)$

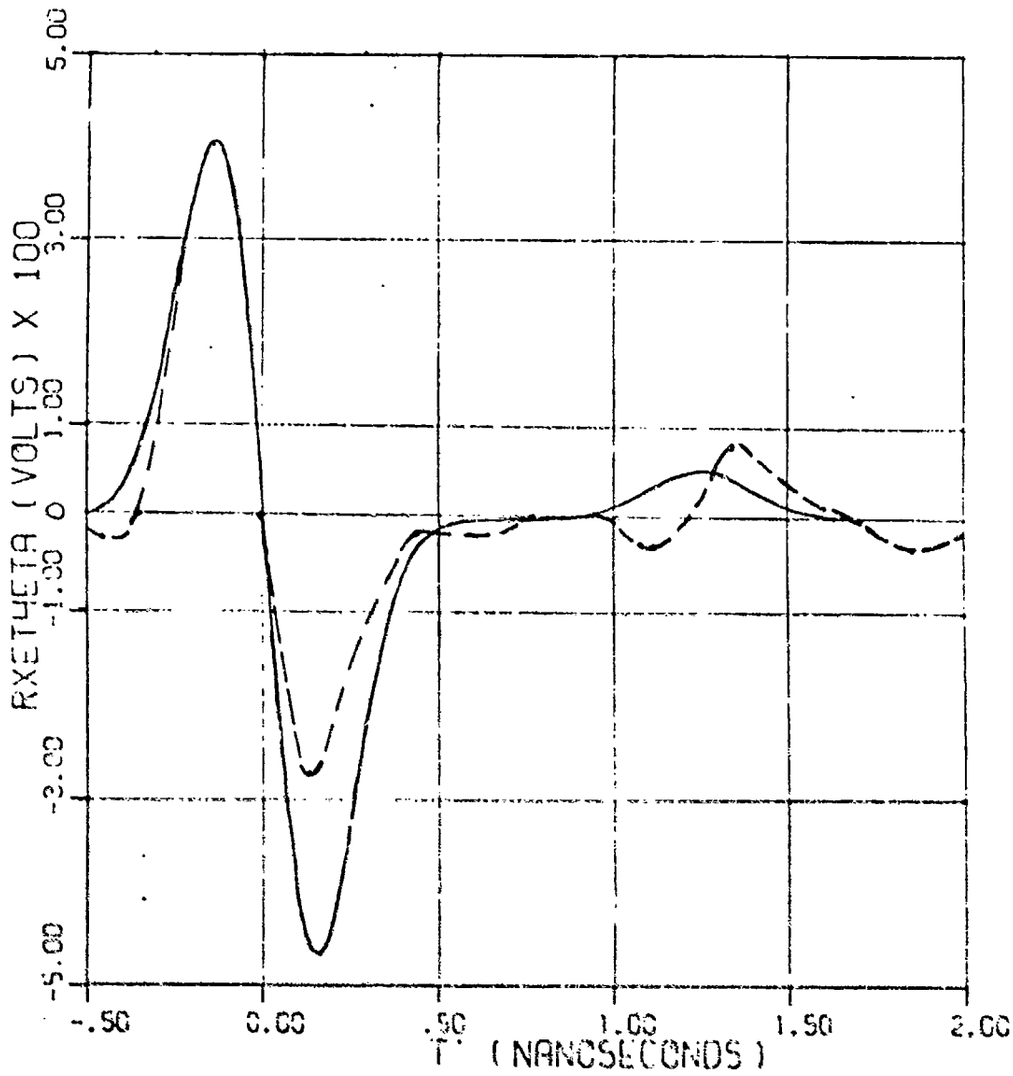

Figure 2.7

Boresight $rE_\theta(\bar{r},t)$ for the Eight-Inch TEM Horn

BDM 8-INCH TEM HORN--50 DEGREES AZIMUTH

-----Experimental Results (Martins et al., 1973:234)
———Theoretical Results from Chernousov Formulation and Computer Runs

$T' = t - (r/v)$

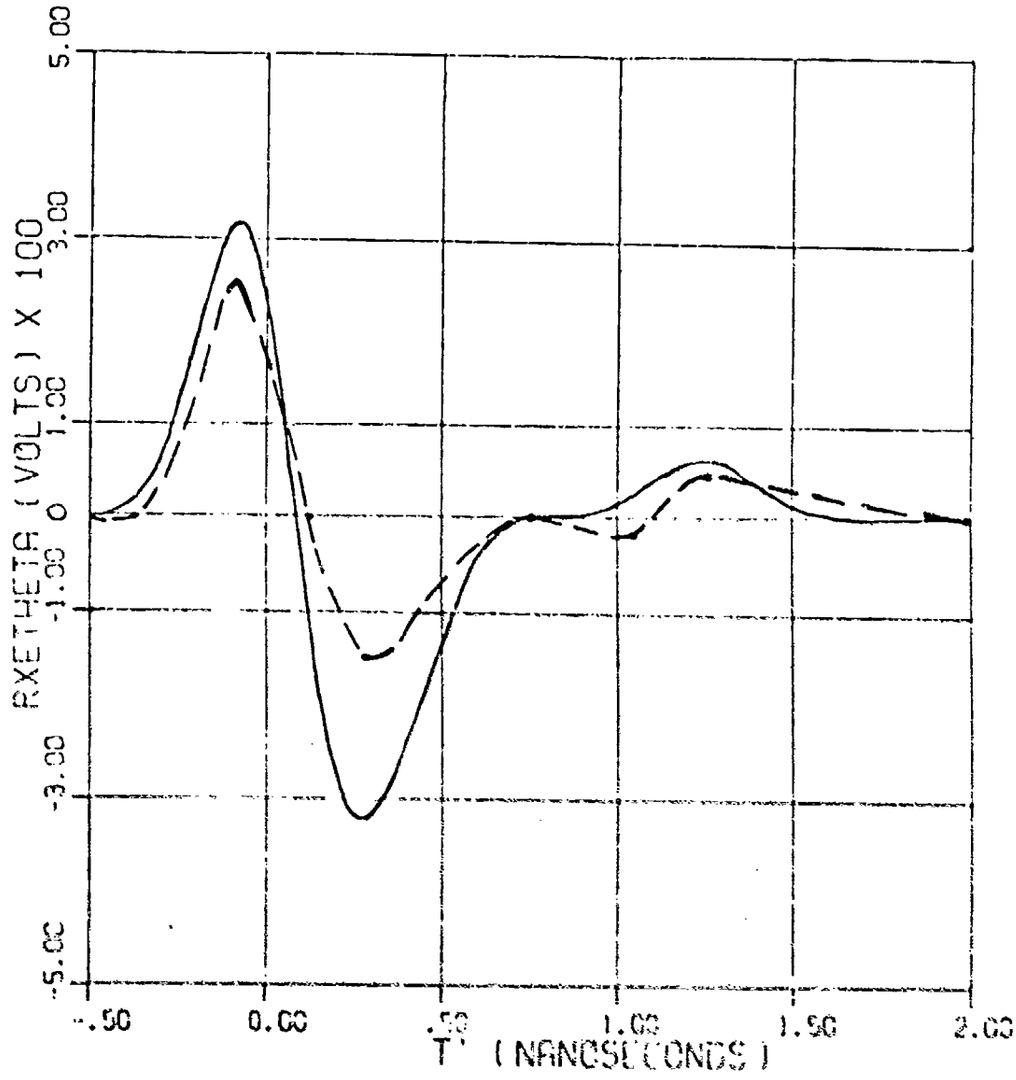

Figure 2.8

$rE_\theta(\bar{r},t)$ at $\phi = 50^\circ$ for the Eight-Inch TEM Horn

BDM 8-INCH TEM HORN--100 DEGREES AZIMUTH

-----Experimental Results (Martins et al., 1973:234)
———Theoretical Results from Chernousov Formulation and Computer Runs

$T' = t - (r/v)$

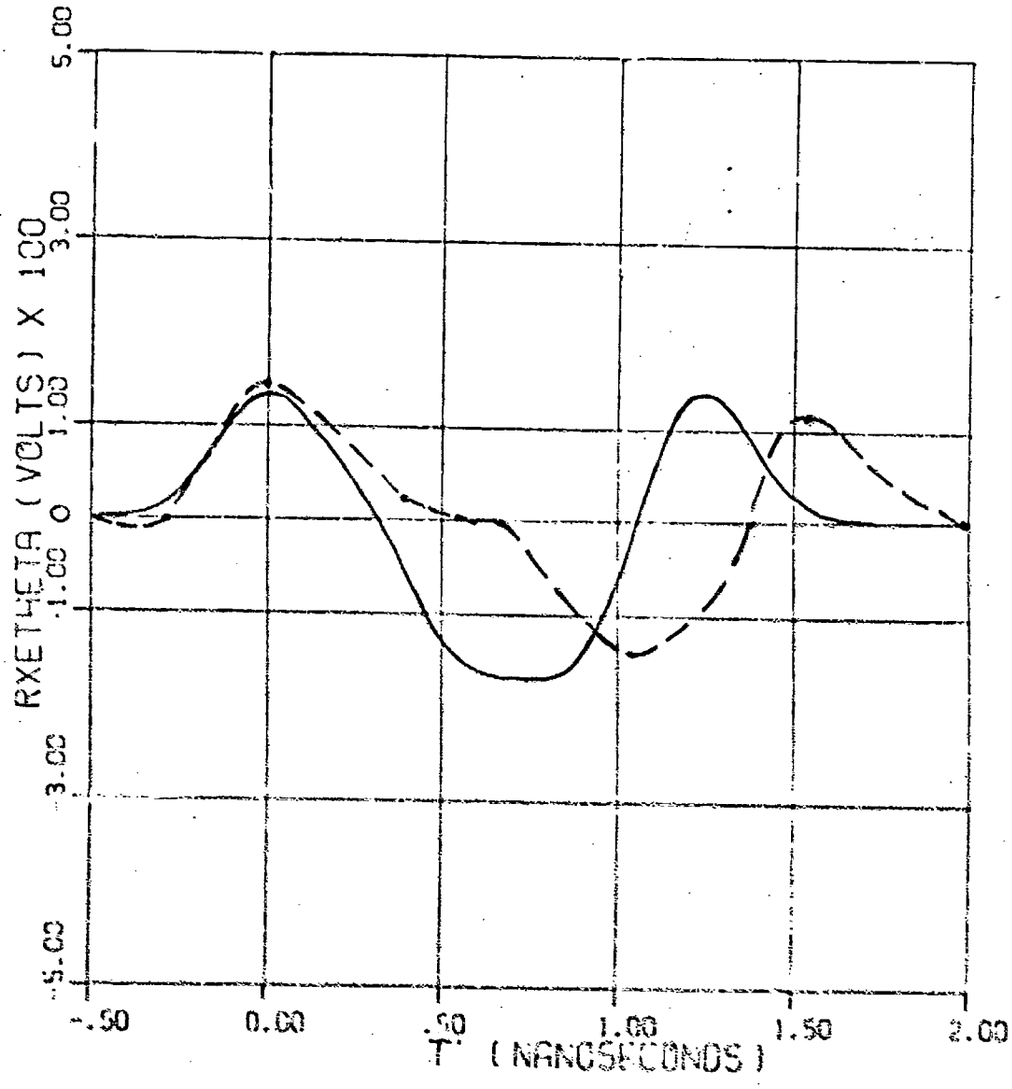

Figure 2.9

$rE_\theta(\bar{r},t)$ at $\phi = 100^\circ$ for the Eight-Inch TEM Horn

maximum amplitude of the boresight response was the same theoretically and experimentally. A discussion of the absolute amplitude of the experimental results is reserved for Chapter 6. Note--in the theoretical numerical computations, $f(\alpha,\beta)$ was normalized to unity for convenience. However, for TEM horns with small flare in the E-plane, the actual value of $f(\alpha,\beta) \simeq 1/(\pi - 2\theta_o)$. Therefore, for the eight-inch TEM horn, $f(\alpha,\beta) \simeq 1/(\sin^{-1}(2h/r_a)) = 5.62$. Therefore, all theoretical and experimental amplitudes shown in Figures 2.7, 2.8, and 2.9 should be multiplied by 5.62.

Consider first the results for the boresight direction shown in Figure 2.7. The theoretical boresight response consists of an approximately symmetric derivative of the exciting gaussian pulse followed by a positive replica of the exciting pulse retarded by the round trip time from the apex. The experimental boresight response is a derivative-type radiation of the exciting gaussian pulse followed by a more complicated series of replicas approximately delayed by the round trip time from the apex. The asymmetry in the experimental derivative response is believed to be due to the rectangular front aperture. That is--the outward propagating spherical wave between the two conducting wedges does not reach the entire front aperture at the same instant in time. The outward propagating wave reaches the center of the front aperture of the eight-inch TEM horn first, and starts to be reflected from this point. As the outward propagating wave progresses, it reaches points symmetrically located on each side of the center of the front aperture until the time when it reaches the edges of the front aperture. Therefore, the experimental positive

part of the gaussian-derivative radiation is somewhat time compressed with respect to the negative part of the gaussian-derivative radiation. This implies that the experimentally measured negative part of the gaussian-derivative radiation is reduced in amplitude and smeared in time with respect to the positive part. This effect is demonstrated in Figures 2.7 and 2.8. The negative going experimental pulses near the round trip time from the apex of the eight-inch TEM horn in the boresight direction appear to be due to the finiteness of the gap at the apex,* which was neglected in the theoretical analysis. Also, as confirmed in a telephone conversation with Martins, some of the scales shown in Martins et al. (1973:234) are incorrect. Figures 55-b and 55-c should have Horizontal = 500 ps/cm. Figure 55-c should have Vertical = 100 mv/cm. Figure 2.9 shows the electric far field of the TEM horn at $\phi = 100^{\circ}$. This is a series of delayed replicas of the gaussian excitation, which is confirmed both theoretically and experimentally. Around the retarded time $T' = t - (r/v) = 0.50$ nanoseconds, the experimental results show a rather flat response which lasts about 300 picoseconds. Therefore, the theoretically computed second and third delayed replicas are displaced in time from the experimentally determined responses by about 300 picoseconds. The reason for the experimentally flat response about $T' = 0.50$ nanoseconds has not been resolved.* Figure 2.10 shows the theoretical relative amplitudes of the theta component of the electric far field at various angular directions in the azimuth plane.

---

* This statement was obtained during a personal conversation with Vasco C. Martins of Martins et al. (1973) at the Rome Air Development Center, Rome, N. Y. on April 2, 1974.

BDM 8-INCH TEM HORN--AZIMUTH RXETHETA

———Theoretical Results from Chernousov Formulation and Computer Runs

$T' = t - (r/v)$

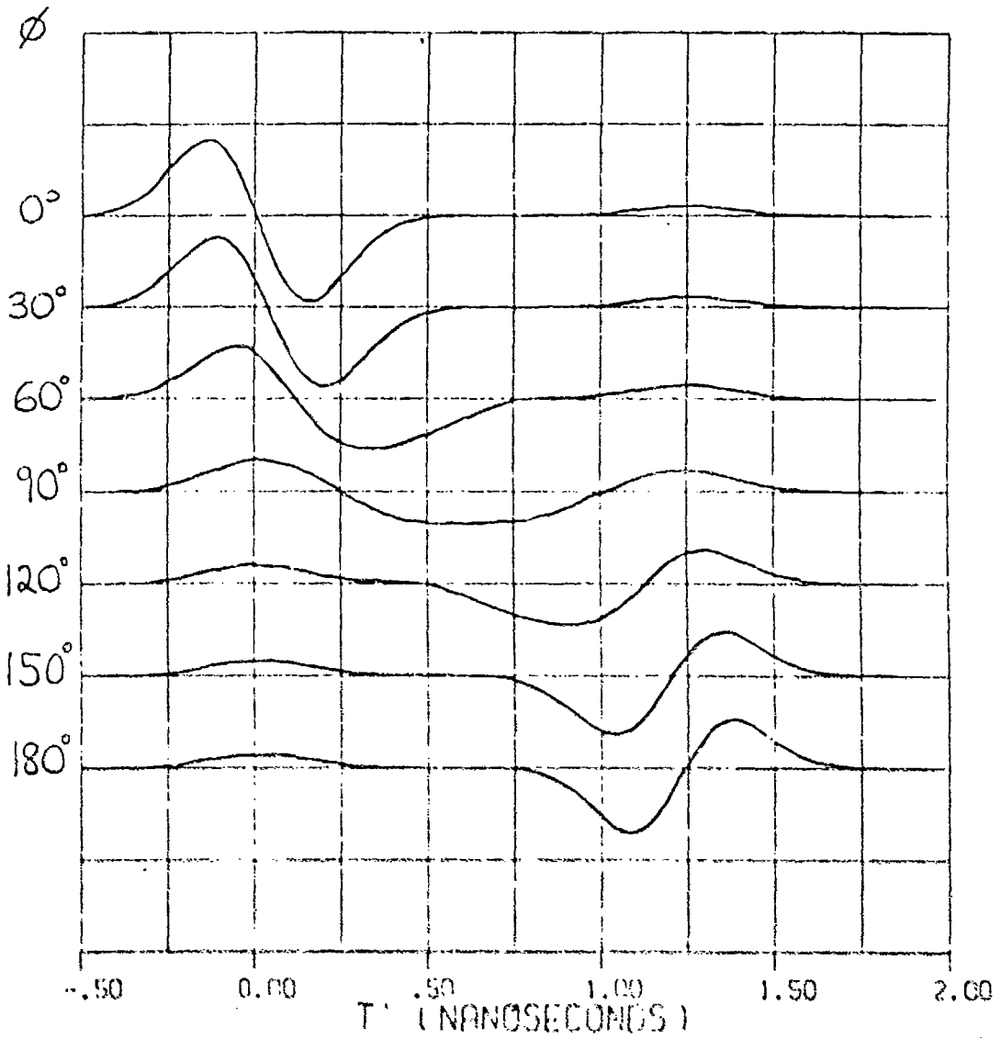

Figure 2.10

Azimuth Plane $rE_\theta(\bar{r},t)$ for the Eight-Inch TEM Horn

Chapter 3

THE TRANSIENT ELECTRIC FAR FIELDS OF AN APPROXIMATE TEM HORN-- A BICONICAL SECTION

3.1 INTRODUCTION

The approximate TEM horn model is two perfectly conducting surfaces which form a section of a biconical antenna. This model is shown in Figure 3.1. The surfaces extend from $r' = 0^+$ to $r' = r_a$ and from $\beta = -\beta_o$ to $\beta = \beta_o$. The surfaces are located at $\alpha = \theta_o$ and $\alpha = \pi - \theta_o$ respectively. When the TEM horn has small flare in the E-plane, that is--when θ_o is on the order of 90^o, the biconical section model is very similar to the Sperry Rand TEM horn or the eight-inch TEM horn studied by Martins et al. (1973).

The electric far fields are found directly from the current sheets $\bar{J}_s$ which flow on the two perfectly conducting surfaces. Approximate closed form solutions for the theta component of the electric far field in the azimuth ($\theta = 90^o$) plane are also found.

3.2 DERIVATION OF THE ELECTRIC FAR FIELDS FROM THE VECTOR POTENTIAL

The fundamental equations used in the derivation are

$$\bar{A}(\bar{r},t) = \frac{\mu}{4\pi}\int_{S'} \frac{\bar{J}_s(\bar{r}',t-R/v)}{R}\, dS' \qquad (3\text{-}1)$$

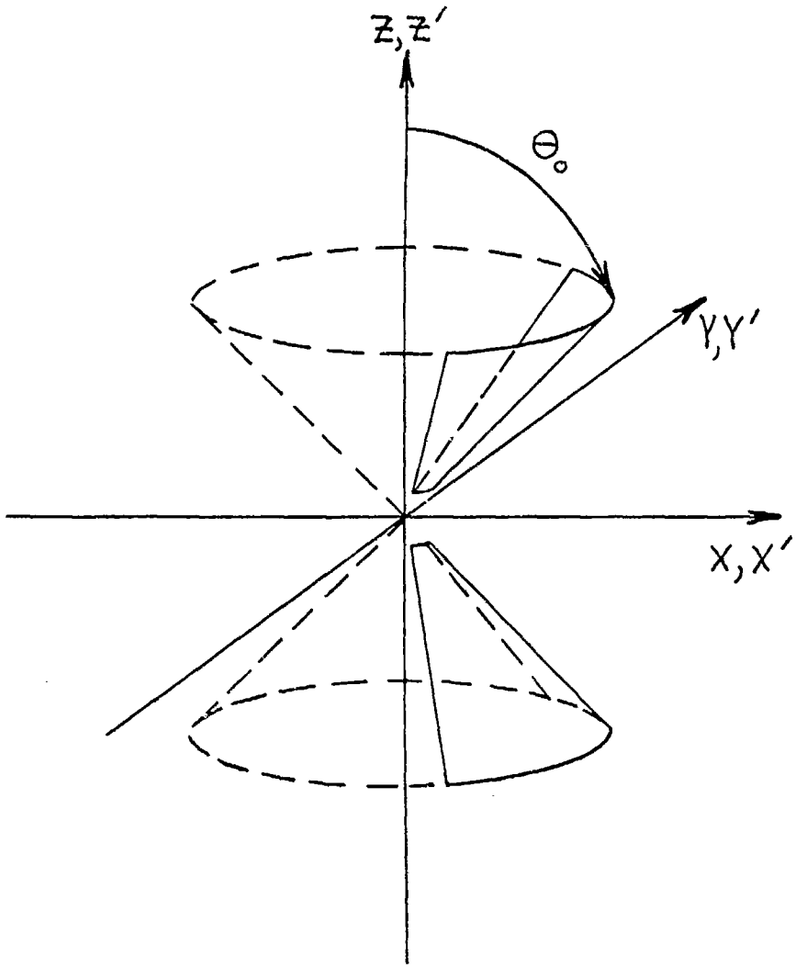

Cartesian source coordinates (x', y', z')
Spherical source coordinates (r', α, β)
Cartesian observation coordinates (x, y, z)
Spherical observation coordinates (r, θ, ϕ)

Figure 3.1

The TEM Horn as a Biconical Section

and

$$\bar{H}(\bar{r},t) = \frac{1}{\mu}\nabla \times \bar{A}(\bar{r},t) \tag{3-2}$$

The various quantities involved in equations (3-1) and (3-2) are:

$\bar{A}$, the electric vector potential,

$R = |\bar{r} - \bar{r}'|$,

s', the surface of integration, and

μ, the permittivity of the medium.

The coordinate systems are indicated in Figure 3.1. In the far field, $\bar{E}(\bar{r},t)$ is found from $\bar{H}(\bar{r},t)$ by the simple relationship

$$\bar{E}(\bar{r},t) = \eta\left[\bar{H}(\bar{r},t) \times \hat{r}\right] \tag{3-3}$$

where η is the impedance of the medium.

Assume that within the region between the two perfectly conducting surfaces the $\bar{E}$ and $\bar{H}$ fields are the same as those assumed for the Sperry Rand derivation in Section 2.1 of Chapter 2. Therefore,

$$\bar{H}(\bar{r}',t) = \frac{\hat{\beta} f(\alpha,\beta)}{\eta r'}\left[V\left(t - \frac{r'}{v}\right) - k_v V\left(t + \frac{r'}{v} - \frac{2r_a}{v}\right)\right] \tag{3-4}$$

k_v and $f(\alpha,\beta)$ are also discussed in Section 2.1 of Chapter 2. The $\bar{J}_s$ current sheets flowing on the upper and lower surfaces are found from the boundary condition

$$\bar{J}_s = \hat{n} \times \bar{H} \tag{3-5}$$

where $\hat{n}$ is the inward unit normal to the surface in question. At the upper surface, $\hat{n} = \hat{\alpha}$. Therefore,

$$\bar{J}_{s_{upper}} = \frac{\hat{r}' f(\theta_o,\beta)}{\eta r'}\left[V\left(t-\frac{r'}{v}\right) - k_v V\left(t+\frac{r'}{v}-\frac{2r_a}{v}\right)\right] \quad (3\text{-}6)$$

At the lower surface, $\hat{n} = -\hat{\alpha}$. Therefore,

$$\bar{J}_{s_{lower}} = -\frac{\hat{r}' f(\pi-\theta_o,\beta)}{\eta r'}\left[V\left(t-\frac{r'}{v}\right) - k_v V\left(t+\frac{r'}{v}-\frac{2r_a}{v}\right)\right] \quad (3\text{-}7)$$

Also, at the perfectly conducting surfaces,

$$ds' = r'\sin\theta_o\, d\beta\, dr' \quad (3\text{-}8)$$

Also, $\mu/\eta = 1/v$, $\sin\theta_o = \sin(\pi - \theta_o)$, and $f(\theta_o,\beta) = f(\pi-\theta_o,\beta)$. Then, substituting (3-6), (3-7), and (3-8) into (3-1),

$$\bar{A}(\bar{r},t)$$

$$= \frac{1}{4\pi v}\left\{\int_0^{r_a}\int_{-\beta_o}^{\beta_o}\frac{\hat{r}_u' f(\theta_o,\beta)}{R_u} V\left(t-\frac{r_u'}{v}-\frac{R_u}{v}\right)\sin\theta_o\, d\beta\, dr'\right.$$

$$-k_v\int_0^{r_a}\int_{-\beta_o}^{\beta_o}\frac{\hat{r}_u' f(\theta_o,\beta)}{R_u} V\left(t+\frac{r_u'}{v}-\frac{2r_a}{v}-\frac{R_u}{v}\right)\sin\theta_o\, d\beta\, dr'$$

$$-\int_0^{r_a}\int_{-\beta_o}^{\beta_o}\frac{\hat{r}_l' f(\theta_o,\beta)}{R_l} V\left(t-\frac{r_l'}{v}-\frac{R_l}{v}\right)\sin\theta_o\, d\beta\, dr'$$

$$\left.+k_v\int_0^{r_a}\int_{-\beta_o}^{\beta_o}\frac{\hat{r}_l' f(\theta_o,\beta)}{R_l} V\left(t+\frac{r_l'}{v}-\frac{2r_a}{v}-\frac{R_l}{v}\right)\sin\theta_o\, d\beta\, dr'\right\} \quad (3\text{-}9)$$

R_u and R_l are the values of R at the upper and lower surfaces respectively. r'_u and r'_l, and $\hat{r}'_u$ and $\hat{r}'_l$, are the values of r' and $\hat{r}'$ at the upper and lower surfaces respectively.

Since only the far fields are desired, R_u and R_l are replaced by their approximate values in the numerator and denominator of (3-9). In the denominator, $R_u \approx R_l \approx r$. In the arguments of V, $R_u \approx r - \hat{r}\cdot\hat{r}'_u$ and $R_l \approx r - \hat{r}\cdot\hat{r}'_l$.

At the upper surface,

$$\hat{r}\cdot\bar{r}'_u = r'(\sin\theta_o\cos\beta\sin\theta\cos\phi + \sin\theta_o\sin\beta\sin\theta\sin\phi + \cos\theta_o\cos\theta) \quad (3\text{-}10)$$

At the lower surface,

$$\hat{r}\cdot\bar{r}'_l = r'(\sin\theta_o\cos\beta\sin\theta\cos\phi + \sin\theta_o\sin\beta\sin\theta\sin\phi - \cos\theta_o\cos\theta) \quad (3\text{-}11)$$

$\hat{r}'_u$ and $\hat{r}'_l$ need to be described in terms of $\theta_o, \beta, \theta, \phi, \hat{r}, \hat{\theta}$, and $\hat{\phi}$ so that the curl operation on the observation coordinates r, θ, ϕ, required by equation (3-2), may be performed.

$$\hat{r}'_u = \sin\theta_o\cos\beta\hat{x} + \sin\theta_o\sin\beta\hat{y} + \cos\theta_o\hat{z} \quad (3\text{-}12)$$

Using the vector identities

$$\hat{x} = \sin\theta\cos\phi\hat{r} + \cos\theta\cos\phi\hat{\theta} - \sin\phi\hat{\phi} \quad (3\text{-}13)$$

$$\hat{y} = \sin\theta\sin\phi\hat{r} + \cos\theta\sin\phi\hat{\theta} + \cos\phi\hat{\phi} \quad (3\text{-}14)$$

$$\hat{z} = \cos\theta\hat{r} - \sin\theta\hat{\theta} \quad (3\text{-}15)$$

in (3-12), $\hat{r}'_u$ may be written as follows.

$$\begin{aligned}\hat{r}'_u = &(\sin\theta_o\cos\beta\sin\theta\cos\phi \\ &+\sin\theta_o\sin\beta\sin\theta\sin\phi+\cos\theta_o\cos\theta)\hat{r} \\ &+(\sin\theta_o\cos\beta\cos\theta\cos\phi \\ &+\sin\theta_o\sin\beta\cos\theta\sin\phi-\cos\theta_o\sin\theta)\hat{\theta} \\ &+(-\sin\theta_o\cos\beta\sin\phi \\ &+\sin\theta_o\sin\beta\cos\phi)\hat{\phi}\end{aligned} \tag{3-16}$$

$\hat{r}'_l$ is the same as $\hat{r}'_u$ with θ_o replaced by $\pi - \theta_o$. Therefore,

$$\begin{aligned}\hat{r}'_l = &(\sin\theta_o\cos\beta\sin\theta\cos\phi \\ &+\sin\theta_o\sin\beta\sin\theta\sin\phi-\cos\theta_o\cos\theta)\hat{r} \\ &+(\sin\theta_o\cos\beta\cos\theta\cos\phi \\ &+\sin\theta_o\sin\beta\cos\theta\sin\phi+\cos\theta_o\sin\theta)\hat{\theta} \\ &+(-\sin\theta_o\cos\beta\sin\phi \\ &+\sin\theta_o\sin\beta\cos\phi)\hat{\phi}\end{aligned} \tag{3-17}$$

Let

$$T = t - \frac{r}{v} \tag{3-18}$$

Also, define

$$V\left(T - \frac{r'}{v} + \frac{\hat{r}\cdot\bar{r}'_u}{v}\right) \triangleq V_{u1} \tag{3-19}$$

$$V\left(T + \frac{r'}{v} - \frac{2r_a}{v} + \frac{\hat{r}\cdot\bar{r}'_u}{v}\right) \triangleq V_{u2} \tag{3-20}$$

$$V\left(T-\frac{r'}{v}+\frac{\hat{r}\cdot\bar{r}\ell'}{v}\right)\triangleq V_{\ell 1} \tag{3-21}$$

$$V\left(T+\frac{r'}{v}-\frac{2r_a}{v}+\frac{\hat{r}\cdot\bar{r}\ell'}{v}\right)\triangleq V_{\ell 2} \tag{3-22}$$

In the spherical coordinates r, θ, ∅,

$$\nabla\times\bar{A}=\left(\frac{1}{r}\frac{\partial A_\phi}{\partial\theta}+\frac{A_\phi}{r\tan\theta}-\frac{1}{r\sin\theta}\frac{\partial A_\theta}{\partial\phi}\right)\hat{r}$$

$$+\left(\frac{1}{r\sin\theta}\frac{\partial A_r}{\partial\phi}-\frac{\partial A_\phi}{\partial r}-\frac{A_\phi}{r}\right)\hat{\theta}$$

$$+\left(\frac{\partial A_\theta}{\partial r}+\frac{A_\theta}{r}-\frac{1}{r}\frac{\partial A_r}{\partial\theta}\right)\hat{\phi} \tag{3-23}$$

Since only the theta and phi components of $\nabla\times\bar{A}$ which vary as 1/r are needed to find the electric far fields of the biconical section, only $\frac{\partial A_\phi}{\partial r}$ and $\frac{\partial A_\theta}{\partial r}$ need to be computed. Realizing that $\eta/\mu = v$, from (3-23), (3-2), and (3-3),

$$E_\theta(\bar{r},t)=v\frac{\partial A_\theta}{\partial r} \tag{3-24}$$

Also, from (3-23), (3-2), and (3-3),

$$E_\phi(\bar{r},t)=v\frac{\partial A_\phi}{\partial r} \tag{3-25}$$

Performing the operation indicated by (3-24) on (3-9) using (3-16) through (3-22),

$$4\pi v r E_\theta(\bar{r},t)$$

$$=-\cos\theta\cos\phi\int_0^{r_a}\int_{-\beta_0}^{\beta_0}f(\theta_0,\beta)\sin^2\theta_0\cos\beta\left[V'_{\ell 1}-k_v V'_{\ell 2}\right]d\beta dr'$$

$$-\cos\theta\sin\phi\int_0^{r_a}\int_{-\beta_o}^{\beta_o} f(\theta_o,\beta)\sin^2\theta_o\sin\beta\left[V'_{u1}-k_v V'_{u2}\right]d\beta dr'$$

$$+\sin\theta\int_0^{r_a}\int_{-\beta_o}^{\beta_o} f(\theta_o,\beta)\sin\theta_o\cos\theta_o\left[V'_{u1}-k_v V'_{u2}\right]d\beta dr'$$

$$+\cos\theta\cos\phi\int_0^{r_a}\int_{-\beta_o}^{\beta_o} f(\theta_o,\beta)\sin^2\theta_o\cos\beta\left[V'_{\ell 1}-k_v V'_{\ell 2}\right]d\beta dr'$$

$$+\cos\theta\sin\phi\int_0^{r_a}\int_{-\beta_o}^{\beta_o} f(\theta_o,\beta)\sin^2\theta_o\sin\beta\left[V'_{\ell 1}-k_v V'_{\ell 2}\right]d\beta dr'$$

$$+\sin\theta\int_0^{r_a}\int_{-\beta_o}^{\beta_o} f(\theta_o,\beta)\sin\theta_o\cos\theta_o\left[V'_{z1}-k_v V'_{\ell 2}\right]d\beta dr' \qquad (3\text{-}26)$$

The primes associated with the various V's indicate differentiation with respect to the argument of the V in question. Performing the operation indicated by (3-25) on (3-9) using (3-16) through (3-22),

$$4\pi r E_\phi(\bar{r},t)$$

$$=\sin\phi\int_0^{r_a}\int_{-\beta_o}^{\beta_o} f(\theta_o,\beta)\sin^2\theta_o\cos\beta\left[V'_{u1}-k_v V'_{u2}\right]d\beta dr'$$

$$-\cos\phi\int_0^{r_a}\int_{-\beta_o}^{\beta_o} f(\theta_o,\beta)\sin^2\theta_o\sin\beta\left[V'_{u1}-k_v V'_{u2}\right]d\beta dr'$$

$$-\sin\phi\int_0^{r_a}\int_{-\beta_0}^{\beta_0} f(\theta_0,\beta)\sin^2\theta_0\cos\beta\left[V\acute{e}_1-k_v V\acute{e}_2\right]d\beta dr'$$

$$+\cos\phi\int_0^{r_a}\int_{-\beta_0}^{\beta_0} f(\theta_0,\beta)\sin^2\theta_0\sin\beta\left[V\acute{e}_1-k_v V\acute{e}_2\right]d\beta dr' \qquad (3\text{-}27)$$

The transient electric far fields of a biconical antenna could be found from equations (3-26) and (3-27) as follows. If the spherical TEM wave described by equations (2-1) and (2-2) in Section 2.1 of Chapter 2 is a reasonable approximation to the electromagnetic fields exciting the biconical antenna, simply replace β_0 by π in the limits of integration in equations (3-26) and (3-27). For wide-angle biconical antennas, $f(\theta_0,\beta) \simeq 1/(\pi - 2\theta_0)$. For other biconical antennas, another form of $f(\theta_0,\beta)$ would have to be determined. Equations (3-26) and (3-27) could then be programmed for execution on a digital computer using a given form for the voltage V(t) exciting the apex of the bicone. The approximate numerical solutions would be valid for an arbitrary observation point $P(\theta,\phi)$ in the far field.

3.3 APPROXIMATE CLOSED FORM SOLUTIONS FOR THE THETA COMPONENT OF THE ELECTRIC FAR FIELD IN THE AZIMUTH PLANE

Consider equation (3-26) for the theta component of the electric far field. In the azimuth ($\theta = 90^\circ$) plane, $\cos\theta = 0$ and $\sin\theta = 1$. Therefore, the first, second, fourth, and fifth lines of (3-26) are zero. Consider now a TEM horn with small flare in the E-plane.

Then $f(\theta_o, \beta) \simeq 1/(\pi - 2\theta_o)$ and $\sin\theta_o\cos\theta_o = (\sin 2\theta_o)/2 \simeq (\pi - 2\theta_o)/2$. Therefore, (3-26) may be written in the azimuth plane as

$$4\pi v r E_\theta(\bar{r},t)\Big|_{\theta = 90^\circ}$$

$$\approx \frac{1}{2}\int_0^{r_a}\int_{-\beta_o}^{\beta_o}\left[V_{u1}' - k_v V_{u2}'\right]d\beta dr' + \frac{1}{2}\int_0^{r_a}\int_{-\beta_o}^{\beta_o}\left[V_{\ell 1}' - k_v V_{\ell 2}'\right]d\beta dr' \quad (3\text{-}28)$$

From (3-10), in the azimuth plane, $\hat{r}\cdot\hat{r}_u' = r'\sin\theta_o\cos(\beta - \phi) \approx r'\cos(\beta - \phi)$. From (3-11), in the azimuth plane, $\hat{r}\cdot\hat{r}_l' = r'\sin\theta_o \times(\cos(\beta - \phi)) \approx r'\cos(\beta - \phi)$. Thus, by inspection of (3-19) through (3-22),

$$4\pi v r E_\theta(\bar{r},t)\Big|_{\theta = 90^\circ}$$

$$\approx \int_0^{r_a}\int_{-\beta_o}^{\beta_o}\left[V_{u1}' - k_v V_{u2}'\right]d\beta dr' \quad (3\text{-}29)$$

Utilizing the substitution

$$\xi_1 = T - \frac{r'}{v} + \frac{r'}{v}\cos(\beta - \phi), \quad (3\text{-}30)$$

$$\int_0^{r_a} V_{u1}'\, dr'$$

$$\approx \frac{v}{1 - \cos(\beta - \phi)}\left\{V\left[T\right] - V\left[T - \frac{r_a}{v}\left(1 - \cos(\beta - \phi)\right)\right]\right\} \quad (3\text{-}31)$$

Utilizing the substitution

$$\xi_2 = T + \frac{r'}{v} - \frac{2r_a}{v} + \frac{r'}{v}\cos(\beta - \phi), \quad (3\text{-}32)$$

$$k_v\int_0^{r_a} V_{u2}'\, dr' \approx \frac{v k_v}{1 + \cos(\beta - \phi)}\left\{V\left[T - \frac{r_a}{v}\left(1 - \cos(\beta - \phi)\right)\right]\right.$$

$$-V\left[T-\frac{2r_a}{v}\right]\Bigg\} \tag{3-33}$$

Consider now the case when the front aperture of the approximate TEM horn is electrically small, that is--when $2r_a\beta_o/v$ and $r_a(\pi - 2\theta_o)/v$ are less than or comparable with the exciting waveform's characteristic time dimensions. Then, the integration over β in (3-29) will be approximated by $2\beta_o$ times the value of the inner integral over r' evaluated at $\hat{\beta}$, where $\hat{\beta}$ is some angle between $-\beta_o$ and β_o. Thus, (3-29) may be written in the azimuth plane as

$$4\pi v r E_\theta(\bar{r},t)\Big|_{\phi = 90^\circ}$$

$$\approx \frac{2\beta_o v}{1-\cos(\hat{\beta}-\phi)}\left\{V[T]-V\left[T-\frac{r_a}{v}\left(1-\cos(\hat{\beta}-\phi)\right)\right]\right\}$$

$$-\frac{2\beta_o v k_v}{1+\cos(\hat{\beta}-\phi)}\left\{V\left[T-\frac{r_a}{v}\left(1-\cos(\hat{\beta}-\phi)\right)\right]\right.$$

$$\left.-V\left[T-\frac{2r_a}{v}\right]\right\} \tag{3-34}$$

Consider first the boresight ($\phi = 0^\circ$) direction. The first two terms of (3-34) may then be combined to form an approximate derivative as follows.

$$\frac{V[T]-V\left[T-\frac{r_a}{v}(1-\cos\hat{\beta})\right]}{\frac{r_a}{v}(1-\cos\hat{\beta})} \triangle \frac{V[T]-V[T-\epsilon]}{\epsilon} \approx V'[T] \tag{3-35}$$

Also, since $\hat{\beta}$ is small, $\cos\hat{\beta}$ is not greatly different from 1, and $1 - \cos\hat{\beta}$ is not greatly different from $1 - \cos\beta_o$. Therefore,

$$E_{\theta_{BORESIGHT}}(\bar{r},t) \approx \frac{r_a \beta_o}{2\pi v r} V'[T] - \frac{k_v \beta_a}{4\pi r}\left\{V\left[T - \frac{r_a}{v}(1-\cos\beta_o)\right] - V\left[T - \frac{2r_a}{v}\right]\right\} \quad (3\text{-}36)$$

Equation (3-36) is identical to equation (2-26) in Section 2.3 of Chapter 2. Therefore, the approximate theta component of the electric far field in the boresight direction using the vector potential approach is self-consistent with the result obtained by the aperture approach.

Consider next the backfire ($\phi = 180^o$) direction. The third and fourth terms of (3-34) may then be combined to form an approximate derivative as follows.

$$\frac{V\left[T - \frac{r_a}{v}(1+\cos\hat{\beta})\right] - V\left[T - \frac{2r_a}{v}\right]}{\frac{r_a}{v}(1-\cos\hat{\beta})}$$

$$\underline{\Delta} \; \frac{V\left[T - \frac{2r_a}{v} + \epsilon\right] - V\left[T - \frac{2r_a}{v}\right]}{\epsilon} \approx V'\left[T - \frac{2r_a}{v}\right] \quad (3\text{-}37)$$

Again, since $\hat{\beta}$ is small, $\cos\hat{\beta}$ is not greatly different from 1, and $1 + \cos\hat{\beta}$ is not greatly different from $1 + \cos\beta_o$. Therefore,

$$E_{\theta_{BACKFIRE}}(\bar{r},t) \approx \frac{\beta_o}{4\pi r}\left\{V[T] - V\left[T - \frac{r_a}{v}(1+\cos\beta_o)\right]\right\} - \frac{k_v r_a \beta_a}{2\pi v r} V'\left[T - \frac{2r_a}{v}\right] \quad (3\text{-}38)$$

Equation (3-38) is identical to the sum of equations (2-13) and (2-29) divided by $4\pi r$. Therefore, the approximate theta component of the electric far field in the backfire direction using the vector potential approach is also self-consistent with the result obtained by the aperture approach discussed in Section 2.3 of Chapter 2.

Consider finally directions in the azimuth plane well removed from the boresight and backfire directions (directions for which ϕ is neither near 0° nor near 180°). Since β_o is small, in these directions $1 - \cos(\hat{\beta} - \phi) \approx 1 - \cos\phi$, and $1 + \cos(\hat{\beta} - \phi) \approx 1 + \cos\phi$. Hence, (3-34) may be written as

$$E_\theta(\bar{r},t)\Big|_{\substack{\phi \not\approx 0^\circ \\ \phi \not\approx 180^\circ}} \approx \frac{\beta_o}{2\pi r(1-\cos\phi)}\left\{V\left[T\right] - V\left[T - \frac{r_a}{v}(1-\cos\phi)\right]\right\}$$

$$- \frac{k_v \beta_o}{2\pi r(1+\cos\phi)}\left\{V\left[T - \frac{r_a}{v}(1-\cos\phi)\right] - V\left[T - \frac{2r_a}{v}\right]\right\} \quad (3\text{-}39)$$

Equation (3-39) is identical to equation (2-30) divided by $4\pi r$. Therefore, using the vector potential approach, in directions well removed from boresight and backfire, the total radiation of the TEM horn consists of a series of delayed replicas of the excitation applied to the apex. However, the derivative radiation of the front aperture as given by equation (2-9) does not appear in (3-39). As discussed in Section 2.4 of Chapter 2, the superposition of the derivative radiation upon the delayed replica radiation is due to the approximation of the TEM horn as a structure of three apertures when the front aperture is electrically very small.

Chapter 4

THE TRANSIENT ELECTRIC FAR FIELDS OF A PARABOLOID REFLECTOR/POINT SOURCE FEED ANTENNA SYSTEM

4.1 INTRODUCTION

Consider the paraboloid reflector shown in Figure 4.1. This figure is identical to Figure C.1 on the second page of Appendix C, and it is repeated here for the convenience of the reader. The various coordinate systems shown in Figure 4.1 are discussed in Section C.1 of Appendix C.

Assume that at the focus of the paraboloid, located at O, there exists a spherical-wave point source radiator which has the following electric far field components in terms of the spherical coordinates ρ, Ψ, ξ.

$$\bar{E}_\Psi = \frac{V_1(\Psi, \xi, t)}{\rho} \hat{\Psi} \tag{4-1}$$

and

$$\bar{E}_\xi = \frac{V_2(\Psi, \xi, t)}{\rho} \hat{\xi} \tag{4-2}$$

That is--it is assumed that the paraboloid reflector is in the far field of the point source. $\bar{E}_\Psi$ and $\bar{E}_\xi$ represent components of a TEM spherical wave propagating in the $\hat{\rho}$ direction. V_1 and V_2 are

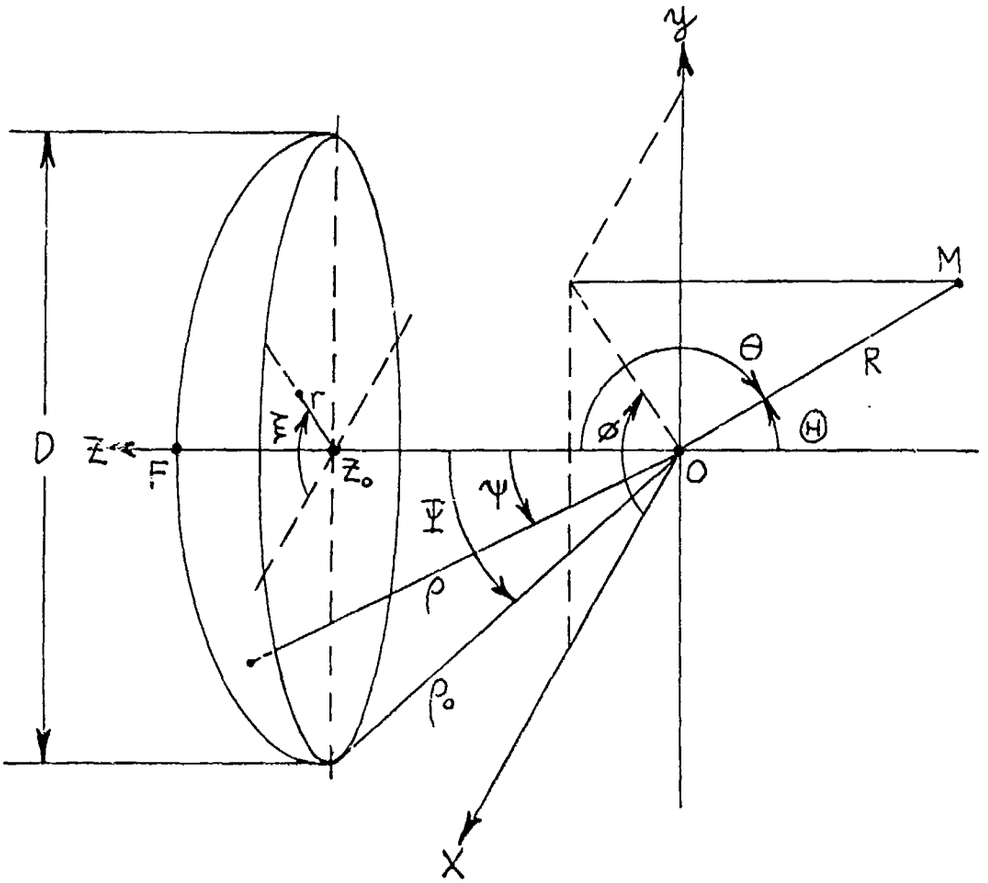

D = exit aperture diameter
M = observation point
OF = f = focal length
z_o = center of exit aperture
Ψ = half-angular aperture
Ⓗ = $\pi - \theta$

Figure 4.1

Geometry for the Paraboloid Reflector/Point Source Feed

general functions of Ψ, Ξ, and t. Functions V_1 and V_2 may be applied to any transient or cw feed which may be approximated as a point source radiator located at the focus of the paraboloid. Thus, V_1 and V_2 are not limited to an approximation of the TEM horn feed.

4.2 THE TRANSIENT ELECTRIC FAR FIELDS OF THE SYSTEM IN TERMS OF THE EXIT APERTURE FIELDS

The electric far fields of the point source as given by equations (4-1) and (4-2), along with their associated magnetic fields, then impinge upon the perfectly conducting paraboloid reflector surface. The complete mathematical details of the derivation of the electric far fields of the paraboloid reflector/point source feed antenna system in terms of the fields over the exit aperture are given in Appendix C.

The derivation of the system far fields in terms of the fields over the exit aperture of the paraboloid utilizes four basic assumptions:

1. The paraboloid reflector is assumed to be sufficiently smooth to allow application of the plane wave boundary conditions at the perfectly conducting surface.
2. The geometrical optics approximation is invoked to afford a one-to-one, point-to-point transformation between the fields at the paraboloid surface and the fields at the exit aperture.
3. The Chernousov formulation requires a closed aperture surface S_a. In keeping with common practice, S_a is taken

as a plane containing the exit aperture of the paraboloid and closed at infinity, and the fields over the non-aperture part of the plane are taken as approximately zero (Ramo and Whinnery, 1956:530,532).

4. Edge effects at the exit aperture are not considered.

Employing the geometrical optics approximation, the values of V_{1A} and V_{2A}, V_1 and V_2 evaluated at the exit aperture respectively, may be easily found. V_{1A} is the same as V_1 if the time retardation from the focus to the exit aperture is taken into account. Also, V_{2A} has the same relationship to V_2. The time retardation from the focus to the exit aperture is simply the length of the optical path divided by v, the velocity of propagation in the medium. Therefore,

$$V_{1A}\left\{\Gamma, \xi, t - \frac{f}{v}\left[\frac{16(f/D)^2+1}{16(f/D)^2}\right]\right\} = V_1\left\{\Psi, \xi, t - \frac{f}{v}\left[\frac{16(f/D)^2+1}{16(f/D)^2}\right]\right\} \tag{4-3}$$

and

$$V_{2A}\left\{\Gamma, \xi, t - \frac{f}{v}\left[\frac{16(f/D)^2+1}{16(f/D)^2}\right]\right\} = V_2\left\{\Psi, \xi, t - \frac{f}{v}\left[\frac{16(f/D)^2+1}{16(f/D)^2}\right]\right\} \tag{4-4}$$

The relationship between Ψ and r in terms of f is given by equation (C-32) on the seventh page of Appendix C. The Chernousov formulation, namely equation (C-65) on the thirteenth page of Appendix C, is now applied to the electromagnetic fields existing over the exit aperture of the paraboloid. The application of the Chernousov (1965) formulation

results in equations (C-92) and (C-93) in Section C.4 of Appendix C. The primes associated with V_{1A} and V_{2A} in equations (C-92) and (C-93) indicate differentiation with respect to the time argument of the V in question. V'_{1A} and V'_{2A} are given by equations (C-68) and (C-69) respectively. The time arguments of V'_{1A} and V'_{2A} are given by equation (C-95).

4.3 TRANSFORMATIONS BETWEEN THE POINT SOURCE FEED OBSERVATION COORDINATES AND THE EXIT APERTURE COORDINATES

The purpose of this section is to determine the transformations between V_1 and V_2, as given in equations (4-1) and (4-2), and the normalized electric far fields of a point source feed, located at the focus of the paraboloid, which has cartesian observation coordinates x_H, y_H, z_H. The subscript "H" is used from here on for all feed coordinates to avoid confusion between feed and paraboloid coordinate systems.

The orientation of the feed cartesian coordinates x_H, y_H, z_H with respect to the paraboloid cartesian coordinates x,y,z is shown in Figure 4.2. The spherical feed coordinates corresponding to the feed cartesian coordinates are r_H, θ_H, ϕ_H. The spherical source coordinates for the paraboloid are ρ, Ψ, Ξ, and the exit aperture coordinates for the paraboloid are r, Ξ, z. The paraboloid source coordinates and exit aperture coordinates are shown in Figure 4.1.

Let the normalized electric far field components of the feed be designated by $r_H E_{\theta H}$ and $r_H E_{\phi H}$. These normalized field components

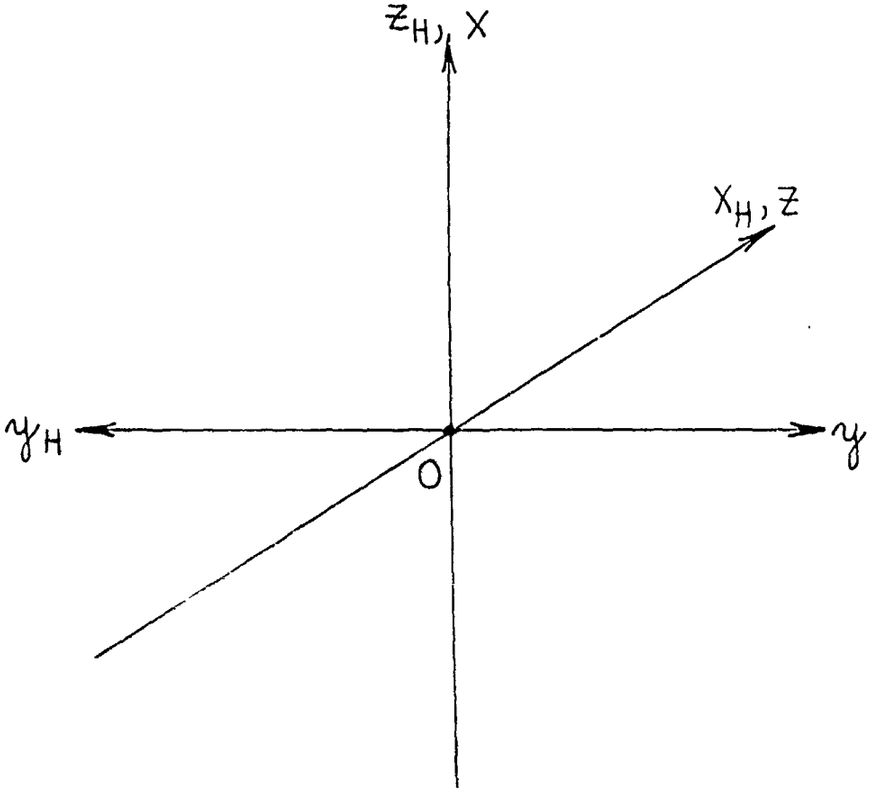

Cartesian feed coordinates (x_H, y_H, z_H)
Spherical feed coordinates (r_H, θ_H, ϕ_H)
Cartesian paraboloid coordinates (x, y, z)
Spherical paraboloid source coordinates (ρ, Ψ, ξ)

Figure 4.2

Feed and Paraboloid Cartesian Coordinates

are physically more typical for a feed than V_1 and V_2, which were used for the sake of mathematical simplicity in the derivation in Appendix C.

First, V_1 and V_2 are found in terms of the normalized field components of the feed and the spherical paraboloid source coordinates ρ, Ψ, ξ. Secondly, V_1 and V_2 are found in terms of the normalized field components of the feed and the paraboloid exit aperture coordinates r, ξ, z.

The relationships between the two cartesian systems are given by

$$x = z_H \tag{4-5}$$

$$y = -y_H \tag{4-6}$$

$$z = x_H \tag{4-7}$$

Also, since the origins of the spherical systems r_H, θ_H, ϕ_H and ρ, Ψ, ξ coincide,

$$\rho = r_H \tag{4-8}$$

The following vector identities are employed.

$$\hat{\theta}_H = \cos\theta_H \cos\phi_H \hat{x}_H + \cos\theta_H \sin\phi_H \hat{y}_H - \sin\theta_H \hat{z}_H \tag{4-9}$$

$$\hat{\phi}_H = -\sin\phi_H \hat{x}_H + \cos\phi_H \hat{y}_H \tag{4-10}$$

$$\hat{x} = \sin\Psi\cos\xi\,\hat{\rho} + \cos\Psi\cos\xi\,\hat{\Psi} - \sin\xi\,\hat{\xi} \tag{4-11}$$

$$\hat{y} = \sin\Psi\sin\xi\,\hat{\rho} + \cos\Psi\sin\xi\,\hat{\Psi} + \cos\xi\,\hat{\xi} \tag{4-12}$$

$$\hat{z} = \cos\Psi\,\hat{\rho} - \sin\Psi\,\hat{\Psi} \tag{4-13}$$

The spherical systems are related to the corresponding cartesian systems by the following relationships.

$$x_H = r_H \sin\theta_H \cos\phi_H \tag{4-14}$$

$$y_H = r_H \sin\theta_H \sin\phi_H \tag{4-15}$$

$$z_H = r_H \cos\theta_H \tag{4-16}$$

$$x = \rho \sin\psi \cos\xi \tag{4-17}$$

$$y = \rho \sin\psi \sin\xi \tag{4-18}$$

$$z = \rho \cos\psi \tag{4-19}$$

Using (4-5) through (4-19), after numerous manipulations,

$$\hat{\theta}_H = -\frac{\cos\psi\cos\xi\,\hat{\psi}}{\sqrt{1-\sin^2\psi\cos^2\xi}} + \frac{\sin\xi\,\hat{\xi}}{\sqrt{1-\sin^2\psi\cos^2\xi}} \tag{4-20}$$

and

$$\hat{\phi}_H = -\frac{\sin\xi\,\hat{\psi}}{\sqrt{1-\sin^2\psi\cos^2\xi}} - \frac{\cos\psi\cos\xi\,\hat{\xi}}{\sqrt{1-\sin^2\psi\cos^2\xi}} \tag{4-21}$$

$V_1(\psi,\xi,t)$ and $V_2(\psi,\xi,t)$, used in the derivation of the electric far fields of the paraboloid reflector/point source feed system, are now found in terms of $r_H E_{\theta H}$ and $r_H E_{\phi H}$, the normalized electric far fields of the point source feed. The normalized electric far field of the feed is

$$r_H \bar{E}(\bar{r}_H, t) = r_H E_{\theta H}(\bar{r}_H, t)\hat{\theta}_H + r_H E_{\phi H}(\bar{r}_H, t)\hat{\phi}_H \tag{4-22}$$

From equations (4-1) and (4-2), the normalized electric far field

exciting the paraboloid may also be written as

$$\rho \bar{E}(\bar{\rho}, t) = V_1(\psi, \xi, t)\hat{\psi} + V_2(\psi, \xi, t)\hat{\xi} \qquad (4\text{-}23)$$

Equating (4-22) and (4-23), and utilizing (4-20) and (4-21),

$$V_1(\psi, \xi, t) = -\frac{(r_H E_{\theta H} \cos\psi \cos\xi + r_H E_{\phi H} \sin\xi)}{\sqrt{1 - \sin^2\psi \cos^2\xi}} \qquad (4\text{-}24)$$

and

$$V_2(\psi, \xi, t) = \frac{(r_H E_{\theta H} \sin\xi - r_H E_{\phi H} \cos\psi \cos\xi)}{\sqrt{1 - \sin^2\psi \cos^2\xi}} \qquad (4\text{-}25)$$

To write (4-24) and (4-25) in terms of the exit aperture coordinates r, ξ, z, the relationships

$$\cos\psi = \frac{(1 - r^2/4f^2)}{(1 + r^2/4f^2)} \qquad (4\text{-}26)$$

and

$$\sin\psi = \frac{r}{f(1 + r^2/4f^2)} \qquad (4\text{-}27)$$

are employed. Therefore,

$$V_1(r, \xi, t) = -\frac{f(1 - r^2/4f^2)\cos\xi\, r_H E_{\theta H}}{\sqrt{f^2(1 + r^2/4f^2)^2 - r^2\cos^2\xi}} - \frac{f(1 + r^2/4f^2)\sin\xi\, r_H E_{\phi H}}{\sqrt{f^2(1 + r^2/4f^2)^2 - r^2\cos^2\xi}} \qquad (4\text{-}28)$$

and

$$V_2(r, \xi, t) = \frac{f(1 + r^2/4f^2)\sin\xi\, r_H E_{\theta H}}{\sqrt{f^2(1 + r^2/4f^2)^2 - r^2\cos^2\xi}}$$

$$-\frac{f(1-r^2/4f^2)\cos\xi\, r_H E_{\phi H}}{\sqrt{f^2(1+r^2/4f^2)^2 - r^2\cos^2\xi}} \qquad (4\text{-}29)$$

4.4 A SOLUTION FOR THE FAR FIELDS OF THE ANTENNA SYSTEM IN THE BORESIGHT DIRECTION FOR AN ISOTROPIC FEED

Consider the case when the point source feed has an $E_{\theta H}$ electric far field component only. In accordance with equations (C-68) and (C-69) in Appendix C, define

$$V'_{\theta H_A} \triangleq \left(r_H E_{\theta H}\right)'_A \qquad (4\text{-}30)$$

That is, $V'_{\theta H_A}$ is the partial derivative of $r_H E_{\theta H}$ with respect to its time argument when $r_H E_{\theta H}$ is evaluated at the exit aperture of the paraboloid.

In the boresight ($\Theta = 0^\circ$) direction, from equation (C-95) in Appendix C, the time argument of $r_H E_{\theta H}$ is $T - (2f/v)$, where $T = t - (R/v)$. Therefore,

$$V'_{\theta H_A}\Big|_{\Theta=0^\circ} = \frac{\partial r_H E_{\theta H}(r, \xi, T-2f/v)}{\partial(T-2f/v)} \qquad (4\text{-}31)$$

Consider as an illustrative example a point source feed whose angular radiation pattern is isotropic (gain $G(\Psi, \Xi) = 1$) or is at least constant over the solid angle subtended by the paraboloid. This produces an exit aperture illumination which varies only as $1/\rho$. (See Silver (1965:419). The isotropic feed is equivalent to Silver's equation (11) on page 419 with $G(\Psi, \Xi) = 1$.) Then

$$\frac{\partial r_H E_{\theta H}(r, \xi, T-2f/v)}{\partial(T-2f/v)} = \frac{d\, r_H E_{\theta H}(T-2f/v)}{d(T-2f/v)} \triangleq V' \qquad (4\text{-}32)$$

From equations (C-68) and (C-69), using (4-28), (4-29), and (4-32),

$$V'_{1A} = -\frac{f(1-r^2/4f^2)\cos\xi\, V'}{\sqrt{f^2(1+r^2/4f^2)^2 - r^2\cos^2\xi}} \tag{4-33}$$

and

$$V'_{2A} = -\frac{f(1+r^2/4f^2)\sin\xi\, V'}{\sqrt{f^2(1+r^2/4f^2)^2 - r^2\cos^2\xi}} \tag{4-34}$$

Define

$$Q = \sqrt{f^2(1+r^2/4f^2)^2 - r^2\cos^2\xi} \tag{4-35}$$

Substituting (4-33) and (4-34) into equations (C-92) and (C-93) in Appendix C, the Θ and ϕ components of the electric far fields of the paraboloid reflector/point source feed antenna system in the boresight ($\Theta = 0^\circ$) direction may be written as follows.

$$RE_\Theta(\bar{R},t)\Big|_{\Theta=0^\circ}$$

$$= \frac{V'}{2\pi v}\left\{-\sin\phi\int_0^{2\pi}\int_0^{D/2}\frac{(1-r^2/4f^2)\sin\xi\cos\xi\, r\,dr\,d\xi}{(1+r^2/4f^2)Q}\right.$$

$$-\cos\phi\int_0^{2\pi}\int_0^{D/2}\frac{(1-r^2/4f^2)\cos^2\xi\, r\,dr\,d\xi}{(1+r^2/4f^2)Q}$$

$$+\sin\phi\int_0^{2\pi}\int_0^{D/2}\frac{\sin\xi\cos\xi\, r\,dr\,d\xi}{Q}$$

$$\left.-\cos\phi\int_0^{2\pi}\int_0^{D/2}\frac{\sin^2\xi\, r\,dr\,d\xi}{Q}\right\} \tag{4-36}$$

$$RE_\phi(\bar{R},t)\Big|_{\Theta=0^\circ}$$

$$= \frac{V'}{2\pi v}\left\{\cos\phi\int_0^{2\pi}\int_0^{D/2}\frac{(1-r^2/4f^2)\sin\xi\cos\xi\, r\,dr\,d\xi}{(1+r^2/4f^2)Q}\right.$$

$$-\sin\phi\int_0^{2\pi}\int_0^{D/2}\frac{(1-r^2/4f^2)\cos^2\xi\, r\,dr\,d\xi}{(1+r^2/4f^2)Q}$$

$$-\cos\phi\int_0^{2\pi}\int_0^{D/2}\frac{\sin\xi\cos\xi\, r\,dr\,d\xi}{Q}$$

$$\left.-\sin\phi\int_0^{2\pi}\int_0^{D/2}\frac{\sin^2\xi\, r\,dr\,d\xi}{Q}\right\} \qquad (4\text{-}37)$$

Equations (4-36) and (4-37) may be simplified by considering the various integrals over ξ. First, utilizing several straightforward trigonometric substitutions,

$$\int_0^{2\pi}\frac{\sin\xi\cos\xi\, d\xi}{Q} = 0 \qquad (4\text{-}38)$$

Secondly, let

$$a^2 = f^2\left(1+r^2/4f^2\right)^2 \qquad (4\text{-}39)$$

Then, after the utilization of a number of trigonometric substitutions,

$$\int_0^{2\pi}\frac{\sin^2\xi\, d\xi}{\sqrt{a^2-r^2\cos^2\xi}} = \frac{4}{a}\int_0^1\frac{\sqrt{1-u^2}\,du}{\sqrt{1-r^2u^2/a^2}} \qquad (4\text{-}40)$$

where $r^2/a^2 \leq 1$ for all r. (Note--$r^2/a^2 = 1$ only when $r = 2f$.) Finally, after utilizing trigonometric substitutions sialr to those used to derive (4-40),

$$\int_0^{2\pi}\frac{\cos^2\xi\, d\xi}{\sqrt{a^2-r^2\cos^2\xi}} = \frac{4}{a}\int_0^1\frac{u^2\,du}{\sqrt{(1-u^2)(1-r^2u^2/a^2)}} \qquad (4\text{-}41)$$

Substituting (4-38), (4-40) and (4-41) into (4-36) and (4-37), with a^2 given by (4-39), $RE_\Theta(\bar{R},t)$ and $RE_\phi(\bar{R},t)$ may be written in the boresight direction as follows.

$$RE_\Theta(\bar{R},t)\Big|_{\Theta=0^\circ}$$

$$=-\frac{2V'\cos\phi}{\pi v f}\left\{\int_0^{D/2}\frac{(1-r^2/4f^2)}{(1+r^2/4f^2)}r\,dr\int_0^1\frac{u^2\,du}{\sqrt{(1-u^2)(1-r^2u^2/a^2)}}\right.$$

$$\left.+\int_0^{D/2}\frac{r\,dr}{(1+r^2/4f^2)}\int_0^1\frac{\sqrt{1-u^2}\,du}{\sqrt{1-r^2u^2/a^2}}\right\} \qquad (4\text{-}42)$$

and

$$RE_\phi(\bar{R},t)\Big|_{\Theta=0^\circ}$$

$$=-\frac{2V'\sin\phi}{\pi v f}\left\{\int_0^{D/2}\frac{(1-r^2/4f^2)}{(1+r^2/4f^2)}r\,dr\int_0^1\frac{u^2\,du}{\sqrt{(1-u^2)(1-r^2u^2/a^2)}}\right.$$

$$\left.+\int_0^{D/2}\frac{r\,dr}{(1+r^2/4f^2)}\int_0^1\frac{\sqrt{1-u^2}\,du}{\sqrt{1-r^2u^2/a^2}}\right\} \qquad (4\text{-}43)$$

The integrands in (4-42) and (4-43) are positive definite for $r < 2f$. Therefore, the integrals themselves are positive for $r < 2f$.

Consider first the boresight direction at $\phi = 0^\circ$. Then $RE_\Theta(\bar{R},t)\big|_{(\Theta,\phi)=(0^\circ,0^\circ)}$ is given by (4-42) with $\cos\phi = 1$, and $RE_\phi(\bar{R},t)\big|_{(\Theta,\phi)=(0^\circ,0^\circ)}$ is zero. Therefore, the form of the electric

far field of the paraboloid reflector/point source feed system in the boresight direction is the negative time derivative of the excitation.

As a check on the $(\Theta,\phi) = (0^\circ,0^\circ)$ results, consider the $(\Theta,\phi) = (0^\circ,90^\circ)$ direction. Then $RE_\Theta(\bar{R},t)\big|_{(\Theta,\phi)=(0^\circ,90^\circ)}$ is zero and $RE_\phi(\bar{R},t)\big|_{(\Theta,\phi)=(0^\circ,90^\circ)}$ is identical to $RE_\Theta(\bar{R},t)\big|_{(\Theta,\phi)=(0^\circ,0^\circ)}$.

The theoretical numerical solution of equation (4-42) for the paraboloid studied by Martins et al. (1973) is shown in Figure 5.5 of Chapter 5. Chapter 5 also presents theoretical solutions for directions away from boresight for the isotropic feed considered in Section 4.4.

In addition, Chapter 5 presents theoretical and experimental solutions for the radiation fields of paraboloid reflector/TEM horn antenna system when the eight-inch TEM horn studied by Martins et al. (1973) is approximated by a point source radiator located at the focus of the paraboloid. In this case, the electric far fields of the TEM horn are not isotropic in the angular coordinates Ψ and ξ. Also, the time waveshape of the horn far fields varies with the angular position (Ψ,ξ) in space. The angular and time variations of the waveshape for the normalized electric far fields of the eight-inch TEM horn are shown in Figures 5.1 through 5.4 in Chapter 5. Figures 5.1 through 5.4 characterize the electric far fields of the eight-inch horn over the exit aperture of the paraboloid.

Chapter 5

THE TRANSIENT ELECTRIC FAR FIELDS OF A PARABOLOID REFLECTOR/TEM HORN FEED ANTENNA SYSTEM

5.1 THE NUMERICALLY COMPUTED ELECTRIC FAR FIELDS OF THE EIGHT-INCH TEM HORN OVER THE EXIT APERTURE

In this chapter, as in Chapter 4, the coordinate systems of the feed are designated by the subscript "H" to avoid confusion between the feed coordinates and the paraboloid coordinates. Equations (B-89) and (B-90) in Section B.5 of Appendix B were programmed in Fortran for execution on a digital computer using unit amplitude gaussian excitation at the apex of the TEM horn. The approximation of the eight-inch TEM horn, studied by Martins et al. (1973), by a Sperry Rand TEM horn is discussed in Section 2.5 of Chapter 2.

Computer runs were performed in both the azimuth and polar planes of the approximate eight-inch TEM horn to characterize the electric far fields over the angular aperture of the paraboloid. The half-angular aperture Ψ of the paraboloid is given in terms of f and D, as shown in Figure 4.1, by the relationship

$$\cos\Psi = \frac{[16(f/D)^2 - 1]}{[16(f/D)^2 + 1]} \qquad (5\text{-}1)$$

The paraboloid used by Martins et al. (1973) had f = 20.16" and D = 48".

Therefore, $\Psi = 61.4^{\circ}$.

In terms of spherical feed observation coordinates r_H, θ_H, ϕ_H, indicated in Figure 4.2, the boresight direction for the feed is $(\theta_H, \phi_H) = (90^{\circ}, 0^{\circ})$. Therefore, since the half-angular aperture of the paraboloid is approximately 60°, azimuth plane runs were performed from $(\theta_H, \phi_H) = (90^{\circ}, 60^{\circ})$ to $(\theta_H, \phi_H) = (90^{\circ}, -60^{\circ})$. Also, polar plane runs were performed from $(\theta_H, \phi_H) = (30^{\circ}, 0^{\circ})$ to $(\theta_H, \phi_H) = (150^{\circ}, 0^{\circ})$. Both $r_H E_{\phi H}$ and $r_H E_{\theta H}$ were considered.

The relative amplitudes of the results of the computer runs for $r_H E_{\theta H}$ and $r_H E_{\phi H}$ are shown in Figures 5.1, 5.2, 5.3, and 5.4. The absolute value of the boresight response shown in Figures 5.1 and 5.2 is the same. The relative amplitude of the boresight response was scaled down in Figure 5.2 so that the family of curves would fit properly on the given grid.

In the azimuth plane, $r_H E_{\theta H}$ is symmetric about the boresight direction. Therefore, $r_H E_{\theta H}(90^{\circ}, \phi_H) = r_H E_{\theta H}(90^{\circ}, -\phi_H)$. In the polar plane, $r_H E_{\theta H}$ is also symmetric about the boresight direction, so that $r_H E_{\theta H}(\theta_H, 0^{\circ}) = r_H E_{\theta H}(90^{\circ} - \theta_H, 0^{\circ})$.

In the azimuth plane, $r_H E_{\phi H}$ is antisymmetric about the boresight direction. Therefore, $r_H E_{\phi H}(90^{\circ}, \phi_H) = -r_H E_{\phi H}(90^{\circ}, -\phi_H)$. In the polar plane, $r_H E_{\phi H}$ is also antisymmetric about the boresight direction, so that $r_H E_{\phi H}(\theta_H, 0^{\circ}) = -r_H E_{\phi H}(90^{\circ} - \theta_H, 0^{\circ})$.

5.2 AN APPROXIMATE CLOSED FORM SOLUTION TO REPRESENT THE ILLUMINATION OF THE EXIT APERTURE

BDM 8-INCH TEM HORN--AZIMUTH RXETHETA

———Theoretical Results from Chernousov Formulation and Computer Runs

$T = t - (r_H/v)$

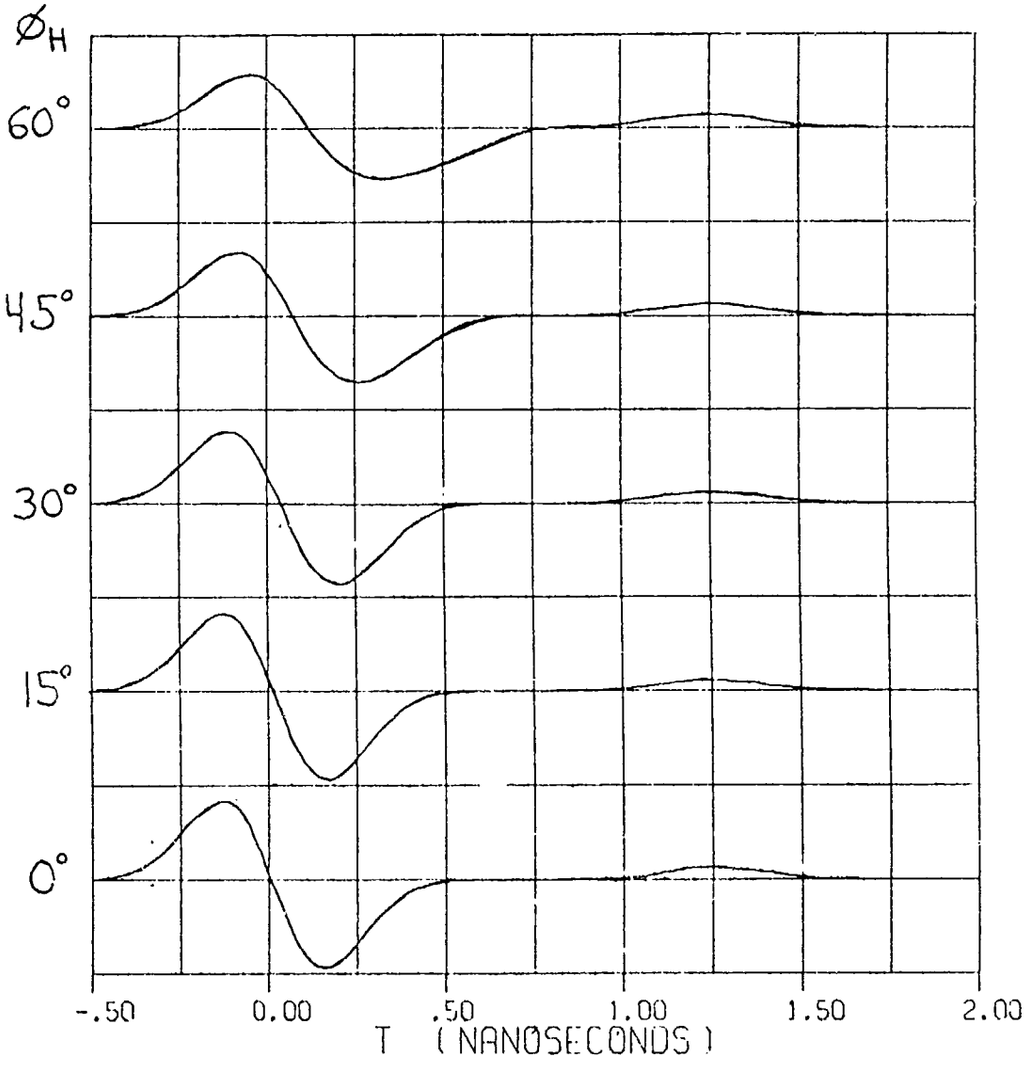

Figure 5.1

$r_H E_{\theta H}$ in the Azimuth ($\theta_H = 90^\circ$) Plane for the Approximate Eight-Inch TEM Horn

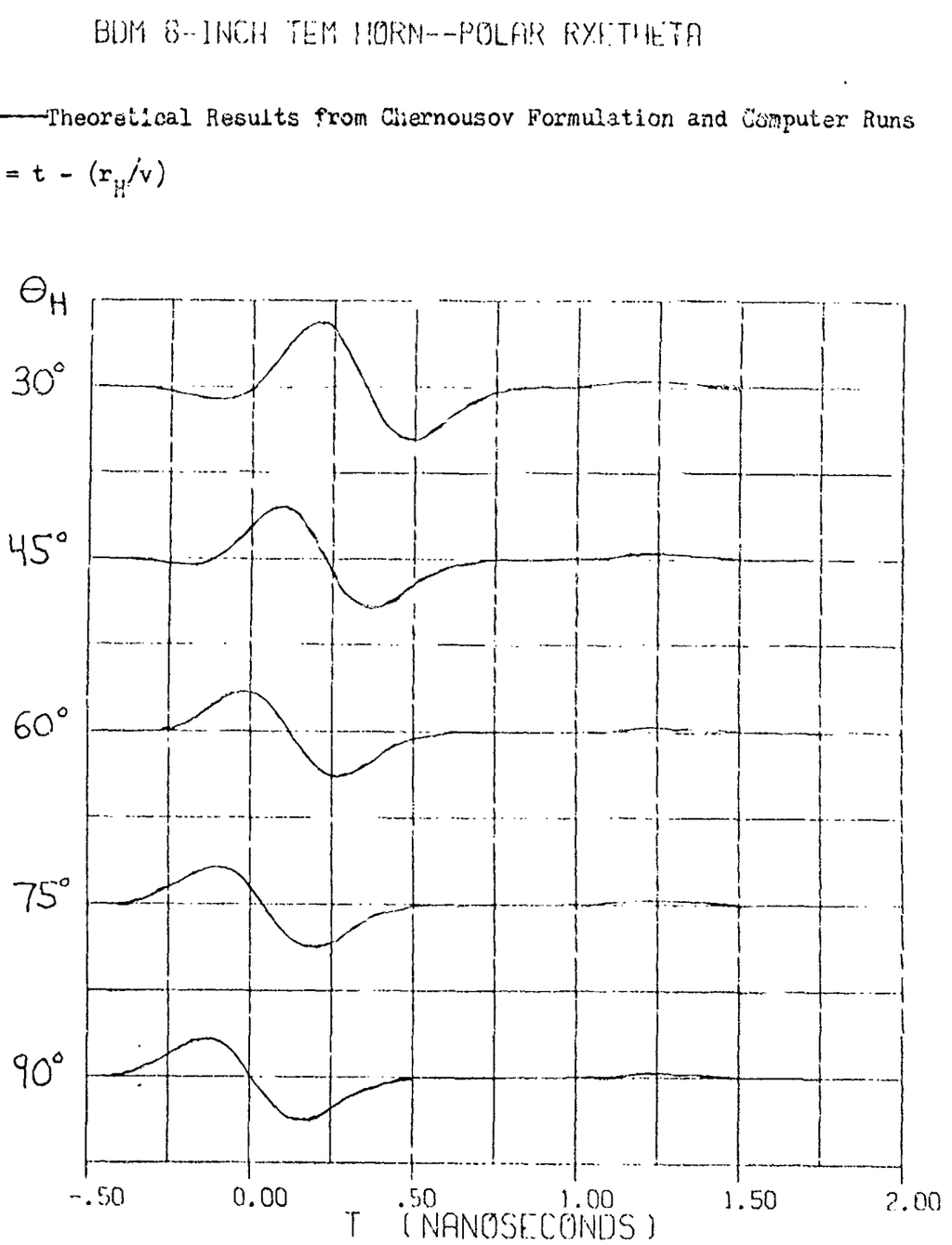

Figure 5.2

$r_H E_{\theta H}$ in the Polar ($\phi_H = 0^\circ$) Plane for the Approximate Eight-Inch TEM Horn

BDM 8-INCH TEM HORN-AZIMUTH (RXEPHI)X100

——Theoretical Results from Chernousov Formulation and Computer Runs

$T = t - (r_H/v)$

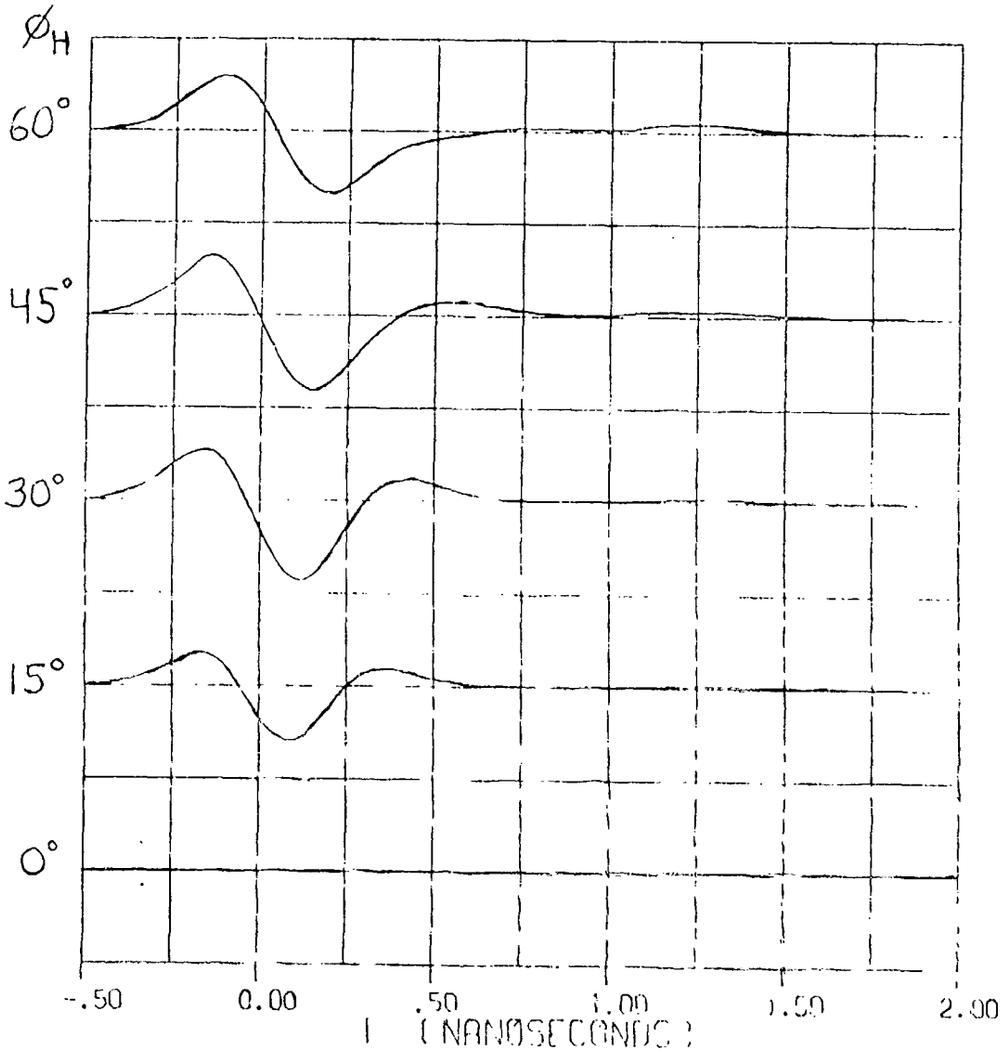

Figure 5.3

$r_H E_{\phi H} x100$ in the Azimuth ($\theta_H = 90^\circ$) Plane for the Approximate Eight-Inch TEM Horn

BDM 8-INCH TEM HORN-POLAR (RXEPHI)X100

———Theoretical Results from Chernousov Formulation and Computer Runs

$T = t - (r_H/v)$

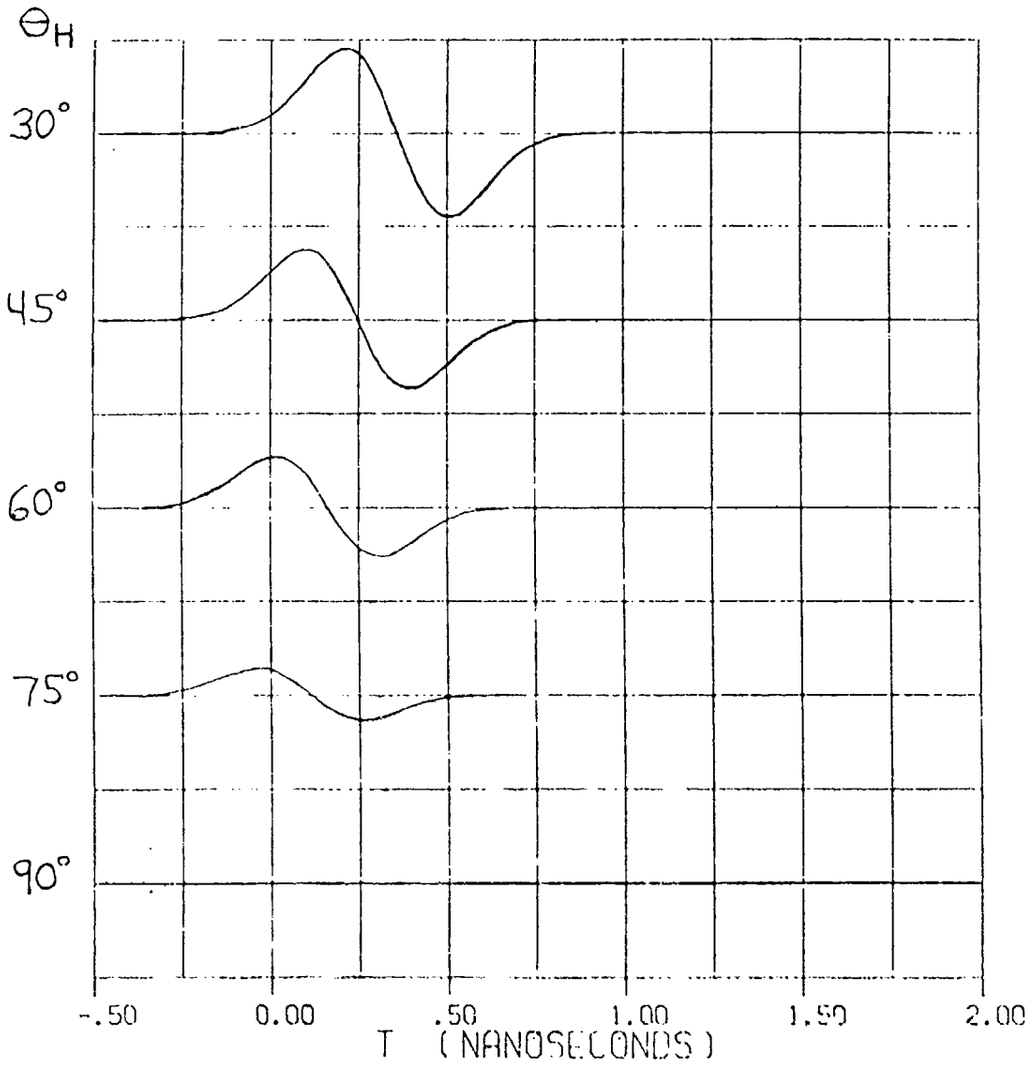

Figure 5.4

$r_H E_{\phi H} x100$ in the Polar ($\phi_H = 0^\circ$) Plane for the Approximate Eight-Inch TEM Horn

The boresight $r_H E_{\theta H}$ response of the approximate eight-inch TEM horn, shown at the bottom of Figure 5.1, is approximately proportional to the derivative of the gaussian excitation at the apex of the TEM horn if the small positive response about the retarded time $T = t - (r_H/v) = 1.25$ nanoseconds is neglected. Therefore, an approximate closed form solution to represent the theta component of the radiation in the boresight direction is

$$r_H E_{\theta H}(t) = -\frac{2Kt}{c^2} e^{-\left(\frac{t}{c}\right)^2} \tag{5-2}$$

for gaussian excitation

$$V(t) = e^{-\left(\frac{t}{c}\right)^2} \tag{5-3}$$

at the apex. K is a constant.

However, Figures 5.1 and 5.2 show additional features of the $r_H E_{\theta H}$ component of the radiation.

1. In both the azimuth and polar planes, the time occurrence of the central zero crossing progresses away from the time T = 0.00 nanoseconds in the boresight direction.
2. There is considerable stretching of the response in time in the azimuth plane for directions away from boresight.
3. There are variations in the amplitudes of the response in both the azimuth and polar planes for directions away from boresight.

Figures 5.3 and 5.4 show the $r_H E_{\phi H}$ component of the radiation with amplitudes relative to the $r_H E_{\theta H}$ component. The amplitudes shown

in Figures 5.3 and 5.4 have been multiplied by 100. Therefore, the maximum value of $r_H E_{\phi H}$ over the angular aperture is approximately 40 db down from the maximum value of $r_H E_{\theta H}$.

To determine an approximate closed form solution to represent the electric far fields of the eight-inch TEM horn over the exit aperture of the paraboloid, with coordinates r, Ξ, z as shown in Figure 4.1, neglect $r_H E_{\phi H}$ with respect to $r_H E_{\theta H}$ and suppose that $r_H E_{\theta H}(r, \Xi, t)$ may be written as

$$r_H E_{\theta H}(r, \Xi, t) = -\frac{2K\left[t - \frac{r}{v}\left(a|\cos\Xi| + b|\sin\Xi|\right)\right]}{\left[\tau_o + \frac{cr}{v}|\sin\Xi|\right]^2} \times \left\{ \frac{e^{-\left[\frac{t - \frac{r}{v}\left(a|\cos\Xi| + b|\sin\Xi|\right)}{\tau_o + \frac{cr}{v}|\sin\Xi|}\right]^2}}{\left[1 + \frac{dr}{D/2}|\sin\Xi|\right]\left[1 - \frac{er}{D/2}|\cos\Xi|\right]} \right\} \quad (5\text{-}4)$$

K is the same constant as in equation (5-2). This form of $r_H E_{\theta H}(r, \Xi, t)$ involves only simple functions of r and Ξ and allows for the various characteristics of the radiation described on the previous page. In equation (5-4), τ_o is the same as τ in equations (5-2) and (5-3). The five parameters a,b,c,d, and e will now be determined from Figures 5.1 and 5.2.

Consider first Figure 5.2 ($\Xi = 0, \pi$). When $r = D/2$, $\theta_H \approx 30^\circ$ because the half-angular aperture of the paraboloid, Ψ, is about 60°. By measuring the difference in time between central zero crossings at $\theta_H = 30^\circ$ and $\theta_H = 90^\circ$, $(aD/2v) = (55/32" - 1")\times 0.50 nsec/"$, or $(aD/2v) = 0.359$ nsec. Since L [illegible]", a = 0.177.

Consider secondly Figure 5.1 ($\xi = \pm\pi/2$) and measure the difference in time between the central zero crossings at $\phi_H = 60^\circ$ and $\phi_H = 0^\circ$. Then $(bD/2v) = (5/4" - 1")x0.50nsec/"$, or $b = 0.0615$.

Thirdly, consider again Figure 5.1 and measure the distances between the maxima of the response at $\phi_H = 60^\circ$ and $\phi_H = 0^\circ$. For a gaussian derivative pulse of the form

$$V(t) = -\frac{2t}{\tau^2} e^{-\left(\frac{t}{\tau}\right)^2} \qquad (5\text{-}5)$$

the distance between maxima is $\tau\sqrt{2}$. Then $(cD/2v) = \tau_{60^\circ} - \tau_{0^\circ}$. $\tau_{60^\circ}\sqrt{2} = (53/32" - 29/32")x0.50nsec/" = 0.375$ nsec, or $\tau_{60^\circ} = 0.265$ nsec. $\tau_{0^\circ} = \tau_o = 0.204$ nsec. Thus $c = 0.030$.

Next, the parameter d is found from Figure 5.1 by measuring the positive maximum amplitudes at $\phi_H = 60^\circ$ and $\phi_H = 0^\circ$. $r_H E_{\theta H}(\phi_H = 0^\circ)$ is proportional to $1/\tau_o$, which is proportional to 13/32". Also, $r_H E_{\theta H}(\phi_H = 60^\circ)$ is proportional to $1/((1 + d)(\tau_o + (cD/2v)))$, which is proportional to 9/32". Solving the ratio of the relative amplitude at $\phi_H = 0^\circ$ to the relative amplitude at $\phi_H = 60^\circ$, $d = 0.110$.

Finally, the parameter e is found from Figure 5.2 by measuring the positive maximum amplitudes at $\theta_H = 30^\circ$ and $\theta_H = 90^\circ$. $r_H E_{\theta H}(\theta_H = 90^\circ)$ is proportional to $1/\tau_o$, which is proportional to 7/32". Also, $r_H E_{\theta H}(\theta_H = 30^\circ)$ is proportional to $1/(\tau_o(1 - e))$, which is proportional to 12/32". Solving the ratio of the relative amplitude at $\theta_H = 90^\circ$ to the relative amplitude at $\theta_H = 30^\circ$, $e = 0.417$.

To summarize, an approximate closed form solution for the $r_H E_{\theta H}$ component of the radiation from the eight-inch TEM horn is

taken as equation (5-4) with the following parameters: τ_o = 204 picoseconds, D = 48", a = 0.177, b = 0.3615, c = 0.030, d = 0.110, and e = 0.417.

5.3 THEORETICAL RESULTS FOR GAUSSIAN-DERIVATIVE ILLUMINATION OF THE EXIT APERTURE FOR AN ISOTROPIC FEED

In this section, as a first order approximation to the electric far fields of the eight-inch TEM horn over the exit aperture of the paraboloid, equation (5-2) is used for $r_H E_{\theta H}$, and the $r_H E_{\phi H}$ component of the electric far field of the eight-inch horn is neglected with respect to the $r_H E_{\theta H}$ component. That is, as discussed in Section 4.4 of Chapter 4, the eight-inch TEM horn is considered as a point source feed, located at the focus of the paraboloid, whose angular radiation pattern is isotropic (gain $G(\Psi, \xi) = 1$) or is at least constant over the solid angle subtended by the paraboloid. This produces an exit aperture illumination which varies only as $1/\rho$. (See Silver (1965, 419). The isotropic feed is equivalent to Silver's equation (11) on page 419 with $G(\Psi, \xi) = 1$.)

In Section 5.4, the illumination used will be a better approximation to the actual tapered illumination produced by the eight-inch TEM horn. This better approximation is given by equation (5-4) and is hereafter identified by the words "tapered illumination".

Equations (C-92) and (C-93) in Appendix C were then programmed in Fortran for execution on a digital computer using equations (4-28) and (4-29) in Chapter 4. The relationship between V_1 and V'_{1A} is given

by equation (C-68) in Appendix C. The relationship between V_2 and V'_{2A} is given by equation (C-69) in Appendix C. In equations (C-68) and (C-69), the retarded time T is given by $T = t - (R/v)$. The spherical observation coordinates R,Θ,ϕ for the paraboloid reflector/TEM horn feed antenna system are indicated in Figure 4.1 of Chapter 4. A complete description and listing of the Fortran program utilizing equation (5-2) is given in Section E.1 of Appendix E.

To employ equation (5-2) for numerical computations, the value of the constant K had to be determined. This was accomplished as follows. For the gaussian-derivative form given by equation (5-2), the maximum value of $r_H E_{\theta H}$ is given by $r_H E_{\theta H max} = (\sqrt{2}/\tau)e^{-1/2}$. The gaussian pulse used by Martins et al. (1973) had a half-amplitude width of 340 picoseconds. Therefore, for this pulse, $\tau = 204$ picoseconds. Consider now Figure 2.7 in Chapter 2. From Figure 2.7, the positive maximum value of the gaussian-derivative response is $r_H E_{\theta H} = 4.088 \times 10^{-2}$. Therefore, for the approximate eight-inch TEM horn, $K = 9.74 \times 10^{-12}$. This value of K was included in the theoretical numerical program to compute the electric far fields of the paraboloid reflector/TEM horn feed antenna system.

The responses shown in subsequent figures in this chapter were computed for the paraboloid reflector, studied by Martins et al. (1973), with f = 20.16" and D = 48".

The theoretical boresight response of the antenna system for an isotropic feed, $RE_{\Theta}(\bar{R},t)\Big|_{(\Theta,\phi)=(0^o,0^o)}$, is shown in Figure 5.5. This response is the negative second derivative of the gaussian

BDM PARABOLOID/FEED SYSTEM--BORESIGHT

———Theoretical Results from Chernousov Formulation and Computer Runs

$T' = t - (R/v)$

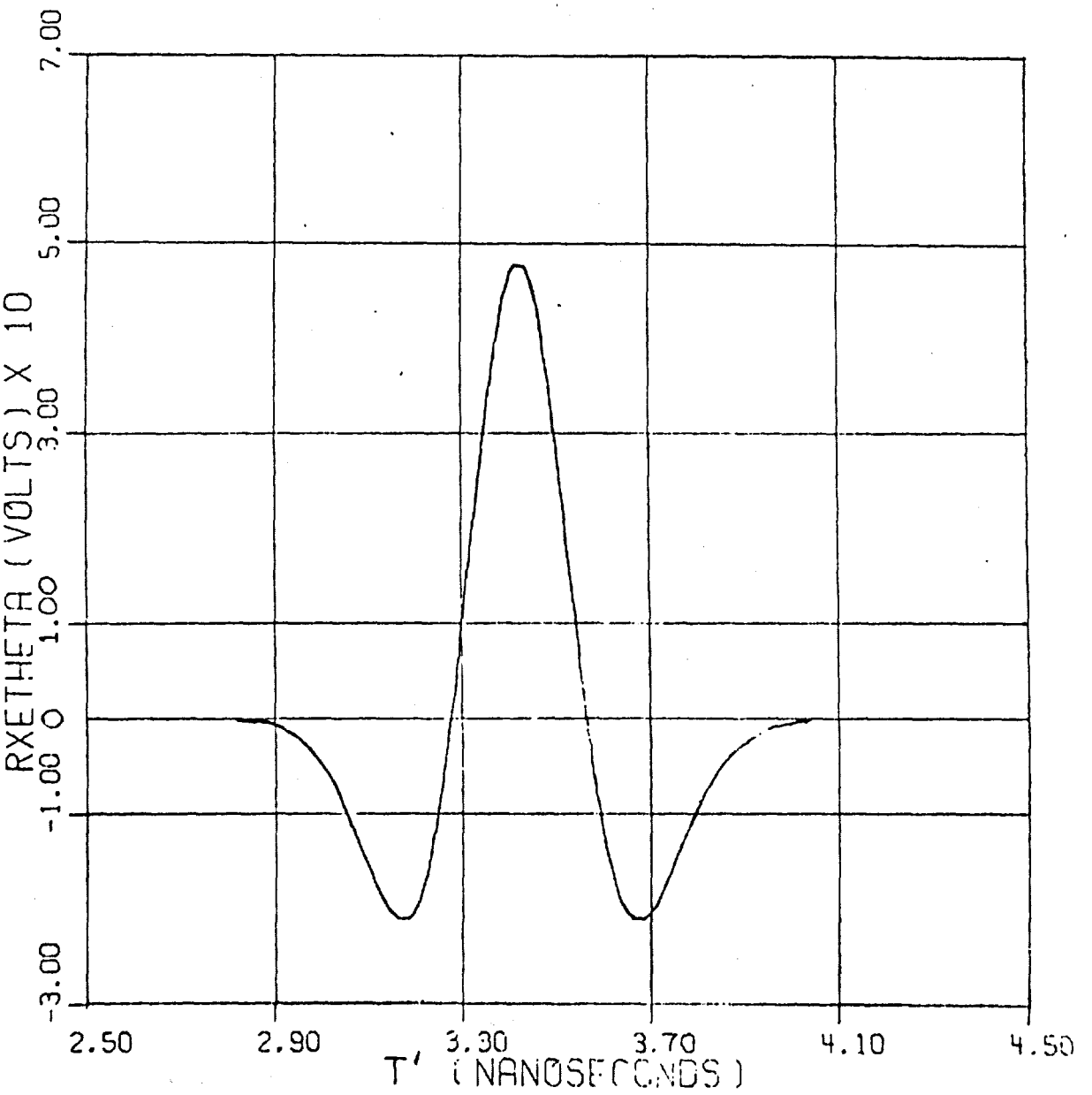

Figure 5.5

Boresight $RE_{\Theta}(\bar{R},t)$ at $\phi = 0^{\circ}$ for the System for an Isotropic Feed

excitation applied to the apex of the TEM horn. The gaussian excitation was assumed to have unit amplitude, as given by equation (5-3). However, as discussed in Section 2.6 of Chapter 2, the illumination function of the TEM horn, $f(\alpha,\beta)$, was normalized to unity for convenience in the theoretical numerical computations. The actual value of $f(\alpha,\beta)$ for the approximate eight-inch TEM horn was shown to be 5.62. Therefore, the value of the theoretical amplitude computed in Figure 5.5 should be multiplied by 5.62. The boresight response shown in Figure 5.5 is the theoretical numerical solution of equation (4-42) in Section 4.4 of Chapter 4 for the paraboloid studied by Martins et al. (1973).

Figure 5.6 shows the relative amplitudes of $RE_{\theta}(\bar{R},t)\Big|_{\phi = 0^{\circ}}$ for several values of θ. The boresight ($\theta = 0^{\circ}$) response is the same as that shown in Figure 5.5. In directions away from boresight in the $\phi = 0^{\circ}$ plane, the response of the system changes from the negative second derivative of the gaussian excitation applied to the apex of the TEM horn to a series of delayed replicas of gaussian derivatives. The center of the response in directions away from boresight is located in time at the center of the negative second derivative response in the boresight direction. Also, the delayed gaussian derivative replicas appear to emanate from opposite edges of the exit aperture of the paraboloid.

As a check on the results shown in Figure 5.6, $RE_{\phi}(\bar{R},t)$ at $\phi = 90^{\circ}$ was computed for the same values of θ. These results are identical to those shown in Figure 5.6.

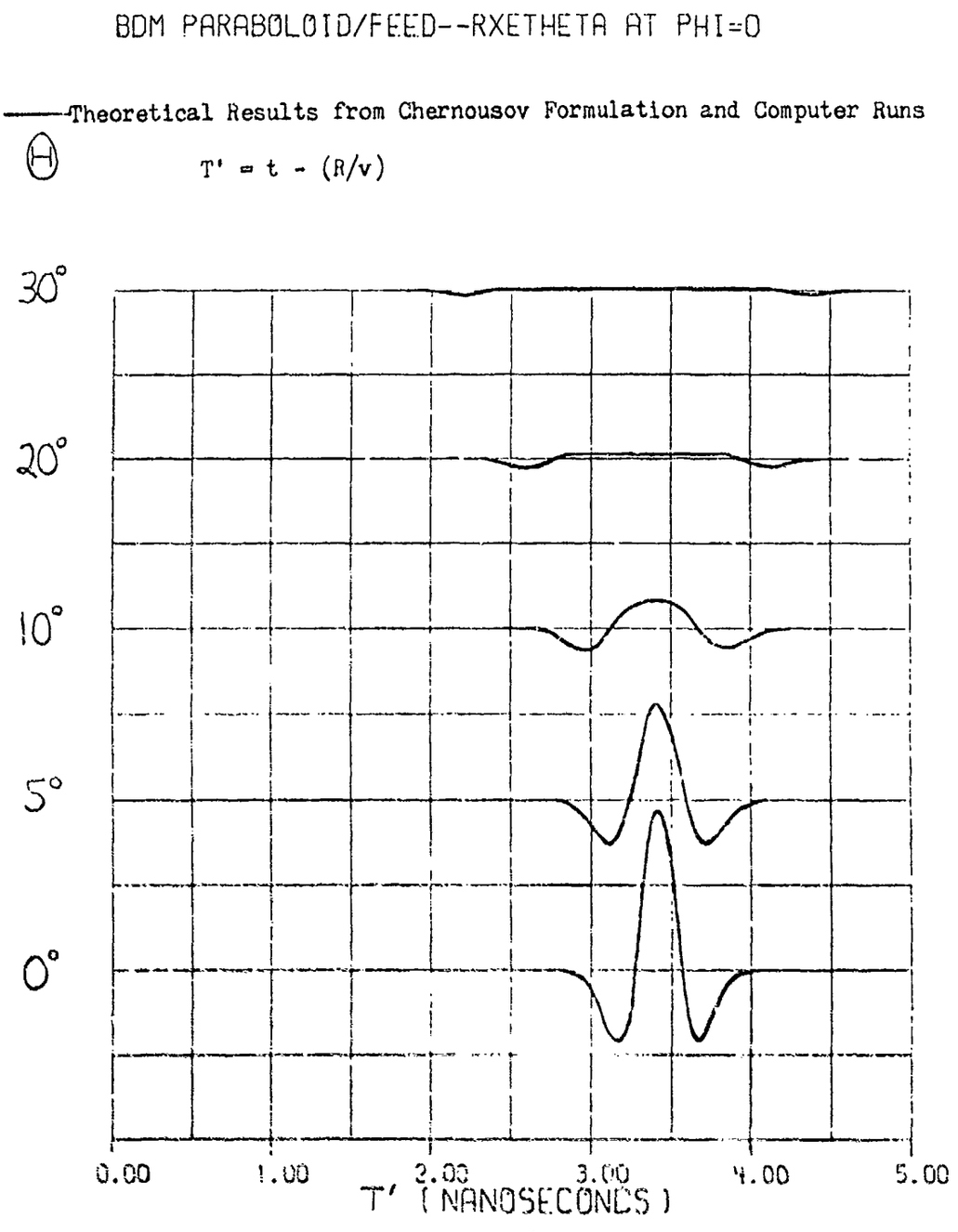

Figure 5.6

$RE_{\Theta}(\bar{R},t)$ at $\phi = 0^{\circ}$ for the System for an Isotropic Feed

5.4 THEORETICAL AND EXPERIMENTAL RESULTS FOR GAUSSIAN-DERIVATIVE TAPERED ILLUMINATION OF THE EXIT APERTURE

In this section, equation (5-4) is used as an approximation to the electric far field component $r_H E_{\theta H}$ of the eight-inch TEM horn over the exit aperture. Also, as in Section 5.3, the $r_H E_{\phi H}$ component of the electric far field of the eight-inch horn is neglected with respect to the $r_H E_{\theta H}$ component.

The Fortran computer program used to determine the theoretical responses for the tapered illumination uses the same equations as those discussed in Section 5.3, except that equation (5-4) was substituted for equation (5-2). A complete description and listing of the Fortran program utilizing equation (5-4) is given in Section E.2 of Appendix E.

Figure 5.7 shows the theoretical and experimentally measured boresight response of the system, that is, $RE_{\Theta}(\bar{R},t)\Big|_{(\Theta,\phi)=(0^\circ,0^\circ)}$. The experimental response, obtained by Martins et al. (1973:235), was normalized to have the same maximum amplitude as the theoretical response. A discussion of the absolute amplitude of the experimental response is reserved for Chapter 6. Also, as discussed in Section 5.3, the values of the amplitudes of both the theoretical and experimental responses shown in Figure 5.7 should be multiplied by 5.62.

The asymmetry of the experimental response in Figure 5.7 is believed to be due to the asymmetry of the experimental gaussian-derivative fields exciting the paraboloid as indicated in Figure 2.7. By comparison of Figure 5.7 with Figure 5.5, the effect of tapering

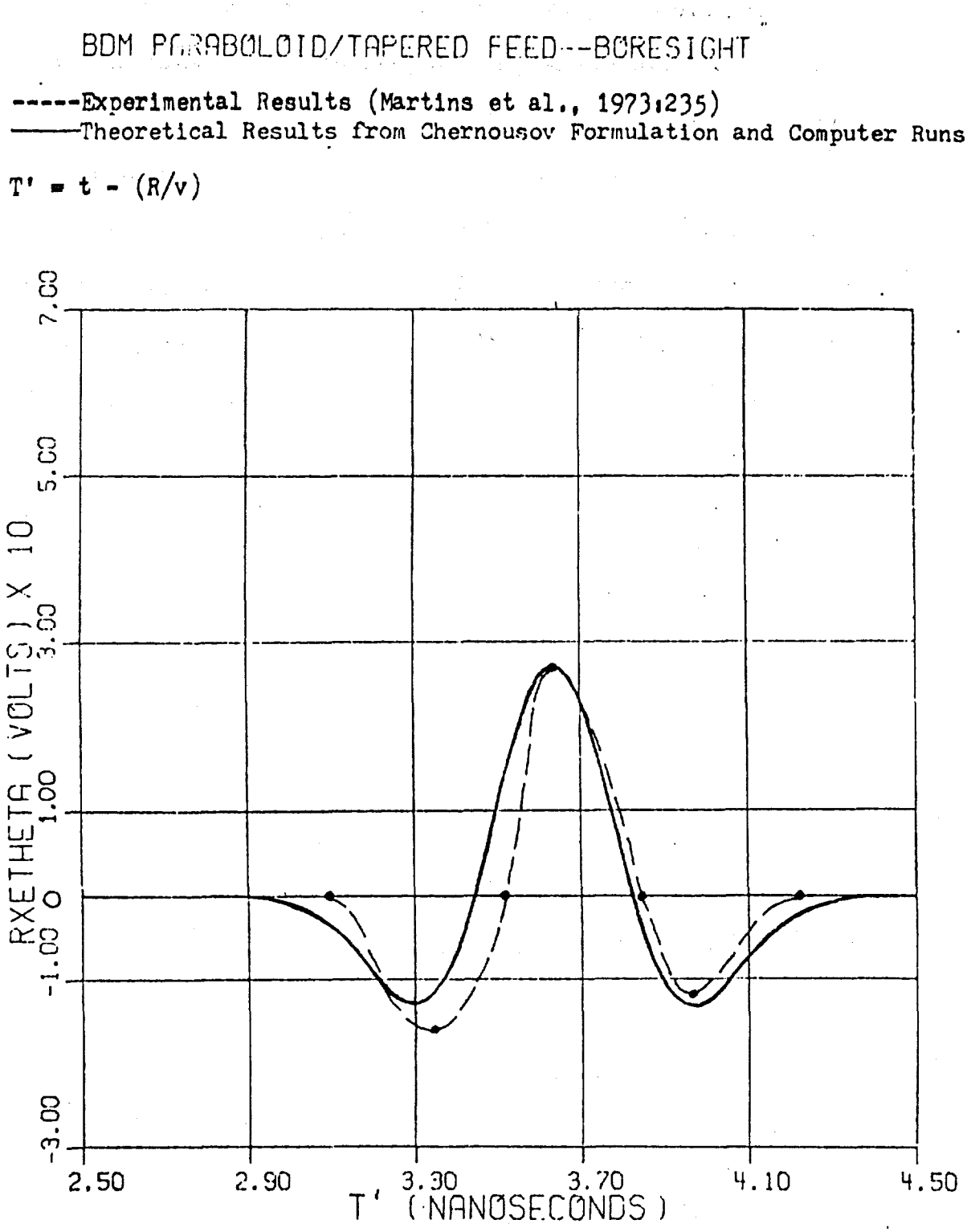

Figure 5.7

Boresight $RE_{\Theta}(\bar{R},t)$ at $\phi = 0^{\circ}$ for the System with Tapered Illumination

the exciting fields in space and time over the exit aperture is to reduce the boresight response in amplitude and to smear the boresight response in time.

Figures 5.8 and 5.9 show the theoretical relative responses for $RE_{\Theta}(\bar{R},t)\Big|_{\phi = 0^o}$ and $RE_{\phi}(\bar{R},t)\Big|_{\phi = 90^o}$ for several values of Θ respectively. The boresight ($\Theta = 0^o$) response for the system is shown to be the same in both Figures 5.8 and 5.9, as expected. This theoretical boresight response is the same as that shown in Figure 5.7.

The results shown in Figure 5.8 indicate that the maximum value of the response regresses from $T' = t - (R/v) = 3.70$ nanoseconds in the boresight direction to $T' = 3.00$ nanoseconds at $\Theta = 30^o$. Analytical attempts were made to demonstrate this regression in closed form, but they proved unsuccessful. This is due to the fact that the function chosen to represent the $r_H E_{\theta H}$ component of the electric far field of the eight-inch horn, namely equation (5-4), involves tapering in both space and time. Therefore, the time function cannot be brought outside the double integrals which represent the far fields of the system in terms of the fields over the exit aperture. Also, the sidelobe structure for the system with tapered illumination of the exit aperture is more complicated than for the case of illumination by an isotropic feed, as given by equation (5-2).

In Figure 5.9, the time regression of the maximum value of the response from the boresight ($\Theta = 0^o$) direction to the $\Theta = 30^o$ direction is much less pronounced, and the results shown in Figure

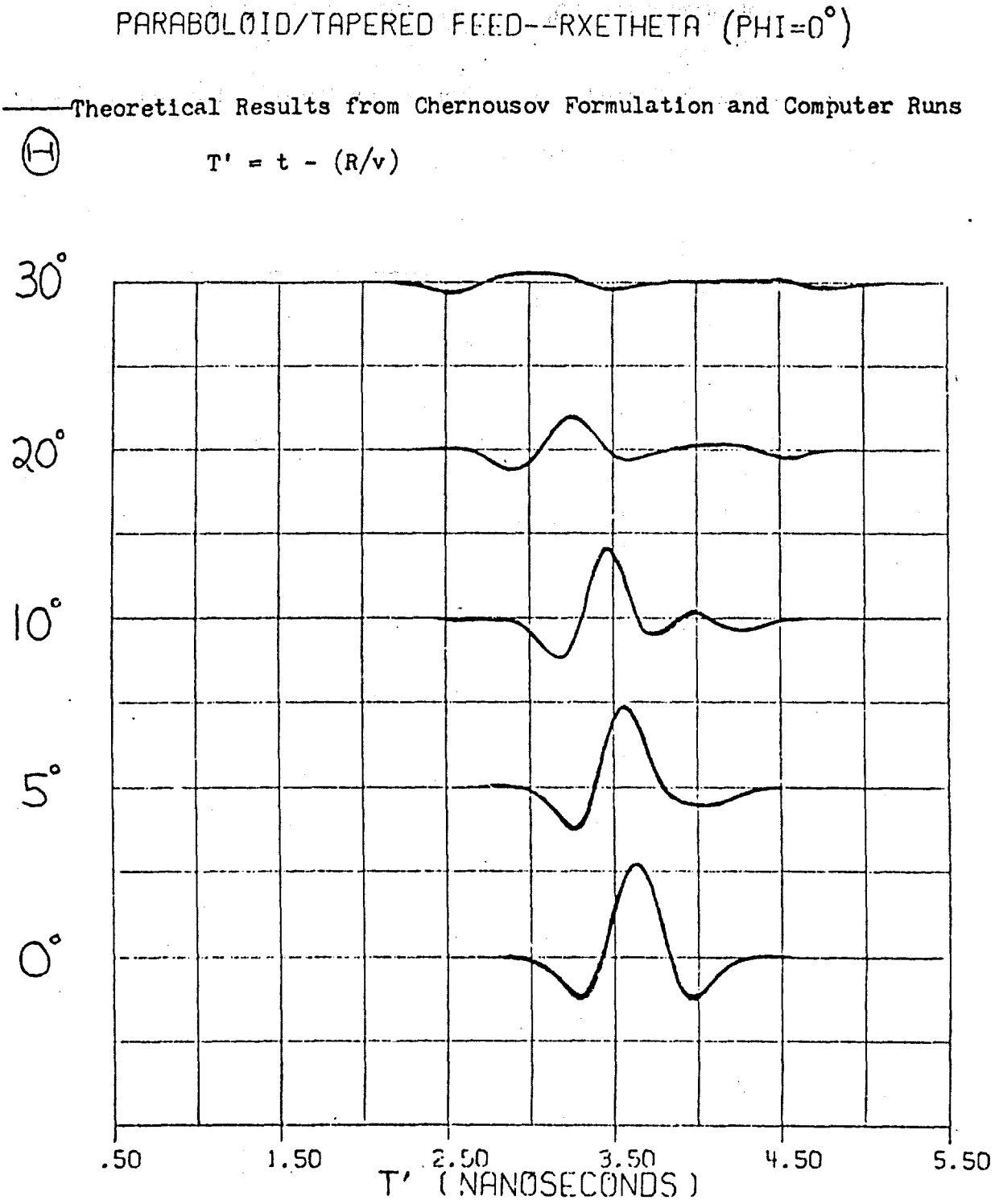

Figure 5.8

$RE_{(H)}(\bar{R},t)$ at $\phi = 0^{\circ}$ for the System with Tapered Illumination

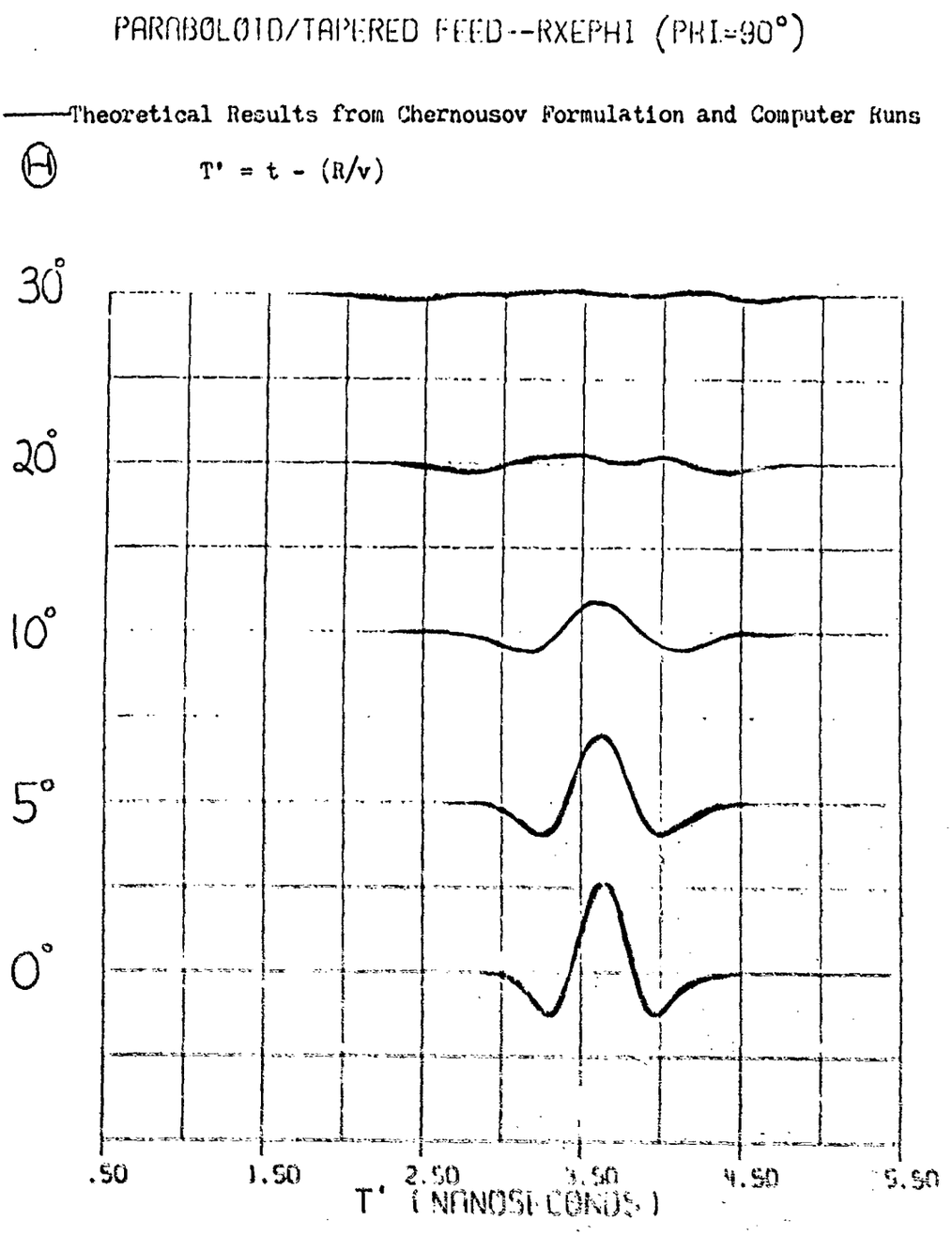

Figure 5.9

$RE_\phi(R,t)$ at $\phi = 90°$ for the System with Tapered Illumination

5.9 are not identical to those shown in Figure 5.8, except in the boresight direction. These effects are also due to the tapering of the illumination of the exit aperture in both space and time.

The inability to arrive at simple closed form solutions to characterize the sidelobe structure of the antenna system could be predicted from the results of equation (4-42) in Chapter 4. That is, equation (4-42) represents the boresight response of the system for illumination of the exit aperture by an isotropic point source feed. Even for this simple case, the response is shown to be of the form of the negative time derivative of the fields exciting the exit aperture multiplied by double integrals in space. Since the inner integrals are similar to elliptic integrals, the double integrals could not be evaluated in closed form. In directions away from boresight, the time function cannot be brought outside the double integrals which represent the far fields of the system in terms of the fields over the exit aperture, even for the simple case of illumination of the exit aperture by an isotropic point source feed.

Chapter 6

CONCLUSIONS AND SUMMARY

6.1 INTRODUCTION

In this chapter are summarized the principal theoretical results obtained in this thesis and comparisons with available experimental data.

6.2 COMPARISON OF THEORY WITH EXPERIMENT

It has turned out to be impracticable to compare the various theoretical results derived in this thesis with the experimental values obtained by Martins et al. (1973) on an absolute basis. The reason is that it appears that further work is necessary to render self-consistent the various transmit and receive measured data in Martins' work with his own theory. There are variations as large as four to one among Martins' theoretically predicted values and experimentally measured values. Also, Martins did not use any sensor whose absolute calibration is established beyond question. Thus, the sensors used by Martins have not been calibrated against a "standard" sensor. The introduction of standards in time domain measurements is an area which needs much more work.

The experimental facilities at the University of Vermont are inadequate to duplicate, much less refine, the key measurements made

by Martins. Because of this, and because of the large degree of uncertainty concerning the absolute values as established by Martins' measurements, it was decided to be impractical to make any comparisons with Martins on an absolute basis. Also, Susman and Lamensdorf (1970, 42-44) made experimental measurements on a relative basis only. Therefore, necessarily, all comparisons between theory and experiment have been made on a relative basis. This is effected by normalizing the experimental boresight response to have the same peak value as the corresponding theoretical boresight response. Once this is done, the theoretical and experimental curves may then be compared with respect to shape, slope, relative values of other peaks, zero crossings, etc.

Figures 2.3, 2.4, and 2.5 show the comparison between theoretically computed responses and experimentally measured responses for the three TEM horns studied experimentally by Susman and Lamensdorf (1970,42-44). The geometry for these three TEM horns is shown in Figure 2.1. As discussed in the previous paragraph, the experimental boresight ($\phi = 0^{o}$) response was normalized to have the same peak value as the theoretically computed response. In general, Figures 2.3, 2.4, and 2.5 show reasonable agreement between theory and experiment. In Figure 2.3, spikes appear on the theoretical results for $\phi = 60^{o}$, 90^{o}, and 120^{o}. This effect is believed to be due to the approximation of the TEM horn as a set of three radiating apertures when the front aperture is electrically small, that is--when the electrical dimensions of the front aperture are less than or comparable with the exciting waveform's characteristic time

dimensions. (For a more detailed discussion see pages 32 and 36.) This spike phenomenon does not occur in directions at or near boresight, which is the important direction for the paraboloid/horn system. Also, there are differences in the dc levels of the theoretical and experimental responses for ϕ between 120° and 180°. This effect is believed to be due to the fact that Susman and Lamensdorf (1970) established the experimental zero level in these directions to be the amplitude of the positive delayed replica response when this amplitude was small and not noticeable experimentally. Finally, for ϕ between 90° and 180°, the experimental responses are smeared in time with respect to the theoretically computed responses. This effect has not been explained theoretically.

The eight-inch TEM horn studied by Martins et al. (1973) is shown in Figure 2.6. This horn was approximated by a horn of the type shown in Figure 2.1, and the approximation is discussed in Section 2.5. The theoretical and experimental results for the eight-inch TEM horn are shown for three angular directions in the azimuth plane in Figures 2.7, 2.8, and 2.9. In Figure 2.7, the experimental boresight response was normalized to have the same peak value as the theoretically computed response. This scaling factor was left unchanged for Figures 2.8 and 2.9. Consider first Figure 2.7. The theoretical boresight response is an approximately symmetric derivative of the exciting gaussian pulse followed by a positive replica of the exciting pulse retarded by the round trip time from the apex. The experimental response is a derivative-type radiation of the exciting gaussian

pulse followed by a more complicated series of delayed replicas approximately delayed in time by the round trip time from the apex. The asymmetry in the experimental derivative response is believed to be due to the effect of the rectangular front aperture of the actual eight-inch horn shown in Figure 2.6. This effect is discussed in Section 2.6. The negative going experimental pulses located near the round trip time from the apex appear to be due to the theoretical neglect of the finiteness of the gap at the apex. Consider secondly Figure 2.8. Again, the experimental asymmetry of the gaussian derivative response is evident. Consider finally Figure 2.9. This figure shows reasonable agreement between theory and experiment except that the experimentally measured response is relatively flat around the retarded time 0.50 nanoseconds for a duration of approximately 300 picoseconds. Thus, the theoretically computed second and third delayed replicas are displaced in time from the experimentally determined second and third delayed replicas by approximately 300 picoseconds. The reason for the experimental flat response about the retarded time 0.50 nanoseconds has not been resolved.

Figure 5.7 shows the theoretical and experimental boresight response for the eight-inch TEM horn feeding the paraboloid studied by Martins et al. (1973). The paraboloid had $f = 20.16"$ and $D = 48"$. The theoretical response was computed by reducing the eight-inch TEM horn to a point source feed located at the focus of the paraboloid, using the geometrical optics approximation, and employing equation (5-4) to represent the normalized electric far fields over the exit

aperture of the paraboloid. The technique of reducing the eight-inch horn to an approximate point source radiator is discussed in Sections 5.1 and 5.2. In Figure 5.7, the experimental response was normalized to have the same peak value as the theoretical response. Reasonable agreement between theory and experiment is indicated. The asymmetry of the experimental response is due to the asymmetry of the experimental gaussian derivative fields exciting the paraboloid as indicated in Figures 2.7 and 2.8.

6.3 SUMMARY

The primary objective of this research was to study theoretically, directly in the time domain, the electromagnetic far fields of a paraboloid reflector fed by a TEM horn. This antenna system is shown in Figure 1.1. The TEM horn, located near the focus of the paraboloid, is excited at its apex by a voltage V(t). The TEM horn consists of two metallic circular sectors separated by a small gap at the apex and flared apart away from the apex. At the present time, no direct time domain models exist to describe the radiation of the TEM horn or the paraboloid reflector/TEM horn antenna system at an arbitrary observation point in the far field.

Specifically, the study of the above antenna system was accomplished as follows. A general theoretical model applicable to aperture antennas of any type excited by electromagnetic fields of any form in space and time is a set of time domain integrals which were derived by Chernousov (1965). The electromagnetic fields over

a closed surface including the aperture surface must be known (or guessed at). The geometry for the Chernousov derivation is shown in Figure A.1, and the complete mathematical details of the Chernousov derivation are presented in Appendix A. The resulting equation which describes the electric far fields of the aperture antenna in terms of the fields exciting the aperture is equation (A-102). The magnetic far fields are related to the electric far fields by the simple relationship (A-103).

The TEM horn of the type studied by Susman and Lamensdorf (1970,1971) is shown in Figure 2.1. As discussed in Section 2.1, this TEM horn was approximated by a set of three radiating apertures. These three apertures consist of a front aperture and two wedge-shaped side apertures. The horn shown in Figure 2.1 was assumed to be excited at its apex by a voltage V(t), and the Chernousov formulation was applied to the fields existing over the three apertures. Complete mathematical details of the application of the Chernousov formulation to the TEM horn are furnished in Appendix B. The resulting expressions for the components of the electric far fields of the TEM horn are given by equations (B-89) and (B-90).

Next, approximate closed form solutions for (B-89) were found in the azimuth plane of the TEM horn when the front aperture is electrically small, that is--when the electrical dimensions of the front aperture are less than or comparable with the exciting waveform's characteristic time dimensions. These closed form solutions give engineering insight into the behavior of the TEM horn, and the

details of the derivation are presented in Section 2.3. Equation (2-26) is the approximate closed form solution for the radiation from the TEM horn in the boresight direction, and it is repeated below for the reader's convenience.

$$E_{\theta_{BORESIGHT}}(\bar{r},t) \approx \frac{r_a \beta_o V'[T]}{2\pi v r} - \frac{k_v \beta_o}{4\pi r}\left\{V\left[T - \frac{r_a}{v}\left(1-\cos\beta_o\right)\right] - V\left[T - \frac{2r_a}{v}\right]\right\} \qquad (6\text{-}1)$$

This radiation is shown to be a combination of two forms of far fields. The first term of (6-1) is a field which is the time derivative of the excitation at the apex. The second and third terms of (6-1) are of the form of delayed replicas of the excitation.

From equations (2-13) and (2-29), the approximate closed form solution for radiation from the TEM horn in the backfire direction is

$$E_{\theta_{BACKFIRE}}(\bar{r},t) \approx -\frac{k_v r_a \beta_o}{2\pi v r} V'\left[T - \frac{2r_a}{v}\right] + \frac{\beta_o}{4\pi r}\left\{V[T] - V\left[T - \frac{r_a}{v}\left(1+\cos\beta_o\right)\right]\right\} \qquad (6\text{-}2)$$

This radiation is also a combination of two forms of far fields. The first term of (6-2) is a negative time derivative of the excitation which occurs at the round trip time from the apex. The second and third terms of (6-2) are of the form of delayed replicas of the excitation. The ratio of the amplitude of the backfire derivative response to the boresight derivative response is minus the reflection coefficient at the front aperture of the TEM horn.

From equations (2-9) and (2-30), the approximate closed form

solution for directions in the azimuth plane well removed from boresight and backfire for the TEM horn is

$$E_\theta(\bar{r},t)\Big|_{\substack{\phi\neq 0^\circ \\ \phi\neq 180^\circ}} \approx \frac{r_a \beta_o}{4\pi v r}\left\{\left[(1+\cos\phi) - k_V(1-\cos\phi)\right]\right.$$

$$\left.\times V'\left[T - \frac{r_a}{v}(1-\cos\phi)\right]\right\} + \left\{\frac{\beta_o}{2\pi r}\left\{\frac{1}{1-\cos\phi}V[T] - \left(\frac{1}{1-\cos\phi}\right.\right.\right.$$

$$\left.\left.\left. + \frac{k_V}{1+\cos\phi}\right)V\left[T - \frac{r_a}{v}(1-\cos\phi)\right] + \frac{k_V}{1+\cos\phi}V\left[T - \frac{2r_a}{v}\right]\right\}\right\} \quad (6\text{-}3)$$

This radiation also consists of two forms. One form is a sum of three delayed replicas of the excitation at the apex of the TEM horn. The amplitude and time occurrence of these replicas depend upon the angular direction in the azimuth plane. The other form is a delayed time derivative of the excitation at the apex whose amplitude and time occurrence also depend upon the angular direction in the azimuth plane.

Equations (B-89) and (B-90) were then programmed in Fortran for execution on a digital computer, in order to determine numerically the electric far fields of a given TEM horn of the type studied by Susman and Lamensdorf (1970,1971). The comparison of theoretical and experimental results for the three TEM horns studied experimentally by Susman and Lamensdorf is presented in Figures 2.3, 2.4, and 2.5. In general, there is good agreement between theory and experiment. A more detailed discussion of the comparison between theory and experiment for Figures 2.3, 2.4, and 2.5 is given in Section 6.2.

The eight-inch TEM horn, studied by Martins et al. (1973), is shown in Figure 2.6. This horn was approximated by the type of TEM horn studied by Susman and Lamensdorf (1970,1971), as discussed in Section 2.5. Utilizing the Fortran program for executing equations (B-89) and (B-90) on a digital computer, the theoretical results were compared with experimental results obtained by Martins et al. (1973) as shown in Figures 2.7, 2.8, and 2.9. In general, there is reasonable agreement between theory and experiment. A more detailed discussion of Figures 2.7, 2.8, and 2.9 is given in Section 6.2.

For the sake of completeness, the theoretical waveforms of relative amplitudes vs. time of the approximate eight-inch TEM horn electric far field are given in Figure 2.10 for various azimuthal directions.

In Chapter 3, an approximate model of the TEM horn is considered to be a section of a biconical antenna. The vector potential formulation is then used to determine the electric far fields of the biconical section in terms of the fields arising within the antenna region due to the excitation $V(t)$ at the apex. Approximate closed form solutions for the electric far field of the biconical section in the azimuth plane are also found. Equation (3-36) is the approximate closed form solution in the boresight direction, and this equation is identical to equation (6-1) obtained using the aperture model of the TEM horn. Equation (3-38) is the approximate closed form solution in the backfire direction and is identical to equation (6-2) obtained using the aperture model. Therefore, in the boresight

and backfire directions, the vector potential approach is self-consistent with the results obtained by the aperture approach. In directions well removed from boresight and backfire, the vector potential approach produces the approximate closed form solution given by equation (3-39). This result differs from the closed form result equation (6-3) obtained from the aperture model in that the derivative radiation of the front aperture given in equation (6-3) does not appear in (3-39). As discussed in Section 2.4, the superposition of the derivative radiation upon the delayed replica radiation is due to the approximation of the TEM horn as a structure of three apertures when the front aperture is electrically very small.

In Chapter 4, the electric far fields of a paraboloid reflector/point source feed antenna system are found in terms of the fields of the feed over the exit aperture of the paraboloid. This was accomplished as follows. It was assumed that at the focus of the paraboloid there exists a spherical-wave point source radiator whose electric far field components may be described by equations (4-1) and (4-2). Next, the following assumptions were made: (1) The paraboloid reflector was assumed to be in the far field of the point source feed. (2) The reflector was assumed to be sufficiently smooth to allow the application of the plane wave boundary conditions at the perfectly conducting surface. (3) The geometrical optics approximation was invoked to afford a one-to-one, point-to-point transformation between the fields at the paraboloid surface and the fields at the exit aperture. (4) The Chernousov (1965) formulation requires

a closed aperture surface. In keeping with common practice, this closed surface is taken as a plane containing the exit aperture of the paraboloid and closed at infinity, and the fields over the non-aperture part of the plane are taken as approximately zero (Ramo and Whinnery, 1956:530,532). (5) Edge effects at the exit aperture are not considered. The Chernousov formulation was then applied to find the electric far fields of the paraboloid reflector/point source feed antenna system in terms of the fields existing over the exit aperture. The excitation used is described by equations (4-1) and (4-2). The complete mathematical details of the application of the Chernousov formulation are presented in Appendix C. The resulting electric far fields of the paraboloid reflector/point source feed are given by equations (C-92) and (C-93).

In Section 4.4, solutions for the electric far fields of the paraboloid reflector/point source feed are derived for the case when the point source feed has an angular radiation pattern which is isotropic (gain = 1) or is at least constant over the solid angle subtended by the paraboloid. The resulting electric far fields are given for the boresight direction by equations (4-42) and (4-43). These equations show that the form of the boresight fields is the negative time derivative of the fields exciting the exit aperture.

Chapter 5 presents theoretical and experimental results for the paraboloid reflector/TEM horn feed antenna system and also theoretical results for a paraboloid reflector fed by an isotropic point source feed. Sections 5.1 and 5.2 present the method of reducing the

eight-inch TEM horn studied by Martins et al. (1973) to a point source feed located at the focus of the paraboloid. This reduction was accomplished as follows. First, the eight-inch TEM horn, shown in Figure 2.6, was approximated by a TEM horn of the type studied by Susman and Lamensdorf (1970,1971), shown in Figure 2.1. Secondly, for unit amplitude gaussian excitation at the apex of the approximate eight-inch TEM horn, equations (B-89) and (B-90) were programmed in Fortran for execution on a digital computer. These equations represent the application of the Chernousov (1965) formulation to the TEM horn, which is considered as a structure of three apertures. Computer runs of (B-89) and (B-90) were then performed to characterize the fields of the eight-inch TEM horn over the angular aperture of the 48-inch paraboloid with f = 20.16" studied by Martins et al. (1973). The results of the computer runs in both the azimuth and polar planes of the horn are shown in Figures 5.1 through 5.4. Thirdly, from the results of the computer runs, an approximate closed form solution for the far fields of the TEM horn was developed. This approximate closed form is given by equation (5-4). By inspection of Figures 5.1 and 5.2, the various parameters involved in equation (5-4) were determined.

Section 5.3 presents theoretical results for the 48-inch paraboloid when fed by an isotropic point source feed located at the focus of the paraboloid. The electric far field of the isotropic point source feed was taken as equation (5-2), and equations (C-92) and (C-93) were programmed in Fortran for execution on a digital computer. The theoretical results of the computer runs for the isotropic

feed are shown in Figures 5.5 and 5.6. Figure 5.5 is the theoretical numerical solution of equation (4-42) for the 48-inch paraboloid. Since the far field of the isotropic feed was assumed to be gaussian derivative in time, the boresight response of the paraboloid fed by the isotropic feed is the negative of the second gaussian derivative in time. This numerical result from the general equation (C-92) confirms the form of the boresight solution given by equation (4-42). Figure 5.6 shows the response of the paraboloid reflector fed by an isotropic feed on boresight and for several directions away from boresight. Away from boresight, the response of the system changes from the negative second gaussian derivative response to delayed replicas of the gaussian derivative fields exciting the exit aperture. These delayed replicas appear to emanate from diametrically opposite points of the exit aperture.

Section 5.4 presents theoretical and experimental results for the 48-inch paraboloid reflector when excited by the point source approximation of the eight-inch TEM horn as given by equation (5-4). Computer runs were performed using equations (C-92) and (C-93), as in Section 5.3, except that equation (5-4) was utilized rather than equation (5-2). The results of these computer runs are shown in Figures 5.7, 5.8, and 5.9. Figure 5.7 shows the theoretically computed and experimentally measured boresight response of the 48-inch paraboloid reflector/eight-inch TEM horn feed system. The experimentally measured response was normalized to have the same maximum amplitude as the theoretical response. Figure 5.7 indicates good

relative agreement between theory and experiment. A more detailed comparison between theory and experiment is given in Section 6.2. The effect of tapering the fields exciting the exit aperture in both space and time, as indicated by comparison of Figure 5.7 with Figure 5.5, is to reduce the boresight response in amplitude and to smear the boresight response in time. Figures 5.8 and 5.9 show the response of the 48-inch paraboloid reflector/eight-inch TEM horn feed antenna system on boresight and for several directions away from boresight for both components of the electric far field of the system. The theoretical boresight response shown in Figures 5.8 and 5.9 is the same, as expected. However, in directions away from boresight, the response of the system changes from a negative second gaussian derivative response to a series of delayed gaussian derivative replicas which are no longer symmetric in amplitude or time with respect to the boresight response. Thus, the sidelobe structure of the 48-inch paraboloid reflector/eight-inch TEM horn feed antenna system is more complicated than the sidelobe structure for the paraboloid reflector fed by an isotropic point source feed, as shown in Figure 5.6. This is due to the fact that the electric far field of the approximate point source TEM horn, as given by equation (5-4), is tapered in both space and time.

REFERENCES

Abo-Zena, A. M. and R. E. Beam (1972), "Transient radiation field of a circular loop antenna," IEEE Transactions on Antennas and Propagation, vol. AP-20, May 1972, pp. 380-383.

Cheng, D. K. and F. I. Tseng (1964), "Transient and steady-state antenna pattern characteristics for arbitrary time signals," IEEE Transactions on Antennas and Propagation, vol. AP-12, July 1964, pp. 492-493.

Chernousov, V. S. (1965), "Nonstationary radiation of antenna systems," Radio Engineering and Electronic Physics, (Russian, English translation), vol. 10, no. 8, 1965, pp. 1246-1252.

Collin, Robert E. and Francis J. Zucker (eds.) (1969), Antenna Theory, Part II, Inter-University Electronics Series, vol. 7. New York: Mc-Graw Hill Book Co., 1969.

Cronson, Harry M. (1969), "An impulse scattering range," Proceedings IEEE, vol. 57, November 1969, p. 2094.

Cronson, H. M. and J. M. Proud (1970a), Wideband Antenna Development, Rome Air Development Center Final Technical Report, RADC-TR-70-74, (Rome, N. Y.), May 1970. (AD 870 224L)

Cronson, Harry M. and Joseph M. Proud, Jr. (1970b), "Time domain ray analysis," Proceedings IEEE, vol. 58, September 1970, pp. 1383-1384.

DeLorenzo, J. D. (1967), "Video time-domain scattering range," IEEE NEREM Record, November 1967, pp. 80-81.

Mandelsman, Morris (1972), Time Domain Impulse Antenna Study, Rome Air Development Center Final Technical Report, RADC-TR-72-105, (Rome, N. Y.), May 1972. (AD 744 837)

Harrison, C. W. Jr. (1962), Tables of Impedance and Radian Effective Half-Length of Electrically Long Cylindrical Antennas of Fixed Length to Diameter Ratio, Sandia Corp., (Albuquerque, N. M.), SCR-576, November 1962.

Harrison, C. W. Jr. (1963a), Tables of Impedance and Radian Effective Length of Wide-Angle Conical Antennas, Sandia Corp., (Albuquerque, N. M.), SCR-662, June 1963.

Harrison, C. W. Jr. (1963b), "The radian effective half-length of cylindrical antennas less than 1.3 wavelengths long," IEEE Transactions on Antennas and Propagation, vol. AP-11, November 1963, pp. 657-660.

Harrison, C. W. Jr. and C. S. Williams, Jr. (1963), Transients in Wide-Angle Conical Antennas, Sandia Corp., (Albuquerque, N. M.), SCR-663, June 1963.

Harrison, C. W. Jr. and C. S. Williams, Jr. (1965), "Transients in wide-angle conical antennas," IEEE Transactions on Antennas and Propagation, vol. AP-13, March 1965, pp. 236-246.

Harrison, C. W. Jr. and R. W. P. King (1967), "On the transient response of an infinite cylindrical antenna," IEEE Transactions on Antennas and Propagation, vol. AP-15, March 1967, pp. 301-302.

Jordan, Edward C. and Keith G. Balmain (1968), Electromagnetic Waves and Radiating Systems. 2d ed.; Englewood Cliffs, N. J.: Prentice-Hall, Inc., 1968.

Knop, Charles M. (1970), "On transient radiation from a log-periodic dipole array," IEEE Transactions on Antennas and Propagation, vol. AP-18, November 1970, pp. 807-808.

Lamensdorf, David (1970), "The transient response of the coaxial cone antenna," IEEE Transactions on Antennas and Propagation, vol. AP-18, November 1970, pp. 799-802.

Martins, Vasco C. et al. (1973), Picosecond Pulse Reflector Antenna Investigation, Rome Air Development Center Final Technical Report, RADC-TR-73-215, (Rome, N. Y.), July 1973. (AD 774 132)

Mayo, B. R. (1961), "Transient behavior of aperture antennas," Proceedings IRE, vol. 49, April 1961, pp. 817-819.

Morgan, S. P. (1962), "Transient behavior of a dipole antenna," Journal of Mathematical Physics, vol. 3, no. 3, 1962, p. 564.

Palciauskas, R. J. and R. E. Beam (1970), "Transient fields of thin cylindrical antennas," IEEE Transactions on Antennas and Propagation, vol. AP-18, March 1970, pp. 276-278.

Polk, C. (1960), "Transient behavior of aperture antennas," Proceedings IRE, vol. 48, July 1960, pp. 1281-1286.

Ramo, Simon and John R. Whinnery (1956), Fields and Waves in Modern Radio. 2d ed.; New York: John Wiley and Sons, Inc., 1956.

Ross, G. F. (1967), "A new wideband antenna receiving element," IEEE NEREM Record, November 1967, pp. 78-79.

Schelkunoff, Sergei A. (1952), Advanced Antenna Theory. New York: John Wiley and Sons, Inc., 1952.

Schelkunoff, Sergei A. and Harald T. Friis (1952), Antennas Theory and Practice. New York: John Wiley and Sons, Inc., 1952.

Schmitt, Hans J. (1960), "Transients in cylindrical antennae," Proceedings IEE (London), pt. C, Monograph no. 377E, April 1960, pp. 292-298.

Schmitt, H. J., C. W. Harrison, Jr., and C. S. Williams, Jr. (1966), "Calculated and experimental response of thin cylindrical antennas to pulse excitation," IEEE Transactions on Antennas and Propagation, vol. AP-14, March 1966, pp. 120-127.

Silver, Samuel (1965), Microwave Antenna Theory and Design, ed. Samuel Silver. New York: Dover Publications, Inc., 1965. (Unabridged and unaltered republication of vol. 12 in the M. I. T. Radiation Laboratory Series (1949).)

Stekert, J. J. and L. J. Fitzgerald (1973), Transient Response of an Asymmetric Cylindrical Antenna, Ikor, Inc., (Burlington, Mass.), January 8, 1973. (Xeroxed.)

Susman, Leon and David Lamensdorf (1970), Picosecond Pulse Antenna Techniques, SRRC-CR-70-21, Sperry Rand Research Center, (Sudbury, Mass.), or Rome Air Development Center Interim Report, RADC-TR-70-205, (Rome, N. Y.), August 1970. (AD 877 569)

Susman, Leon and David Lamensdorf (1971), Picosecond Pulse Antenna Techniques, SRRC-CR-71-4, Sperry Rand Research Center, (Sudbury, Mass.), or Rome Air Development Center Final Technical Report, RADC-TR-71-64, (Rome, N. Y.), February 1971. (AD 884 646)

Tseng, F. I. and D. K. Cheng (1964), "Antenna pattern response to arbitrary time signals," Canadian Journal of Physics, vol. 42, July 1964, pp. 1358-1368.

Wu, T. T. (1961), "Transient response of a dipole antenna," Journal of Mathematical Physics, vol. 2, November-December 1961, pp. 892-894.

Appendix A

DERIVATION OF THE CHERNOUSOV EQUATIONS

The purpose of this appendix is to fill in the details of the derivation of the equations which appear in the terse paper by Chernousov (1965).

The general theoretical expressions which were used in this research are a set of integrals first derived by Chernousov (1965). These integrals are derived directly in the time domain. They describe the electromagn tic fields arising from a closed aperture surface S_a in a homogeneous source-free medium excited by fields of any form in space and time. The fields exciting the aperture surface must be known (or guessed at). The Huygens-Kirchhoff principle is used in the derivation--that is, the electromagnetic fields arising from S_a are calculated from secondary sources at the antenna surface due to the boundary conditions there.

The derivation of the basic equations parallels the development given in Jordan and Balmain (1968,313-315,466-469). The geometry for the problem is shown in Figure A.1. The various quantities used in the derivation are:

$\bar{r}_s$, the vector from the origin to the surface element ds,

$\hat{n}$, the outward normal to ds,

$\bar{r}$, the vector from the origin to the observation point $M(\bar{r})$,

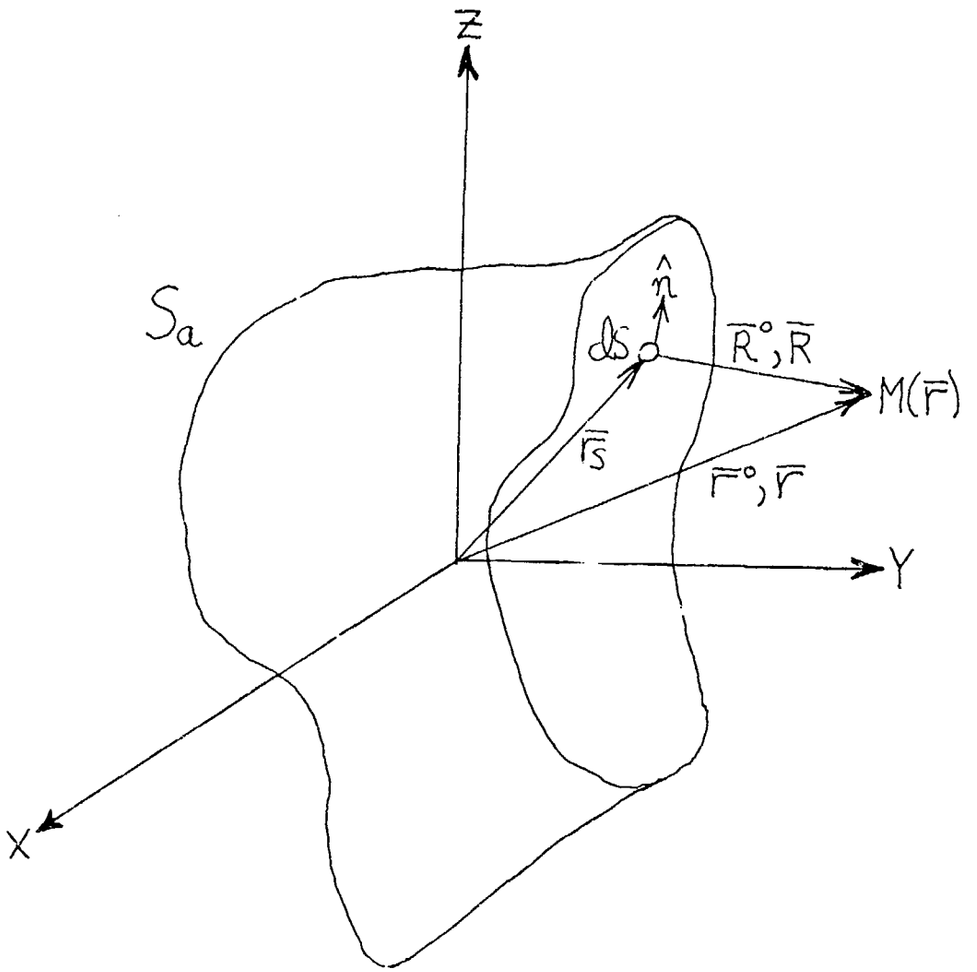

Figure A.1

Geometry for the Chernousov Derivation

$\bar{r}^o$, the unit vector in the $\bar{r}$ direction,

$\bar{R}$, the vector from ds to $M(\bar{r})$,

$\bar{R}^o$, the unit vector in the $\bar{R}$ direction

η, the impedance of the medium,

μ, the permeability of the medium,

ϵ, the permittivity of the medium, and

v, the velocity of propagation in the medium.

Including both a fictitious magnetic current $\bar{M}$ and a fictitious magnetic charge density ρ_m as well as an electric current $\bar{J}$ and an electric charge density ρ, Maxwell's equations would be written as follows:*

$$\nabla \times \bar{H} = \dot{\bar{D}} + \bar{J} \tag{A-1}$$

$$\nabla \times \bar{E} = -\dot{\bar{B}} - \bar{M} \tag{A-2}$$

$$\nabla \cdot \bar{E} = \rho/\epsilon \tag{A-3}$$

$$\nabla \cdot \bar{H} = \rho_m/\mu \tag{A-4}$$

Define the total electric field $\bar{E}$ as

$$\bar{E} = \bar{E}^e + \bar{E}^m \tag{A-5}$$

---

* A dot over a quantity indicates partial differentiation with respect to time. Two dots indicate second partial differentiation with respect to time.

Define the total magnetic field $\bar{H}$ as

$$\bar{H} = \bar{H}^e + \bar{H}^m \tag{A-6}$$

Writing Maxwell's equations for magnetic currents and charges only,

$$\nabla \times \bar{H}^m = \epsilon \dot{\bar{E}}^m \tag{A-7}$$

$$\nabla \times \bar{E}^m = -\mu \dot{\bar{H}}^m - \bar{M} \tag{A-8}$$

$$\nabla \cdot \bar{H}^m = \rho_m / \mu \tag{A-9}$$

$$\nabla \cdot \bar{E}^m = 0 \tag{A-10}$$

Writing Maxwell's equations for electric currents and charges only,

$$\nabla \times \bar{H}^e = \epsilon \dot{\bar{E}} + \bar{J} \tag{A-11}$$

$$\nabla \times \bar{E}^e = -\mu \dot{\bar{H}}^e \tag{A-12}$$

$$\nabla \cdot \bar{H}^e = 0 \tag{A-13}$$

$$\nabla \cdot \bar{E}^e = \rho / \epsilon \tag{A-14}$$

First, Maxwell's equations for electric charges and currents only are considered. (A-13) is satisfied if $\bar{H}^e$ is the curl of some vector, say $\bar{A}_E$. Therefore, define

$$\mu H^e \triangleq \nabla \times \bar{A}_E \tag{A-15}$$

Substituting (A-15) into (A-12),

$$\nabla \times \left(E^e + \dot{\bar{A}}_E \right) = 0 \tag{A-16}$$

(A-16) is satisfied if $\bar{E}^e + \dot{\bar{A}}_E$ is the gradient of a scalar, say V. Therefore, define

$$\bar{E}^e \underline{\Delta} -\nabla V - \dot{\bar{A}}_E \tag{A-17}$$

(A-11) and (A-14) may now be used to derive differential equations for the potential functions $\bar{A}_E$ and V. Substituting (A-15) and (A-17) into (A-11) yields

$$\frac{1}{\mu}\nabla\times\nabla\times\bar{A}_E = -\epsilon\nabla\dot{V} - \epsilon\ddot{\bar{A}}_E + \bar{J} \tag{A-18}$$

Using the vector identity

$$\nabla\times\nabla\times\bar{A}_E = \nabla\nabla\cdot\bar{A}_E - \nabla^2\bar{A}_E \tag{A-19}$$

in (A-18),

$$\nabla^2\bar{A}_E - \mu\epsilon\ddot{\bar{A}}_E = -\mu\bar{J} + \mu\epsilon\nabla\dot{V} + \nabla\nabla\cdot\bar{A}_E \tag{A-20}$$

(A-20) is one of the differential equations for $\bar{A}_E$ and V. Substituting (A-17) into (A-14),

$$\nabla^2 V + \nabla\cdot\dot{\bar{A}}_E = -\rho/\epsilon \tag{A-21}$$

(A-21) is the other differential equation for $\bar{A}_E$ and V. Equations (A-20) and (A-21) are coupled--that is, they both involve $\bar{A}_E$ and V. To uncouple them, the "electric" Lorentz gauge condition is employed. According to this condition, set

$$\nabla\cdot\bar{A}_E = -\mu\epsilon\dot{V} \tag{A-22}$$

The electric Lorentz gauge condition is equivalent to

$$V = -\frac{1}{\mu\epsilon}\int \nabla\cdot \bar{A}_E\, dt \qquad \text{(A-23)}$$

Using (A-22), (A-20) may be written as

$$\nabla^2\bar{A}_E - \mu\epsilon\ddot{\bar{A}}_E = -\mu\bar{J} \qquad \text{(A-24)}$$

Using (A-22) in (A-21),

$$\nabla^2 V - \mu\epsilon\ddot{V} = -\rho/\epsilon \qquad \text{(A-25)}$$

Equations (A-24) and (A-25) are the decoupled set for $\bar{A}_E$ and V. The potential function which solves (A-24) is known to be

$$\bar{A}_E(\bar{r},t) = \frac{\mu}{4\pi}\oint_{S_a}\frac{\bar{J}(\bar{r}_s, t - R/v)}{R}\,ds \qquad \text{(A-26)}$$

$\bar{A}_E(\bar{r},t)$ may be shown to satisfy (A-24) by substitution. V is given in terms of $\bar{A}_E$ by (A-23).

Maxwell's equations for magnetic charges and currents only are now considered. (A-10) will be satisfied if $\bar{E}^m$ is the curl of some vector, say $\bar{A}_H$. Therefore, define

$$\epsilon\bar{E}^m = -\nabla\times\bar{A}_H \qquad \text{(A-27)}$$

Substituting (A-27) into (A-7),

$$\nabla\times\left(\bar{H}^m + \dot{\bar{A}}_H\right) = 0 \qquad \text{(A-28)}$$

(A-28) is satisfied if $\bar{H}^m + \dot{\bar{A}}_H$ is the gradient of a scalar, say $\mathcal{F}$. Therefore, let

$$\overline{H}^m = -\nabla\mathcal{F} - \dot{\overline{A}}_H \tag{A-29}$$

(A-27) and (A-29) satisfy equations (A-7) and (A-10). (A-8) and (A-9) may now be used to derive differential equations for the potential functions $\bar{A}_H$ and $\mathcal{F}$. Substituting (A-27) and (A-29) into (A-8),

$$-\frac{1}{\epsilon}\nabla\times\nabla\times\overline{A_H} = \mu\nabla\dot{\mathcal{F}} + \mu\ddot{\overline{A}}_H - \overline{M} \tag{A-30}$$

Using the vector identity

$$\nabla\times\nabla\times\overline{A_H} = \nabla\nabla\cdot\overline{A_H} - \nabla^2\overline{A_H} \tag{A-31}$$

in (A-30),

$$\nabla^2\overline{A_H} - \mu\epsilon\ddot{\overline{A}}_H = -\epsilon\overline{M} + \mu\epsilon\nabla\dot{\mathcal{F}} + \nabla\nabla\cdot\overline{A_H} \tag{A-32}$$

This is one of the differential equations for $\bar{A}_H$ and $\mathcal{F}$. Substituting (A-29) into (A-9),

$$\nabla^2\mathcal{F} + \nabla\cdot\dot{\overline{A}}_H = -\rho_m/\mu \tag{A-33}$$

This is the other differential equation for $\bar{A}_H$ and $\mathcal{F}$. (A-32) and (A-33) are coupled--that is, they both involve $\bar{A}_H$ and $\mathcal{F}$. To uncouple them, the "magnetic" Lorentz gauge condition is employed. According to this condition, set

$$\nabla\cdot\overline{A_H} = -\mu\epsilon\dot{\mathcal{F}} \tag{A-34}$$

The magnetic Lorentz gauge condition is equivalent to

$$\mathcal{F} = -\frac{1}{\mu\epsilon}\int \nabla\cdot\overline{A_H}\,dt \qquad \text{(A-35)}$$

Using the gauge condition (A-34), (A-32) may be written as

$$\nabla^2\overline{A_H} - \mu\epsilon\ddot{\overline{A_H}} = -\epsilon\overline{M} \qquad \text{(A-36)}$$

Using (A-34) in (A-33),

$$\nabla^2\mathcal{F} - \mu\epsilon\ddot{\mathcal{F}} = -\rho_m/\mu \qquad \text{(A-37)}$$

(A-36) and (A-37) are the decoupled set for $\bar{A}_H$ and $\mathcal{F}$. The potential function which solves (A-36) is known to be

$$\overline{A_H}(\bar{r},t) = \frac{\epsilon}{4\pi}\oint_{S_a}\frac{\overline{M}(\bar{r}_s, t - R/v)}{R}\,ds \qquad \text{(A-38)}$$

$\bar{A}_H(\bar{r},t)$ may be shown to satisfy (A-36) by substitution. $\mathcal{F}$ is given in terms of $\bar{A}_H$ by (A-35). The results for $\bar{E}(\bar{r},t)$ and $\bar{H}(\bar{r},t)$ are found using (A-5) and (A-6). Adding (A-17) and (A-27),

$$\overline{E}(\bar{r},t) = -\nabla V - \dot{\overline{A}}_E - \frac{1}{\epsilon}\nabla\times\overline{A_H} \qquad \text{(A-39)}$$

$\bar{E}(\bar{r},t)$ may be written entirely in terms of the integrals defining V, $\bar{A}_E$, and $\bar{A}_H$. Using (A-23), (A-26), and (A-28) in (A-39),

$$\overline{E}(\bar{r},t)$$

$$= \frac{1}{4\pi\epsilon}\nabla\nabla\cdot\oint_{S_a}\left\{\frac{1}{R}\int_{t_i}^{t-R/v}\overline{J}(\bar{r}_s,t')\,dt'\right\}ds$$

$$-\frac{\mu}{4\pi}\oint_{S_a}\frac{1}{R}\,\frac{\partial \bar{J}(\bar{r}_s,\,t-R/v)}{\partial t}\,ds$$

$$-\frac{1}{4\pi}\nabla\times\oint_{S_a}\frac{\bar{M}(\bar{r}_s,\,t-R/v)}{R}\,ds \qquad \text{(A-40)}$$

The limits of the time integral in (A-40) may be explained physically as follows. The excitation starts at time t_i. All contributions from ds are then integrated from t_i to retarded time t - R/v to account for the finite velocity of propagation, v, in the medium. It is understood that the time integral is zero for all t - R/v less than t_i.

Adding (A-15) and (A-29),

$$\bar{H}(\bar{r},\,t)=-\nabla\mathcal{F}-\dot{\bar{A}}_H+\frac{1}{\mu}\nabla\times\bar{A}_E \qquad \text{(A-41)}$$

$\bar{H}(\bar{r},t)$ may be written entirely in terms of the integrals defining $\mathcal{F}$, $\bar{A}_E$, and $\bar{A}_H$. Using (A-26), (A-35), and (A-38) in (A-41),

$$\bar{H}(\bar{r},\,t)$$

$$=\frac{1}{4\pi\mu}\nabla\nabla\cdot\oint_{S_a}\left\{\frac{1}{R}\int_{t_i}^{t-R/v}\bar{M}(\bar{r}_s,\,t')\,dt'\right\}ds$$

$$-\frac{\epsilon}{4\pi}\oint_{S_a}\frac{1}{R}\,\frac{\partial \bar{M}(\bar{r}_s,\,t-R/v)}{\partial t}\,ds$$

$$+\frac{1}{4\pi}\nabla\times\oint_{S_a}\frac{\overline{J}(\bar{r}_s,\,t-R/v)}{R}\,ds \qquad \text{(A-42)}$$

As discussed in Jordan and Balmain (1968;468-469), for a source-free aperture surface, the equivalent electric current $\bar{J}$ and magnetic current $\bar{M}$ are

$$\overline{M}(\bar{r}_s,t-R/v)=-\hat{n}\times\overline{E}(\bar{r}_s,t-R/v) \qquad \text{(A-43)}$$

$$\overline{J}(\bar{r}_s,t-R/v)=\hat{n}\times\overline{H}(\bar{r}_s,t-R/v) \qquad \text{(A-44)}$$

The $\bar{E}$ and $\bar{H}$ fields used in (A-43) and (A-44) are the excitation fields which illuminate the aperture surface. Using (A-43) and (A-44) in (A-40),

$$\begin{aligned}\overline{E}(\bar{r},t)&=\frac{1}{4\pi\epsilon}\nabla\nabla\cdot\oint_{S_a}\left\{\frac{1}{R}\int_{t_i}^{t-R/v}\left[\hat{n}\times\overline{H}(\bar{r}_s,t')\right]dt'\right\}ds\\&-\frac{\mu}{4\pi}\oint_{S_a}\frac{1}{R}\,\frac{\partial\left[\hat{n}\times\overline{H}(\bar{r}_s,t-R/v)\right]}{\partial t}\,ds\\&+\frac{1}{4\pi}\nabla\times\oint_{S_a}\frac{\left[\hat{n}\times\overline{E}(\bar{r}_s,t-R/v)\right]}{R}\,ds\end{aligned} \qquad \text{(A-45)}$$

Using (A-43) and (A-44) in (A-42),

$$\overline{H}(\bar{r},t)=-\frac{1}{4\pi\mu}\nabla\nabla\cdot\oint_{S_a}\left\{\frac{1}{R}\int_{t_i}^{t-R/v}\left[\hat{n}\times\overline{E}(\bar{r}_s,t')\right]dt'\right\}ds$$

$$+\frac{\epsilon}{4\pi}\oint_{S_a}\frac{1}{R}\frac{\partial[\hat{n}\times\bar{E}(\bar{r}_s,t-R/v)]}{\partial t}\,ds$$

$$+\frac{1}{4\pi}\nabla\times\oint_{S_a}\frac{[\hat{n}\times\bar{H}(\bar{r}_s,t-R/v)]}{R}\,ds \qquad \text{(A-46)}$$

(A-45) and (A-46) are the correct versions of the two equations given by Chernousov (1965:1247). In the Chernousov article, $\bar{E}$ and $\bar{H}$ are transposed in two places. The subsequent equations in the Chernousov article are correct.

Let

$$\bar{H}(\bar{r}_s,t-R/v)=H(\bar{r}_s,t-R/v)\bar{H}^{\circ} \qquad \text{(A-47)}$$

and

$$\bar{E}(\bar{r}_s,t-R/v)=E(\bar{r}_s,t-R/v)\bar{E}^{\circ} \qquad \text{(A-48)}$$

Realizing that $\mu\epsilon = 1/v^2$, $\bar{E}(\bar{r},t)$ may be written as

$$\bar{E}(\bar{r},t)$$

$$=-\frac{1}{4\pi\epsilon}\oint_{S_a}\left\{\frac{1}{v^2R}\frac{\partial[\bar{H}(\bar{r}_s,t-R/v)]}{\partial t}[\hat{n}\times\bar{H}^{\circ}]\right.$$

$$-\epsilon\nabla\times[\hat{n}\times\bar{E}^{\circ}E(\bar{r}_s,t-R/v)]/R$$

$$\left.-\nabla\nabla\cdot\frac{1}{R}\int_{t_i}^{t-R/v}[\hat{n}\times\bar{H}^{\circ}H(\bar{r}_s,t')]\,dt'\right\}ds \qquad \text{(A-49)}$$

Let a be an arbitrary scalar and $\bar{B}$ an arbitrary vector. Then

$$\nabla \times (a\bar{B}) = \nabla a \times \bar{B} + a\nabla \times \bar{B} \tag{A-50}$$

Using (A-50) in (A-49),

$$-\epsilon \nabla \times \frac{\left[\hat{n} \times \bar{E}^{\circ} E(\bar{r}_s, t - R/v)\right]}{R}$$

$$= \epsilon \left[\hat{n} \times \bar{E}^{\circ} \times \nabla \left(\frac{E(\bar{r}_s, t - R/v)}{R} \right)\right] \tag{A-51}$$

Let A be an arbitrary scalar and $\bar{a}$ be an arbitrary vector. Then

$$\nabla\nabla\cdot(A\bar{a}) = \nabla A \nabla \cdot \bar{a} + A\nabla\nabla\cdot\bar{a}$$

$$+\nabla A \times (\nabla \times \bar{a}) + (\bar{a}\cdot\nabla)\nabla A + (\nabla A \cdot \nabla)\bar{a} \tag{A-52}$$

Let

$$A = \frac{1}{R} \int_{t_i}^{t - R/v} H(\bar{r}_s, t')\, dt' \tag{A-53}$$

and

$$\bar{a} = \hat{n} \times \bar{H}^{\circ} \tag{A-54}$$

Then

$$\nabla\nabla\cdot\frac{1}{R}\int_{t_i}^{t-R/v}\left[\hat{n}\times\bar{H}^{\circ} H(\bar{r}_s, t')\right] dt'$$

$$= \left[(\hat{n}\times\bar{H}^{\circ})\cdot\nabla\right]\nabla\left(\frac{1}{R}\int_{t_i}^{t-R/v}\bar{H}(\bar{r}_s, t')\, dt'\right) \tag{A-55}$$

Using (A-51) and (A-55) in (A-49), $\bar{E}(\bar{r},t)$ may be written as

$$\overline{E}(\overline{r},t)$$

$$= -\frac{1}{4\pi\epsilon}\oint_{S_a}\left\{\frac{1}{v^2R}\frac{\partial H(\overline{r}_s,t-R/v)}{\partial t}[\hat{n}\times\overline{H}^o]\right.$$

$$+\epsilon\left[[\hat{n}\times\overline{E}^o]\times\nabla\left(\frac{E(\overline{r}_s,t-R/v)}{R}\right)\right]$$

$$\left.-\left([\hat{n}\times\overline{H}^o]\cdot\nabla\right)\nabla\left(\frac{1}{R}\int_{t_i}^{t-R/v}H(\overline{r}_s,t')\,dt'\right)\right\}ds \qquad \text{(A-56)}$$

Using $\mu\epsilon = 1/v^2$, (A-46) may be written as

$$\overline{H}(\overline{r},t)$$

$$= \frac{1}{4\pi\mu}\oint_{S_a}\left\{\frac{1}{v^2R}\frac{\partial E(\overline{r}_s,t-R/v)}{\partial t}[\hat{n}\times\overline{E}^o]\right.$$

$$+\mu\nabla\times\frac{[\hat{n}\times\overline{H}^o H(\overline{r}_s,t-R/v)]}{R}$$

$$\left.-\nabla\nabla\cdot\frac{1}{R}\int_{t_i}^{t-R/v}[\hat{n}\times\overline{E}^o E(\overline{r}_s,t')]\,dt'\right\}ds \qquad \text{(A-57)}$$

From (A-50)

$$\mu\nabla\times\left[\hat{n}\times\overline{H}^o\frac{H(\overline{r}_s,t-R/v)}{R}\right] = -\mu\left[\hat{n}\times\overline{H}^o\times\nabla\left(\frac{H(\overline{r}_s,t-R/v)}{R}\right)\right] \qquad \text{(A-58)}$$

From (A-52)

$$\nabla\nabla\cdot\frac{1}{R}\int_{t_i}^{t-R/v}[\hat{n}\times\bar{E}^{\circ}\,E(\bar{r}_s,t')]dt'$$
$$=[(\hat{n}\times\bar{E}^{\circ})\cdot\nabla]\nabla\left(\frac{1}{R}\int_{t_i}^{t-R/v}E(\bar{r}_s,t')dt'\right) \qquad \text{(A-59)}$$

Using (A-58) and (A-59) in (A-57),

$$\bar{H}(\bar{r},t)$$
$$=\frac{1}{4\pi\mu}\oint_{S_a}\left\{\frac{1}{v^2R}\frac{\partial E(\bar{r}_s,t-R/v)}{\partial t}[\hat{n}\times\bar{E}^{\circ}]\right.$$
$$-\mu\left[[\hat{n}\times\bar{H}^{\circ}]\times\nabla\left(\frac{H(\bar{r}_s,t-R/v)}{R}\right)\right]$$
$$\left.-\left([\hat{n}\times\bar{E}^{\circ}]\cdot\nabla\right)\nabla\left(\frac{1}{R}\int_{t_i}^{t-R/v}E(\bar{r}_s,t')dt'\right)\right\}ds \qquad \text{(A-60)}$$

Consider

$$Q=-\frac{1}{v^2R}\frac{\partial F(\bar{r}_s,t-R/v)}{\partial t}[\hat{n}\times\bar{F}^{\circ}]$$
$$+\left([\hat{n}\times\bar{F}^{\circ}]\cdot\nabla\right)\nabla\left(\frac{1}{R}\int_{t_i}^{t-R/v}F(\bar{r}_s,t')dt'\right) \qquad \text{(A-61)}$$

where $\bar{F}$ may be either $\bar{E}$ or $\bar{H}$. $\bar{F}^{\circ}$ is the unit vector in the $\bar{F}$ direction.

$$\nabla\left(\frac{1}{R}\int_{t_i}^{t-R/v}F(\bar{r}_s,t')dt'\right)=\frac{1}{R}\nabla\int_{t_i}^{t-R/v}F(\bar{r}_s,t')dt'+\int_{t_i}^{t-R/v}F(\bar{r}_s,t')dt'\nabla\left(\frac{1}{R}\right) \qquad \text{(A-62)}$$

$$\nabla(R^n)=nR^{n-1}\bar{R}^{\circ} \qquad \text{(A-63)}$$

$$\nabla\int_{t_i}^{t-R/v} F(\bar{r}_s,t')\,dt' = -\frac{\bar{R}^\circ}{v}F(\bar{r}_s,t-R/v) \qquad \text{(A-64)}$$

Using (A-63) and (A-64), (A-62) may be written as

$$\nabla\left(\frac{1}{R}\int_{t_i}^{t-R/v} F(\bar{r}_s,t')\,dt'\right) = -\frac{\bar{R}^\circ}{vR}F(\bar{r}_s,t-R/v) - \frac{\bar{R}^\circ}{R}\int_{t_i}^{t-R/v} F(\bar{r}_s,t')\,dt' \qquad \text{(A-65)}$$

Let $\bar{a}$ and $\bar{b}$ be two arbitrary vectors. Let A be an arbitrary scalar function. Then

$$(\bar{b}\cdot\nabla)(\bar{a}A) = \bar{a}(\bar{b}\cdot\nabla A) + A(\bar{b}\cdot\nabla\bar{a}) \qquad \text{(A-66)}$$

To employ identity (A-66), let

$$\bar{a} = \bar{R}^\circ \qquad \text{(A-67)}$$

$$\bar{b} = [\hat{n}\times\bar{F}^\circ] \qquad \text{(A-68)}$$

and

$$A = \left[-\frac{F(\bar{r}_s,t-R/v)}{vR} - \frac{1}{R^2}\int_{t_i}^{t-R/v} F(\bar{r}_s,t')\,dt'\right] \qquad \text{(A-69)}$$

With A given by (A-69),

$$\nabla A = -\frac{1}{vR}\nabla F(\bar{r}_s,t-R/v) - \frac{F(\bar{r}_s,t-R/v)}{v}\nabla\left(\frac{1}{R}\right) - \frac{1}{R^2}\cdot\nabla\int_{t_i}^{t-R/v} F(\bar{r}_s,t')\,dt' - \int_{t_i}^{t-R/v} F(\bar{r}_s,t')\,dt'\,\nabla\left(\frac{1}{R^2}\right) \qquad \text{(A-70)}$$

$$\nabla F(\bar{r}_s, t - R/v) = -\frac{\bar{R}^o}{v}\frac{\partial F(\bar{r}_s, t-R/v)}{\partial(t-R/v)} \tag{A-71}$$

$\bar{b}\cdot\nabla\bar{a}$ is found with $\bar{b} = \hat{n}\times\bar{F}^o$ and $\bar{a} = \bar{R}^o$.

$$\bar{R}^o = \frac{\bar{R}}{R} = \frac{(x-x')\hat{a}_x + (y-y')\hat{a}_y + (z-z')\hat{a}_z}{\left[(x-x')^2 + (y-y')^2 + (z-z')^2\right]^{1/2}} \tag{A-72}$$

$$\frac{\partial\bar{R}^o}{\partial x} = \frac{\hat{a}_x}{R} - \frac{\bar{R}}{R^3}(x-x') \tag{A-73}$$

$$(\bar{b}\cdot\nabla\bar{a})_x = \left[\hat{n}\times\bar{F}^o\right]_x\frac{\hat{a}_x}{R} - \left[\hat{n}\times\bar{F}^o\right]_x\frac{\bar{R}}{R^3}(x-x') \tag{A-74}$$

The expressions for $(\bar{b}\cdot\nabla\bar{a})_y$ and $(\bar{b}\cdot\nabla\bar{a})_z$ are similar to (A-74).

Therefore,

$$\bar{b}\cdot\nabla\bar{a} = \frac{\left[\hat{n}\times\bar{F}^o\right]}{R} - \frac{\bar{R}}{R^3}\left(\left[\hat{n}\times\bar{F}^o\right]\cdot\bar{R}\right) \tag{A-75}$$

or

$$\bar{b}\cdot\nabla\bar{a} = \frac{\left[\hat{n}\times\bar{F}^o\right]}{R} - \frac{\bar{R}^o}{R}\left(\left[\hat{n}\times\bar{F}^o\right]\cdot\bar{R}^o\right) \tag{A-76}$$

Substituting (A-63), (A-64), and (A-71) into (A-70),

$$\nabla A = \frac{\bar{R}^o}{v^2R}\frac{\partial F(\bar{r}_s, t-R/v)}{\partial(t-R/v)} + \frac{2\bar{R}^o}{vR^2}F(\bar{r}_s, t-R/v) + \frac{2\bar{R}^o}{R^3}\int_{t_i}^{t-R/v} F(\bar{r}_s, t')\,dt' \tag{A-77}$$

From (A-77) with $\bar{b} = \hat{n}\times\bar{F}^o$,

$$(\bar{b}\cdot\nabla A) = \frac{\bar{R}^o}{v^2R}\cdot\left[\hat{n}\times\frac{\partial\bar{F}(\bar{r}_s, t-R/v)}{\partial(t-R/v)}\right]$$

$$+\frac{2\bar{R}^{\circ}}{vR^2}\cdot\left[\hat{n}\times\bar{F}(\bar{r}_s,t-R/v)\right]$$

$$+\frac{2\bar{R}'}{R^3}\cdot\left[\hat{n}\times\int_{t_i}^{t-R/v}\bar{F}(\bar{r}_s,t')\,dt'\right] \qquad \text{(A-78)}$$

From (A-76) with $A=\left[\frac{-F(\bar{r}_s,t-R/v)}{vR}\right]-\frac{1}{R^2}\int_{t_i}^{t-R/v}F(\bar{r}_s,t')\,dt'\Big]$,

$$A(\bar{b}\cdot\nabla\bar{a})=-\frac{\hat{n}\times\bar{F}(\bar{r}_s,t-R/v)}{vR^2}-\frac{\hat{n}\times\int_{t_i}^{t-R/v}\bar{F}(\bar{r}_s,t')\,dt'}{R^3}$$

$$+\frac{\bar{R}^{\circ}}{vR^2}\left(\left[\hat{n}\times\bar{F}(\bar{r}_s,t-R/v)\right]\cdot\bar{R}^{\circ}\right)$$

$$+\frac{\bar{R}^{\circ}}{R^3}\left(\left[\hat{n}\times\int_{t_i}^{t-R/v}\bar{F}(\bar{r}_s,t')\,dt'\right]\cdot\bar{R}^{\circ}\right) \qquad \text{(A-79)}$$

From (A-78) with $\bar{a}=\bar{R}^{\circ}$,

$$\bar{a}(\bar{b}\cdot\nabla A)=\bar{R}^{\circ}\left(\frac{\bar{R}^{\circ}}{v^2R}\left[\hat{n}\times\frac{\partial\bar{F}(\bar{r}_s,t-R/v)}{\partial(t-R/v)}\right]\right)$$

$$+\bar{R}^{\circ}\left(\frac{2\bar{R}^{\circ}}{vR^2}\cdot\left[\hat{n}\times\bar{F}(\bar{r}_s,t-R/v)\right]\right)$$

$$+\bar{R}^{\circ}\left(\frac{2\bar{R}^{\circ}}{R^3}\cdot\left[\hat{n}\times\int_{t_i}^{t-R/v}\bar{F}(\bar{r}_s,t')\,dt'\right]\right) \qquad \text{(A-80)}$$

Using (A-79) and (A-80), (A-61) may be written as

$$-\frac{1}{v^2R}\frac{\partial F(\bar{r}_s,t-R/v)}{\partial(t-R/v)}\left[\hat{n}\times\bar{F}^{\circ}\right]+\left(\left[\hat{n}\times\bar{F}^{\circ}\right]\cdot\nabla\right)\nabla\left(\frac{1}{R}\int_{t_i}^{t-R/v}F(\bar{r}_s,t')\,dt'\right)$$

$$=-\frac{1}{v^2R}\frac{\partial F(\bar{r}_s,t-R/v)}{\partial(t-R/v)}\left[\hat{n}\times\bar{F}^{\circ}\right]+\frac{1}{v^2R}\bar{R}^{\circ}\left(\bar{R}^{\circ}\cdot\left[\hat{n}\times\frac{\partial\bar{F}(\bar{r}_s,t-R/v)}{\partial(t-R/v)}\right]\right)$$

$$+\frac{1}{vR^2}3\bar{R}^o\left(\bar{R}^o\cdot\left[\hat{n}\times\bar{F}(\bar{r}_s,t-R/v)\right]\right)-\frac{1}{vR^2}\left[\hat{n}\times\bar{F}(\bar{r}_s,t-R/v)\right]$$

$$+\frac{1}{R^3}3\bar{R}^o\left(\bar{R}^o\cdot\left[\hat{n}\times\int_{t_i}^{t-R/v}\bar{F}(\bar{r}_s,t')\,dt'\right]\right)$$

$$-\frac{1}{R^3}\left[\hat{n}\times\int_{t_i}^{t-R/v}\bar{F}(\bar{r}_s,t')\,dt'\right] \qquad \text{(A-81)}$$

The first two terms of (A-81) may be combined using the following method.

$$-\frac{1}{v^2R}\frac{\partial\bar{F}(\bar{r}_s,t-R/v)}{\partial(t-R/v)}\left[\hat{n}\times\bar{F}^o\right]=-\frac{1}{v^2R}\hat{n}\times\frac{\partial\bar{F}(\bar{r}_s,t-R/v)}{\partial(t-R/v)} \qquad \text{(A-82)}$$

But

$$\frac{\partial\bar{F}(\bar{r}_s,t-R/v)}{\partial(t-R/v)}=\frac{\partial\bar{F}(\bar{r}_s,t-R/v)}{\partial t} \qquad \text{(A-83)}$$

because R is not a function of time. Therefore,

$$\text{first two terms}=\frac{1}{v^2R}\frac{\partial\bar{F}(\bar{r}_s,t-R/v)}{\partial t}\left(-\left[\hat{n}\times\bar{F}^o\right]+\bar{R}^o\left(\bar{R}^o\cdot\left[\hat{n}\times\bar{F}^o\right]\right)\right) \qquad \text{(A-84)}$$

Let $\bar{a}$, $\bar{b}$, and $\bar{c}$ be arbitrary vectors. Then

$$\bar{a}\times(\bar{b}\times\bar{c})=\bar{b}(\bar{a}\cdot\bar{c})-\bar{c}(\bar{a}\cdot\bar{b}) \qquad \text{(A-85)}$$

Let $\bar{a}=\bar{R}^o$, $\bar{b}=\bar{R}^o$, and $\bar{c}=\hat{n}\times\bar{F}^o$. Then

$$\bar{R}^o\times\left[\bar{R}^o\times\left[\hat{n}\times\bar{F}^o\right]\right]=-\left[\hat{n}\times\bar{F}^o\right]+\bar{R}^o\left(\bar{R}^o\cdot\left[\hat{n}\times\bar{F}^o\right]\right) \qquad \text{(A-86)}$$

Substituting (A-86) into (A-84),

$$-\frac{\partial \bar{F}(\bar{r}_s, t-R/v)}{v^2 R\ \partial t}\left[\hat{n}\times\bar{F}^{\circ}\right]+\frac{1}{v^2 R}\bar{R}^{\circ}\left(\bar{R}^{\circ}\cdot\left[\hat{n}\times\frac{\partial \bar{F}(\bar{r}_s, t-R/v)}{\partial(t-R/v)}\right]\right)$$

$$=\frac{1}{v^2 R}\left[\bar{R}^{\circ}\times\left[\bar{R}^{\circ}\times\left[\hat{n}\times\frac{\partial \bar{F}(\bar{r}_s, t-R/v)}{\partial(t-R/v)}\right]\right]\right] \qquad \text{(A-87)}$$

Using (A-87) in (A-81),

$$-\frac{1}{v^2 R}\frac{\partial \bar{F}(\bar{r}_s, t-R/v)}{\partial t}\left[\hat{n}\times\bar{F}^{\circ}\right]+\left(\left[\hat{n}\times\bar{F}^{\circ}\right]\cdot\nabla\right)\nabla\left(\frac{1}{R}\int_{t_i}^{t-R/v}\bar{F}(\bar{r}_s, t')\,dt'\right)$$

$$=\frac{1}{v^2 R}\left[\bar{R}^{\circ}\times\left[\bar{R}^{\circ}\times\left[\hat{n}\times\frac{\partial \bar{F}(\bar{r}_s, t-R/v)}{\partial(t-R/v)}\right]\right]\right]$$

$$+\frac{3\bar{R}^{\circ}}{v R^2}\left(\bar{R}^{\circ}\cdot\left[\hat{n}\times\bar{F}(\bar{r}_s, t-R/v)\right]\right)-\frac{1}{v R^2}\left[\hat{n}\times\bar{F}(\bar{r}_s, t-R/v)\right]$$

$$+\frac{3\bar{R}^{\circ}}{R^3}\left(\bar{R}^{\circ}\cdot\left[\hat{n}\times\int_{t_i}^{t-R/v}\bar{F}(\bar{r}_s, t')\,dt'\right]\right)-\frac{1}{R^3}\left[\hat{n}\times\int_{t_i}^{t-R/v}\bar{F}(\bar{r}_s, t')\,dt'\right] \qquad \text{(A-88)}$$

Consider now $\left[\hat{n}\times\bar{F}^{\circ}\right]\times\nabla\left(\frac{F(\bar{r}_s, t-R/v)}{R}\right)$.

From (A-63),

$$\left[\hat{n}\times\bar{F}^{\circ}\right]\times F(\bar{r}_s, t-R/v)\nabla\left(\frac{1}{R}\right)=\frac{\bar{R}^{\circ}}{R^2}\times\left[\hat{n}\times\bar{F}(\bar{r}_s, t-R/v)\right] \qquad \text{(A-89)}$$

From (A-71),

$$\frac{\left[\hat{n}\times\bar{F}^{\circ}\right]}{R}\times\nabla F(\bar{r}_s, t-R/v)=\frac{1}{v R}\bar{R}^{\circ}\times\left[\hat{n}\times\frac{\partial \bar{F}(\bar{r}_s, t-R/v)}{\partial(t-R/v)}\right] \qquad \text{(A-90)}$$

Therefore,

$$\left[\hat{n}\times\bar{F}\right]\times\nabla\left(\frac{F(\bar{r}_s,t-R/v)}{R}\right)$$

$$=\frac{1}{vR}\bar{R}^\circ\times\left[\hat{n}\times\frac{\partial\bar{F}(\bar{r}_s,t-R/v)}{\partial(t-R/v)}\right]$$

$$+\frac{1}{R^2}\bar{R}^\circ\times\left[\hat{n}\times\bar{F}(\bar{r}_s,t-R/v)\right] \qquad \text{(A-91)}$$

Substituting (A-88) and (A-91) into (A-56) and (A-60), $\bar{E}(\bar{r},t)$ and $\bar{H}(\bar{r},t)$ may be written everywhere as follows.

$$\bar{E}(\bar{r},t)=\frac{1}{4\pi\epsilon}\oint_{S_a}\left\{\frac{1}{v^2R}\left[\bar{R}^\circ\times\left[\bar{R}^\circ\times\left[\hat{n}\times\frac{\partial\bar{H}(\bar{r}_s,t-R/v)}{\partial(t-R/v)}\right]\right]\right]\right.$$

$$+\frac{3\bar{R}^\circ}{vR^2}\left(\bar{R}^\circ\cdot\left[\hat{n}\times\bar{H}(\bar{r}_s,t-R/v)\right]\right)-\frac{1}{vR^2}\left[\hat{n}\times\bar{H}(\bar{r}_s,t-R/v)\right]$$

$$+\frac{3\bar{R}^\circ}{R^3}\left(\bar{R}^\circ\cdot\left[\hat{n}\times\int_{t_i}^{t-R/v}\bar{H}(\bar{r}_s,t')\,dt'\right]\right)-\frac{1}{R^3}\left[\hat{n}\times\int_{t_i}^{t-R/v}\bar{H}(\bar{r}_s,t')\,dt'\right]$$

$$-\frac{\epsilon}{vR}\left[\bar{R}^\circ\times\left[\hat{n}\times\frac{\partial\bar{E}(\bar{r}_s,t-R/v)}{\partial(t-R/v)}\right]\right]$$

$$\left.-\frac{\epsilon}{R^2}\left[\bar{R}^\circ\times\left[\hat{n}\times\bar{E}(\bar{r}_s,t-R/v)\right]\right]\right\}ds \qquad \text{(A-92)}$$

$$\bar{H}(\bar{r},t)=\frac{1}{4\pi\mu}\oint_{S_a}\left\{-\frac{1}{v^2R}\left[\bar{R}^\circ\times\left[\bar{R}^\circ\times\left[\hat{n}\times\frac{\partial\bar{E}(\bar{r}_s,t-R/v)}{\partial(t-R/v)}\right]\right]\right]\right.$$

$$-\frac{3\bar{R}^\circ}{vR^2}\left(\bar{R}^\circ\cdot\left[\hat{n}\times\bar{E}(\bar{r}_s,t-R/v)\right]\right)+\frac{1}{vR^2}\left[\hat{n}\times\bar{E}(\bar{r}_s,t-R/v)\right]$$

$$-\frac{3\bar{R}^\circ}{R^3}\left(\bar{R}^\circ\cdot\left[\hat{n}\times\int_{t_i}^{t-R/v}\bar{E}(\bar{r}_s,t')\,dt'\right]\right)+\frac{1}{R^3}\left[\hat{n}\times\int_{t_i}^{t-R/v}\bar{E}(\bar{r}_s,t')\,dt'\right]$$

$$-\frac{\mu}{vR}\left[\bar{R}^\circ\times\left[\hat{n}\times\frac{\partial\bar{H}(\bar{r}_s,t-R/v)}{\partial(t-R/v)}\right]\right]$$

$$\left.-\frac{\mu}{R^2}\left[\bar{R}^\circ\times\left[\hat{n}\times\bar{H}(\bar{r}_s,t-R/v)\right]\right]\right\}ds \qquad \text{(A-93)}$$

Equations (A-88) and (A-91) are now examined to see under what conditions $1/R^2$ and $1/R^3$ terms may be neglected with respect to $1/R$ terms. From (A-91),

$$\frac{1}{v}\left|\frac{\partial\bar{F}(\bar{r}_s,t-R/v)}{\partial(t-R/v)}\right|\gg\frac{1}{R}\left|\bar{F}(\bar{r}_s,t-R/v)\right| \qquad \text{(A-94)}$$

From (A-88),

$$\frac{1}{v^2}\left|\frac{\partial\bar{F}(\bar{r}_s,t-R/v)}{\partial(t-R/v)}\right|\gg\frac{1}{vR}\left|\bar{F}(\bar{r}_s,t-R/v)\right|\gg\frac{1}{R^2}\left|\int_{t_i}^{t-R/v}\bar{F}(\bar{r}_s,t')\,dt'\right| \qquad \text{(A-95)}$$

Keeping only terms of the order of $1/R$ in the general expressions for $\bar{E}(\bar{r},t)$ and $\bar{H}(\bar{r},t)$ as given in (A-92) and (A-93), and realizing that

$v\epsilon = 1/\eta$ and $v\mu = \eta$, $\bar{E}(\bar{r},t)$ and $\bar{H}(\bar{r},t)$ may be written in the far field as

$$\bar{E}(\bar{r},t) = \frac{1}{4\pi v}\oint_{S_a}\frac{1}{R}\left\{\eta\left[\bar{R}^\circ\times\left[\bar{R}^\circ\times\left[\hat{n}\times\frac{\partial\bar{H}(\bar{r}_s,t-R/v)}{\partial t}\right]\right]\right]\right.$$
$$\left.-\left[\bar{R}^\circ\times\left[\hat{n}\times\frac{\partial\bar{E}(\bar{r}_s,t-R/v)}{\partial t}\right]\right]\right\}ds \qquad \text{(A-96)}$$

$$\bar{H}(\bar{r},t) = -\frac{1}{4\pi v}\oint_{S_a}\frac{1}{R}\left\{\frac{1}{\eta}\left[\bar{R}^\circ\times\left[\bar{R}^\circ\times\left[\hat{n}\times\frac{\partial\bar{E}(\bar{r}_s,t-R/v)}{\partial t}\right]\right]\right]\right.$$
$$\left.+\left[\bar{R}^\circ\times\left[\hat{n}\times\frac{\partial\bar{H}(\bar{r}_s,t-R/v)}{\partial t}\right]\right]\right\}ds \qquad \text{(A-97)}$$

(A-96) and (A-97) may be simplified further by replacing R with its approximate value in the far field. In terms of $\bar{r}$ and $\bar{r}_s$, $\bar{R}$ is given by by $\bar{R} = \bar{r} - \bar{r}_s$. Therefore,

$$R = \sqrt{(\bar{r}-\bar{r}_s)\cdot(\bar{r}-\bar{r}_s)} = \sqrt{r^2 - 2\bar{r}\cdot\bar{r}_s + r_s^2}$$
$$= r\sqrt{1 - \frac{2\bar{r}\cdot\bar{r}_s}{r} + \left(\frac{r_s}{r}\right)^2} \qquad \text{(A-98)}$$

From the series

$$(1-X)^{1/2} = 1 - \frac{X}{2} + \cdots, \quad X^2 < 1, \qquad \text{(A-99)}$$

$$R = r\sqrt{1 - \frac{2\bar{r}^\circ\cdot\bar{r}_s}{r} + \left(\frac{r_s}{r}\right)^2} \cong r - \bar{r}^\circ\cdot\bar{r}_s \qquad \text{(A-100)}$$

Consider finally the quantity t - (R/v). Let T = t - (r/v). Then

$$t - R/v \cong T + \frac{\bar{r}^\circ\cdot\bar{r}_s}{v} \qquad \text{(A-101)}$$

Replacing 1/R by 1/r, and neglecting the angle between $\bar{R}^o$ and $\bar{r}^o$,

$$\bar{E}(\bar{r},t) = -\frac{1}{4\pi v r}\left[\bar{r}^o \times \oint_{S_a}\left\{\left[\hat{n}\times\frac{\partial \bar{E}\left(\bar{r}_s, T+\frac{\bar{r}^o\cdot\bar{r}_s}{v}\right)}{\partial t}\right]\right.\right.$$

$$\left.\left. -\eta\left[\bar{r}^o\times\left[\hat{n}\times\frac{\partial \bar{H}\left(\bar{r}_s, T+\frac{\bar{r}^o\cdot\bar{r}_s}{v}\right)}{\partial t}\right]\right]\right\} ds\right] \qquad \text{(A-102)}$$

(A-102) is the central equation which was used in the subsequent research.

In the far field, $\bar{H}(\bar{r},t)$ may be found from $\bar{E}(\bar{r},t)$ by the simple relationship

$$\bar{H}(\bar{r},t) = \frac{1}{\eta}\left[\bar{r}^o \times \bar{E}(r,t)\right] \qquad \text{(A-103)}$$

Appendix B

DERIVATION OF THE ELECTRIC FAR FIELDS OF THE SPERRY RAND TEM HORN ANTENNA UTILIZING THE CHERNOUSOV METHOD

B.1 INTRODUCTION

This appendix presents a detailed mathematical derivation of the electric far fields of the TEM horn antenna, shown in Figure B.1, first studied experimentally by Susman and Lamensdorf (1970,1971). This TEM horn consists of two perfectly conducting circular sectors of angle ϕ_o and radius r_a separated by a small gap at the apex and by a distance 2h at $r' = r_a$. As derived in Appendix A, the equation used to determine the electric far fields is

$$\bar{E}(\bar{r},t) = -\frac{1}{4\pi v r}\left[\bar{r}^o \times \oint_{S_a}\left\{\left[\hat{n} \times \frac{\partial \bar{E}(\bar{r}_s, T+\frac{\bar{r}^o\cdot\bar{r}_s}{v})}{\partial t}\right] - \eta\left[\bar{r}^o \times \left[\hat{n} \times \frac{\partial \bar{H}(\bar{r}_s, T+\frac{\bar{r}^o\cdot\bar{r}_s}{v})}{\partial t}\right]\right]\right\} ds\right] \quad \text{(B-1)}$$

The various quantities used in (B-1) are:

$\bar{r}_s$, the vector from the origin to the surface element ds,

$\hat{n}$, the outward normal to ds,

$\bar{r}$, the vector from the origin to the observation point,

T, the retarded time, defined by $T = t - r/v$,

$\bar{r}^o$, the unit vector in the $\bar{r}$ direction,

v, the velocity of propagation in the medium, and

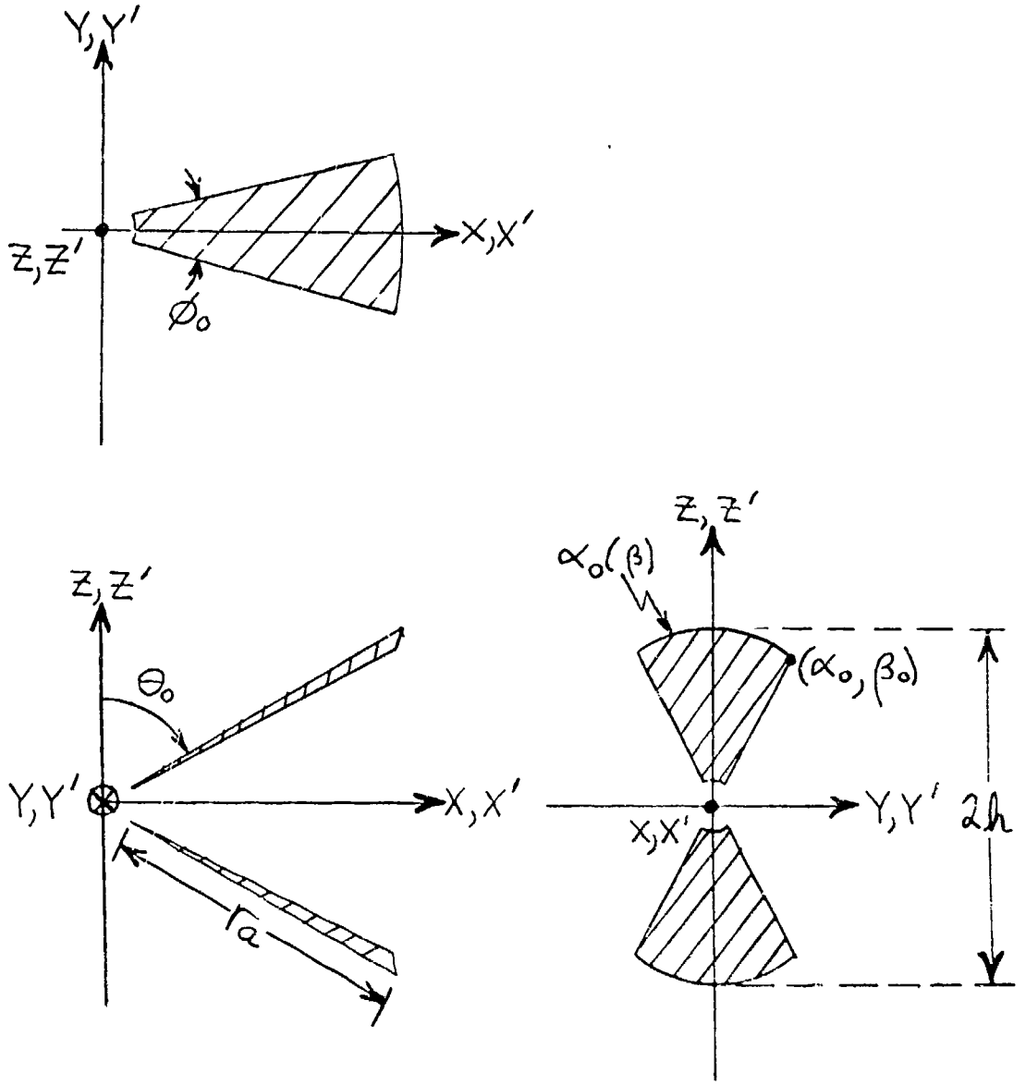

Cartesian source coordinates (x',y',z')
Spherical source coordinates (r',α,β)
Cartesian observation coordinates (x,y,z)
Spherical observation coordinates (r,θ,ϕ)

Figure B.1

The TEM Horn Antenna

η , the impedance of the medium.

Assume that in the region between the two metallic wedges comprising the TEM horn

$$\bar{E}(\bar{r},t) = \frac{\hat{\alpha} f(\alpha,\beta)}{r'} \left[V(t - r'/v) + k_v V(t + r'/v - 2r_a/v) \right] \quad \text{(B-2)}$$

That is, if the apex is excited by V(t), the $\bar{E}$ field within the horn arises from a forward propagating voltage V(t - r'/v) and a reflected voltage $k_v V(t + r'/v - 2r_a/v)$ propagating backward from the front aperture located at $r' = r_a$. k_v is the effective voltage reflection coefficient determined from

$$k_v = \frac{Z_{eff} - Z_o}{Z_{eff} + Z_o} \quad \text{(B-3)}$$

Z_{eff} is the effective terminating impedance of the front aperture, and Z_o is the characteristic impedance of the TEM horn. $f(\alpha,\beta)$ is the function which describes the taper of the $\bar{E}$ field in the two angular coordinates α and β. Assuming that the $\bar{E}$ and $\bar{H}$ fields comprise a TEM pair propagating in the free space which fills the TEM horn,

$$\bar{H}(\bar{r},t) = \frac{\hat{\beta} f(\alpha,\beta)}{\eta r'} \left[V(t - r'/v) - k_v V(t + r'/v - 2r_a/v) \right] \quad \text{(B-4)}$$

As discussed in Chapter 2, three apertures consisting of free space are considered:

1. a front aperture which is a spherical sector at $r' = r_a$ extending from $\alpha = \alpha_o(\beta)$ to $\alpha = \pi - \alpha_o(\beta)$ and from $\beta = -\beta_o$ to $\beta = \beta_o$,
2. a wedge-shaped side aperture located at $\beta = \beta_o$ extending

from $r' = 0$ to $r' = r_a$ and from $\alpha = \alpha_o$ to $\alpha = \pi - \alpha_o$, and

3. another wedge-shaped side aperture located at $\beta = -\beta_o$ extending from $r' = 0$ to $r' = r_a$ and from $\alpha = \alpha_o$ to $\alpha = \pi - \alpha_o$.

B.2 RADIATION FROM THE FRONT APERTURE

Consider first the front aperture located at $r' = r_a$. The spherical source coordinates descibing the fields at the various apertures are (r', α, β). The spherical observation coordinates describing the radiated fields are (r, θ, ϕ). At the front aperture

$$\hat{n} = \hat{r}' = \sin\alpha\cos\beta\hat{x} + \sin\alpha\sin\beta\hat{y} + \cos\alpha\hat{z} \tag{B-5}$$

$$\bar{r}^o = \hat{r} = \sin\theta\cos\phi\hat{x} + \sin\theta\sin\phi\hat{y} + \cos\theta\hat{z} \tag{B-6}$$

$$\bar{r}_s = r_a\hat{r}' = r_a\left[\sin\alpha\cos\beta\hat{x} + \sin\alpha\sin\beta\hat{y} + \cos\alpha\hat{z}\right] \tag{B-7}$$

Therefore,

$$\hat{n}\times\hat{\alpha} = \hat{r}'\times\hat{\alpha} = \hat{\beta} \tag{B-8}$$

Also,

$$\hat{\beta} = -\sin\beta\hat{x} + \cos\beta\hat{y} \tag{B-9}$$

In terms of the spherical coordinates (r, θ, ϕ),

$$\hat{x} = \sin\theta\cos\phi\hat{r} + \cos\theta\cos\phi\hat{\theta} - \sin\phi\hat{\phi} \tag{B-10}$$

$$\hat{y} = \sin\theta\sin\phi\hat{r} + \cos\theta\sin\phi\hat{\theta} + \cos\phi\hat{\phi} \tag{B-11}$$

$$\hat{z} = \cos\theta\,\hat{r} - \sin\theta\,\hat{\theta} \tag{B-12}$$

Therefore,

$$\hat{\beta} = -\sin\beta\sin\theta\cos\phi\,\hat{r} - \sin\beta\cos\theta\cos\phi\,\hat{\theta} + \sin\beta\sin\phi\,\hat{\phi} + \cos\beta\sin\theta\sin\phi\,\hat{r} + \cos\beta\cos\theta\sin\phi\,\hat{\theta} + \cos\beta\cos\phi\,\hat{\phi} \tag{B-13}$$

From (B-13),

$$\left[\hat{r}^{\circ}\times\left[\hat{n}\times\hat{\alpha}\right]\right] = \left[\hat{r}\times\hat{\beta}\right] = -\sin\beta\cos\theta\cos\phi\,\hat{\phi} - \sin\beta\sin\phi\,\hat{\theta} + \cos\beta\cos\theta\sin\phi\,\hat{\phi} - \cos\beta\cos\phi\,\hat{\theta} \tag{B-14}$$

Also,

$$\left[\hat{r}^{\circ}\times\left[\hat{n}\times\hat{\beta}\right]\right] = \hat{r}\times(-\hat{\alpha}) \tag{B-15}$$

In terms of cartesian coordinates (x,y,z),

$$\hat{\alpha} = \cos\alpha\cos\beta\,\hat{x} + \cos\alpha\sin\beta\,\hat{y} - \sin\alpha\,\hat{z} \tag{B-16}$$

Using (B-10), (B-11), and (B-12) in (B-16),

$$\begin{aligned}\hat{\alpha} &= \cos\alpha\cos\beta\sin\theta\cos\phi\,\hat{r} + \cos\alpha\cos\beta\cos\theta\cos\phi\,\hat{\theta} \\ &\quad - \cos\alpha\cos\beta\sin\phi\,\hat{\phi} + \cos\alpha\sin\beta\sin\theta\sin\phi\,\hat{r} \\ &\quad + \cos\alpha\sin\beta\cos\theta\sin\phi\,\hat{\theta} + \cos\alpha\sin\beta\cos\phi\,\hat{\phi} \\ &\quad - \sin\alpha\cos\theta\,\hat{r} + \sin\alpha\sin\theta\,\hat{\theta}\end{aligned} \tag{B-17}$$

The next quantity which must be found is

$$[\bar{r}^{\circ}\times[\bar{r}^{\circ}\times[\hat{n}\times\hat{\beta}]]]=[\hat{r}\times[\hat{r}\times(-\hat{\alpha})]] \qquad \text{(B-18)}$$

Using (B-17),

$$\begin{aligned}[\bar{r}^{\circ}\times[\bar{r}^{\circ}\times[\hat{n}\times\hat{\beta}]]] &= \cos\alpha\cos\beta\cos\theta\cos\phi\,\hat{\theta}\\ &-\cos\alpha\cos\beta\sin\phi\,\hat{\phi}\\ &+\cos\alpha\sin\beta\cos\theta\sin\phi\,\hat{\theta}\\ &+\cos\alpha\sin\beta\cos\phi\,\hat{\phi}\\ &+\sin\alpha\sin\theta\,\hat{\theta}\end{aligned} \qquad \text{(B-19)}$$

From (B-2), at the front aperture at $r' = r_a$,

$$\bar{E}_{front}(\bar{r},t)=\frac{\hat{\alpha}f_1(\alpha,\beta)}{r_a}(1+k_v)V(t-r_a/v) \qquad \text{(B-20)}$$

Also, from (B-4) at the front aperture,

$$\bar{H}_{front}(\bar{r},t)=\frac{\hat{\beta}f_2(\alpha,\beta)}{\eta r_a}(1-k_v)V(t-r_a/v) \qquad \text{(B-21)}$$

From (B-5) and (B-7),

$$\begin{aligned}(\bar{r}^{\circ}\cdot\bar{r}_s)_{front} = r_a(&\sin\alpha\cos\beta\sin\theta\cos\phi\\ &+\sin\alpha\sin\beta\sin\theta\sin\phi\\ &+\cos\alpha\cos\theta)\end{aligned} \qquad \text{(B-22)}$$

Define

$$V_1' \triangleq \frac{dV\left[T - r_a/v + \left(\frac{\bar{r}^o \cdot \bar{r}_s}{v}\right)_{front}\right]}{d\left[T - r_a/v + \left(\frac{\bar{r}^o \cdot \bar{r}_s}{v}\right)_{front}\right]} \tag{B-23}$$

Also, at the front aperture

$$ds = r_a^2 \sin\alpha \, d\alpha \, d\beta \tag{B-24}$$

Using (B-14), (B-19), (B-20), (B-21), and (B-23) in (B-1), $rE_{\theta front}(\bar{r},t)$ and $rE_{\phi front}(\bar{r},t)$ may be written as follows.

$$\begin{aligned}
rE_{\theta front}(\bar{r},t) &= \left(\frac{r_a/v}{4\pi}\right)\Bigg\{\Bigg[(1+k_V)\sin\phi \int_{-\beta_o}^{\beta_o}\int_{\alpha_o(\beta)}^{\pi-\alpha_o(\beta)} \sin\beta \sin\alpha f(\alpha,\beta) V_1' \, d\alpha \, d\beta \\
&+ (1+k_V)\cos\phi \int_{-\beta_o}^{\beta_o}\int_{\alpha_o(\beta)}^{\pi-\alpha_o(\beta)} \cos\beta \sin\alpha f(\alpha,\beta) V_1' \, d\alpha \, d\beta \\
&+ (1-k_V)\cos\theta\cos\phi \int_{-\beta_o}^{\beta_o}\int_{\alpha_o(\beta)}^{\pi-\alpha_o(\beta)} \cos\beta\cos\alpha\sin\alpha f(\alpha,\beta) V_1' \, d\alpha \, d\beta \\
&+ (1-k_V)\cos\theta\sin\phi \int_{-\beta_o}^{\beta_o}\int_{\alpha_o(\beta)}^{\pi-\alpha_o(\beta)} \sin\beta\cos\alpha\sin\alpha f(\alpha,\beta) V_1' \, d\alpha \, d\beta \\
&+ (1-k_V)\sin\theta \int_{-\beta_o}^{\beta_o}\int_{\alpha_o(\beta)}^{\pi-\alpha_o(\beta)} \sin^2\alpha f(\alpha,\beta) V_1' \, d\alpha \, d\beta\Bigg]\Bigg\}
\end{aligned} \tag{B-25}$$

$$rE_{\phi front}(\bar{r},t)$$

$$= \left(\frac{r_a/v}{4\pi}\right)\left\{(1+k_v)\cos\theta\cos\phi\int_{-\beta_o}^{\beta_o}\int_{\alpha_o(\beta)}^{\pi-\alpha_o(\beta)}\sin\beta\sin\alpha f(\alpha,\beta)V_1'\,d\alpha\,d\beta\right.$$

$$-(1+k_v)\cos\theta\sin\phi\int_{-\beta_o}^{\beta_o}\int_{\alpha_o(\beta)}^{\pi-\alpha_o(\beta)}\cos\beta\sin\alpha f(\alpha,\beta)V_1'\,d\alpha\,d\beta$$

$$-(1-k_v)\sin\phi\int_{-\beta_o}^{\beta_o}\int_{\alpha_o(\beta)}^{\pi-\alpha_o(\beta)}\cos\beta\cos\alpha\sin\alpha f(\alpha,\beta)V_1'\,d\alpha\,d\beta$$

$$\left.+(1-k_v)\cos\phi\int_{-\beta_o}^{\beta_o}\int_{\alpha_o(\beta)}^{\pi-\alpha_o(\beta)}\sin\beta\cos\alpha\sin\alpha f(\alpha,\beta)V_1'\,d\alpha\,d\beta\right\} \quad \text{(B-26)}$$

The functions $\alpha_o(\beta)$ and β_o are discussed in the fourth section of this appendix.

B.3 RADIATION FROM THE WEDGE-SHAPED SIDE APERTURES

Consider now the two wedge-shaped side apertures. Let them be designated by the subscripts 1 and 2 respectively. The wedge located at $\beta=\beta_o$ is a surface of constant β with

$$\hat{n}_1 = \hat{\beta}_o \quad \text{(B-27)}$$

The second wedge located at $\beta=-\beta_o$ is a surface of constant β with

$$\hat{n}_2 = -\hat{\beta}_o \tag{B-28}$$

Also,

$$\overline{r_{s_1}} = r'\left[\sin\alpha\cos\beta_o\hat{x} + \sin\alpha\sin\beta_o\hat{y} + \cos\alpha\,\hat{z}\right] \tag{B-29}$$

and

$$\overline{r_{s_2}} = r'\left[\sin\alpha\cos\beta_o\hat{x} - \sin\alpha\sin\beta_o\hat{y} + \cos\alpha\,\hat{z}\right] \tag{B-30}$$

From (B-2), at the first wedge aperture W_1

$$\overline{E}_{W_1}(\bar{r}',t) = \frac{\hat{\alpha}_1 f(\alpha,\beta_o)}{r'}\left[V(t-r'/v) + k_v V(t+r'/v - 2r_a/v)\right] \tag{B-31}$$

and

$$\overline{H}_{W_1}(\bar{r}',t) = \frac{\hat{\beta}_1 f(\alpha,\beta_o)}{\eta\, r'}\left[V(t-r'/v) - k_v V(t+r'/v - 2r_a/v)\right] \tag{B-32}$$

Several cross products must now be determined.

$$\hat{n}_1 \times \hat{\alpha}_1 = \hat{\beta}_o \times \hat{\alpha}_1 = -\overline{r_{s_1}} \tag{B-33}$$

where

$$\hat{r}_{s_1} = \frac{\overline{r_{s_1}}}{1} \tag{B-34}$$

$$\hat{n}_1 \times \hat{\beta}_1 = \hat{\beta}_o \times \hat{\beta}_o = 0 \tag{B-35}$$

Therefore, to find the far field radiation due to the first wedge-shaped side aperture, W_1, $\left[\bar{E}^o \times \left[\hat{n}_1 \times \hat{\alpha}_1\right]\right]$ must be determined. In terms of cartesian coordinates (x,y,z),

$$-\hat{r}_{s_1} = -\sin\alpha\cos\beta_o\hat{x} - \sin\alpha\sin\beta_o\hat{y} - \cos\alpha\hat{z} \qquad \text{(B-36)}$$

Using (B-36), (B-10), (B-11), and (B-12), $-\hat{r}_{s_1}$ may be written as

$$\begin{aligned}
-\hat{r}_{s_1} = &-\sin\alpha\cos\beta_o\sin\theta\cos\phi\,\hat{r} \\
&-\sin\alpha\cos\beta_o\cos\theta\cos\phi\,\hat{\theta} \\
&+\sin\alpha\cos\beta_o\sin\phi\,\hat{\phi} \\
&-\sin\alpha\sin\beta_o\sin\theta\sin\phi\,\hat{r} \\
&-\sin\alpha\sin\beta_o\cos\theta\sin\phi\,\hat{\theta} \\
&-\sin\alpha\sin\beta_o\cos\phi\,\hat{\phi} \\
&-\cos\alpha\cos\theta\,\hat{r} + \cos\alpha\sin\theta\,\hat{\theta}
\end{aligned} \qquad \text{(B-37)}$$

Therefore,

$$\begin{aligned}
\left[\hat{r}^o \times \left[\hat{n}_1 \times \hat{\alpha}_1\right]\right] &= \hat{r} \times (-\hat{r}_{s_1}) \\
&= -\sin\alpha\cos\beta_o\cos\theta\cos\phi\,\hat{\phi} \\
&\quad -\sin\alpha\cos\beta_o\sin\phi\,\hat{\theta} \\
&\quad -\sin\alpha\sin\beta_o\cos\theta\sin\phi\,\hat{\phi} \\
&\quad +\sin\alpha\sin\beta_o\cos\phi\,\hat{\theta} \\
&\quad +\cos\alpha\sin\theta\,\hat{\phi}
\end{aligned} \qquad \text{(B-38)}$$

From (B-6) and (B-29),

$$\bar{r}^{\circ}\cdot\bar{r}_{s_1} = (\sin\alpha\cos\beta_o\sin\theta\cos\phi + \sin\alpha\sin\beta_o\sin\theta\sin\phi + \cos\alpha\cos\theta)\,r' \tag{B-39}$$

Define

$$V_2' \triangleq \frac{dV\left[T - r'/v + \frac{\bar{r}^{\circ}\cdot\bar{r}_{s_1}}{v}\right]}{d\left[T - r'/v + \frac{\bar{r}^{\circ}\cdot\bar{r}_{s_1}}{v}\right]} + k_V\frac{dV\left[T + r'/v - 2r_a/v + \frac{\bar{r}^{\circ}\cdot\bar{r}_{s_1}}{v}\right]}{d\left[T + r'/v - 2r_a/v + \frac{\bar{r}^{\circ}\cdot\bar{r}_{s_1}}{v}\right]} \tag{B-40}$$

At the wedge aperture W_1,

$$ds_{W_1} = r'dr'd\alpha \tag{B-41}$$

Using (B-31), (B-38), and (B-40) in (B-1), $rE_{\theta W_1}(\bar{r},t)$ and $rE_{\phi W_1}(\bar{r},t)$ may be written as follows.

$$rE_{\theta W_1}(\bar{r},t) = \frac{(1/v)}{4\pi}\left\{\sin\phi\cos\beta_o\int_{\alpha_o}^{\pi-\alpha_o}\int_0^{r_a}\sin\alpha\, f(\alpha,\beta_o)V_2'\,dr'd\alpha - \cos\phi\sin\beta_o\int_{\alpha_o}^{\pi-\alpha_o}\int_0^{r_a}\sin\alpha\, f(\alpha,\beta_o)V_2'\,dr'd\alpha\right\} \tag{B-42}$$

$$r E_{\phi W_1}(\bar{r},t)$$

$$= \frac{(1/v)}{4\pi}\Bigg\{\cos\theta\cos\phi\cos\beta_0 \int_{\alpha_0}^{\pi-\alpha_0}\int_0^{r_a} \sin\alpha\, f(\alpha,\beta_0) V_2' dr' d\alpha$$

$$+\cos\theta\sin\phi\sin\beta_0 \int_{\alpha_0}^{\pi-\alpha_0}\int_0^{r_a} \sin\alpha\, f(\alpha,\beta_0) V_2' dr' d\alpha$$

$$-\sin\theta \int_{\alpha_0}^{\pi-\alpha_0}\int_0^{r_a} \cos\alpha\, f(\alpha,\beta_0) V_2' dr' d\alpha \Bigg\} \qquad \text{(B-43)}$$

The function α_0 is discussed in the fourth section of this appendix.

Consider now the second wedge aperture, W_2. From (B-2),

$$\bar{E}_{W_2}(\bar{r},t) = \frac{\hat{\alpha}_2 f(\alpha,-\beta_0)}{r'}\left[V(t-r'/v)+k_v V(t+r'/v-\frac{2r_a}{v})\right] \qquad \text{(B-44)}$$

Also, from (B-4),

$$\bar{H}_{W_2}(\bar{r},t) = \frac{\hat{\beta}_2 f(\alpha,-\beta_0)}{\eta r'}\left[V(t-r'/v)-k_v V(t+r'/v-\frac{2r_a}{v})\right] \qquad \text{(B-45)}$$

Again, several cross products must now be found.

$$\hat{n}_2 \times \hat{\alpha}_2 = -\hat{\beta}_0 \times \hat{\alpha}_2 = \hat{r}_{s_2} \qquad \text{(B-46)}$$

where

$$\hat{r}_{s_2} = \frac{\bar{r}_{s_2}}{r'} \qquad \text{(B-47)}$$

$$\hat{n}_2 \times \hat{\beta}_2 = -\hat{\beta}_o \times \hat{\beta}_o = 0 \qquad \text{(B-48)}$$

Therefore, to find the far field radiation due to the second wedge aperture, W_2, $\left[\bar{F}^o \times \left[\hat{n}_2 \times \hat{\alpha}_2\right]\right]$ must be determined. In terms of cartesian coordinates (x,y,z),

$$\hat{r}_{s_2} = \sin\alpha\cos\beta_o \hat{x} - \sin\alpha\sin\beta_o \hat{y} + \cos\alpha \hat{z} \qquad \text{(B-49)}$$

Using (B-10), (B-11), and (B-12) in (B-49), $\hat{r}_{s_2}$ may be written as

$$\begin{aligned}
\hat{r}_{s_2} &= \sin\alpha\cos\beta_o \sin\theta\cos\phi\, \hat{r} + \sin\alpha\cos\beta_o\cos\theta\cos\phi\, \hat{\theta} \\
&\quad - \sin\alpha\cos\beta_o \sin\phi\, \hat{\phi} - \sin\alpha\sin\beta_o \sin\theta\sin\phi\, \hat{r} \\
&\quad - \sin\alpha\sin\beta_o\cos\theta\sin\phi\, \hat{\theta} - \sin\alpha\sin\beta_o \cos\phi\, \hat{\phi} \\
&\quad + \cos\alpha\cos\theta\, \hat{r} - \cos\alpha\sin\theta\, \hat{\theta}
\end{aligned} \qquad \text{(B-50)}$$

$$\begin{aligned}
\left[\bar{F}^o \times \left[\hat{n}_2 \times \hat{\alpha}_2\right]\right] &= \hat{r} \times \hat{r}_{s_2} \\
&= \sin\alpha\cos\beta_o\cos\theta\cos\phi\, \hat{\phi} + \sin\alpha\cos\beta_o \sin\phi\, \hat{\theta} \\
&\quad - \sin\alpha\sin\beta_o\cos\theta\sin\phi\, \hat{\phi} + \sin\alpha\sin\beta_o \cos\phi\, \hat{\theta} \\
&\quad - \cos\alpha\sin\theta\, \hat{\phi}
\end{aligned} \qquad \text{(B-51)}$$

From (B-6) and (B-30),

$$\bar{r}^{\circ}\cdot\bar{r}_{s_2} = (\sin\alpha\cos\beta_o\sin\theta\cos\phi - \sin\alpha\sin\beta_o\sin\theta\sin\phi + \cos\alpha\cos\theta)\,r' \qquad \text{(B-52)}$$

Define

$$V_3' \triangleq \frac{dV\left[T - r'/v + \frac{\bar{r}^{\circ}\cdot\bar{r}_{s_2}}{v}\right]}{d\left[T - r'/v + \frac{\bar{r}^{\circ}\cdot\bar{r}_{s_2}}{v}\right]} + k_v\frac{dV\left[T + r'/v - 2r_a/v + \frac{\bar{r}^{\circ}\cdot\bar{r}_{s_2}}{v}\right]}{d\left[T + r'/v - 2r_a/v + \frac{\bar{r}^{\circ}\cdot\bar{r}_{s_2}}{v}\right]} \qquad \text{(B-53)}$$

At the wedge aperture W_2,

$$dS_{W_2} = r'\,dr'\,d\alpha \qquad \text{(B-54)}$$

Also, from considerations of symmetry

$$f(\alpha,\beta_o) = f(\alpha,-\beta_o) \qquad \text{(B-55)}$$

Using (B-44), (B-51), and (B-53) in (B-2), $rE_{\theta W_2}(\bar{r},t)$ and $rE_{\phi W_2}(\bar{r},t)$ may be written as follows.

$$rE_{\theta W_2}(\bar{r},t) = \frac{(1/v)}{4\pi}\left\{-\sin\phi\cos\beta_o\int_{\alpha_o}^{\pi-\alpha_o}\int_0^{r_a}\sin\alpha\,f(\alpha,\beta_o)\,V_3'\,dr'\,d\alpha - \cos\phi\sin\beta_o\int_{\alpha_o}^{\pi-\alpha_o}\int_0^{r_a}\sin\alpha\,f(\alpha,\beta_o)\,V_3'\,dr'\,d\alpha\right\} \qquad \text{(B-56)}$$

$$rE_\phi w_2(\bar{r},t)$$

$$= \frac{(1/v)}{4\pi}\left\{-\cos\theta\cos\phi\cos\beta_o \int_{\alpha_o}^{\pi-\alpha_o}\int_0^{r_a} \sin\alpha\, f(\alpha,\beta_o) V_3' dr' d\alpha \right.$$

$$+\cos\theta\sin\phi\sin\beta_o \int_{\alpha_o}^{\pi-\alpha_o}\int_0^{r_a} \sin\alpha\, f(\alpha,\beta_o) V_3' dr' d\alpha$$

$$\left. +\sin\theta \int_{\alpha_o}^{\pi-\alpha_o}\int_0^{r_a} \cos\alpha\, f(\alpha,\beta_o) V_3' dr' d\alpha \right\} \qquad \text{(B-57)}$$

The function α_o is discussed in the following section of this appendix.

B.4 LIMITS OF INTEGRATION

The purpose of this section is to determine the limits of integration $\alpha_o(\beta)$, β_o, and α_o in terms of the easily measured TEM horn parameters ϕ_o and θ_o shown in Figure B.1. Consider now the coordinate systems shown in Figure B.2. The x"y"z" system is a right-handed cartesian system. The 'y'z' system is also a right-handed cartesian system obtained by rotating the x"y"z" system through a clockwise angle γ from the z" axis in the x"z" plane.

$$X' = OM' = OP\cos(\gamma+\delta) \qquad \text{(B-58)}$$

$$Z' = ON' = OP\sin(\gamma+\delta) \qquad \text{(B-59)}$$

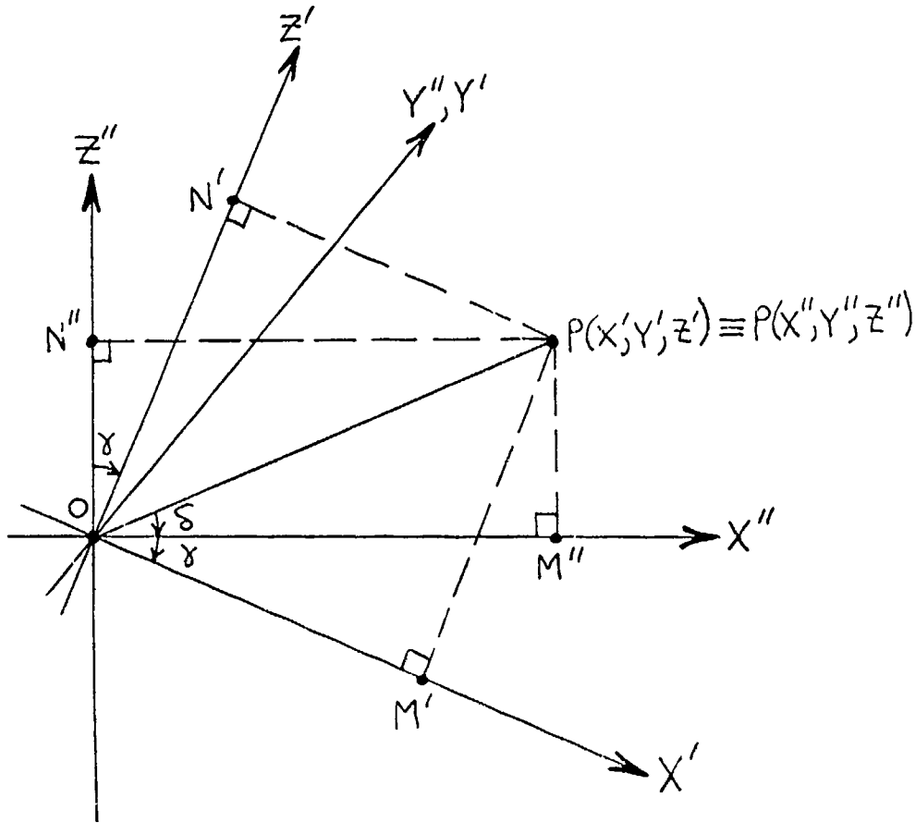

Figure B.2

Coordinate Systems to Determine the Limits of Integration

Therefore,

$$X' = OP\cos\delta\cos\gamma - OP\sin\delta\sin\gamma \tag{B-60}$$

$$Z' = OP\cos\delta\sin\gamma + OP\sin\delta\cos\gamma \tag{B-61}$$

But

$$X'' = OM'' = OP\cos\delta \tag{B-62}$$

and

$$Z'' = ON'' = OP\sin\delta \tag{B-63}$$

Therefore, the coordinate transformations may be written as

$$\begin{pmatrix} X' \\ Z' \end{pmatrix} = \begin{pmatrix} \cos\gamma & -\sin\gamma \\ \sin\gamma & \cos\gamma \end{pmatrix} \begin{pmatrix} X'' \\ Z'' \end{pmatrix} \tag{B-64}$$

The inverse coordinate transformations are given by

$$\begin{pmatrix} X'' \\ Z'' \end{pmatrix} = \begin{pmatrix} \cos\gamma & \sin\gamma \\ -\sin\gamma & \cos\gamma \end{pmatrix} \begin{pmatrix} X' \\ Z' \end{pmatrix} \tag{B-65}$$

Consider one wedge of the TEM horn lying in the x"y" plane and symmetric about the x" axis. The equation of the circle describing the outer edge of this wedge of the TEM horn in double-primed coordinates

is given by

$$x''^2 + y''^2 = r_a^2 \tag{B-66}$$

Using coordinate transformations (B-65), (B-66) may be expressed as

$$x'^2\cos^2\gamma + 2x'z'\sin\gamma\cos\gamma + z'^2\sin^2\gamma + y'^2 = r_a^2 \tag{B-67}$$

But on the surface of the sphere including the front aperture located at $r' = r_a$,

$$x' = r_a \sin\alpha\cos\beta \tag{B-68}$$

$$y' = r_a \sin\alpha\sin\beta \tag{B-69}$$

$$z' = r_a \cos\alpha \tag{B-70}$$

In order to determine $\alpha_c(\beta)$, α as a function of β and γ must be found. Using (B-68), (B-69), and (B-70) in (B-67),

$$r_a^2\sin^2\alpha\cos^2\beta\cos^2\gamma + 2r_a^2\sin\alpha\cos\alpha\cos\beta\sin\gamma\cos\gamma + r_a^2\cos^2\alpha\sin^2\gamma + r_a^2\sin^2\alpha\sin^2\beta = r_a^2 \tag{B-71}$$

After several manipulations utilizing the identity $\sin^2 x + \cos^2 x = 1$, (B-71) reduces to

$$(\sin\alpha\cos\beta\sin\gamma - \cos\alpha\cos\gamma)^2 = 0 \tag{B-72}$$

or

$$\alpha = \tan^{-1}\left(\frac{\cot\gamma}{\cos\beta}\right) \tag{B-73}$$

In polar coordinates in the double-primed coordinate system,

$$x''^2 = r_a^2 \cos^2 \phi'' \tag{B-74}$$

Also,

$$y'' = y' = r_a \sin\alpha \sin\beta \tag{B-75}$$

Therefore, using (B-74) and (B-75) in (B-66)

$$\cos^2 \phi'' + \sin^2\alpha \sin^2\beta = 1 \tag{B-76}$$

From (B-73),

$$\sin^2\alpha = \frac{\cot^2\gamma}{\cos^2\beta + \cot^2\gamma} \tag{B-77}$$

Substituting (B-77) in (B-76),

$$\cos^2\phi'' + \frac{\cot^2\gamma}{(\cos^2\beta + \cot^2\gamma)} \sin^2\beta = 1 \tag{B-78}$$

Solving (B-78) for $\cos^2\beta$,

$$\cos^2\beta = \frac{\cos^2\phi''}{1 + \frac{(1-\cos^2\phi'')}{\cot^2\gamma}} \tag{B-79}$$

Considering β to be a positive angle between 0 and π,

$$\beta = \cos^{-1}\left[\frac{\cos\phi''}{\sqrt{1 + \frac{(1-\cos^2\phi'')}{\cot^2\gamma}}}\right] \tag{B-80}$$

Finally, α is found as a function of β'' and γ. From (B-73),

$$\sin^2\beta = 1 - \cot^2\alpha \cot^2\gamma \tag{B-81}$$

Using (B-81) in (B-76),

$$\cos^2\phi'' + \sin^2\alpha\left(1 - \cot^2\alpha\cot^2\gamma\right) = 1 \qquad \text{(B-82)}$$

Solving (B-82) for $\cos^2\alpha$,

$$\cos^2\alpha = \frac{\cos^2\phi''}{1 + \cot^2\gamma} \qquad \text{(B-83)}$$

Therefore,

$$\alpha = \cos^{-1}\left(\frac{\cos\phi''}{\sqrt{1 + \cot^2\gamma}}\right) \qquad \text{(B-84)}$$

Referring to Figures B.1 and B.2, at the upper wedge of the TEM horn,

$$\gamma = \frac{\pi}{2} - \theta_o \qquad \text{(B-85)}$$

The limits of integration $\alpha_o(\beta)$, β_o, and α_o may then be written as follows. Using (B-85) in (B-73),

$$\alpha_o(\beta) = \tan^{-1}\left(\frac{\tan\theta_o}{\cos\beta}\right) \qquad \text{(B-86)}$$

Referring again to Figures B.1 and B.2, the limit of ϕ'' is $\phi_o/2$. Therefore, using (B-85) in (B-80),

$$\beta_o = \cos^{-1}\left[\frac{\cos(\phi_o/2)}{\sqrt{1 + \dfrac{\left(1 - \cos^2(\phi_o/2)\right)}{\tan^2\theta_o}}}\right] \qquad \text{(B-87)}$$

and, using (B-85) in (B-84),

$$\alpha_o = \cos^{-1}\left(\frac{\cos(\phi_o/2)}{\sqrt{1 + \tan^2\theta_o}}\right) \qquad \text{(B-88)}$$

B.5 SUMMARY

The total electric far fields of the TEM horn are due to the sum of the radiation from the front aperture and the wedge-shaped side apertures. The theta component is the sum of (B-25), (B-42), and (B-56). Therefore,

$$
\begin{aligned}
r E_\theta(r,t) = \frac{(r_a/v)}{4\pi}\Bigg\{ & (1+k_v)\sin\phi \int_{-\beta_o}^{\beta_o}\int_{\alpha_o(\beta)}^{\pi-\alpha_o(\beta)} \sin\beta \sin\alpha f(\alpha,\beta) V_1' \, d\alpha \, d\beta \\
& + (1+k_v)\cos\phi \int_{-\beta_o}^{\beta_o}\int_{\alpha_o(\beta)}^{\pi-\alpha_o(\beta)} \cos\beta \sin\alpha f(\alpha,\beta) V_1' \, d\alpha \, d\beta \\
& + (1-k_v)\cos\theta\cos\phi \int_{-\beta_o}^{\beta_o}\int_{\alpha_o(\beta)}^{\pi-\alpha_o(\beta)} \cos\beta\cos\alpha \sin\alpha f(\alpha,\beta) V_1' \, d\alpha \, d\beta \\
& + (1-k_v)\cos\theta\sin\phi \int_{-\beta_o}^{\beta_o}\int_{\alpha_o(\beta)}^{\pi-\alpha_o(\beta)} \sin\beta\cos\alpha\sin\alpha f(\alpha,\beta) V_1' \, d\alpha \, d\beta \\
& + (1-k_v)\sin\theta \int_{-\beta_o}^{\beta_o}\int_{\alpha_o(\beta)}^{\pi-\alpha_o(\beta)} \sin^2\alpha f(\alpha,\beta) V_1' \, d\alpha \, d\beta \Bigg\}
\end{aligned}
$$

$$+\frac{(1/v)}{4\pi}\left\{\sin\phi\cos\beta_0\int_{\alpha_0}^{\pi-\alpha_0}\int_0^{r_a}\sin\alpha\, f(\alpha,\beta_0)V_2'\,dr'd\alpha\right.$$

$$\left.-\cos\phi\sin\beta_0\int_{\alpha_0}^{\pi-\alpha_0}\int_0^{r_a}\sin\alpha\, f(\alpha,\beta_0)V_2'\,dr'd\alpha\right\}$$

$$+\frac{(1/v)}{4\pi}\left\{-\sin\phi\cos\beta_0\int_{\alpha_0}^{\pi-\alpha_0}\int_0^{r_a}\sin\alpha\, f(\alpha,\beta_0)V_3'\,dr'd\alpha\right.$$

$$\left.-\cos\phi\sin\beta_0\int_{\alpha_0}^{\pi-\alpha_0}\int_0^{r_a}\sin\alpha\, f(\alpha,\beta_0)V_3'\,dr'd\alpha\right\} \qquad \text{(B-69)}$$

V_1', V_2', and V_3' are given by (B-23), (B-40), and (B-53) respectively. The limits $\alpha_0(\beta)$ and β_0 are given by (B-86) and (B-87) respectively. The phi component is the sum of (B-26), (B-43), and (B-57). Therefore,

$$rE_\phi(\bar{r},t)$$

$$=\frac{(r_a/v)}{4\pi}\left\{(1+k_v)\cos\theta\cos\phi\int_{-\beta_0}^{\beta_0}\int_{\alpha_0(\beta)}^{\pi-\alpha_0(\beta)}\sin\beta\sin\alpha\, f(\alpha,\beta)V_1'\,d\alpha d\beta\right.$$

$$-(1+k_v)\cos\theta\sin\phi\int_{-\beta_0}^{\beta_0}\int_{\alpha_0(\beta)}^{\pi-\alpha_0(\beta)}\cos\beta\sin\alpha\, f(\alpha,\beta)V_1'\,d\alpha d\beta$$

$$-(1-k_v)\sin\phi\int_{-\beta_0}^{\beta_0}\int_{\alpha_0(\beta)}^{\pi-\alpha_0(\beta)}\cos\beta\cos\alpha\sin\alpha\, f(\alpha,\beta)V_1'\,d\alpha d\beta$$

$$\left.+(1-k_v)\cos\phi\int_{-\beta_0}^{\beta_0}\int_{\alpha_0(\beta)}^{\pi-\alpha_0(\beta)}\sin\beta\cos\alpha\sin\alpha\, f(\alpha,\beta)V_1'\,d\alpha d\beta\right\}$$

$$+\frac{(1/v)}{4\pi}\Bigg\{\cos\theta\cos\phi\cos\beta_0\int_{\alpha_0}^{\pi-\alpha_0}\int_0^{r_a}\sin\alpha\, f(\alpha,\beta_0)V_2'\,dr'd\alpha$$

$$+\cos\theta\sin\phi\sin\beta_0\int_{\alpha_0}^{\pi-\alpha_0}\int_0^{r_a}\sin\alpha\, f(\alpha,\beta)V_2'\,dr'd\alpha$$

$$-\sin\theta\int_{\alpha_0}^{\pi-\alpha_0}\int_0^{r_a}\cos\alpha\, f(\alpha,\beta_0)V_2'\,dr'd\alpha\Bigg\}$$

$$+\frac{(1/v)}{4\pi}\Bigg\{-\cos\theta\cos\phi\cos\beta_0\int_{\alpha_0}^{\pi-\alpha_0}\int_0^{r_a}\sin\alpha\, f(\alpha,\beta_0)V_3'\,dr'd\alpha$$

$$+\cos\theta\sin\phi\sin\beta_0\int_{\alpha_0}^{\pi-\alpha_0}\int_0^{r_a}\sin\alpha\, f(\alpha,\beta_0)V_3'\,dr'd\alpha$$

$$+\sin\theta\int_{\alpha_0}^{\pi-\alpha_0}\int_0^{r_a}\cos\alpha\, f(\alpha,\beta_0)V_3'\,dr'd\alpha\Bigg\} \qquad \text{(B-90)}$$

The limit α_0 is given by (B-88).

Appendix C

DERIVATION OF THE ELECTRIC FAR FIELDS OF THE PARABOLOID REFLECTOR/POINT SOURCE FEED UTILIZING THE CHERNOUSOV METHOD

C.1 INTRODUCTION

In this appendix, the Chernousov (1965) formulation is used to derive the transient electric far fields of a paraboloid reflector fed by a transient TEM spherical-wave point source located at the focus of the paraboloid. The reflector is assumed to be perfectly conducting, to be in the far field of the feed, and to be sufficiently smooth to allow application of the plane wave boundary conditions at the reflector surface.

The geometrical optics approximation is invoked to allow a one-to-one, point-to-point transformation of the fields emanating from the focus to the fields at the exit aperture. The electric far fields of the paraboloid reflector/point source system are then formulated in terms of the fields existing at the exit aperture.

Four coordinate systems are used in the derivation. These systems are shown in Figure C.1. To describe the relation of the point source feed pattern to the reflector surface, a cartesian coordinate system x,y,z and a spherical system ρ, Ψ, ξ are used. The focus of the paraboloid, 0, is located at the origin of the cartesian

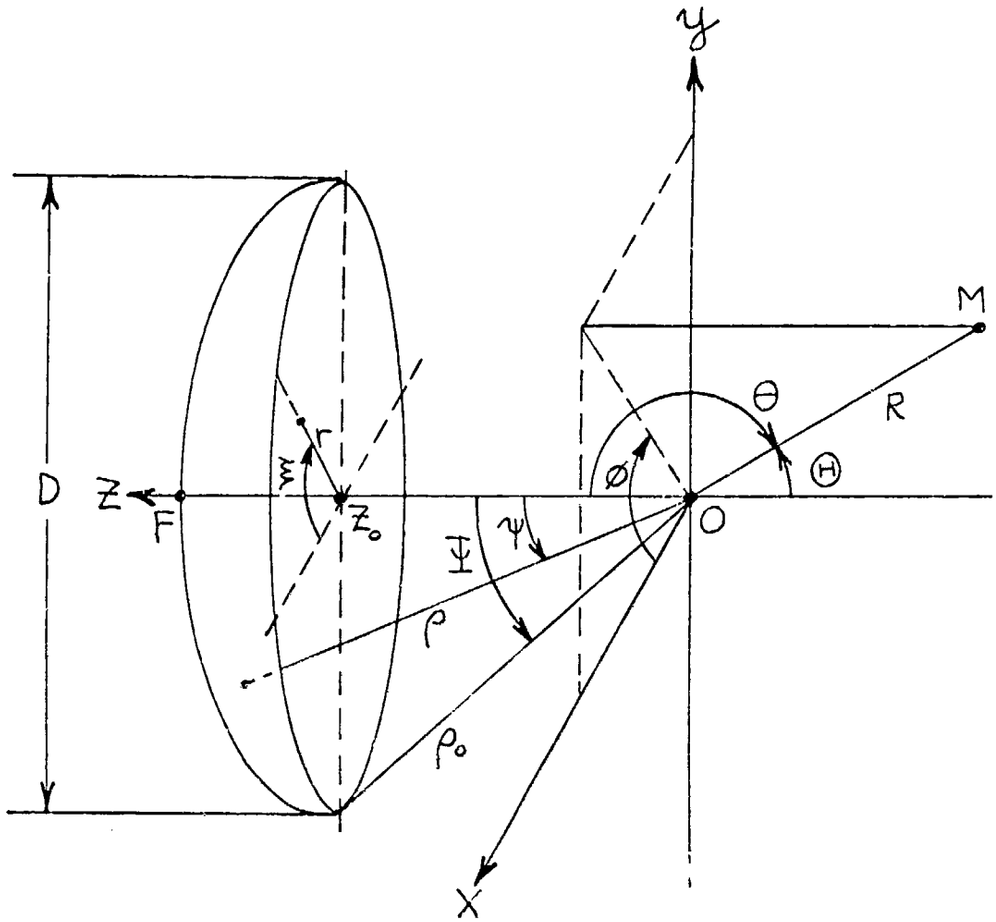

D = exit aperture diameter
M = observation point
OF = f = focal length
z_o = center of exit aperture
Ψ_o = half-angular aperture
Θ = π - θ

Figure C.1

Geometry for the Paraboloid Reflector/Point Source Feed

system, and the z-axis is the axis of revolution of the paraboloid. To describe the observation point in the far field of the antenna system, a spherical coordinate system R,θ,ϕ is used. The origin of this system is at the origin of the x,y,z system. To describe the distribution of fields over the exit aperture, a polar system r,ξ,z is used. The r,ξ plane is parallel to the x,y plane, and the origin is located at the focus of the paraboloid.

C.2 THE GENERAL FORM OF THE FAR FIELDS ARISING FROM THE POINT SOURCE AT THE FOCUS

Assume that at the focus of the paraboloid, located at O, there exists a spherical-wave point source described by the following radiated $\bar{E}$ and $\bar{H}$ fields. It is assumed that the paraboloid reflector is in the far field of the point source. That is, the $\bar{E}$-field components of the radiation from the point source may be described as

$$\bar{E}_\psi = \frac{V_1(\psi, \xi, t)}{\rho}\,\hat{\psi} \tag{C-1}$$

and

$$\bar{E}_\xi = \frac{V_2(\psi, \xi, t)}{\rho}\,\hat{\xi} \tag{C-2}$$

(ρ, ψ, ξ) are the spherical coordinates discussed in Section C.1. V_1 and V_2 are general functions of ψ, ξ, and t. $\bar{E}_\psi$ and $\bar{E}_\xi$ are the $\bar{E}$-field components of TEM waves propagating in the $\hat{\rho}$ direction. Therefore,

$$\bar{H}_\xi = \frac{V_1(\psi, \xi, t)}{\eta\rho}\,\hat{\xi} \tag{C-3}$$

and

$$\overline{H}\psi = -\frac{V_2(\psi,\xi,t)}{\eta\rho}\hat{\psi} \tag{C-4}$$

where η is the impedance of the medium.

Functions V_1 and V_2 may apply to any feed for the paraboloid reflector which is approximated by a transient (or cw) spherical-wave point source located at the focus.

C.3 GENERAL GEOMETRICAL PROPERTIES OF THE PARABOLOID REFLECTOR

The vertex of the paraboloid is located at $(x,y,z) = (0,0,F)$. The axis of revolution of the paraboloid is the z-axis. The equation of the paraboloid is

$$x^2 + y^2 = 4f(f - z) \tag{C-5}$$

as given in Collin and Zucker (1969,39).

With respect to the spherical source coordinate system,

$$x = \rho \sin\psi \cos\xi \tag{C-6}$$

$$y = \rho \sin\psi \sin\xi \tag{C-7}$$

$$z = \rho \cos\psi \tag{C-8}$$

Substituting (C-6), (C-7), and (C-8) into (C-5),

$$\rho = \frac{2f}{1 + \cos\psi} \tag{C-9}$$

(C-9) is also given in Collin and Zucker (1969:39). However,

$$\frac{1+\cos\psi}{2} = \cos^2\frac{\psi}{2} \tag{C-10}$$

Therefore,

$$\rho = f\sec^2\frac{\psi}{2} \tag{C-11}$$

To determine the unit normal to the paraboloid surface, $\hat{n}_p$, in the spherical ρ,ψ,ξ system, the gradient of the equation of the surface is taken and then properly normalized. For a scalar function g,

$$\nabla g = \frac{\partial g}{\partial \rho}\hat{\rho} + \frac{1}{\rho}\frac{\partial g}{\partial \psi}\hat{\psi} + \frac{1}{\rho\sin\psi}\frac{\partial g}{\partial \xi}\hat{\xi} \tag{C-12}$$

Therefore,

$$\nabla\left[f - \rho\cos^2\frac{\psi}{2}\right]$$

$$= -\cos^2\left(\frac{\psi}{2}\right)\hat{\rho} + \frac{1}{\rho}\left[-2\cos\frac{\psi}{2}\left(-\sin\frac{\psi}{2}\right)\frac{1}{2}\right]\hat{\psi} \tag{C-13}$$

$$\left|\nabla\left[f-\rho\cos^2\frac{\psi}{2}\right]\right|^2 = \cos^4\frac{\psi}{2} + \sin^2\frac{\psi}{2}\cos^2\frac{\psi}{2} \tag{C-14}$$

or

$$\left|\nabla\left[f-\rho\cos^2\frac{\psi}{2}\right]\right|^2 = \cos^2\frac{\psi}{2} \tag{C-15}$$

Therefore,

$$\hat{n}_p = \frac{\nabla\left[f-\rho\cos^2\frac{\psi}{2}\right]}{\cos\frac{\psi}{2}} \tag{C-16}$$

Substituting (C-13) into (C-16),

$$\hat{n}_p = -\cos\frac{\Psi}{2}\hat{\rho} + \sin\frac{\Psi}{2}\hat{\psi} \qquad \text{(C-17)}$$

(C-17) is also given in Collin and Zucker (1969:39).

To determine the relationship between the focal length f, the exit aperture diameter D, and the half-angular aperture Ψ, equation (C-11) is used. The various quantities used in this derivation are indicated in Figure C.1. At the edge of the reflector,

$$\sin\Psi = \frac{D}{2\rho_0} \qquad \text{(C-18)}$$

From (C-11),

$$\cos^2\frac{\Psi}{2} = \frac{f}{\rho_0} \qquad \text{(C-19)}$$

From (C-18),

$$\frac{1}{\rho_0} = \frac{2\sin\Psi}{D} \qquad \text{(C-20)}$$

Therefore, substituting (C-20) into (C-19),

$$\cos^2\frac{\Psi}{2} = \frac{2f}{D}\sin\Psi \qquad \text{(C-21)}$$

Solving (C-21) for $\cos\Psi$,

$$\cos\Psi = \frac{16(f/D)^2 - 1}{16(f/D)^2 + 1} \qquad \text{(C-22)}$$

z_0, ρ, and several trigonometric functions of Ψ are also determined in terms of the exit aperture coordinates r, ξ, z.

$$x^2 + y^2 = r^2 \qquad \text{(C-23)}$$

When $z = z_o$,

$$r^2 = \left(\frac{D}{2}\right)^2 = \frac{D^2}{4} \tag{C-24}$$

Substituting (C-23) and (C-24) into (C-5),

$$\frac{D^2}{4} = 4f(f - z_o) \tag{C-25}$$

or

$$z_o = \frac{D\left[16(f/D)^2 - 1\right]}{16(f/D)} \tag{C-26}$$

Substituting (C-23) into (C-5) and solving for z,

$$z = f\left(1 - \frac{r^2}{4f^2}\right) \tag{C-27}$$

But

$$\rho^2 = z^2 + r^2 \tag{C-28}$$

Substituting (C-27) into (C-28) and solving for ρ,

$$\rho = f\left(1 + \frac{r^2}{4f^2}\right) \tag{C-29}$$

As shown in Figure C.1,

$$\cos\Psi = \frac{z}{\rho} \tag{C-30}$$

$$\sin\Psi = \frac{r}{\rho} \tag{C-31}$$

Using (C-27) and (C-29) in (C-30),

$$\cos\Psi = \frac{\left[1 - \frac{r^2}{4f^2}\right]}{\left[1 + \frac{r^2}{4f^2}\right]} \tag{C-32}$$

Using (C-29) in (C-31),

$$\sin\psi = \frac{r}{f\left[1+\frac{r^2}{4f^2}\right]} \tag{C-33}$$

To determine $\sin\frac{\psi}{2}$ and $\cos\frac{\psi}{2}$, the trigonometric identities

$$\cos^2\frac{\psi}{2} = \frac{1+\cos\psi}{2} \tag{C-34}$$

and

$$\sin^2\frac{\psi}{2} = \frac{1-\cos\psi}{2} \tag{C-35}$$

are employed. Using (C-35) in (C-32),

$$\sin\frac{\psi}{2} = \frac{\frac{r}{2f}}{\left[1+\frac{r^2}{4f^2}\right]^{1/2}} \tag{C-36}$$

Using (C-34) in (C-32),

$$\cos\frac{\psi}{2} = \frac{1}{\left[1+\frac{r^2}{4f^2}\right]^{1/2}} \tag{C-37}$$

C.4 THE ELECTRIC FAR FIELDS OF THE PARABOLOID REFLECTOR/POINT SOURCE IN TERMS OF THE FIELDS AT THE EXIT APERTURE

The derivation in this section utilizes four assumptions:

1. The reflected fields at the paraboloid surface are found by applying plane wave boundary conditions.
2. The geometrical optics approximation is invoked to afford a one-to-one, point-to-point transformation between the fields at the paraboloid surface and the fields at the exit aperture.

3. The Chernousov formulation requires a closed surface S_a. In keeping with common practice, S_a is taken as a plane containing the exit aperture and closed at infinity, and the fields over the non-aperture part of the plane are taken as approximately zero (Ramo and Whinnery, 1956:530,532).

4. Edge effects at the exit aperture are not considered.

The plane wave boundary conditions for the electric fields at the paraboloid surface are

$$\hat{n}_p \times \hat{e}_r = -\hat{n}_p \times \hat{e}_i \tag{C-38}$$

and

$$\hat{n}_p \cdot \hat{e}_r = \hat{n}_p \cdot \hat{e}_i \tag{C-39}$$

where $\hat{e}_i$ and $\hat{e}_r$ are unit vectors in the direction of the incident and reflected electric fields respectively. $\hat{n}_p$ is the unit vector normal to the paraboloid. Using (C-1) and (C-2), the incident electric field at the paraboloid surface, $\bar{E}_i$, may be written as

$$\bar{E}_i = \frac{V_1(\Psi, \Xi, t - \frac{\rho}{v})}{\rho} \hat{\psi} + \frac{V_2(\Psi, \Xi, t - \frac{\rho}{v})}{\rho} \hat{\xi} \tag{C-40}$$

The unit vector, $\hat{n}_p$, normal to the paraboloid is

$$\hat{n}_p = -\cos\frac{\Psi}{2}\hat{\xi} + \sin\frac{\Psi}{2}\hat{\psi} \tag{C-41}$$

From (C-38), (C-40), and (C-41),

$$\hat{n}_p \times \bar{E}_r = \frac{V_1(\Psi, \Xi, t - \frac{\rho}{v})}{\rho} \cos\frac{\Psi}{2}\hat{\xi}$$

$$- \frac{V_2(\Psi, \Xi, t - \frac{\rho}{v})}{\rho} \cos\frac{\Psi}{2}\hat{\psi} - \frac{V_2(\Psi, \Xi, t - \frac{\rho}{v})}{\rho} \sin\frac{\Psi}{2}\hat{\rho} \tag{C-42}$$

From (C-39), (C-40), and (C-41),

$$\hat{n}_p \cdot \bar{E}_r = \sin\frac{\Psi}{2}\,\frac{V_1(\Psi, \xi, t - \frac{\rho}{c})}{\rho} \qquad \text{(C-43)}$$

First, the reflected $\bar{E}$ and $\bar{H}$ fields at the exit aperture are found. Consider the expressions for $\hat{n}_p \times \bar{E}_r$ and $\hat{n}_p \cdot \bar{E}_r$. From (C-42),

$$\hat{n}_p \times \bar{E}_r = \frac{V_1}{\rho}\cos\frac{\Psi}{2}\,\hat{\xi} - \frac{V_2}{\rho}\cos\frac{\Psi}{2}\,\hat{\Psi} - \frac{V_2}{\rho}\sin\frac{\Psi}{2}\,\hat{\rho} \qquad \text{(C-44)}$$

From (C-43),

$$\hat{n}_p \cdot \bar{E}_r = \frac{V_1}{\rho}\sin\frac{\Psi}{2} \qquad \text{(C-45)}$$

Describing the reflected electric field $\bar{E}_r$ in terms of normal and tangential components,

$$\bar{E}_r = (\hat{n}_p \cdot \bar{E}_r)\hat{n}_p + (\hat{n}_p \times \bar{E}_r) \times \hat{n}_p \qquad \text{(C-46)}$$

Utilizing (C-41),

$$(\hat{n}_p \cdot \bar{E}_r)\hat{n}_p = -\frac{V_1}{\rho}\sin\frac{\Psi}{2}\cos\frac{\Psi}{2}\,\hat{\rho} + \frac{V_1}{\rho}\sin^2\frac{\Psi}{2}\,\hat{\Psi} \qquad \text{(C-47)}$$

and

$$(\hat{n}_p \times \bar{E}_r) \times \hat{n}_p = -\frac{V_1}{\rho}\cos^2\frac{\Psi}{2}\,\hat{\Psi} - \frac{V_1}{\rho}\sin\frac{\Psi}{2}\cos\frac{\Psi}{2}\,\hat{\rho} - \frac{V_2}{\rho}\cos^2\frac{\Psi}{2}\,\hat{\xi} - \frac{V_2}{\rho}\sin^2\frac{\Psi}{2}\,\hat{\xi} \qquad \text{(C-48)}$$

Therefore, employing the trigonometric identities

$$2\sin\frac{\Psi}{2}\cos\frac{\Psi}{2} = \sin\Psi \qquad \text{(C-49)}$$

and

$$\cos^2\frac{\psi}{2} - \sin^2\frac{\psi}{2} = \cos\psi \tag{C-50}$$

$$\bar{E}_r = -\frac{V_1}{\rho}\sin\psi\,\hat{\rho} - \frac{V_1}{\rho}\cos\psi\,\hat{\psi} - \frac{V_2}{\rho}\hat{\xi} \tag{C-51}$$

To find the reflected electric field at the exit aperture, $\bar{E}_{rA}$, the geometrical optics approximation is applied. Since all of the reflected rays from the paraboloid surface are parallel, the field intensity remains constant in magnitude between the paraboloid surface and the exit aperture. The geometrical optics approximation also implies that the reflected field at the exit aperture can have no $\hat{z}$ component. Utilizing the vector identities

$$\hat{\rho} = \sin\psi\cos\xi\,\hat{x} + \sin\psi\sin\xi\,\hat{y} + \cos\psi\,\hat{z} \tag{C-52}$$

$$\hat{\psi} = \cos\psi\cos\xi\,\hat{x} + \cos\psi\sin\xi\,\hat{y} - \sin\psi\,\hat{z} \tag{C-53}$$

$\bar{E}_{rA}$ may be written as

$$\bar{E}_{rA} = -\frac{V_{1A}}{\rho}\sin^2\psi\cos\xi\,\hat{x} - \frac{V_{1A}}{\rho}\sin^2\psi\sin\xi\,\hat{y}$$
$$-\frac{V_{1A}}{\rho}\cos^2\psi\cos\xi\,\hat{x} - \frac{V_{1A}}{\rho}\cos^2\psi\sin\xi\,\hat{y}$$
$$-\frac{V_{2A}}{\rho}\hat{\xi} \tag{C-54}$$

V_{1A} and V_{2A} are the functions V_1 and V_2 respectively, evaluated at the exit aperture. But in the exit aperture coordinates r, ξ, z,

$$\hat{r} = \cos\xi\,\hat{x} + \sin\xi\,\hat{y} \tag{C-55}$$

Therefore,

$$\bar{E}_{rA} = -\frac{V_{1A}}{\rho}\hat{r} - \frac{V_{2A}}{\rho}\hat{\xi} \tag{C-56}$$

To determine the reflected magnetic field at the exit aperture, $\bar{H}_{rA}$, the condition

$$\bar{H}_{r_1} = \frac{1}{\eta}\left[-\hat{z} \times \bar{E}_{rA}\right] \tag{C-57}$$

is employed. (C-57) simply states that $\bar{E}_{rA}$ and $\bar{H}_{rA}$ comprise a TEM pair propagating in the $-\hat{z}$ direction. Substituting (C-56) into (C-57), $\bar{H}_{rA}$ may be written as

$$\bar{H}_{rA} = \frac{V_{1A}}{\eta\rho}\hat{\xi} - \frac{V_{2A}}{\eta\rho}\hat{r} \tag{C-58}$$

To complete the Chernousov (1965) formulation in terms of $\bar{E}_{rA}$ and $\bar{H}_{rA}$ over the exit aperture in the coordinates r, ξ, z, V_{1A} and V_{2A} must be found. Using (C-29) in (C-37),

$$\frac{\cos\frac{\psi}{2}}{\rho} = \frac{1}{f\left[1 + \frac{r^2}{4f^2}\right]^{3/2}} \tag{C-59}$$

Using (C-29) in (C-36),

$$\frac{\sin^2\frac{\psi}{2}}{\rho} = \frac{\frac{r^2}{4f^2}}{f\left[1 + \frac{r^2}{4f^2}\right]^2} \tag{C-60}$$

Employing the geometrical optics approximation, V_{1A} is the same as V_1 if the time retardation from the focus to the exit aperture is taken into account. Also, V_{2A} has the same relationship to V_2. The time retardation from the focus to the exit aperture is the length of the optical path divided by v, the velocity of propagation in the medium.

By inspection of Figure C.1,

$$\frac{\text{optical path}}{v} = \frac{\rho}{v} + \frac{z - z_o}{v} = \frac{f}{v} + \frac{f - z_o}{v} \qquad \text{(C-61)}$$

Substituting (C-26) into (C-61),

$$\frac{\text{optical path}}{v} = \frac{f}{v} + \frac{D}{v}\left[\frac{1}{16(f/D)}\right] = \frac{f}{v}\left[\frac{16(f/D)^2 + 1}{16(f/D)^2}\right] \qquad \text{(C-62)}$$

Therefore,

$$V_{1A}\left\{r, \xi, t - \frac{f}{v}\left[\frac{16(f/D)^2 + 1}{16(f/D)^2}\right]\right\} = V_1\left\{\psi, \xi, t - \frac{f}{v}\left[\frac{16(f/D)^2 + 1}{16(f/D)^2}\right]\right\} \qquad \text{(C-63)}$$

and

$$V_{2A}\left\{r, \xi, t - \frac{f}{v}\left[\frac{16(f/D)^2 + 1}{16(f/D)^2}\right]\right\} = V_2\left\{\psi, \xi, t - \frac{f}{v}\left[\frac{16(f/D)^2 + 1}{16(f/D)^2}\right]\right\} \qquad \text{(C-64)}$$

The relationship between ψ and r in terms of f is given by (C-32).

Consider the Chernousov far field formulation of the fields over the exit aperture in terms of the spherical observation coordinates R, θ, ϕ.

$$\bar{E}(\bar{R}, t) = -\frac{1}{4\pi v R}\int_{S_A}\left\{\left[\bar{R}^o \times \left[\hat{n} \times \frac{\partial \bar{E}_{rA}}{\partial t}\right]\right]\right\} ds + \frac{1}{4\pi v R}\int_{S_A} \eta\left[\bar{R}^o \times \left[\bar{R}^o \times \left[\hat{n} \times \frac{\partial \bar{H}_{rA}}{\partial t}\right]\right]\right] ds \qquad \text{(C-65)}$$

This equation is of the same form as equation (A-102) on the last page of Appendix A. The various quantities involved in (C-65) are:

ds, the differential surface element of the exit aperture,

$\bar{E}_{rA}$, the reflected $\bar{E}$ field evaluated at the exit aperture,

$\bar{H}_{rA}$, the reflected $\bar{H}$ field evaluated at the exit aperture,

$\hat{n}$, the unit vector outward from the exit aperture,

$\bar{R}^{o}$, the unit vector in the $\bar{R}$ direction,

S_A, the surface of the exit aperture,

v, the velocity of propagation in the medium, and

η, the impedance of the medium.

The open surface of the exit aperture, S_A, is taken as an approximation to the closed surface S_a required by the Chernousov formulation. This is because edge effects are not considered, and because the fields over the remainder of the closed surface are considered to be negligible. $T = t - (R/v)$, and $\bar{r}_s$ is given by (C-77).

Since neither ρ, Ψ, ξ nor r, ξ, z are functions of time,

$$\frac{\partial \bar{E}_{rA}}{\partial t} = \frac{\partial \bar{E}_{rA}\left(\bar{r}_s, T + \frac{\bar{R}^{o} \cdot \bar{r}_s}{v}\right)}{\partial\left(T + \frac{\bar{R}^{o} \cdot \bar{r}_s}{v}\right)} \tag{C-66}$$

From (C-56),

$$\frac{\partial \bar{E}_{rA}}{\partial t} = -\frac{V_{1A}'}{\rho}\hat{r} - \frac{V_{2A}'}{\rho}\hat{\xi} \tag{C-67}$$

Where

$$V_{1A}' = \frac{\partial V_1\left\{r, \xi, T - \frac{f}{v}\left[\frac{16(f/D)^2 + 1}{16(f/D)^2}\right] + \frac{\bar{R}^{o} \cdot \bar{r}_s}{v}\right\}}{\partial\left\{T - \frac{f}{v}\left[\frac{16(f/D)^2 + 1}{16(f/D)^2}\right] + \frac{\bar{R}^{o} \cdot \bar{r}_s}{v}\right\}} \tag{C-68}$$

and

$$V_{2A}' = \frac{\partial V_2\left\{r, \xi, T - \frac{f}{v}\left[\frac{16(f/D)^2 + 1}{16(f/D)^2}\right] + \frac{\bar{R}^{o} \cdot \bar{r}_s}{v}\right\}}{\partial\left\{T - \frac{f}{v}\left[\frac{16(f/D)^2 + 1}{16(f/D)^2}\right] + \frac{\bar{R}^{o} \cdot \bar{r}_s}{v}\right\}} \tag{C-69}$$

From (C-58),

$$\frac{\partial \bar{H}_{rA}}{\partial t} = \frac{V'_{1A}}{\eta \rho}\hat{\xi} - \frac{V'_{2A}}{\eta \rho}\hat{r} \tag{C-70}$$

Let

$$\frac{\partial \bar{E}_{rA}}{\partial t} \triangleq \bar{E}'_A \tag{C-71}$$

and

$$\frac{\partial \bar{H}_{rA}}{\partial t} \triangleq \bar{H}'_A \tag{C-72}$$

$\bar{E}'_A$ and $\bar{H}'_A$ are easily found in terms of the exit aperture coordinates r, ξ, z by the use of (C-29) in (C-67) and (C-70).

$$\frac{\partial \bar{E}_{rA}}{\partial t} \triangleq \bar{E}'_A = -\frac{V'_{1A}}{f\left[1+\frac{r^2}{4f^2}\right]}\hat{r} - \frac{V'_{2A}}{f\left[1+\frac{r^2}{4f^2}\right]}\hat{\xi} \tag{C-73}$$

$$\frac{\partial \bar{H}_{rA}}{\partial t} \triangleq \bar{H}'_A = \frac{V'_{1A}}{\eta f\left[1+\frac{r^2}{4f^2}\right]}\hat{\xi} - \frac{V'_{2A}}{\eta f\left[1+\frac{r^2}{4f^2}\right]}\hat{r} \tag{C-74}$$

The surface element ds at the exit aperture is

$$ds = r\,dr\,d\xi \tag{C-75}$$

The unit vector in the $\bar{R}$ direction, $\bar{R}^o$, is given by

$$\bar{R}^o = \frac{\bar{R}}{R} = \sin\theta\cos\phi\hat{x} + \sin\theta\sin\phi\hat{y} + \cos\theta\hat{z} \tag{C-76}$$

The vector $\bar{r}_s$ from the origin to the exit aperture surface element ds is

$$\bar{r}_s = z_o\hat{z} + r\hat{r} \tag{C-77}$$

But

$$\hat{r} = \cos\xi\,\hat{x} + \sin\xi\,\hat{y} \tag{C-78}$$

Therefore,

$$\bar{r}_S = z_o\hat{z} + r\cos\xi\,\hat{x} + r\sin\xi\,\hat{y} \tag{C-79}$$

and

$$\bar{R}^\circ \cdot \bar{r}_S = r(\cos\xi\sin\theta\cos\phi + \sin\xi\sin\theta\sin\phi) + z_o\cos\theta \tag{C-80}$$

$$-\left[\bar{R}^\circ \times \left[\hat{n} \times \bar{E}_A'\right]\right] \text{ and } \eta\left[\bar{R}^\circ \times \left[\bar{R}^\circ \times \left[\hat{n} \times \bar{H}_A'\right]\right]\right]$$

must now be determined. From (C-67) and (C-71),

$$\rho\bar{E}_A' = -V_{1A}'\hat{r} - V_{2A}'\hat{\xi} \tag{C-81}$$

The unit vector $\hat{n}$ normal to the exit aperture is $-\hat{z}$. Therefore,

$$\hat{n} \times \rho\bar{E}_A' = V_{1A}'\hat{\xi} - V_{2A}'\hat{r} \tag{C-82}$$

But

$$\hat{r} = \cos\xi\,\hat{x} + \sin\xi\,\hat{y} \tag{C-83}$$

$$\hat{\xi} = -\sin\xi\,\hat{x} + \cos\xi\,\hat{y} \tag{C-84}$$

Also,

$$\hat{x} = \sin\theta\cos\phi\,\hat{R} + \cos\theta\cos\phi\,\hat{\theta} - \sin\phi\,\hat{\phi} \tag{C-85}$$

$$\hat{y} = \sin\theta\sin\phi\,\hat{R} + \cos\theta\sin\phi\,\hat{\theta} + \cos\phi\,\hat{\phi} \tag{C-86}$$

$$\hat{z} = \cos\theta\,\hat{R} - \sin\theta\,\hat{\theta} \tag{C-87}$$

Substituting (C-83), (C-84), (C-85), (C-86), and (C-87) into (C-82),

$$\begin{aligned}
-\left[\bar{R}^{\circ} \times \left[\hat{n} \times \rho \bar{E}'_A\right]\right] &= V'_{1A} \sin\xi \cos\theta \cos\phi\,\hat{\phi} \\
&+ V'_{1A} \sin\xi \sin\phi\,\hat{\theta} \\
&- V'_{1A} \cos\xi \cos\theta \sin\phi\,\hat{\phi} \\
&+ V'_{1A} \cos\xi \cos\phi\,\hat{\theta} \\
&+ V'_{2A} \cos\xi \cos\theta \cos\phi\,\hat{\phi} \\
&+ V'_{2A} \cos\xi \sin\phi\,\hat{\theta} \\
&+ V'_{2A} \sin\xi \cos\theta \sin\phi\,\hat{\phi} \\
&- V'_{2A} \sin\xi \cos\phi\,\hat{\theta}
\end{aligned} \tag{C-88}$$

Also,

$$\eta\left[\hat{n} \times \rho \bar{H}'_A\right] = V'_{1A}\,\hat{r} + V'_{2A}\,\hat{\xi} \tag{C-89}$$

Substituting (C-83), (C-84), (C-85), (C-86), and (C-87) into (C-89),

$$\begin{aligned}
\eta\left[\bar{R}^{\circ} \times \left[\bar{R}^{\circ} \times \left[\hat{n} \times \rho \bar{H}'_A\right]\right]\right] &= -V'_{1A} \cos\xi \cos\theta \cos\phi\,\hat{\theta} \\
&+ V'_{1A} \cos\xi \sin\phi\,\hat{\phi} \\
&- V'_{1A} \sin\xi \cos\theta \sin\phi\,\hat{\theta} \\
&- V'_{1A} \sin\xi \cos\phi\,\hat{\phi} \\
&+ V'_{2A} \sin\xi \cos\theta \cos\phi\,\hat{\theta}
\end{aligned}$$

$$-V'_{2A}\sin\xi\sin\phi\,\hat{\phi}$$
$$-V'_{2A}\cos\xi\cos\theta\sin\phi\,\hat{\theta}$$
$$-V'_{2A}\cos\xi\cos\phi\,\hat{\phi} \qquad \text{(C-90)}$$

Let

$$\textcircled{H} = \pi - \theta \qquad \text{(C-91)}$$

This notation is used for consistency with engineering practice since $\textcircled{H} = 0$ is the boresight direction for the antenna system and $\textcircled{H} = \pi$ is the backfire direction for the antenna system.

Using (C-29), (C-88), and (C-90), the Chernousov expressions for the electric far fields of the paraboloid reflector/point source feed system may be written in the spherical observation coordinates R, θ, ϕ as

$$RE_{\textcircled{H}}(\bar{R},t)$$

$$= \frac{1}{4\pi v f}\Bigg\{(1+\cos\textcircled{H})\sin\phi\int_0^{2\pi}\int_0^{D/2}\frac{V'_{1A}\sin\xi\, r\,dr\,d\xi}{(1+r^2/4f^2)}$$

$$+(1+\cos\textcircled{H})\cos\phi\int_0^{2\pi}\int_0^{D/2}\frac{V'_{1A}\cos\xi\, r\,dr\,d\xi}{(1+r^2/4f^2)}$$

$$+(1+\cos\textcircled{H})\sin\phi\int_0^{2\pi}\int_0^{D/2}\frac{V'_{2A}\cos\xi\, r\,dr\,d\xi}{(1+r^2/4f^2)}$$

$$-(1+\cos\Theta)\cos\phi\int_0^{2\pi}\int_0^{D/2}\frac{V'_{2A}\sin\xi\, r\,dr\,d\xi}{(1+r^2/4f^2)}\Bigg\} \quad (C\text{-}92)$$

and

$$RE_\phi(\bar{R},t)$$

$$=\frac{1}{4\pi vf}\Bigg\{-(1+\cos\Theta)\cos\phi\int_0^{2\pi}\int_0^{D/2}\frac{V'_{1A}\sin\xi\, r\,dr\,d\xi}{(1+r^2/4f^2)}$$

$$+(1+\cos\Theta)\sin\phi\int_0^{2\pi}\int_0^{D/2}\frac{V'_{1A}\cos\xi\, r\,dr\,d\xi}{(1+r^2/4f^2)}$$

$$-(1+\cos\Theta)\cos\phi\int_0^{2\pi}\int_0^{D/2}\frac{V'_{2A}\cos\xi\, r\,dr\,d\xi}{(1+r^2/4f^2)}$$

$$-(1+\cos\Theta)\sin\phi\int_0^{2\pi}\int_0^{D/2}\frac{V'_{2A}\sin\xi\, r\,dr\,d\xi}{(1+r^2/4f^2)}\Bigg\} \quad (C\text{-}93)$$

V'_{1A} and V'_{2A} are given by (C-68) and (C-69) respectively. Equations (C-92) and (C-93) are not restricted to the TEM horn feed. They apply to any feed which may be approximated by a transient (or cw) TEM spherical-wave point source located at the focus of the paraboloid.

Using (C-26) and (C-91) in (C-80), $(\bar{R}^o\cdot\bar{r}_s)/v$ may be written in spherical observation coordinates R,Θ,ϕ as

$$\frac{\bar{R}^o\cdot\bar{r}_s}{v}=\frac{r}{v}\left(\cos\xi\sin\Theta\cos\phi+\sin\xi\sin\Theta\sin\phi\right)$$

$$-\frac{f}{v}\left[\frac{16(f/D)^2-1}{16(f/D)^2}\right]\cos\Theta \quad (C\text{-}94)$$

The time arguments of V'_{1A} and V'_{2A} as given by (C-68) and (C-69) may then be written as

$$T - \frac{f}{v}\left[\frac{16(f/D)^2 + 1}{16(f/D)^2}\right] + \frac{\bar{R}^o \cdot \bar{r}_s}{v}$$

$$= T - \frac{f}{v}\left(1 + \cos\Theta\right) - \frac{f}{v}\left(1 - \cos\Theta\right)\frac{1}{16(f/D)^2}$$

$$+ \frac{r}{v}\left(\cos\xi \sin\Theta\cos\phi + \sin\xi\sin\Theta\sin\phi\right) \qquad \text{(C-95)}$$

Appendix D

DESCRIPTION AND LISTING OF THE FORTRAN PROGRAMS TO COMPUTE THE ELECTRIC FAR FIELDS OF TEM HORN ANTENNAS

D.1 PROGRAM FOR GAUSSIAN EXCITATION AT THE APEX

This section describes and lists the Fortran IV program which computes the electric far fields of the TEM horn antenna from equations (B-89) and (B-90) as given in Section B.5. The geometry for the TEM horn is shown in Figure B.1 on the second page of Appendix B. The program was written for the Xerox XDS Sigma 6 digital computer (with 80k words of main memory) located at the Cook Physical Science Building at the University of Vermont.

The program assumes unit gaussian excitation at the apex of the TEM horn. That is, V(t) is given by

$$V(t) = e^{-\left(\frac{t}{\tau}\right)^2} \qquad \text{(D-1)}$$

The mainline program establishes various constants and quantities which are used throughout the analysis, increments the discrete values of time at which the electric far fields are computed, and computes the numerical value of (B-89) and (B-90) at the various

discrete times. The mainline also calls several subroutines which perform other functions.

SUBROUTINE INPUT reads the input data for the program. The first line of data read is MODE, an integer set equal to 1, 2, or 3. When MODE equals 1, only the theta component of the electric far fields is computed. When MODE equals 2, only the phi component of the electric far fields is computed. When MODE equals 3, both the theta and phi components are computed. MODE was incorporated into the program to conserve execution time if only the theta component or only the phi component is desired.

The second line of data read are HEIGHT, RAINCH, PHIZD, and WIDTH. HEIGHT is the parameter h in inches. RAINCH is the parameter r_a in inches. PHIZD is the parameter ϕ_o in degrees. WIDTH is the 3-db width of the gaussian pulse exciting the TEM horn in seconds.

The third line of data read are two integers, NDIV and NPTS. NDIV establishes a subdivision criterion for the numerical integration routine. For best accuracy in the numerical integration routine, NDIV should be an even integer, at least as large as 4. Larger values may be used, depending upon limits for execution time. NPTS is an integer determining the number of discrete values of time at which the field components will be computed at each observation point $P(\theta,\phi)$. The maximum value for NPTS is 200. An approximate minimum value for NPTS to properly characterize the electric far fields may be found from the largest of $npts_1$, $npts_2$, and $npts_3$, where

$$npts_1 = \frac{4\Gamma a}{\tau v} \qquad \text{(D-2)}$$

$$npts_2 = \frac{4\Gamma a \phi_0}{\tau v} \qquad \text{(D-3)}$$

$$npts_3 = \frac{8h}{\tau v} \qquad \text{(D-4)}$$

v is the velocity of propagation in the medium. τ is related to WIDTH by the relationship

$$\tau = \frac{WIDTH}{2\sqrt{\ln 2}} \qquad \text{(D-5)}$$

The fourth line of data read is ZEFF and ZZERO. ZEFF is the effective terminating impedance of the front aperture of the TEM horn in ohms, and ZZERO is the characteristic impedance of the TEM horn in ohms. If time domain reflectometry were used to measure ZZERO and the reflection coefficient k_v from the front aperture, ZEFF could be calculated from the relationship

$$ZEFF = ZZERO\left(\frac{1+k_v}{1-k_v}\right) \qquad \text{(D-6)}$$

The fifth and following lines of data read are the locations of the observation points at which the electric far fields are to be computed. THETAD is the parameter θ in degrees. PHID is the parameter ϕ in degrees. One observation point THETAD,PHID is read per line. As many observation points as desired may be listed, depending upon the time limits for execution.

The following is an example input file used to execute the program.

```
3
0.6,7.3,59.0,340.0E-12
8,80
283.0,50.0
90.0,0.0
90.0,30.0
90.0,60.0
90.0,90.0
90.0,120.0
90.0,150.0
90.0,180.0
```

For the example shown, MODE was set equal to 3 so that both $rE_\theta(\bar{r},t)$ and $rE_\phi(\bar{r},t)$ were computed. The horn dimensions were h = 0.6", r_a = 7.3", and $\phi_o = 59.0^\circ$. WIDTH was 340.0 picoseconds. NDIV was set equal to 8 and NPTS was set equal to 80. The effective terminating impedance of the front aperture was 283.0 ohms, and the characteristic impedance of the TEM horn was 50.0 ohms. The electric far fields were computed at seven different observation points: $P(\theta,\phi)$ = $(90.0^\circ,0.0^\circ)$, $(90.0^\circ,30.0^\circ)$, $(90.0^\circ,60.0^\circ)$, $(90.0^\circ,90.0^\circ)$, $(90.0^\circ,120.0^\circ)$, $(90.0^\circ,150.0^\circ)$, and $(90.0^\circ,180.0^\circ)$.

The program for gaussian excitation with the associated Fortran library routines required approximately 10k words of memory. The execution for the example input file required 89.7 minutes of central processing unit time. The execution time for the program varies directly as NPTS and directly as the number of observation points $P(\theta,\phi)$. Also, the execution time varies approximately as $NDIV^2$.

SUBROUTINE TSETUP computes the limits of integration α_o and β_o, and establishes the numerical time window for the field computations. ALPHAZ is α_o in radians. BETAZ is β_o in radians. The low end of the time window, TMIN, is determined from

$$TMIN = -3\tau \tag{D-7}$$

The high end of the time window, TMAX, is determined from

$$TMAX = (2r_a/v) + 3\tau \tag{D-8}$$

The numerical time window TMAX - TMIN was established so that execution time would not be wasted computing many double integrals at times for which the physical fields would be negligible with respect to their maximum value.

SUBROUTINE SUBDIV establishes the subdivisions for the numerical integration routine. NFRONT is the number of subdivisions used to divide the alpha integration at the front aperture. NFRONT is determined from

$$NFRONT = NDIV\left[1 + \frac{r_a}{\tau V}(\pi - 2\theta_o)\right] \tag{D-9}$$

MFRONT is the number of subdivisions used to divide the beta integration at the front aperture. MFRONT is determined from

$$MFRONT = NDIV\left[1 + \frac{r_a}{\tau V}\phi_o\right] \tag{D-10}$$

NSIDE is the number of subdivisions used to divide the alpha integration at the wedge-shaped side apertures. NSIDE is determined from

$$NSIDE = NDIV\left[1 + \frac{r_a}{\tau V}(\pi - 2\alpha_o)\right] \tag{D-11}$$

MSIDE is the number of subdivisions used to divide the r' integration at the wedge-shaped side apertures. MSIDE is determined from

$$MSIDE = NDIV\left[1 + \frac{r_a}{2v}\right] \qquad \text{(D-12)}$$

SUBROUTINE DBLINT(G,X1,X2,Y1,Y2,N,M) computes the iterated double integral of G(X,Y) from X1(Y) to X2(Y) and then from Y1 to Y2 using N equal subdivisions in X2(Y) - X1(Y) and M equal subdivisions in Y. The subroutine uses the "iterated" trapezoidal rule. For greatest accuracy, N and M should be even integers. The trapezoidal rule integration was chosen as a compromise between precision of integration and execution time required.

FUNCTION FRONT(ALPHA,BETA) determines the integrand for the front aperture. In this function subroutine, the taper $f(\alpha,\beta)$ was assumed to be unity. This assumption would affect the absolute values of the electric far fields computed. It can be shown that for TEM horns with small flare in the E-plane

$$f(\alpha,\beta) \simeq \frac{1}{\pi - 2\theta_0} \qquad \text{(D-13)}$$

Therefore, the absolute value of the fields computed should be multiplied by (D-13) for horns with small E plane flare. For TEM horns with arbitrary flare in the E and H planes, another form of $f(\alpha,\beta)$ would have to be determined, depending upon the geometry of the horn in question. However, all horns which were studied numerically did have small E-plane flare, so that (D-13) would be the appropriate multiplying factor to find the absolute value of the far fields.

FUNCTION SIDE(ALPHA,RPRIME) determines the integrands for the wedge-shaped side apertures. Again, in this function subroutine,

$f(\alpha, \beta_o)$ was assumed to be unity. This assumption affects the absolute value of the fields computed. The same comments as for FUNCTION FRONT(ALPHA,BETA) apply.

FUNCTION ALPHA1(BETA), FUNCTION ALPHA2(BETA), FUNCTION ALPHA3(BETA), and FUNCTION ALPHA4(BETA) establish the limits of integration $\alpha_o(\beta)$, $\pi - \alpha_o(\beta)$, α_o, and $\pi - \alpha_o$ respectively.

SUBROUTINE OUTPUT generates the numerical output of the program. This subroutine contains sufficient Hollerith statements to be self-explanatory. SUBROUTINE OUTPUT was programmed to be able to handle a wide range of horn dimensions, pulse widths, terminating impedance, and characteristic impedance.

A listing of the Fortran IV program for gaussian excitation at the apex of the TEM horn follows on the next page.

```
C  MAINLINE FOR THE TEM HORN TRANSIENT RESPONSE CONSIDERING
C  BOTH THE FRONT AND WEDGE-SHAPED SIDE APERTURES
C  USING NUMERICAL INTEGRATION OF
C  GAUSSIAN EXCITATION AT THE APEX
      DIMENSION RETHET(200), REPHI(200), TRET (200)
      COMMON/BLCK1/SINT
      COMMON/BLCK2/NFRONT,MFRONT,NSIDE,MSIDE
      COMMON/BLCK3/TTHETZ
      COMMON/BLCK4/TPRIME,ATIME,TAU,RA,V,PI
      COMMON/BLCK5/SITHET,COTHET,SIPHI,COPHI
      COMMON/BLCK6/THETAZ,PHIZ,ALPHAZ,BETAZ
      COMMON/BLCK7/TMAX,TMIN
      COMMON/BLCK8/HEIGHT,RAINCH,PHIZD,WIDTH
      COMMON/BLCK9/NDIV,NPTS
      COMMON/BLCK10/THETAD,PHID
      COMMON/BLCK11/ICOUNT
      COMMON/BLCK12/RETHET,REPHI,TRET
      COMMON/BLCK13/INDEXA,INDEXB
      COMMON/BLCK14/ANGLE,RADFAC
      COMMON/BLCK15/ZEFF,ZZERO,REFL
      COMMON/BLCK16/MODE
      COMMON/BLCK17/SBETAZ,CBETAZ
      EXTERNAL FRONT,SIDE,ALPHA1,ALPHA2,ALPHA3,ALPHA4
      ICOUNT = 0
1000  CALL INPUT
      IF (THETAD) 1500,1005,1005
1005  RA = RAINCH/39.3700
      V = 2.99776E+08
      PI = 3.14159
      ANGLE = ASIN(HEIGHT/RAINCH)
      THETAZ = (PI/2.0) - ANGLE
      RADFAC = PI/180.0
      PHIZ = RADFAC*PHIZD
      THETA = RADFAC*THETAD
      PHI = RADFAC*PHID
      ATIME = RA/V
      FACT1 = ATIME/(4.0*PI)
      FACT2 = (1.0/V)/(4.0*PI)
      CPLUS = 1.0 + REFL
      CMINUS = 1.0 - REFL
      TAU = WIDTH/(2.0*SQRT(ALOG(2.0)))
      TTHETZ = TAN(THETAZ)
      SITHET = SIN(THETA)
      COTHET = COS(THETA)
      SIPHI = SIN(PHI)
      COPHI = COS(PHI)
      CALL TSETUP
      SBETAZ = SIN(BETAZ)
      CBETAZ = COS(BETAZ)
      CALL SUBDIV
C  ROUTINE TO COMPUTE RXETHETA(R,T-R/V) AND/OR
C  RXEPHI(R,T-R/V) FROM THE CHERNOUSOV EXPRESSION
```

```
      NTIME = 0
      DO 1300 NTIME = 1,NPTS,1
      AMTIME = NTIME - 1
      ANPTS = NPTS - 1
      TPRIME = TMIN + ((AMTIME/ANPTS)*(TMAX - TMIN))
      ATHETA = 0.0
      APHI = 0.0
      BTHETA = 0.0
      BPHI = 0.0
      INDEXA = 0
      INDEXB = 0
1100  GO TO (1101,1102,1101), MODE
1101  KOUNTA = 5
      GO TO 1105
1102  KOUNTA = 4
1105  DO 1175 INDEXA = 1,KOUNTA,1
     0CALL DBLINT(FRONT,ALPHA1,ALPHA2,
     1-BETAZ,BETAZ,NFRONT,MFRONT)
      GO TO (1110,1120,1130,1140,1150), INDEXA
1110  ATHETA = (CPLUS*SIPHI*SINT) + ATHETA
      APHI = (CPLUS*COTHET*COPHI*SINT) + APHI
      GO TO 1175
1120  ATHETA = (CPLUS*COPHI*SINT) + ATHETA
      APHI = -(CPLUS*COTHET*SIPHI*SINT) + APHI
      GO TO 1175
1130  ATHETA = (CMINUS*COTHET*COPHI*SINT) + ATHETA
      APHI = -(CMINUS*SIPHI*SINT) + APHI
      GO TO 1175
1140  ATHETA = (CMINUS*COTHET*SIPHI*SINT) + ATHETA
      APHI = (CMINUS*COPHI*SINT) + APHI
      GO TO 1175
1150  ATHETA = (CMINUS*SITHET*SINT) + ATHETA
1175  CONTINUE
1200  GO TO (1201,1202,1202), MODE
1201  KOUNTB = 2
      GO TO 1205
1202  KOUNTB = 4
1205  DO 1275 INDEXB = 1,KOUNTB,1
     0CALL DBLINT(SIDE,ALPHA3,ALPHA4,
     10.0,RA,NSIDE,MSIDE)
      GO TO (1206,1207,1207), MODE
1206  GO TO (1210,1230), INDEXB
1207  GO TO (1210,1220,1230,1240), INDEXB
1210 0BTHETA = (SIPHI*CBETAZ*SINT)
     1-(COPHI*SBETAZ*SINT) + BTHETA
     0BPHI = (COTHET*COPHI*CBETAZ*SINT)
     1+(COTHET*SIPHI*SBETAZ*SINT) + BPHI
      GO TO 1275
1220  BPHI = -(SITHET*SINT) + BPHI
      GO TO 1275
1230 0BTHETA = -(SIPHI*CBETAZ*SINT)
     1-(COPHI*SBETAZ*SINT) + BTHETA
```

```
     0BPHI = -(COTHET*COPHI*CBETAZ*SINT)
     1+(COTHET*SIPHI*SBETAZ*SINT) + BPHI
      GO TO 1275
1240  BPHI = (SITHET*SINT) + BPHI
1275  CONTINUE
      RETHET(NTIME) = (FACT1*ATHETA) + (FACT2*BTHETA)
      REPHI(NTIME) = (FACT1*APHI) + (FACT2*BPHI)
      TRET(NTIME) = TPRIME
1300  CONTINUE
      ICOUNT = ICOUNT + 1
      CALL OUTPUT
      GO TO 1000
1500  END
C  SUBROUTINE TO READ INPUT DATA
C  FOR THE TEM HORN TRANSIENT RESPONSE PROGRAM
C  DATA READ ARE EXECUTION MODE DESIRED,
C  HORN DIMENSIONS AND ANGLES,
C  HALF-WIDTH OF THE EXCITING VOLTAGE PULSE,
C  A SUBDIVISION CRITERION FOR THE NUMERICAL INTEGRATION,
C  NUMBER OF COMPUTED POINTS AT EACH OBSERVATION POINT,
C  EFFECTIVE TERMINATING IMPEDANCE OF THE FRONT APERTURE,
C  CHARACTERISTIC IMPEDANCE OF THE HORN, AND
C  LOCATION OF THE OBSERVATION POINT P(THETA,PHI).
      SUBROUTINE INPUT
      COMMON/BLCK8/HEIGHT,RAINCH,PHIZD,WIDTH
      COMMON/BLCK9/NDIV,NPTS
      COMMON/BLCK10/THETAD,PHID
      COMMON/BLCK11/ICOUNT
      COMMON/BLCK15/ZEFF,ZZERO,REFL
      COMMON/BLCK16/MODE
      IF (ICOUNT) 1501,1501,1530
1501  READ (105,1505) MODE
1505  FORMAT(I)
      READ (105,1510) HEIGHT,RAINCH,PHIZD,WIDTH
1510  FORMAT(4E.1)
      READ (105,1520) NDIV,NPTS
1520  FORMAT(2I)
      READ (105,1525) ZEFF,ZZERO
1525  FORMAT(2E.1)
      REFL = (ZEFF - ZZERO)/(ZEFF + ZZERO)
1530  READ (105,1540) THETAD,PHID
1540  FORMAT(2E.1)
      RETURN
      END
C  SUBROUTINE TO ESTABLISH THE TIME WINDOW
C  AND COMPUTE THE TEM HORN ANGLES
      SUBROUTINE TSETUP
      COMMON/BLCK4/TPRIME,ATIME,TAU,RA,V,PI
      COMMON/BLCK6/THETAZ,PHIZ,ALPHAZ,BETAZ
      COMMON/BLCK7/TMAX,TMIN
      ALPHZ1 = COS(PHIZ/2.0)
      ALPHZ2 = (TAN(THETAZ))**2.0
```

```
      ALPHZ3 = SQRT(1.0 + ALPHZ2)
      ALPHAZ = ACOS(ALPHZ1/ALPHZ3)
      BETAZ1 = 1.0 - (ALPHZ1**2.0)
      BETAZ2 = SQRT(1.0 + (BETAZ1/ALPHZ2))
      BETAZ = ACOS(ALPHZ1/BETAZ2)
      TMAX = (2.0*ATIME) + (3.0*TAU)
      TMIN = -(3.0*TAU)
      RETURN
      END
C  SUBROUTINE TO ESTABLISH SUBDIVISIONS
C  FOR THE NUMERICAL INTEGRATION ROUTINE
      SUBROUTINE SUBDIV
      COMMON/BLCK2/NFRONT,MFRONT,NSIDE,MSIDE
      COMMON/BLCK4/TPRIME,ATIME,TAU,RA,V,PI
      COMMON/BLCK6/THETAZ,PHIZ,ALPHAZ,BETAZ
      COMMON/BLCK9/NDIV,NPTS
      NSTART = (ATIME/TAU)*(PI - (2.0*THETAZ))
      NSTART = NSTART + 1
      NFRONT = NDIV*NSTART
      MSTART = (ATIME/TAU)*PHIZ
      MSTART = MSTART + 1
      MFRONT = NDIV*MSTART
      JSTART = (ATIME/TAU)*(PI - (2.0*ALPHAZ))
      JSTART = JSTART + 1
      NSIDE = NDIV*JSTART
      KSTART = (ATIME/TAU)
      KSTART = KSTART + 1
      MSIDE = NDIV*KSTART
      RETURN
      END
C  SUBROUTINE TO COMPUTE THE ITERATED DOUBLE INTEGRAL
C  OF G(X,Y) FROM X1(Y) TO X2(Y) AND THEN FROM Y1 TO Y2
C  USING N EQUAL SUBDIVISIONS IN X2(Y) - X1(Y)
C  AND M EQUAL SUBDIVISIONS IN Y.
C  THE SUBROUTINE USES THE ITERATED TRAPEZOIDAL RULE.
C  FOR GREATEST ACCURACY, N AND M SHOULD BE EVEN.
      SUBROUTINE DOUINT(G,X1,X2,Y1,Y2,N,M)
      COMMON/BLCK1/SINT
      EXTERNAL G,X1,X2
      EXTERNAL FRONT,SIDE,ALPHA1,ALPHA2,ALPHA3,ALPHA4
      AN = N
      AM = M
      DELTAY = (Y2 - Y1)/AM
      J = 0
      DO 260 J = 1,M+1,2
      L = J - 1
      AJ = J
      AL = L
      I = 0
      YL = Y1 + (AL*DELTAY)
      YJ = Y1 + (AJ*DELTAY)
      U = X1(YL)
```

```
      V = X1(YJ)
      DELTXL = (X2(YL) - U)/AN
      DELTXJ = (X2(YJ) - V)/AN
      DO 130 I = 1,N+1,2
      K = I - 1
      AI = I
      AK = K
      XKL = U + (AK*DELTXL)
      XIL = U + (AI*DELTXL)
      XKJ = V + (AK*DELTXJ)
      XIJ = V + (AI*DELTXJ)
      A = G(XKL,YL)
      B = G(XIL,YL)
      C = G(XKJ,YJ)
      D = G(XIJ,YJ)
      IF (I - 1) 5,5,30
5     RL = (A/2.0) + B
      RJ = (C/2.0) + D
      GO TO 130
30    IF (I - (N + 1)) 35,65,65
35    RL = A + B + RL
      RJ = C + D + RJ
      GO TO 130
65    RL = A + (B/2.0) + RL
      RJ = C + (D/2.0) + RJ
130   CONTINUE
      RL = RL*DELTXL
      RJ = RJ*DELTXJ
      IF (J - 1) 195,195,220
195   R = (RL/2.0) + RJ
      GO TO 260
220   IF (J - (M + 1)) 225,255,255
225   R = RL + RJ + R
      GO TO 260
255   R = RL + (RJ/2.0) + R
260   CONTINUE
      SINT = R*DELTAY
      RETURN
      END
C  DEFINE THE INTEGRAND FOR THE FRONT
C  APERTURE, FRONT(ALPHA,BETA).
      FUNCTION FRONT(ALPHA,BETA)
      COMMON/BLCK4/TPRIME,ATIME,TAU,RA,V,PI
      COMMON/BLCK5/SITHET,COTHET,SIPHI,COPHI
      COMMON/BLCK13/INDEXA,INDEXB
      SIALPH = SIN(ALPHA)
      COALPH = COS(ALPHA)
      SIBETA = SIN(BETA)
      COBETA = COS(BETA)
C  DEFINE THE ARGUMENT OF V* FOR THE FRONT
C  APERTURE, ARGF = (T* - (RA/V) + (R0.RS/V)),
      ARGAF = SIALPH*COBETA*SITHET*COPHI
```

```
      ARGBF = SIALPH*SIBETA*SITHET*SIPHI
      ARGCF = COALPH*COTHET
      ARGDF = ARGAF + ARGBF + ARGCF
      ARGF = TPRIME - ATIME + (ATIME*ARGDF)
C  DEFINE V' FOR THE FRONT APERTURE.
      VPRF = -2.0*(ARGF/(TAU**2.0))*EXP(-((ARGF/TAU)**2.0))
C  DEFINE THE ANGULAR TAPER OF THE EXCITATION
C  FOR THE FRONT APERTURE, TAPERF = F(ALPHA,BETA).
      TAPERF = 1.0
      DEDTF = TAPERF*VPRF
      GO TO (310,320,330,340,350), INDEXA
310   FRONT = SIBETA*SIALPH*DEDTF
      RETURN
320   FRONT = COBETA*SIALPH*DEDTF
      RETURN
330   FRONT = COBETA*COALPH*SIALPH*DEDTF
      RETURN
340   FRONT = SIBETA*COALPH*SIALPH*DEDTF
      RETURN
350   FRONT = SIALPH*SIALPH*DEDTF
      RETURN
      END
C  DEFINE THE INTEGRAND FOR THE WEDGE-SHAPED
C  SIDE APERTURES, SIDE(ALPHA,RPRIME).
      FUNCTION SIDE(ALPHA,RPRIME)
      COMMON/BLCK4/TPRIME,ATIME,TAU,RA,V,PI
      COMMON/BLCK5/SITHET,COTHET,SIPHI,COPHI
      COMMON/BLCK6/THETAZ,PHIZ,ALPHAZ,BETAZ
      COMMON/BLCK13/INDEXA,INDEXB
      COMMON/BLCK15/ZEFF,ZZERO,REFL
      COMMON/BLCK16/MODE
      COMMON/BLCK17/SBETAZ,CBETAZ
      SIALPH = SIN(ALPHA)
      COALPH = COS(ALPHA)
      WTIME = RPRIME/V
      ARGAS = SIALPH*CBETAZ*SITHET*COPHI
      ARGBS = SIALPH*SBETAZ*SITHET*SIPHI
      ARGCS = COALPH*COTHET
C  DEFINE THE ARGUMENTS OF V' FOR
C  THE WEDGE-SHAPED SIDE APERTURES.
C  ARGV1A = (T' - (R'/V) + (R0.RS1/V))
      ARGDS = ARGAS + ARGBS + ARGCS
      ARGV1A = TPRIME - WTIME + (WTIME*ARGDS)
C  ARGV1B = (T' + (R'/V) - (2RA/V) + (R0.RS1/V))
      ARGV1B = TPRIME + WTIME - (2.0*ATIME) + (WTIME*ARGDS)
C  ARGW2A = (T' - (R'/V) + (R0.RS2/V))
      ARGES = ARGAS + ARGBS + ARGCS
      ARGW2A = TPRIME - WTIME + (WTIME*ARGES)
C  ARGW2B = (T' + (R'/V) - (2RA/V) + (R0.RS2/V))
      ARGW2B = TPRIME + WTIME - (2.0*ATIME) + (WTIME*ARGES)
C  DEFINE THE VARIOUS V'S FOR
C  THE WEDGE-SHAPED SIDE APERTURES.
```

```
      C = -2.0/(TAU**2.0)
      VPRW1A = C*ARGW1A*EXP(-((ARGW1A/TAU)**2.0))
      VPRW1B = C*ARGW1B*EXP(-((ARGW1B/TAU)**2.0))
      VPRW2A = C*ARGW2A*EXP(-((ARGW2A/TAU)**2.0))
      VPRW2B = C*ARGW2B*EXP(-((ARGW2B/TAU)**2.0))
C  DEFINE THE ANGULAR TAPER OF THE EXCITATION
C  FOR THE WEDGE-SHAPED SIDE APERTURES,
C  TAPERS = F(ALPHA,BETAZ).
      TAPERS = 1.0
      DEDTW1 = TAPERS*(VPRW1A + (REFL*VPRW1B))
      DEDTW2 = TAPERS*(VPRW2A + (REFL*VPRW2B))
      GO TO (500,600,600), MODE
500   GO TO (510,520), INDEXB
510   SIDE = SIALPH*DEDTW1
      RETURN
520   SIDE = SIALPH*DEDTW2
      RETURN
600   GO TO (510,610,520,620), INDEXB
610   SIDE = COALPH*DEDTW1
      RETURN
620   SIDE = COALPH*DEDTW2
      RETURN
      END
C  DEFINE THE LOWER LIMIT OF INTEGRATION ON ALPHA
C  FOR THE FRONT APERTURE, ALPHA1(BETA).
      FUNCTION ALPHA1(BETA)
      COMMON/BLCK3/TTHETZ
      ALPHA1 = ATAN(TTHETZ/COS(BETA))
      RETURN
      END
C  DEFINE THE UPPER LIMIT OF INTEGRATION ON ALPHA
C  FOR THE FRONT APERTURE, ALPHA2(BETA).
      FUNCTION ALPHA2(BETA)
      COMMON/BLCK4/TPRIME,ATIME,TAU,RA,V,PI
      EXTERNAL ALPHA1
      ALPHA2 = PI - ALPHA1(BETA)
      RETURN
      END
C  DEFINE THE LOWER LIMIT OF INTEGRATION ON ALPHA
C  FOR THE WEDGE-SHAPED SIDE APERTURES, ALPHA3(BETA).
      FUNCTION ALPHA3(BETA)
      COMMON/BLCK6/THETAZ,PHIZ,ALPHAZ,BETAZ
      ALPHA3 = ALPHAZ
      RETURN
      END
C  DEFINE THE UPPER LIMIT OF INTEGRATION ON ALPHA
C  FOR THE WEDGE-SHAPED SIDE APERTURES, ALPHA4(BETA).
      FUNCTION ALPHA4(BETA)
      COMMON/BLCK4/TPRIME,ATIME,TAU,RA,V,PI
      COMMON/BLCK6/THETAZ,PHIZ,ALPHAZ,BETAZ
      ALPHA4 = PI - ALPHAZ
      RETURN
```

```
      END
C  SUBROUTINE TO GENERATE THE NUMERICAL OUTPUT
C  OF THE TEM HORN TRANSIENT RESPONSE PROGRAM
      SUBROUTINE OUTPUT
      DIMENSION RETHET(200), REPHI(200), TRET(200)
      COMMON/BLCK2/NFRONT,MFRONT,NSIDE,MSIDE
      COMMON/BLCK4/TPRIME,ATIME,TAU,RA,V,PI
      COMMON/BLCK6/THETAZ,PHIZ,ALPHAZ,BETAZ
      COMMON/BLCK7/TMAX,TMIN
      COMMON/BLCK8/HEIGHT,RAINCH,PHIZD,WIDTH
      COMMON/BLCK9/NDIV,NPTS
      COMMON/BLCK10/THETAD,PHID
      COMMON/BLCK11/ICOUNT
      COMMON/BLCK12/RETHET,REPHI,TRET
      COMMON/BLCK14/ANGLE,RADFAC
      COMMON/BLCK15/ZEFF,ZZERO,REFL
      COMMON/BLCK16/MODE
      IF (ICOUNT - 1) 1501,1501,1900
1501  WRITE (108,1505)
1505  FORMAT('CONSIDER A TEM HORN WITH')
      WRITE (108,1510) PHIZD
1510  FORMAT('A WEDGE ANGLE OF ',F6.1,' DEGREES,')
      WRITE (108,1515) HEIGHT
1515  FORMAT('A HEIGHT H = ',F6.1,' INCHES,')
      WRITE (108,1520) RAINCH
1520  FORMAT('AND A LENGTH L = ',F6.1,' INCHES.')
      WRITE (108,1525) ZZERO
1525 0FORMAT(/'THE CHARACTERISTIC IMPEDANCE OF THIS HORN'
     1/'WAS FOUND TO BE ',F7.1,' OHMS.')
      WRITE (108,1530) ZEFF
1530 0FORMAT('THE EFFECTIVE TERMINATING IMPEDANCE'
     1/'WHICH WAS USED WAS ',F7.1,' OHMS.')
      WRITE (108,1535) REFL
1535 0FORMAT('THEREFORE,THE EFFECTIVE VOLTAGE REFLECTION'
     1/'COEFFICIENT COMPUTED WAS ',F6.3,'.')
      WRITE (108,1540)
1540 0FORMAT(/'THE CHERNOUSOV ANALYSIS OF THIS HORN'
     1/'WAS PERFORMED USING GAUSSIAN EXCITATION')
      PWIDTH = WIDTH*(1.0E+12)
      WRITE (108,1545) PWIDTH
1545  FORMAT('WITH A HALF-WIDTH OF ',F7.1,' PICOSECONDS.')
      WRITE (108,1550) MODE
1550  FORMAT(/'THE PROGRAM WAS EXECUTED IN MODE ',I1,'.')
      GO TO (1555,1560,1565), MODE
1555  WRITE (108,1556)
1556  FORMAT('RXETHETA(R,T-R/V) ONLY WAS COMPUTED')
      GO TO 1570
1560  WRITE (108,1561)
1561  FORMAT('RXEPHI(R,T-R/V) ONLY WAS COMPUTED')
      GO TO 1570
1565  WRITE (108,1566)
1566 0FORMAT('BOTH RXETHETA(R,T-R/V) AND'
```

```
     1/'RXEPHI(R,T-R/V) WERE COMPUTED')
1570  WRITE (108,1575) NPTS
1575 0FORMAT('AT ',I3,' EQUALLY SPACED VALUES OF'
     1/'RETARDED TIME T'' = T-R/V WHICH FELL WITHIN'
     2/'THE NUMERICALLY ESTABLISHED TIME WINDOW.')
      TLOWER = TMIN*(1.0E+09)
      TUPPER = TMAX*(1.0E+09)
      WRITE (108,1580) TLOWER,TUPPER
1580 0FORMAT('TIME WINDOW STARTED AT ',F7.3,' NANOSECONDS'
     1/'AND ENDED AT ',F7.3,' NANOSECONDS.')
      WWIDTH = TUPPER - TLOWER
      WRITE (108,1585) WWIDTH
1585  FORMAT('THE WINDOW WIDTH WAS ',F7.3,' NANOSECONDS.')
      WRITE (108,1590)
1590  FORMAT(/'FOR THE NUMERICAL INTEGRATION ROUTINE,')
      WRITE (108,1595) NFRONT,MFRONT
1595 0FORMAT('THE FRONT APERTURE WAS DIVIDED'
     1/'INTO ',I4,' SUBDIVISIONS IN ALPHA,'
     2/'AND ',I4,' SUBDIVISIONS IN BETA.')
      WRITE (108,1600) NSIDE,MSIDE
1600 0FORMAT('THE WEDGE-SHAPED SIDE APERTURES WERE DIVIDED'
     1/'INTO ',I4,' SUBDIVISIONS IN ALPHA,'
     2/'AND ',I4,' SUBDIVISIONS IN R''.')
1900  WRITE (108,1905) ICOUNT
1905  FORMAT(///'OBSERVATION POINT P(THETA,PHI) # ',I3)
      WRITE (108,1910) THETAD,PHID
1910 0FORMAT('THETA = ',F6.1,' DEGREES, ',
     1'PHI = ',F6.1,' DEGREES')
      GO TO (1915,1935,1915), MODE
1915  WRITE (108,1920)
1920 0FORMAT(/'A TABLE OF T-R/V,RXETHETA(R,T-R/V) FOLLOWS.'
     1/'T-R/V IS IN NANOSECONDS AND RXETHETA IS IN VOLTS.')
      JIVE = 0
      DO 1930 JIVE = 1,NPTS,1
      TNANO = (TRET(JIVE))*(1.0E+09)
      WRITE (108,1925) TNANO,RETHET(JIVE)
1925  FORMAT(F7.3,',',1PE10.3)
1930  CONTINUE
1935  GO TO (1960,1940,1940), MODE
1940  WRITE (108,1945)
1945 0FORMAT(/'A TABLE OF T-R/V,RXEPHI(R,T-R/V) FOLLOWS.'
     1/'T-R/V IS IN NANOSECONDS AND RXEPHI IS IN VOLTS.')
      JAZZ = 0
      DO 1955 JAZZ = 1,NPTS,1
      TNANO = (TRET(JAZZ))*(1.0E+09)
      WRITE (108,1950) TNANO,REPHI(JAZZ)
1950  FORMAT(F7.3,',',1PE10.3)
1955  CONTINUE
1960  RETURN
      END
```

D.2 PROGRAM FOR ERROR FUNCTION EXCITATION AT THE APEX

This section describes and lists the Fortran IV program which computes the electric far fields of the TEM horn antenna from equations (B-89) and (B-90) as given in Section B.5. The geometry for the TEM horn is shown in Figure B.1 on the second page of appendix B. The program was written for the Xerox XDS Sigma 6 digital computer (with 80k words of main memory) located at the Cook Physical Science Building at the University of Vermont.

The program assumes unit error function excitation at the apex of the TEM horn. That is, V(t) is given by

$$V(t) = \frac{1}{\tau\sqrt{\pi}} \int_{-\infty}^{t} e^{-\left(\frac{\xi}{\tau}\right)^2} d\xi \qquad \text{(D-14)}$$

This program is the same as the program discussed in Section D.1, except for four differences.

First, the quantity WIDTH read in the second line of data of SUBROUTINE INPUT is the 3-db width of the derivative of V(t) given by (D-14). That is, WIDTH is determined from

$$V'(t) = \frac{1}{\tau\sqrt{\pi}} e^{-\left(\frac{t}{\tau}\right)^2} \qquad \text{(D-15)}$$

with

$$\tau = \frac{WIDTH}{2\sqrt{\ln 2}} \qquad \text{(D-16)}$$

Secondly, since this program was used mainly to determine $rE_\theta(\bar{r},t)$ in the azimuth plane of the TEM horns studied experimentally by Susman and Lamensdorf (1970,1971), the discrete values of time at which the fields were computed were adaptively spaced within the numerical time window. This was accomplished as follows. SUBROUTINE TSETUP establishes the values of TMIN and TMAX. In the mainline program, another value of time, TMID, is established depending upon the value of ϕ at the desired observation point $P(\theta,\phi)$ in the azimuth plane ($\theta = 90^\circ$). Half of the discrete values of time are placed between TMIN and TMID, and the other half are placed between TMID and TMAX. If ϕ is between 0° and 90°, TMID is given by

$$TMID = \frac{r_a}{v}\left(1-\cos\phi\right)+3\tau \qquad \text{(D-17)}$$

If ϕ is between 90° and 180°, TMID is given by

$$TMID = \frac{r_a}{v}\left(1-\cos\phi\right)-3\tau \qquad \text{(D-18)}$$

Finally, FUNCTION FRONT(ALPHA,BETA) and FUNCTION SIDE(ALPHA, RPRIME) were modified to account for the unit error function excitation of the apex as given by (D-14).

The execution time and space requirement of this program are approximately the same as the program for gaussian excitation discussed in Section D.1. For the sake of completeness, a complete listing of the Fortran IV program for unit error function excitation at the apex of the TEM horn follows on the next page.

```
C  MAINLINE FOR THE TEM HORN TRANSIENT RESPONSE CONSIDERING
C  BOTH THE FRONT AND WEDGE-SHAPED SIDE APERTURES
C  USING NUMERICAL INTEGRATION OF
C  ERROR FUNCTION EXCITATION AT THE APEX
C  AND ADAPTIVE TIME INCREMENTS
C  WITHIN THE NUMERICAL TIME WINDOW
      DIMENSION RETHET(200), REPHI(200), TRET (200)
      COMMON/BLCK1/SINT
      COMMON/BLCK2/NFRONT,MFRONT,NSIDE,MSIDE
      COMMON/BLCK3/TTHETZ
      COMMON/BLCK4/TPRIME,ATIME,TAU,RA,V,PI
      COMMON/BLCK5/SITHET,COTHET,SIPHI,COPHI
      COMMON/BLCK6/THETAZ,PHIZ,ALPHAZ,BETAZ
      COMMON/BLCK7/TMAX,TMIN
      COMMON/BLCK8/HEIGHT,RAINCH,PHIZD,WIDTH
      COMMON/BLCK9/NDIV,NPTS
      COMMON/BLCK10/THETAD,PHID
      COMMON/BLCK11/ICOUNT
      COMMON/BLCK12/RETHET,REPHI,TRET
      COMMON/BLCK13/INDEXA,INDEXB
      COMMON/BLCK14/ANGLE,RADFAC
      COMMON/BLCK15/ZEFF,ZZERO,REFL
      COMMON/BLCK16/MODE
      COMMON/BLCK17/SBETAZ,CBETAZ
      EXTERNAL FRONT,SIDE,ALPHA1,ALPHA2,ALPHA3,ALPHA4
      ICOUNT = 0
1000  CALL INPUT
      IF (THETAD) 1500,1005,1005
1005  RA = RAINCH/39.3700
      V = 2.99776E+08
      PI = 3.14159
      ANGLE = ASIN(HEIGHT/RAINCH)
      THETAZ = (PI/2.0) - ANGLE
      RADFAC = PI/180.0
      PHIZ = RADFAC*PHIZD
      THETA = RADFAC*THETAD
      PHI = RADFAC*PHID
      ATIME = RA/V
      FACT1 = ATIME/(4.0*PI)
      FACT2 = (1.0/V)/(4.0*PI)
      CPLUS = 1.0 + REFL
      CMINUS = 1.0 - REFL
      TAU = WIDTH/(2.0*SQRT(ALOG(2.0)))
      TTHETZ = TAN(THETAZ)
      SITHET = SIN(THETA)
      COTHET = COS(THETA)
      SIPHI = SIN(PHI)
      COPHI = COS(PHI)
      CALL TSETUP
      SBETAZ = SIN(BETAZ)
      CBETAZ = COS(BETAZ)
      CALL SUBDIV
```

```
C  ROUTINE TO COMPUTE RXETHETA(R,T-R/V) AND/OR
C  RXEPHI(R,T-R/V) FROM THE CHERNOUSOV EXPRESSION
      NTIME = 0
      DO 1300 NTIME = 1,NPTS,1
      IF (PHID - 90.0) 1050,1050,1060
1050  TMID = (ATIME*(1.0 - COPHI)) + (3.0*TAU)
      GO TO 1070
1060  TMID = (ATIME*(1.0 - COPHI)) - (3.0*TAU)
1070  IF (NTIME - (NPTS/2)) 1080,1080,1090
1080  AMTIME = NTIME - 1
      ANPTS = (NPTS/2) - 1
      TPRIME = TMIN + ((AMTIME/ANPTS)*(TMID - TMIN))
      GO TO 1095
1090  AMTIME = NTIME - (NPTS/2)
      ANPTS = NPTS/2
      TPRIME = TMID + ((AMTIME/ANPTS)*(TMAX - TMID))
1095  ATHETA = 0.0
      APHI = 0.0
      BTHETA = 0.0
      BPHI = 0.0
      INDEXA = 0
      INDEXB = 0
1100  GO TO (1101,1102,1101), MODE
1101  KOUNTA = 5
      GO TO 1105
1102  KOUNTA = 4
1105  DO 1175 INDEXA = 1,KOUNTA,1
     0CALL DBLINT(FRONT,ALPHA1,ALPHA2,
     1-BETAZ,BETAZ,NFRONT,MFRONT)
      GO TO (1110,1120,1130,1140,1150), INDEXA
1110  ATHETA = (CPLUS*SIPHI*SINT) + ATHETA
      APHI = (CPLUS*COTHET*COPHI*SINT) + APHI
      GO TO 1175
1120  ATHETA = (CPLUS*COPHI*SINT) + ATHETA
      APHI = -(CPLUS*COTHET*SIPHI*SINT) + APHI
      GO TO 1175
1130  ATHETA = (CMINUS*COTHET*COPHI*SINT) + ATHETA
      APHI = -(CMINUS*SIPHI*SINT) + APHI
      GO TO 1175
1140  ATHETA = (CMINUS*COTHET*SIPHI*SINT) + ATHETA
      APHI = (CMINUS*COPHI*SINT) + APHI
      GO TO 1175
1150  ATHETA = (CMINUS*SITHET*SINT) + ATHETA
1175  CONTINUE
1200  GO TO (1201,1202,1202), MODE
1201  KOUNTB = 2
      GO TO 1205
1202  KOUNTB = 4
1205  DO 1275 INDEXB = 1,KOUNTB,1
     0CALL DBLINT(SIDE,ALPHA3,ALPHA4,
     10.0,RA,NSIDE,MSIDE)
      GO TO (1206,1207,1207), MODE
```

```
 1206  GO TO (1210,1230), INDEXB
 1207  GO TO (1210,1220,1230,1240), INDEXB
 1210 0BTHETA = (SIPHI*CBETAZ*SINT)
      1-(COPHI*SBETAZ*SINT) + BTHETA
      0BPHI = (COTHET*COPHI*CBETAZ*SINT)
      1+(COTHET*SIPHI*SBETAZ*SINT) + BPHI
       GO TO 1275
 1220  BPHI = -(SITHET*SINT) + BPHI
       GO TO 1275
 1230 0BTHETA = -(SIPHI*CBETAZ*SINT)
      1-(COPHI*SBETAZ*SINT) + BTHETA
      0BPHI = -(COTHET*COPHI*CBETAZ*SINT)
      1+(COTHET*SIPHI*SBETAZ*SINT) + BPHI
       GO TO 1275
 1240  BPHI = (SITHET*SINT) + BPHI
 1275  CONTINUE
       RETHET(NTIME) = (FACT1*ATHETA) + (FACT2*BTHETA)
       REPHI(NTIME) = (FACT1*APHI) + (FACT2*BPHI)
       TPRT(NTIME) = TPRIME
 1300  CONTINUE
       ICOUNT = ICOUNT + 1
       CALL OUTPUT
       GO TO 1000
 1500  END
C  SUBROUTINE TO READ INPUT DATA
C  FOR THE TEM HORN TRANSIENT RESPONSE PROGRAM
C  DATA READ ARE EXECUTION MODE DESIRED,
C  HORN DIMENSIONS AND ANGLES,
C  HALF-WIDTH OF THE EXCITING VOLTAGE PULSE,
C  A SUBDIVISION CRITERION FOR THE NUMERICAL INTEGRATION,
C  NUMBER OF COMPUTED POINTS AT EACH OBSERVATION POINT,
C  EFFECTIVE TERMINATING IMPEDANCE OF THE FRONT APERTURE,
C  CHARACTERISTIC IMPEDANCE OF THE HORN, AND
C  LOCATION OF THE OBSERVATION POINT P(THETA,PHI).
       SUBROUTINE INPUT
       COMMON/BLCK8/HEIGHT,RAINCH,PHIZD,WIDTH
       COMMON/BLCK9/NDIV,NPTS
       COMMON/BLCK10/THETAD,PHID
       COMMON/BLCK11/ICOUNT
       COMMON/BLCK15/ZEFF,ZZERO,REFL
       COMMON/BLCK16/MODE
       IF (ICOUNT) 1501,1501,1530
 1501  READ (105,1505) MODE
 1505  FORMAT(1)
       READ (105,1510) HEIGHT,RAINCH,PHIZD,WIDTH
 1510  FORMAT(4E.1)
       READ (105,1520) NDIV,NPTS
 1520  FORMAT(2I)
       READ (105,1525) ZEFF,ZZERO
 1525  FORMAT(2E.1)
       REFL = (ZEFF - ZZERO)/(ZEFF + ZZERO)
 1530  READ (105,1540) THETAD,PHID
```

```
1540  FORMAT(2E.1)
      RETURN
      END
C  SUBROUTINE TO ESTABLISH THE TIME WINDOW
C  AND COMPUTE THE TEM HORN ANGLES
      SUBROUTINE TSETUP
      COMMON/BLCK4/TPRIME,ATIME,TAU,RA,V,PI
      COMMON/BLCK6/THETAZ,PHIZ,ALPHAZ,BETAZ
      COMMON/BLCK7/TMAX,TMIN
      ALPHZ1 = COS(PHIZ/2.0)
      ALPHZ2 = (TAN(THETAZ))**2.0
      ALPHZ3 = SQRT(1.0 + ALPHZ2)
      ALPHAZ = ACOS(ALPHZ1/ALPHZ3)
      BETAZ1 = 1.0 - (ALPHZ1**2.0)
      BETAZ2 = SQRT(1.0 + (BETAZ1/ALPHZ2))
      BETAZ = ACOS(ALPHZ1/BETAZ2)
      TMAX = (2.0*ATIME) + (3.0*TAU)
      TMIN = -(3.0*TAU)
      RETURN
      END
C  SUBROUTINE TO ESTABLISH SUBDIVISIONS
C  FOR THE NUMERICAL INTEGRATION ROUTINE
      SUBROUTINE SUBDIV
      COMMON/BLCK2/NFRONT,MFRONT,NSIDE,MSIDE
      COMMON/BLCK4/TPRIME,ATIME,TAU,RA,V,PI
      COMMON/BLCK6/THETAZ,PHIZ,ALPHAZ,BETAZ
      COMMON/BLCK9/NDIV,NPTS
      NSTART = (ATIME/TAU)*(PI - (2.0*THETAZ))
      NSTART = NSTART + 1
      NFRONT = NDIV*NSTART
      MSTART = (ATIME/TAU)*PHIZ
      MSTART = MSTART + 1
      MFRONT = NDIV*NSTART
      JSTART = (ATIME/TAU)*(PI - (2.0*ALPHAZ))
      JSTART = JSTART + 1
      NSIDE = NDIV*JSTART
      KSTART = (ATIME/TAU)
      KSTART = KSTART + 1
      MSIDE = NDIV*KSTART
      RETURN
      END
C  SUBROUTINE TO COMPUTE THE ITERATED DOUBLE INTEGRAL
C  OF G(X,Y) FROM X1(Y) TO X2(Y) AND THEN FROM Y1 TO Y2
C  USING N EQUAL SUBDIVISIONS IN X2(Y) - X1(Y)
C  AND M EQUAL SUBDIVISIONS IN Y.
C  THE SUBROUTINE USES THE ITERATED TRAPEZOIDAL RULE.
C  FOR GREATEST ACCURACY, N AND M SHOULD BE EVEN.
      SUBROUTINE DBLINT(G,X1,X2,Y1,Y2,N,M)
      COMMON/BLCK1/SINT
      EXTERNAL G,X1,X2
      EXTERNAL FRONT,SIDE,ALPHA1,ALPHA2,ALPHA3,ALPHA4
      AN = N
```

```
      AM = M
      DELTAY = (Y2 - Y1)/AM
      J = 0
      DO 260 J = 1,M+1,2
      L = J - 1
      AJ = J
      AL = L
      I = 0
      YL = Y1 + (AL*DELTAY)
      YJ = Y1 + (AJ*DELTAY)
      U = X1(YL)
      V = X1(YJ)
      DELTXL = (X2(YL) - U)/AN
      DELTXJ = (X2(YJ) - V)/AN
      DO 130 I = 1,N+1,2
      K = I - 1
      AI = I
      AK = K
      XKL = U + (AK*DELTXL)
      XIL = U + (AI*DELTXL)
      XKJ = V + (AK*DELTXJ)
      XIJ = V + (AI*DELTXJ)
      A = G(XKL,YL)
      B = G(XIL,YL)
      C = G(XKJ,YJ)
      D = G(XIJ,YJ)
      IF (I - 1) 5,5,30
5     RL = (A/2.0) + B
      RJ = (C/2.0) + D
      GO TO 130
30    IF (I - (N + 1)) 35,65,65
35    RL = A + B + RL
      RJ = C + D + RJ
      GO TO 130
65    RL = A + (B/2.0) + RL
      RJ = C + (D/2.0) + RJ
130   CONTINUE
      RL = RL*DELTXL
      RJ = RJ*DELTXJ
      IF (J - 1) 195,195,220
195   R = (RL/2.0) + RJ
      GO TO 260
220   IF (J - (M + 1)) 225,255,255
225   R = RL + RJ + R
      GO TO 260
255   R = RL + (RJ/2.0) + R
260   CONTINUE
      SINT = R*DELTAY
      RETURN
      END
C  DEFINE THE INTEGRAND FOR THE FRONT
C  APERTURE, FRONT(ALPHA,BETA).
```

```
      FUNCTION FRONT(ALPHA,BETA)
      COMMON/BLCK4/TPRIME,ATIME,TAU,RA,V,PI
      COMMON/BLCK5/SITHET,COTHET,SIPHI,COPHI
      COMMON/BLCK13/INDEXA,INDEXB
      SIALPH = SIN(ALPHA)
      COALPH = COS(ALPHA)
      SIBETA = SIN(BETA)
      COBETA = COS(BETA)
C  DEFINE THE ARGUMENT OF V' FOR THE FRONT
C  APERTURE, ARGF = (T' - (RA/V) + (R0.RS/V)).
      ARGAF = SIALPH*COBETA*SITHET*COPHI
      ARGBF = SIALPH*SIBETA*SITHET*SIPHI
      ARGCF = COALPH*COTHET
      ARGDF = ARGAF + ARGBF + ARGCF
      ARGF = TPRIME - ATIME + (ATIME*ARGDF)
C  DEFINE V' FOR THE FRONT APERTURE.
      VPRF = (EXP(-((ARGF/TAU)**2.0)))/(1.77245*TAU)
C  DEFINE THE ANGULAR TAPER OF THE EXCITATION
C  FOR THE FRONT APERTURE, TAPERF = F(ALPHA,BETA).
      TAPERF = 1.0
      DEDTF = TAPERF*VPRF
      GO TO (310,320,330,340,350), INDEXA
310   FRONT = SIBETA*SIALPH*DEDTF
      RETURN
320   FRONT = COBETA*SIALPH*DEDTF
      RETURN
330   FRONT = COBETA*COALPH*SIALPH*DEDTF
      RETURN
340   FRONT = SIBETA*COALPH*SIALPH*DEDTF
      RETURN
350   FRONT = SIALPH*SIALPH*DEDTF
      RETURN
      END
C  DEFINE THE INTEGRAND FOR THE WEDGE-SHAPED
C  SIDE APERTURES, SIDE(ALPHA,RPRIME).
      FUNCTION SIDE(ALPHA,RPRIME)
      COMMON/BLCK4/TPRIME,ATIME,TAU,RA,V,PI
      COMMON/BLCK5/SITHET,COTHET,SIPHI,COPHI
      COMMON/BLCK6/THETAZ,PHIZ,ALPHAZ,BETAZ
      COMMON/BLCK13/INDEXA,INDEXB
      COMMON/BLCK15/ZEFF,ZZERO,REFL
      COMMON/BLCK16/MODE
      COMMON/BLCK17/SBETAZ,CBETAZ
      SIALPH = SIN(ALPHA)
      COALPH = COS(ALPHA)
      WTIME = RPRIME/V
      ARGAS = SIALPH*CBETAZ*SITHET*COPHI
      ARGBS = SIALPH*SBETAZ*SITHET*SIPHI
      ARGCS = COALPH*COTHET
C  DEFINE THE ARGUMENTS OF V' FOR
C  THE WEDGE-SHAPED SIDE APERTURES.
C  ARGVIA = (T' - (R'/V) + (R0.RS1/V))
```

```
      ARGDS = ARGAS + ARGBS + ARGCS
      ARGW1A = TPRIME - WTIME + (WTIME*ARGDS)
C  ARGW1B = (T' + (R'/V) - (2RA/V) + (R0.RS1/V))
      ARGW1B = TPRIME + WTIME - (2.0*ATIME) + (WTIME*ARGDS)
C  ARGW2A = (T' - (R'/V) + (R0.RS2/V))
      ARGES = ARGAS - ARGBS + ARGCS
      ARGW2A = TPRIME - WTIME + (WTIME*ARGES)
C  ARGW2B = (T' + (R'/V) - (2RA/V) + (R0.RS2/V))
      ARGW2B = TPRIME + WTIME - (2.0*ATIME) + (WTIME*ARGES)
C  DEFINE THE VARIOUS V'S FOR
C  THE WEDGE-SHAPED SIDE APERTURES.
      DENOM = 1.77245*TAU
      VPRW1A = (EXP(-((ARGW1A/TAU)**2.0)))/DENOM
      VPRW1B = (EXP(-((ARGW1B/TAU)**2.0)))/DENOM
      VPRW2A = (EXP(-((ARGW2A/TAU)**2.0)))/DENOM
      VPRW2B = (EXP(-((ARGW2B/TAU)**2.0)))/DENOM
C  DEFINE THE ANGULAR TAPER OF THE EXCITATION
C  FOR THE WEDGE-SHAPED SIDE APERTURES,
C  TAPERS = F(ALPHA,BETAZ).
      TAPERS = 1.0
      DEDTW1 = TAPERS*(VPRW1A + (REFL*VPRW1B))
      DEDTW2 = TAPERS*(VPRW2A + (REFL*VPRW2B))
      GO TO (500,600,600), MODE
500   GO TO (510,520), INDEXB
510   SIDE = SIALPH*DEDTW1
      RETURN
520   SIDE = SIALPH*DEDTW2
      RETURN
600   GO TO (510,610,520,620), INDEXB
610   SIDE = COALPH*DEDTW1
      RETURN
620   SIDE = COALPH*DEDTW2
      RETURN
      END
C  DEFINE THE LOWER LIMIT OF INTEGRATION ON ALPHA
C  FOR THE FRONT APERTURE, ALPHA1(BETA).
      FUNCTION ALPHA1(BETA)
      COMMON/BLCK3/TTHETZ
      ALPHA1 = ATAN(TTHETZ/COS(BETA))
      RETURN
      END
C  DEFINE THE UPPER LIMIT OF INTEGRATION ON ALPHA
C  FOR THE FRONT APERTURE, ALPHA2(BETA).
      FUNCTION ALPHA2(BETA)
      COMMON/BLCK4/TPRIME,ATIME,TAU,RA,V,PI
      EXTERNAL ALPHA1
      ALPHA2 = PI - ALPHA1(BETA)
      RETURN
      END
C  DEFINE THE LOWER LIMIT OF INTEGRATION ON ALPHA
C  FOR THE WEDGE-SHAPED SIDE APERTURES, ALPHA3(BETA).
      FUNCTION ALPHA3(BETA)
```

```
      COMMON/BLCK6/THETAZ,PHIZ,ALPHAZ,BETAZ
      ALPHA3 = ALPHAZ
      RETURN
      END
C  DEFINE THE UPPER LIMIT OF INTEGRATION ON ALPHA
C  FOR THE WEDGE-SHAPED SIDE APERTURES, ALPHA4(BETA).
      FUNCTION ALPHA4(BETA)
      COMMON/BLCK4/TPRIME,ATIME,TAU,RA,V,PI
      COMMON/BLCK6/THETAZ,PHIZ,ALPHAZ,BETAZ
      ALPHA4 = PI - ALPHAZ
      RETURN
      END
C  SUBROUTINE TO GENERATE THE NUMERICAL OUTPUT
C  OF THE TEM HORN TRANSIENT RESPONSE PROGRAM
      SUBROUTINE OUTPUT
      DIMENSION RETHET(200), REPHI(200), TRET(200)
      COMMON/BLCK2/NFRONT,MFRONT,NSIDE,MSIDE
      COMMON/BLCK4/TPRIME,ATIME,TAU,RA,V,PI
      COMMON/BLCK6/THETAZ,PHIZ,ALPHAZ,BETAZ
      COMMON/BLCK7/TMAX,TMIN
      COMMON/BLCK8/HEIGHT,RAINCH,PHIZD,WIDTH
      COMMON/BLCK9/NDIV,NPTS
      COMMON/BLCK10/THETAD,PHID
      COMMON/BLCK11/ICOUNT
      COMMON/BLCK12/RETHET,REPHI,TRET
      COMMON/BLCK14/ANGLE,RADFAC
      COMMON/BLCK15/ZEFF,ZZERO,REFL
      COMMON/BLCK16/MODE
      IF (ICOUNT - 1) 1501,1501,1900
1501  WRITE (108,1505)
1505  FORMAT('CONSIDER A TEM HORN WITH')
      WRITE (108,1510) PHIZD
1510  FORMAT('A WEDGE ANGLE OF ',F6.1,' DEGREES,')
      WRITE (108,1515) HEIGHT
1515  FORMAT('A HEIGHT H = ',F6.1,' INCHES,')
      WRITE (108,1520) RAINCH
1520  FORMAT('AND A LENGTH L = ',F6.1,' INCHES.')
      WRITE (108,1525) ZZERO
1525 0FORMAT(/'THE CHARACTERISTIC IMPEDANCE OF THIS HORN'
     1/'WAS FOUND TO BE ',F7.1,' OHMS.')
      WRITE (108,1530) ZEFF
1530 0FORMAT('THE EFFECTIVE TERMINATING IMPEDANCE'
     1/'WHICH WAS USED WAS ',F7.1,' OHMS.')
      WRITE (108,1535) REFL
1535 0FORMAT('THEREFORE,THE EFFECTIVE VOLTAGE REFLECTION'
     1/'COEFFICIENT COMPUTED WAS ',F6.3,'.')
      WRITE (108,1540)
1540 0FORMAT(/'THE CHERNOUSOV ANALYSIS OF THIS HORN'
     1/'WAS PERFORMED USING A GAUSSIAN VOLTAGE DERIVATIVE')
      PWIDTH = WIDTH*(1.0E+12)
      WRITE (108,1545) PWIDTH
1545  FORMAT('WITH A HALF-WIDTH OF ',F7.1,' PICOSECONDS.')
```

```
      WRITE (108,1550) MODE
1550  FORMAT(/'THE PROGRAM WAS EXECUTED IN MODE ',I1,'.')
      GO TO (1555,1560,1565), MODE
1555  WRITE (108,1556)
1556  FORMAT('RXETHETA(R,T-R/V) ONLY WAS COMPUTED')
      GO TO 1570
1560  WRITE (108,1561)
1561  FORMAT('RXEPHI(R,T-R/V) ONLY WAS COMPUTED')
      GO TO 1570
1565  WRITE (108,1566)
1566 0FORMAT('BOTH RXETHETA(R,T-R/V) AND'
     1/'RXEPHI(R,T-R/V) WERE COMPUTED')
1570  WRITE (108,1575) NPTS
1575 0FORMAT('AT ',I3,' DIFFERENT VALUES OF'
     1/'RETARDED TIME T'' = T-R/V WHICH FELL WITHIN'
     2/'THE NUMERICALLY ESTABLISHED TIME WINDOW.')
      TLOWER = TMIN*(1.0E+09)
      TUPPER = TMAX*(1.0E+09)
      WRITE (108,1580) TLOWER,TUPPER
1580 0FORMAT('TIME WINDOW STARTED AT ',F7.3,' NANOSECONDS'
     1/'AND ENDED AT ',F7.3,' NANOSECONDS.')
      WWIDTH = TUPPER - TLOWER
      WRITE (108,1585) WWIDTH
1585  FORMAT('THE WINDOW WIDTH WAS ',F7.3,' NANOSECONDS.')
      WRITE (108,1590)
1590  FORMAT(/'FOR THE NUMERICAL INTEGRATION ROUTINE,')
      WRITE (108,1595) NFRONT,MFRONT
1595 0FORMAT('THE FRONT APERTURE WAS DIVIDED'
     1/'INTO ',I4,' SUBDIVISIONS IN ALPHA,'
     2/'AND ',I4,' SUBDIVISIONS IN BETA.')
      WRITE (108,1600) NSIDE,MSIDE
1600 0FORMAT('THE WEDGE-SHAPED SIDE APERTURES WERE DIVIDED'
     1/'INTO ',I4,' SUBDIVISIONS IN ALPHA,'
     2/'AND ',I4,' SUBDIVISIONS IN R''.')
1900  WRITE (108,1905) ICOUNT
1905  FORMAT(///'OBSERVATION POINT P(THETA,PHI) # ',I3)
      WRITE (108,1910) THETAD,PHID
1910 0FORMAT('THETA = ',F6.1,' DEGREES, '
     1'PHI = ',F6.1,' DEGREES')
      GO TO (1915,1935,1915), MODE
1915  WRITE (108,1920)
1920 0FORMAT(/'A TABLE OF T-R/V,RXETHETA(R,T-R/V) FOLLOWS.'
     1/'T-R/V IS IN NANOSECONDS AND RXETHETA IS IN VOLTS.')
      JIVE = 0
      DO 1930 JIVE = 1,NPTS,1
      TNANO = (TRET(JIVE))*(1.0E+09)
      WRITE (108,1925) TNANO,RETHET(JIVE)
1925  FORMAT(F7.3,',',1PE10.3)
1930  CONTINUE
1935  GO TO (1960,1940,1940), MODE
1940  WRITE (108,1945)
1945 0FORMAT(/'A TABLE OF T-R/V,RXEPHI(R,T-R/V) FOLLOWS.'
```

```
     1/'T-R/V IS IN NANOSECONDS AND RXEPHI IS IN VOLTS.')
      JAZZ = 0
      DO 1955 JAZZ = 1,NPTS,1
      TNANO = (TRET(JAZZ))*(1.0E+09)
      WRITE (108,1950) TNANO,REPHI(JAZZ)
1950  FORMAT(F7.3,',',1PE10.3)
1955  CONTINUE
1960  RETURN
      END
```

Appendix E

DESCRIPTION AND LISTING OF THE FORTRAN PROGRAMS TO COMPUTE THE ELECTRIC FAR FIELDS OF A PARABOLOID REFLECTOR/POINT SOURCE FEED ANTENNA SYSTEM

E.1 PROGRAM FOR AN ISOTROPIC FEED

This section describes and lists the Fortran IV program which computes the electric far fields of a paraboloid reflector fed by an isotropic point source feed located at the focus of the paraboloid. The program utilizes equations (C-92) and (C-93) along with equations (4-28) and (4-29). The normalized electric far field components of the feed, $r_H E_{\theta H}$ and $r_H E_{\phi H}$ respectively, are discussed in Section 4.3. The program was written for the Xerox XDS Sigma 6 digital computer (with 80k words of main memory) located at the Cook Physical Science Building at the University of Vermont.

The isotropic feed considered in this section had an $r_H E_{\theta H}$ field component given by equation (5-2). The $r_H E_{\phi H}$ component was neglected with respect to the $r_H E_{\theta H}$ component.

The mainline program establishes various constants and quantities which are used throughout the analysis, increments the discrete values of time at which the electric far fields are computed, and computes the numerical value of (C-92) and (C-93) at the various

discrete times. The mainline also calls several subroutines which perform other functions.

SUBROUTINE INPUT reads the input data for the program. The first line of data read is FINCH and DINCH. FINCH is the focal length of the paraboloid in inches, and DINCH is the diameter of the exit aperture of the paraboloid in inches. The second line of data read is FEED, which is an alphanumeric string of characters to describe the point source feed which is exciting the paraboloid. FEED may be any string of alphanumeric characters up to 72 spaces in length. The third line of data read is WIDTH, which is the 3-db width of the gaussian pulse exciting the feed in seconds. The fourth line of data read is two integers, NDIV and NPTS. NDIV establishes a subdivision criterion for the numerical integration routine. For best accuracy in the numerical integration routine, NDIV should be an integer at least as large as 2. Larger values may be used, depending upon limits for execution time. NPTS is an integer determining the number of discrete values of time at which the field components will be computed at each observation point $P(\Theta,\phi)$ in the far field of the paraboloid. The maximum value of NPTS allowed is 200. An approximate minimum value for NPTS to properly characterize the electric far fields may be found from

$$NPTS = \frac{2D}{\tau V} \qquad (E\text{-}1)$$

where D is the exit aperture diameter, τ is the characteristic parameter of the gaussian pulse exciting the feed as given by equation (5-3),

and v is the velocity of propagation in the medium. τ is related to WIDTH by the relationship

$$\tau = \frac{\text{WIDTH}}{2\sqrt{\ln 2}} \qquad \text{(E-2)}$$

The fifth and following lines of data read are the locations of the observation points at which the electric far fields are to be computed. THETAD is the parameter θ in degrees. PHID is the parameter ϕ in degrees. One observation point THETAD,PHID is read per line. As many observation points as desired may be listed, depending upon the time limits for execution.

The following is an example input file used to execute the program.

```
20.2,48.0
AN ISOTROPIC GAUSSIAN-DERIVATIVE PULSE.
340.0E-12
2,50
30.0,0.0
20.0,0.0
10.0,0.0
5.0,0.0
0.0,0.0
```

For the example shown, the focal length of the paraboloid was 20.2", and the exit aperture diameter was 48.0". Therefore, FINCH = 20.2 and DINCH = 48.0. FEED was the alphanumeric string "AN ISOTROPIC GAUSSIAN-DERIVATIVE PULSE.". WIDTH was 340.0 picoseconds. NDIV was set equal to 2, and NPTS was set equal to 50. The electric far fields were computed at five different observation points: $P(\theta,\phi)$ = $(30.0^\circ, 0.0^\circ)$, $(20.0^\circ,0.0^\circ)$, $(10.0^\circ,0.0^\circ)$, $(5.0^\circ,0.0^\circ)$, and $(0.0^\circ,0.0^\circ)$.

The program for an isotropic feed with the associated Fortran

library routines required approximately 9.5k words of memory. The execution for the example input file required 173.1 minutes of central processing unit time. The execution time for the program varies directly as NPTS and directly as the number of observation points $P(\Theta,\phi)$. Also, the execution time varies approximately as $NDIV^2$.

SUBROUTINE TSETUP establishes the numerical time window for the field computations. The low end of the time window, TMIN, is determined from

$$TMIN = \frac{f}{v}\left(1+\cos\Theta\right) + \frac{f}{v}\left(1-\cos\Theta\right)\frac{D^2}{16f^2} - \frac{D}{2v}\sin\Theta - 3\tau \qquad \text{(E-3)}$$

The high end of the time window, TMAX, is determined from

$$TMAX = \frac{f}{v}\left(1+\cos\Theta\right) + \frac{f}{v}\left(1-\cos\Theta\right)\frac{D^2}{16f^2} + \frac{D}{2v}\sin\Theta + 5\tau \qquad \text{(E-4)}$$

The numerical time window TMAX - TMIN was established so that execution time would not be wasted computing many double integrals at times for which the physical fields would be negligible with respect to their maximum value.

SUBROUTINE SUBDIV establishes the subdivisions for the numerical integration routine. NR is the number of subdivisions used to divide the integration in r at the exit aperture. NR is determined from

$$NR = NDIV\left[\frac{D}{2\tau v} + 1\right] \qquad \text{(E-5)}$$

MXI is the number of subdivisions used to divide the integration in ξ at the exit aperture. MXI is determined from

$$MXI = NDIV\left[\frac{\pi D}{2V} + 1\right] \qquad \text{(E-6)}$$

SUBROUTINE DBLINT(G,X1,X2,Y1,Y2,N,M) computes the double integral of G(X,Y) from X1 to X2 and then from Y1 to Y2 using N equal subdivisions in X and M equal subdivisions in Y. The subroutine uses the trapezoidal rule. The trapezoidal rule integration was chosen as a compromise between precision of integration and execution time required.

SUBROUTINE OUTPUT generates the numerical output of the program. This subroutine contains sufficient Hollerith statements to be self-explanatory. SUBROUTINE OUTPUT was programmed to be able to handle a wide range of focal length and exit aperture diameter, pulse widths, and alphanumeric strings describing the feed exciting the paraboloid.

FUNCTION VTHETA(R,XI) describes the partial time derivative of equation (5-2) evaluated at the exit aperture of the paraboloid. Since the $r_H E_{\phi H}$ component of the normalized electric far field of the isotropic feed was neglected with respect to the $r_H E_{\theta H}$ component, no corresponding FUNCTION VPHI(R,XI) was included in the program.

A listing of the Fortran IV program for the isotropic feed described by equation (5-2) exciting a paraboloid reflector follows on the next page.

```
C  MAINLINE FOR THE TRANSIENT RESPONSE OF
C  A PARABOLOID REFLECTOR/FEED ANTENNA SYSTEM
C  IN TERMS OF THE FIELDS EXCITING THE EXIT APERTURE.
C  THE FEED IS CONSIDERED TO BE A POINT-SOURCE RADIATOR
C  LOCATED AT THE FOCUS OF THE PARABOLOID.
C  THE FIELDS OF THE FEED EXCITING THE EXIT APERTURE
C  ARE DESCRIBED IN THE FUNCTIONS VTHETA AND VPHI.
      DIMENSION RETHET(200), REPHI(200), TRET(200)
      COMMON/BLCK1/SINT
      COMMON/BLCK2/NP,NXI
      COMMON/BLCK3/F,D,FINCH,DINCH
      COMMON/BLCK4/TPRIME,DTIME,FTIME,RATIO,TAU,V,PI
      COMMON/BLCK5/SITHET,COTHET,SIPHI,COPHI
      COMMON/BLCK6/FEED(18)
      COMMON/BLCK7/TMAX,TMIN
      COMMON/BLCK8/WIDTH
      COMMON/BLCK9/NDIV,NPTS
      COMMON/BLCK10/THETAD,PHID
      COMMON/BLCK11/ICOUNT,INDEX
      COMMON/BLCK12/RETHET,REPHI,TRET
      EXTERNAL VTHETA,VPHI
      ICOUNT = 0
1000  CALL INPUT
      IF (THETAD) 1500,1005,1005
1005  F = FINCH/39.3700
      D = DINCH/39.3700
      V = 2.99776E+08
      PI = 3.14159
      RADFAC = PI/180.0
      THETA = RADFAC*THETAD
      PHI = RADFAC*PHID
      FACT = 1.0/(4.0*PI*V)
      TAU = WIDTH/(2.0*SQRT(ALOG(2.0)))
      DTIME = D/V
      FTIME = F/V
      RATIO = (D**2.0)/(16.0*(F**2.0))
      SITHET = SIN(THETA)
      COTHET = COS(THETA)
      SIPHI = SIN(PHI)
      COPHI = COS(PHI)
      CARD = 1.0 + COTHET
      CALL TSETUP
      CALL SOLDIV
C  ROUTINE TO COMPUTE RXETHETA(R,T-R/V) AND
C  RXEPHI(R,T-R/V) FROM THE CHERNOUSOV EXPRESSION
      NTIME = 0
      DO 1300 NTIME = 1,NPTS,1
      ANTIME = NTIME - 1
      ANPTS = NPTS - 1
      TPRIME = TMIN + ((ANTIME/ANPTS)*(TMAX - TMIN))
      ATHETA = 0.0
      APHI = 0.0
```

```
      INDEX = 0
      DO 1175 INDEX = 1,4,1
     0CALL DBLINT(VTHETA,0.0,(D/2.0),
     10.0,(2.0*PI),NR,MXI)
      GO TO (1110,1120,1130,1120), INDEX
1110  ATHETA = -(SIPHI*SINT) + ATHETA
      APHI = (COPHI*SINT) + APHI
      GO TO 1175
1120  ATHETA = -(COPHI*SINT) + ATHETA
      APHI = -(SIPHI*SINT) + APHI
      GO TO 1175
1130  ATHETA = (SIPHI*SINT) + ATHETA
      APHI = -(COPHI*SINT) + APHI
1175  CONTINUE
C  INCLUDE NEXT STATEMENT IF VPHI = 0
      GO TO 1280
      DO 1275 INDEX = 1,4,1
     0CALL DBLINT(VPHI,0.0,(D/2.0),
     10.0,(2.0*PI),NR,MXI)
      GO TO (1210,1220,1210,1240), INDEX
1210  ATHETA = -(SIPHI*SINT) + ATHETA
      APHI = (COPHI*SINT) + APHI
      GO TO 1275
1220  ATHETA = -(COPHI*SINT) + ATHETA
      APHI = -(SIPHI*SINT) + APHI
      GO TO 1275
1240  ATHETA = (COPHI*SINT) + ATHETA
      APHI = (SIPHI*SINT) + APHI
1275  CONTINUE
1280  RETHET(NTIME) = FACT*CARD*ATHETA
      REPHI(NTIME) = FACT*CARD*APHI
      TRET(NTIME) = TPRIME
1300  CONTINUE
      ICOUNT = ICOUNT + 1
      CALL OUTPUT
      GO TO 1000
1500  END
C  SUBROUTINE TO READ INPUT DATA
C  FOR THE PARABOLOID/FEED TRANSIENT RESPONSE PROGRAM.
C  DATA READ ARE THE FOCAL LENGTH AND DIAMETER,
C  THE NAME OF THE FEED EXCITING THE PARABOLOID,
C  THE HALF-AMPLITUDE WIDTH OF THE EXCITING PULSE,
C  A SUBDIVISION CRITERION FOR THE NUMERICAL INTEGRATION,
C  NUMBER OF COMPUTED POINTS AT EACH OBSERVATION POINT,
C  AND LOCATION OF THE OBSERVATION POINT P(THETA,PHI).
      SUBROUTINE INPUT
      COMMON/BLCK3/F,D,FINCH,DINCH
      COMMON/BLCK6/FEED(18)
      COMMON/BLCK8/WIDTH
      COMMON/BLCK9/NDIV,NPTS
      COMMON/BLCK10/THETAD,PHID
      COMMON/BLCK11/ICOUNT,INDEX
```

```
      IF (ICOUNT) 1501,1501,1550
1501  READ (105,1510) FINCH,DINCH
1510  FORMAT(2E.1)
      READ (105,1520) FEED
1520  FORMAT(18A4)
      READ (105,1530) WIDTH
1530  FORMAT(E.1)
      READ (105,1540) NDIV,NPTS
1540  FORMAT(2I)
1550  READ (105,1510) THETAD,PHID
      RETURN
      END
C  SUBROUTINE TO ESTABLISH THE NUMERICAL TIME WINDOW
      SUBROUTINE TSETUP
      COMMON/BLCK4/TPRIME,DTIME,FTIME,RATIO,TAU,V,PI
      COMMON/BLCK5/SITHET,COTHET,SIPHI,COPHI
      COMMON/BLCK7/TMAX,TMIN
      T1 = FTIME*(1.0 + COTHET)
      T2 = FTIME*(1.0 - COTHET)*RATIO
      T3 = (DTIME*SITHET)/2.0
      TMIN = T1 + T2 - T3 - (3.0*TAU)
      TMAX = T1 + T2 + T3 + (5.0*TAU)
      RETURN
      END
C  SUBROUTINE TO ESTABLISH SUBDIVISIONS
C  FOR THE NUMERICAL INTEGRATION ROUTINE
      SUBROUTINE SUBDIV
      COMMON/BLCK2/NR,MXI
      COMMON/BLCK4/TPRIME,DTIME,FTIME,RATIO,TAU,V,PI
      COMMON/BLCK9/NDIV,NPTS
      NSTART = DTIME/(2.0*TAU)
      NSTART = NSTART + 1
      NR = NDIV*NSTART
      MSTART = (PI*DTIME)/TAU
      MSTART = MSTART + 1
      MXI = NDIV*MSTART
      RETURN
      END
C  SUBROUTINE TO COMPUTE THE DOUBLE INTEGRAL
C  OF G(X,Y) FROM X1 TO X2 AND Y1 TO Y2
C  USING N EQUAL SUBDIVISIONS IN X
C  AND M EQUAL SUBDIVISIONS IN Y.
C  THE SUBROUTINE USES THE TRAPEZOIDAL RULE.
      SUBROUTINE DBLINT(G,X1,X2,Y1,Y2,N,M)
      COMMON/BLCK1/SINT
      EXTERNAL G
      EXTERNAL VTHETA,VPHI
      AN = N
      AM = M
      DELTAX = (X2 - X1)/AN
      DELTAY = (Y2 - Y1)/AM
      J = 0
```

```
      DO 260 J = 1,M+1,1
      AJ = J - 1
      Y = Y1 + (AJ*DELTAY)
      I = 0
      DO 130 I = 1,N+1,1
      AI = I - 1
      X = X1 + (AI*DELTAX)
      A = G(X,Y)
      IF (I - 1) 5,5,30
5     RX = A/2.0
      GO TO 130
30    IF (I - (N+1)) 35,65,65
35    RX = A + RX
      GO TO 130
65    RX = (A/2.0) + RX
130   CONTINUE
      RX = RX*DELTAX
      IF (J - 1) 195,195,220
195   R = RX/2.0
      GO TO 260
220   IF (J - (M+1)) 225,255,255
225   R = RX + R
      GO TO 260
255   R = (RX/2.0) + R
260   CONTINUE
      SINT = R*DELTAY
      RETURN
      END
C  SUBROUTINE TO GENERATE THE NUMERICAL OUTPUT
C  OF THE PARABOLOID/FEED TRANSIENT RESPONSE PROGRAM
      SUBROUTINE OUTPUT
      DIMENSION RETHET(200), REPHI(200), TRET(200)
      COMMON/BLCK2/NR,MXI
      COMMON/BLCK3/F,D,FINCH,DINCH
      COMMON/BLCK4/TPRIME,DTIME,FTIME,RATIO,TAU,V,PI
      COMMON/BLCK6/FEED(18)
      COMMON/BLCK7/TMAX,TMIN
      COMMON/BLCK8/WIDTH
      COMMON/BLCK9/NDIV,NPTS
      COMMON/BLCK10/THETAD,PHID
      COMMON/BLCK11/ICOUNT,INDEX
      COMMON/BLCK12/RETHET,REPHI,TRET
      IF (ICOUNT - 1) 1501,1501,1900
1501  WRITE (108,1505)
1505  FORMAT('CONSIDER A PARABOLOID REFLECTOR')
      WRITE (108,1510) FINCH
1510  FORMAT('WITH A FOCAL LENGTH OF ',F7.1,' INCHES')
      WRITE (108,1515) DINCH
1515  FORMAT('AND A DIAMETER OF ',F7.1,' INCHES.')
      WRITE (108,1520) F/D
1520  FORMAT('THE F/D RATIO IN THIS CASE IS ',F7.3,' .')
      WRITE (108,1525) FEED
```

```
1525 0FORMAT(/'THE APPROXIMATE EXIT APERTURE FIELDS'
     1/'WERE DETERMINED FOR EXCITATION BY'
     2/,18A4)
      PWIDTH = WIDTH*(1.0E+12)
      WRITE (108,1530) PWIDTH
1530 0FORMAT(/'THE CHERNOUSOV ANALYSIS FOR THE'
     1/'PARABOLOID/FEED ANTENNA SYSTEM WAS PERFORMED FOR'
     2/'A PULSE WITH HALF-WIDTH OF ',F8.1,' PICOSECONDS.')
      WRITE (108,1535)
1535 0FORMAT(/'BOTH RXETHETA(R,T-R/V) AND'
     1/'RXEPHI(R,T-R/V) WERE COMPUTED')
      WRITE (108,1540) NPTS
1540 0FORMAT('AT ',I3,' EQUALLY SPACED VALUES OF'
     1/'RETARDED TIME T'' = (T - R/V) WHICH FELL WITHIN'
     2/'THE NUMERICALLY ESTABLISHED TIME WINDOW.')
      WRITE (108,1550) NR,MXI
1550 0FORMAT(/'FOR THE NUMERICAL INTEGRATION ROUTINE,'
     1/'THE EXIT APERTURE WAS DIVIDED'
     2/'INTO ',I4,' SUBDIVISIONS IN R,'
     3/'AND ',I4,' SUBDIVISIONS IN XI.')
1900  WRITE (108,1905) ICOUNT
1905  FORMAT(///'OBSERVATION POINT P(THETA,PHI) # ',I3)
      WRITE (108,1910) THETAD,PHID
1910 0FORMAT('THETA = ',F6.1,' DEGREES, ',
     1'PHI = ',F6.1,' DEGREES')
      TLOWER = TMIN*(1.0E+09)
      TUPPER = TMAX*(1.0E+09)
      WWIDTH = TUPPER - TLOWER
      WRITE (108,1915) TLOWER,TUPPER,WWIDTH
1915 0FORMAT(/'TIME WINDOW STARTED AT ',F9.3,' NANOSECONDS'
     1/'AND ENDED AT ',F9.3,' NANOSECONDS.'
     2/'THE WINDOW WIDTH WAS ',F9.3,' NANOSECONDS.')
      WRITE (108,1920)
1920 0FORMAT(/'A TABLE OF T-R/V,RXETHETA(R,T-R/V) FOLLOWS.'
     1/'T-R/V IS IN NANOSECONDS AND RXETHETA IS IN VOLTS.')
      JIVE = 0
      DO 1930 JIVE = 1,NPTS,1
      TNANO = (TRET(JIVE))*(1.0E+09)
      WRITE (108,1925) TNANO,RETHET(JIVE)
1925  FORMAT(F9.3,',',1PE10.3)
1930  CONTINUE
      WRITE (108,1945)
1945 0FORMAT(/'A TABLE OF T-R/V,RXEPHI(R,T-R/V) FOLLOWS.'
     1/'T-R/V IS IN NANOSECONDS AND RXEPHI IS IN VOLTS.')
      JAZZ = 0
      DO 1955 JAZZ = 1,NPTS,1
      TNANO = (TRET(JAZZ))*(1.0E+09)
      WRITE (108,1950) TNANO,REPHI(JAZZ)
1950  FORMAT(F9.3,',',1PE10.3)
1955  CONTINUE
      RETURN
      END
```

```
C  DESCRIBE THE EXIT APERTURE FIELDS
C  DUE TO THE THETA COMPONENT
C  OF THE RADIATION FROM THE FEED, V1,
C  AND DEFINE THE CORRESPONDING APERTURE INTEGRANDS, VTHETA.
      FUNCTION VTHETA(R,XI)
      COMMON/BLCK3/F,D,FINCH,DINCH
      COMMON/BLCK4/TPRIME,DTIME,FTIME,RATIO,TAU,V,PI
      COMMON/BLCK5/SITHET,COTHET,SIPHI,COPHI
      COMMON/BLCK11/ICOUNT,INDEX
C  DEFINE THE TIME ARGUMENT OF THE THETA COMPONENT.
      SIXI = SIN(XI)
      COXI = COS(XI)
      FSQ = F**2.0
      ARGA = FTIME*(1.0 + COTHET)
      ARGB = FTIME*(1.0 - COTHET)*RATIO
      ARGC = COXI*SITHET*COPHI
      ARGD = SIXI*SITHET*SIPHI
      ARGE = (R/V)*(ARGC + ARGD)
      ARG = TPRIME - ARGA - ARGB + ARGE
C  DEFINE THE FORM OF THE FEED'S THETA COMPONENT
C  OVER THE EXIT APERTURE, V1.
      TAUSQ = TAU**2.0
      ARGTAU = (ARG/TAU)**2.0
      V1 = (2.0/TAUSQ)*((2.0*ARGTAU) - 1.0)*EXP(-ARGTAU)
      V1 = V1*(9.74E-12)
C  DEFINE THE EXIT APERTURE INTEGRANDS
C  CORRESPONDING TO THE FEED'S THETA COMPONENT.
      RSQ = R**2.0
      Q = RSQ/(4.0*FSQ)
      QMINUS = 1.0 - Q
      QPLUS = 1.0 + Q
      DENOM = SQRT((FSQ*(QPLUS**2.0)) - (RSQ*COXI*COXI))
      GO TO (1971,1972,1973,1974), INDEX
1971  VTHETA=(V1*(QMINUS/QPLUS)*SIXI*COXI*R)/DENOM
      RETURN
1972  VTHETA=(V1*(QMINUS/QPLUS)*COXI*COXI*R)/DENOM
      RETURN
1973  VTHETA=(V1*SIXI*COXI*R)/DENOM
      RETURN
1974  VTHETA=(V1*SIXI*SIXI*R)/DENOM
      RETURN
      END
```

E.2 PROGRAM FOR TAPERED ILLUMINATION

This program is identical to the Fortran IV program described in Section E.1, except that equation (5-4) is utilized rather than equation (5-2) to describe the $r_H E_{\theta H}$ component of the electric far field of the point source feed located at the focus of the paraboloid. In this section, as in Section E.1, the $r_H E_{\phi H}$ component of the normalized electric far field of the feed was neglected with respect to the $r_H E_{\theta H}$ component.

In the program for tapered illumination of the exit aperture of the paraboloid, FUNCTION VTHETA(R,XI) describes the partial derivative of equation (5-4) with respect to time evaluated at the exit aperture of the paraboloid.

The execution time and space requirement of this program are approximately the same as the program discussed in Section E.1. For the sake of completeness, a listing of the routine FUNCTION VTHETA(R, XI) is given on the following pages.

```
C  DESCRIBE THE EXIT APERTURE FIELDS
C  DUE TO THE THETA COMPONENT
C  OF THE RADIATION FROM THE FEED, V1,
C  AND DEFINE THE CORRESPONDING APERTURE INTEGRANDS, VTHETA.
      FUNCTION VTHETA(R,XI)
      COMMON/BLCK3/F,D,FINCH,DINCH
      COMMON/BLCK4/TPRIME,DTIME,FTIME,RATIO,TAU,V,PI
      COMMON/BLCK5/SITHET,COTHET,SIPHI,COPHI
      COMMON/BLCK11/ICOUNT,INDEX
C  DEFINE THE TIME ARGUMENT OF THE THETA COMPONENT.
      SIXI = SIN(XI)
      COXI = COS(XI)
      FSQ = F**2.0
      ARGA = FTIME*(1.0 + COTHET)
      ARGB = FTIME*(1.0 - COTHET)*RATIO
      ARGC = COXI*SITHET*COPHI
      ARGD = SIXI*SITHET*SIPHI
      ARGE = (R/V)*(ARGC + ARGD)
      ARG1 = TPRIME - ARGA - ARGB + ARGE
      AA = 0.177
      BB = 0.0615
      CC = 0.030
      DD = 0.110
      EE = 0.417
      ABSI = ABS(SIXI)
      ABCO = ABS(COXI)
      ARGF = AA*ABCO
      ARGG = BB*ABSI
      ARG2 = (R/V)*(ARGF + ARGG)
      ARG = ARG1 - ARG2
C  DEFINE THE FORM OF THE FEED'S THETA COMPONENT
C  OVER THE EXIT APERTURE, V1.
      TAUA = TAU + ((CC*R*ABSI)/V)
      TAUASQ = TAUA**2.0
      ARGTAU = (ARG/TAUA)**2.0
      V1 = (2.0/TAUASQ)*((2.0*ARGTAU) - 1.0)*EXP(-ARGTAU)
      DENOM1 = 1.0 + ((2.0*DD*R*ABSI)/D)
      DENOM2 = 1.0 - ((2.0*EE*R*ABCO)/D)
      V1 = V1/(DENOM1*DENOM2)
      V1 = V1*(9.74E-12)
C  DEFINE THE EXIT APERTURE INTEGRANDS
C  CORRESPONDING TO THE FEED'S THETA COMPONENT.
      RSQ = R**2.0
      Q = RSQ/(4.0*FSQ)
      QMINUS = 1.0 - Q
      QPLUS = 1.0 + Q
      DENOM = SQRT((FSQ*(QPLUS**2.0)) - (RSQ*COXI*COXI))
      GO TO (1971,1972,1973,1974), INDEX
1971  VTHETA=(V1*(QMINUS/QPLUS)*SIXI*COXI*R)/DENOM
      RETURN
1972  VTHETA=(V1*(QMINUS/QPLUS)*COXI*COXI*R)/DENOM
      RETURN
```

```
1973  VTHETA=(V1*SIXI*COXI*R)/DENOM
      RETURN
1974  VTHETA=(V1*SIXI*SIXI*R)/DENOM
      RETURN
      END
```

MISSION
of
Rome Air Development Center

RADC is the principal AFSC organization charged with planning and executing the USAF exploratory and advanced development programs for electromagnetic intelligence techniques, reliability and compatibility techniques for electronic systems, electromagnetic transmission and reception, ground based surveillance, ground communications, information displays and information processing. This Center provides technical or management assistance in support of studies, analyses, development planning activities, acquisition, test, evaluation, modification, and operation of aerospace systems and related equipment.

Source AFSCR 23-50, 11 May 70